# VERTICAL GREENING IN URBAN BUILT ENVIRONMENTS

Kanchane Randev Akmimana Gunawardena

This thesis is submitted for the degree of

*Doctor of Philosophy*

Peterhouse Cambridge

July 2021

# Declaration

This thesis is the result of my own work and includes nothing which is the outcome of work done in collaboration except as declared in the thesis acknowledgments, publications statement, and specified in the text. I further state that no substantial part of my thesis has already been submitted, or is being concurrently submitted for any such degree, diploma or other qualification at the University of Cambridge, or any other University or similar institution except as declared in the thesis acknowledgments, publications statement, and specified in the text.

This thesis does not exceed the prescribed word limit of the University of Cambridge, Architecture and History of Art Degree Committee. The word count is 74,595 (including the abstract and introductory pages; but excluding the bibliography text).

**Kanchane R. Gunawardena**
BA(Hons), M.Arch(*Bath*), M.Phil(*Cantab*)
RIBA Chartered Architect

Cambridge, England
July 2021

# Abstract


VERTICAL GREENING IN URBAN BUILT ENVIRONMENTS

Kanchane R. Gunawardena

To meet the challenge of implementing green infrastructure enhancements to address climate risks in densely built cities, attention has been directed in recent times towards encouraging surface greening approaches. The thesis presented here acknowledged this trend and examined how the typology described as '**vertical greening**' contributes to this climate resilience enhancement of urban built environments. The project engaged with case study-based quantitative measurements and simulation methods to answer research questions concerned with the microclimate modification and resultant energy use influence presented by installations, in building-scale sheltered environments (e.g., an indoor atrium and a semi-outdoor court), and outdoor neighbourhood-scale canyon environments. It also engaged with qualitative interview and observational methods to address concerns related to the maintenance and sustainability of wider application of installations.

The key monitoring findings from temperate climate sheltered applications highlighted hygrothermal and airflow **modifications to be most apparent within the 1-2 m proximate zone**, with other phenomena typically introducing airflow mixing to disrupt influence distribution. The potencies of these were relatively modest, and less than those presented in the literature for outdoor installations (maximum mean air temperature reduction of 0.3 K and relative humidity increase of 5.5% at the indoor atrium study, in contrast to 0.9 K air temperature reduction and 13.7% relative humidity increase at the semi-outdoor court study). The modifications nevertheless presented **thermal sensation and diversity opportunity to occupants as a significant benefit**. The building-scale simulation findings of the same temperate climate case studies highlighted these influences to contribute to thermally moderated microclimates. For the semi-outdoor court this translated to surface flux reductions, with living wall application offering the most (84-90%), followed by green façade application (37-44%). Such reductions could translate to **energy use savings if the occupied environments implement mechanical cooling**. This was exemplified by the indoor study simulations, where a net annual energy consumption saving for the atrium zone was estimated (69% with living wall and 71% with green façade application). The neighbourhood-scale simulation results also demonstrated widespread outdoor application to have **improved the thermal climate of street canyons to benefit pedestrians** (summer daytime cool island occurrences increased by 39% for central urban and 3.4% for suburban canyons), as well as present **annual net energy use savings to the canyon buildings** (between 0.8 and 5.2%). These benefits were pronounced most for the central urban than suburban context, while living walls presented greater influence than traditional green façades in both urban backgrounds.

The synthesis of both observational and simulation findings broadly supports the wider applicability of such installations in densely built temperate climate cities; with the thesis discussing concerns and making recommendations for installation designers. Furthermore, the **project presents two novel model coupling pathways for assessing building and neighbourhood-scale vertical greening influence**, which would enable urban planners, architects, and installation designers to expediently utilise this typology of green infrastructure to enhance urban built environments and benefit the health, comfort, and wellbeing of their ever-growing occupant populations.

# Thesis preface

This doctoral project is considered as a progression of the author's Master of Philosophy project at the Martin Centre for Architectural and Urban Studies in Cambridge, where overheating risk was quantified in relation to the warming climate of London. The desire to engage and examine green infrastructural enhancements was in response to the need to develop passive strategies that mitigates such identified overheating risk, while also presenting a multitude of other ecosystem service benefits to urban built environments and their ever-growing occupant populations.

The inspiration to pursue the project and the generation of research questions was also influenced by several preceding years of architectural practice, where the author as a Chartered Architect had engaged with the design and implementation of several building and urban design projects integrating green infrastructural enhancements. The research design and narrative of this project has therefore been informed by the author's longstanding commitment and practical engagement with environmental design principles.

*Dedicated to my loving parents, Dr and Mrs Mahinda and Anoma Gunawardena;*

*&*

*paternal grandfather, the late Don Carlin Gunawardena, Professor of Botany, and maternal grandfather, the late M. A. A. Akmimana, Surveyor*

*...for inspiring my doctoral studies.*

# Acknowledgements

I would like to thank the United Kingdom Engineering and Physical Sciences Research Council (EPSRC) for funding this studentship award; and the Bruckmann Fund at Peterhouse, Kettle's Yard Cambridge, and Santander Universities for funding fieldwork related travel.

I am most grateful to my supervisor Koen Steemers, Professor of Sustainable Design, for his insightful direction, guidance, and support in researching and writing this thesis. The monitoring work presented in this thesis could not have been carried out without the resources he kindly secured, while his constructive criticism helped to focus the narrative, and guided the design, development, and publishing of the peer-reviewed papers supporting this work.

I would also like to thank the following academics from the Department of Architecture: Dr Minna Sunikka-Blank (my advisor), Dr Maximilian Sternberg (former tutor), Professor Ying Jin (Director of the Martin Centre), and Professor François Penz (Head of the Department); Professor Howard Griffiths from the Department of Plant Sciences; and Dr Tristan Kershaw from the Department of Architecture and Civil Engineering at the University of Bath, for their support and guidance; …

> …Dr Shiwei Fan from the Department of Chemistry for loaning monitoring equipment; and the Department of Engineering, Central Technical Services for assisting with apparatus assembly; …
>
> …University of Cambridge Estate Management, Living Laboratory for Sustainability Coordinators, for their enthusiasm for the project; and the Cambridge Conservation Initiative, Facilities Manager at the David Attenborough Building in Cambridge, for providing access and support to carry out monitoring work at the site; …
>
> …living wall consultant and supplier Scotscape Limited for providing access to the St Edmund's Terrace, London case study, along with the residents of the said residence for their corporation and support; and …
>
> …all expert practitioners, consultants, installation managers, and key decisionmakers interviewed; and the anonymous journal peer-reviewers and conference participants for their constructive criticism and comments.

Finally, I would like to thank the doctoral studies cohort and the members of the Behaviour and Building Performance (BBP) research group at the Department of Architecture for their support and comradeship; …

> …the Martin Centre for Architectural and Urban Studies at the Department of Architecture for their academic and administrative support; …
>
> …my College, Peterhouse; Graduate Tutor, Professor Steven Connor; and fellow Middle Combination Room Petreans, Alexander and Francesco, for the kind support offered over the course of my studies here in Cambridge; and …
>
> …Mr Martin Gledhill from the University of Bath, for being a pillar of encouragement throughout my architectural scholarship.

EPSRC
Engineering and Physical Sciences
Research Council

The Martin Centre
for Architectural and Urban Studies

# Publications statement

**Title:** Vertical greening in urban built environments

**Subject:** Architecture, Environmental Design

**Doctoral student:** Kanchane R. Gunawardena

**Supervisor:** Professor Koen Steemers

**Advisor**: Dr Minna Sunikka-Blank

**External advisor**: Dr Tristan Kershaw

This thesis is supported by the following original peer-reviewed journal publications:

**Gunawardena, K.**, Wells, M. J., & Kershaw, T. (2017). *Utilising green and bluespace to mitigate urban heat island intensity.* Science of the Total Environment, 584–585, 1040–1055.

**Gunawardena, K.**, & Steemers, K. (2019a). *Living walls in indoor environments.* Building and Environment, 148 (November 2018), 478–487.

**Gunawardena, K.**, Kershaw, T., & Steemers, K. (2019). *Simulation pathway for estimating heat island influence on urban/suburban building space-conditioning loads and response to façade material changes.* Building and Environment, 150 (January), 195–205.

**Gunawardena, K.**, & Steemers, K. (2020a). *Urban living walls: reporting on maintenance challenges from a review of European installations.* Architectural Science Review, 63(6), 526–535.

**Gunawardena, K.**, & Steemers, K. (2020b). *Living wall influence on the microclimates of sheltered urban conditions: results from monitoring studies.* Architectural Science Review, 64(3), 235-246.

…and the following peer-reviewed conference papers:

**Gunawardena, K.**, Mccullen, N., & Kershaw, T. (2017). *Heat island influence on space-conditioning loads of urban and suburban office buildings.* In: Cities and Climate Conference 2017, Potsdam: Potsdam Institute for Climate Impact Research, pp. 1–13.

**Gunawardena, K.**, & Kershaw, T. (2017). *Urban climate influence on building energy use.* In: M. P. Burlando, Massimiliano; Canepa, Maria; Magliocco, Adriano; Perini, Katia, Repetto, ed., International Conference on Urban Comfort and Environmental Quality URBAN-CEQ, Genoa: Genoa University Press, pp. 175–84.

**Gunawardena, K.**, & Steemers, K. (2019b). *Living wall influence on microclimates: an indoor case study.* In: CISBAT 2019 Special Issue of Journal of Physics: Conference Series, IOP Science, 1343, 012188, pp. 1–6. And in: CISBAT 2019, Climate Resilient Cities - Energy Efficiency and Renewables in the Digital Era, Lausanne: École Polytechnique Fédérale de Lausanne, pp. 1–6.

**Gunawardena, K.**, & Steemers, K. (2020c). *Characterising living wall microclimate modifications in sheltered urban conditions: findings from two monitored case studies.* In: J. Rodríguez-Álvarez & J. C. Gonçalves, eds., Planning Post Carbon Cities. Proceedings of the 35th PLEA Conference on Passive and Low Energy Architecture. Volume 1, A Coruña: University of A Coruña, pp. 606–11.

# Author contributions

For the aforementioned published papers, the author was the principal and first author, and led research development and principal drafting.

*Gunawardena, K., Wells, M. J., & Kershaw, T. (2017):*

The author was responsible for the standard review, analysis, drawing conclusions, producing illustrations, and principal drafting. External advisor and co-author, Dr Tristan Kershaw supervised the review, edited the draft, and provided support and guidance throughout the process. External biodiversity expert and second co-author, Dr M. J. Wells contributed by reviewing and editing the final draft.

*Gunawardena, K., & Steemers, K. (2019a):*

The author was responsible for the standard review, analysis, drawing conclusions, producing illustrations, and principal drafting. The author's supervisor and co-author, Professor Koen Steemers supervised the review and provided support and guidance throughout the process, including the review of the final draft.

*Gunawardena, K., Kershaw, T., & Steemers, K. (2019):*

The author was responsible for designing the research, modifying the code of an established urban climate framework to complement the research design, carrying out simulations, analysis of results, drawing conclusions, producing illustrations, and principal drafting. External advisor and co-author, Dr Tristan Kershaw supervised the research, edited the draft, and provided support and guidance throughout the process. Professor Koen Steemers was the second co-author and contributed by reviewing research results and the final draft.

*Gunawardena, K., & Steemers, K. (2020a):*

The author was responsible for designing the research, conducting fieldwork at ten case-studies, collecting data, conducting interviews and transcribing, analysis of results, drawing conclusions, producing illustrations, and principal drafting. Professor Koen Steemers was the co-author and contributed by reviewing research results and the final draft.

*Gunawardena, K., & Steemers, K. (2020b):*

The author was responsible for designing the research, conducting fieldwork at two case-studies, collecting data, analysis of results, drawing conclusions, producing illustrations, and principal drafting. Professor Koen Steemers was the co-author of the paper and contributed by reviewing research results and the final draft.

# Contents

# Abbreviations

| | |
|---|---|
| AC | Air-conditioning |
| AFFL | Above finish floor level (relative to the given building floor) |
| AGL | Above ground/grade level |
| ALW | Active living wall (living wall variant) |
| AR | Aspect ratio |
| ASL | Above sea level |
| AT | Air temperature \| $T_{air}$ |
| BEM | Building energy model |
| CAM | Crassulacean acid metabolism (photosynthesis pathway) |
| CCC | Committee on Climate Change (independent body advising the United Kingdom Government) |
| CF | CaixaForum Museum in Madrid, Spain (case study) |
| CFD | Computational fluid dynamics |
| CFU | Colony-forming units (number of living and viable microbial organisms in a culture sample) |
| CIBSE | Chartered Institution of Building Services Engineers (United Kingdom) |
| Ctrl | Control (reference to probe/dataset) |
| DAB | David Attenborough Building in Cambridge (case study) |
| EF | East-facing (façade/wall) |
| EPSRC | Engineering and Physical Sciences Research Council (United Kingdom) |
| FAO | Food and Agriculture Organization (United Nations) |
| GF | Green façade (vertical greening category) |
| GR | Glazing ratio |
| HDPE | High-density polyethylene (material) |
| HVAC | Heating, ventilation, and air-conditioning |
| IPCC | Intergovernmental Panel on Climate Change (United Nations) |
| IR | Infrared radiation |
| LAI | Leaf area index |
| LW | Living wall (vertical greening category) |
| MODIS | Moderate Resolution Imaging Spectroradiometer, onboard NASA satellites |
| NASA | National Aeronautics and Space Administration (United States) |
| NF | North-facing (façade/wall) |
| PAR | Photosynthetically active radiation |
| PBL | Planetary boundary-layer |
| PM | Particulate matter |
| PPD | Predicted percentage of dissatisfied (thermal comfort index) |
| QB | Quai Branly Museum in Paris, France (case study) |
| RBL | Rural boundary-layer |
| RH | Relative humidity |
| RHS | Royal Horticultural Society (United Kingdom) |
| SD | Standard deviation |
| SET | St. Edmund's Terrace court in London (case study) |
| SF | South-facing (façade/wall) |
| SI | Site inspection at case study |
| Sp. | Species not fully identified |
| Spp. | Multiple species, *Species pluralis* (Latin) |
| ST | Surface temperature \| $T_{surf}$ |
| UBL | Urban boundary-layer |

| | |
|---|---|
| UCL | Urban canopy layer |
| UCM | Urban canopy layer model |
| UHI | Urban heat island |
| UV | Ultraviolet radiation |
| UWG | Urban Weather Generator (simulation model, [1]) |
| VG | Vertical greening |
| VOC | Volatile organic compound |
| WBGT | Wet-bulb globe temperature (heat stress index) |
| WF | West-facing (façade/wall) |
| WMO | World Meteorological Organization (United Nations) |

# Nomenclature

| Symbol | Description | Unit |
|---|---|---|
| $\alpha$ | Absorptivity | |
| $\theta_{leaf}$ | Angle, of leaf orientation | [degrees] |
| $k$ | Coefficient, canopy attenuation | |
| $h_{Hw}$ | Coefficient, convective surface heat transfer | [W·m$^{2}$·K$^{-1}$] |
| $r \mid r_s$ | Coefficient, Pearson correlation \| Spearman correlation | |
| $\acute{a} \mid \acute{b} \mid \acute{c}$ | Coefficients, material roughness | |
| $g_{asul} \mid g_{asll}$ | Conductance, actual stomatal of upper (adaxial) \| lower (abaxial) leaf | [mol·m$^{-2}$·s$^{-1}$] |
| $g_c$ | Conductance, of heat through the air | [mol·m$^{-2}$·s$^{-1}$] |
| $g_v$ | Conductance, of vapour through the air | [mol·m$^{-2}$·s$^{-1}$] |
| $g_r$ | Conductance, radiative | [mol·m$^{-2}$·s$^{-1}$] |
| $g_s$ | Conductance, stomatal | [mol·m$^{-2}$·s$^{-1}$] |
| $Q_{C_{Hw}}$ | Conduction, heat flux through the vegetated façade | [W·m$^{-2}$] |
| $Q_{C_{veg}}$ | Conduction, through vertical greening plant stems to host surface | [W·m$^{-2}$] |
| $\gamma$ | Constant, psychrometric | [K$^{-1}$] |
| $\gamma^*$ | Constant, psychrometric apparent | [K$^{-1}$] |
| $\sigma$ | Constant, Stefan-Boltzmann = $5.67 \cdot 10^{-8}$ | [W·m$^{-2}$·K$^{-4}$] |
| $vk$ | Constant, Von Karman = 0.40 | |
| $Q_{E_{Hw}}$ | Convection, latent heat flux (when living wall) | [W·m$^{-2}$] |
| $Q_{h_{Hw}}$ | Convection, sensible heat flux (when living wall) | [W·m$^{-2}$] |
| $Q_{\mathrm{H}_{Hw}}$ | Convection, sensible heat flux (for green façade) | [W·m$^{-2}$] |
| $Q_{E_{veg}}$ | Convection, latent flux from transpiration | [W·m$^{-2}$] |
| $Q_{h_{veg}}$ | Convection, sensible flux from vegetation | [W·m$^{-2}$] |
| $M_i$ | Datapoint, measured, $i$ = 1, ..., $n_{tot}$ | |
| $S_i$ | Datapoint, simulated, $i$ = 1, ..., $n_{tot}$ | |
| $n_{tot}$ | Datapoints, total | |
| $sm$ | Datapoints, used to smoothen curve | |
| $\dot{\rho}$ | Density | [kg·m$^{-3}$] |
| $z_{veg}$ | Depth, canopy | [m] |
| $d_0$ | Depth, displacement | [m] |
| $D_{IR}$ | Distance, between target object and infrared sensor | [m] |
| $\varepsilon$ | Emissivity | |
| $F_{ext}$ | Factor, for exterior forced convection conditions = 1.40 | |
| $\psi_m \mid \psi_h$ | Factors, stability correction for momentum \| heat | |
| $AH$ | Humidity, absolute; expressed as vapour density | [g·m$^{-3}$] |
| $RH \mid rH$ | Humidity, relative; as percentage \| as ratio | [%] |

| Symbol | Description | Unit |
|---|---|---|
| $\lambda$ | Latent heat of vaporisation of water = 44,000 | [J·mol$^{-1}$] |
| $D$ | Length, leaf characteristic dimension in wind direction | [m] |
| $z_m \mid z_h$ | Length, of roughness for momentum \| heat | [m] |
| $\hat{\rho}_{air}$ | Molar density of air | [mol·m$^{-3}$] |
| $R$ | Molar gas constant = 8.31 | [J·mol$^{-1}$·K$^{-1}$] |
| $M_w$ | Molecular weight of water = 18.015 | [g·mol$^{-1}$] |
| $P_{air}$ | Pressure, atmospheric | [kPa] |
| $Q_{leaf}$ | Radiation, absorbed by plant layer | [W·m$^{-2}$] |
| $Q_{R_{lw}}$ | Radiation, longwave | [W·m$^{-2}$] |
| $Q_{R_{lw_{veg}}}$ | Radiation, longwave flux emissions from vegetation | [W·m$^{-2}$] |
| $Q_{R_{lw_{air}}}$ | Radiation, longwave flux attenuated by atmosphere | [W·m$^{-2}$] |
| $Q_{R_{lw_{tot}}}$ | Radiation, longwave flux captured by the detector FPA of thermal camera | [W·m$^{-2}$] |
| $Q_{R_{lw_{ref}}}$ | Radiation, longwave flux first emitted by background and then reflected by the target object | [W·m$^{-2}$] |
| $Q_{R_{lw_{obj}}}$ | Radiation, longwave flux from target object surface | [W·m$^{-2}$] |
| $Q_{R_{lw_{Gr}}}$ | Radiation, longwave flux from the ground | [W·m$^{-2}$] |
| $Q_{R_{lw_{Sky}}}$ | Radiation, longwave flux from the sky | [W·m$^{-2}$] |
| $Q_{R_{lw,Ex}}$ | Radiation, longwave net exchange between foliage-to-host/substrate | [W·m$^{-2}$] |
| $Q_{R_{sw}}$ | Radiation, shortwave (direct and diffused) | [W·m$^{-2}$] |
| $I_{max}$ | Irradiation, shortwave maximum incident on leaves | [W·m$^{-2}$] |
| $I_{tot}$ | Irradiation, total shortwave radiation incident on vertical greening surface | [W·m$^{-2}$] |
| $\rho$ | Reflectivity / albedo | |
| $\omega_g/\omega_g^{sat}$ | Saturation ratio of substrate | |
| $\Delta$ | Slope of the saturation vapour pressure function | [kPa·K$^{-1}$] |
| $\eta_{wilt}$ | Soil moisture, level below which plant wilts permanently | |
| $\eta_{root}$ | Soil moisture, minimum value in plant root zone | |
| $c_p$ | Specific heat capacity | [J·kg$^{-1}$·K$^{-1}$] |
| $c_{p_{air}}$ | Specific heat of air at constant pressure = 29.3 | [J·mol$^{-1}$·K$^{-1}$] |
| $Q_P$ | Storage, biochemical energy from plant photosynthesis | [W·m$^{-2}$] |
| $\Delta Q_{S_{Hw}}$ | Storage, net thermal energy storage of vegetated facade | [W·m$^{-2}$] |
| $Q_{S_{Hw}}$ | Storage, thermal energy in host-wall | [J·m$^{-2}$·K$^{-1}$] |
| $\Delta Q_{s_{veg}}$ | Storage, thermal energy in vertical greening plant layer | [W·m$^{-2}$] |
| $T$ | Temperature | [°C] |
| $\Delta T_{\mathrm{veg}}$ | Temperature difference, between $T_{leaf}$ and $T_{air}$ | [K] |
| $T_{air} \mid \boldsymbol{T}_{air}$ | Temperature, of air in Celsius \| Kelvin | [°C] \| [K] |
| $ST_{leaf}$ | Temperature, of canopy surface leaves | [°C] |
| $\kappa$ | Thermal conductivity | [W·m$^{-1}$·K$^{-1}$] |
| $\dot{D}$ | Thermal diffusivity | [m$^2$·s$^{-1}$] |
| $I$ | Thermal inertia | [J·m$^{-2}$·K$^{-1}$·s$^{-0.5}$] |
| $t_i$ | Time, intervals $t_i$, $i = 1, ..., n$. | [s] |
| $\tau$ | Transmissivity | |
| $e_s(T)$ | Vapour pressure of air at saturation | [kPa] |
| $e_a$ | Vapour pressure of air, partial | [kPa] |
| $V$ | Velocity | [m·s$^{-1}$] |
| $V_{air_{Cz}}$ | Velocity, of air immediately above canopy | [m·s$^{-1}$] |
| $V_{air_C}$ | Velocity, of air within canopy | [m·s$^{-1}$] |
| $F$ | View-factor | |
| $W$ | Width | [m] |

| **Subscript** | **Description** |
|---|---|
| *air* | Air |
| *atm* | Atmosphere |
| *can* | Canyon |
| *dew* | Dewpoint |
| *Gr* | Ground |
| *Hw* | Installation host-wall |
| *leaf* | leaf |
| *lw* | Longwave radiation |
| *ref* | Reflected |
| *sw* | Shortwave radiation |
| *Sky* | Sky |
| *sub* | Substrate |
| *obj* | Target object |
| *surf* | Target surface ($surf_1$: vegetated front; $surf_2$: non-vegetated back surface of the wall) |
| *tot* | Total |
| *veg* | Vegetation community / canopy |

# Key definitions

**$\Delta T_{UHI}$:** Intensity of the urban heat island effect, defined as the maximum difference in surface proximate $T_{air}$ between the urban city centre ($T_{urb}$) and the rural area ($T_{rur}$); $\Delta T_{UHI} = T_{urb} - T_{rur}$ [2].

**Analysis pathway:** Refers to the course of action to be taken to achieve the specified result [3], (e.g., assessment of vertical greening influence).

**Canopy:** The sheltering cover formed by the leafy upper branches and crowns of plants [4]. The thesis uses the term to refer to leafy branches of any plant community, including vertical plant cover.

**Comfort:** Described as a state of physical ease and freedom from pain or constraint [3].

**Compaction:** Also referred to as 'the compact city', is an urban development model that promotes concentrated and efficient land-use with the aid of integrated and well-served public transport. Higher density is assumed here to reduce fuel consumption, thereby leading to lower economic and environmental costs [5].

**Dispersed:** Urban development model with low-density; supported by free-market trends [5].

**Ecosystem services:** Processes or materials that are naturally provided by ecosystems, such as clean water, energy, climate regulation, phytoremediation, and nutrient cycling [4].

**Flourishing:** The state of living organisms that grow and develop in a healthy and vigorous way, particularly as the result of a hospitable environment [3].

**Health:** The World Health Organisation (WHO) definition describes it as 'a state of complete physical, mental, and social wellbeing and not merely the absence of disease or infirmity' [4].

**Heat:** Described as a form of energy that is transferred from one body to another following a temperature gradient by the processes of conduction, convection, and radiation [6].

**Heatwave:** The World Meteorological Organization (WMO) definition describes it as 'when the daily maximum temperature of more than five consecutive days exceeds the average maximum temperature by 5°C, the normal period being 1961-1990' (www.metoffice.gov.uk).

**Mean radiant temperature (MRT):** Mean temperature of all the surfaces that surround an object [6].

**Morphology:** The study of the structure and form of organisms or objects [4]. E.g., organisms such as plants and their constituent parts such as the canopy, or inanimate objects such as urban settlements.

**Risk:** Described as a measure of the probability that something of value such as life, health, property, or the environment, experiencing harm or damage from a particular hazard [4].

**Sensation:** The result of messages from the organism's sensory receptors registering in the brain as information about the immediate environment [7].

**Sheltered environment:** Microscale conditions that are not well-coupled with the mesoscale (i.e., background) climate. Such conditions could be considered as either 'semi-indoor' or 'semi-outdoor' environments.

**Thermal alliesthesia:** 'The hedonic qualities of the thermal environment are determined as much by the general thermal state of the subject as by the environment itself' [8].

**Temperate climate:** Mid-latitude climate with mild temperatures and moderate levels of rainfall, both varying from season-to-season [4]; (includes Köppen Cfb: 'Oceanic climate', e.g., London and Paris).

**Thermal comfort:** 'The condition of mind that expresses satisfaction with the thermal environment' [6,9].

**Vertical greening:** Is described as the intentional effort to cover vertical built surfaces to a significant degree with plant life [10].

**Wellbeing:** The Oxford Dictionary defines it as a state of mental and physical health, as well as social wellness, satisfaction with their lives, and experiencing a good quality of life [11].

**Thesis notes:**

- All images and illustrations have been captured or illustrated by the author, except where otherwise stated and referenced.
- All city climates presented either within parenthesis at first introduction or otherwise, are in accordance with the Köppen-Geiger Climate Classification System.
- Plant varieties are referred to by their binomial name throughout, with the common name(s) presented within parenthesis at first introduction.
- The term 'summer' broadly refers to the cooling season (May-to-September), and 'winter' refers to the heating season (the residual).
- The 'experts' or 'consultants' consulted as part of the methodologies of Chapter 3 and 8, included individuals with a wide range of qualifications and designations. They represented agricultural engineers, horticultural experts, ecologists, and individuals that identified themselves as 'living wall consultants' with suitable qualification in the management of plant integrated systems.
- In all boxplots from henceforth, the symbol '×' represents the mean value for the dataset.

# Chapter 1

## INTRODUCTION

Environmental thermal loading on urban buildings is expected to increase resulting from the combined influence of a warming climate, increasing frequency and severity of extreme heat events, and the heat island effect. As means to mitigate the heat-related risks presented, green infrastructure enhancements have been widely supported by an expanding body of research findings, which in turn has informed numerous planning policies encouraging greater implementation. The challenge of realising enhancements in densely built cities however has necessitated the consideration of alternative approaches such as surface greening. Early efforts promoted horizontal greening (commonly referred to as 'green-roofing'), although in recent years 'vertical greening' (VG) has gained increased prominence in efforts to exploit the underutilised and abundant vertical surfaces of urban buildings.

This thesis examines the hypothesis that *'vertical greening enhances heat-related climate resilience in temperate climate urban built environments'*. A range of quantitative and qualitative methods have been engaged to answer five secondary research questions, concerned with the characterisation of microclimate modification influence presented by vertical greening installations in sheltered (indoor and semi-outdoor) and outdoor environments, and resulting implications for ensuring the sustainable enhancement of occupancy conditions (i.e., hygrothermal and wind flow impact on comfort and wellbeing) and operation (i.e., space-conditioning energy use) of such future urban built environments.

## 1.1 Research framework

### 1.1.1 Problem definition

#### Problem: climate warming

There is sound scientific evidence to support a warming trend in the global climate, and significant contribution made by anthropogenic emissions towards its continued occurrence [12,13]. The recently published Sixth Assessment Report by the Intergovernmental Panel on Climate Change (IPCC) warns that the mean global temperature increase above preindustrial levels will exceed the 2 K threshold by mid-twenty-first-century, unless drastic reductions in greenhouse gas emissions are urgently actioned [14]. The reality of this warming trend has been evident in the United Kingdom for some time, with mean temperature over the most recent decade (2009-18) on average 0.3 K warmer than the previous (1981-2010), while the ten warmest years in the series dating from 1884 having occurred since 2002 [15]. The warming climate is also projected to increase the frequency and severity of extreme heat events in the summer [14]. This too has been experienced in recent times, with the notable example of the 2019 late-July heatwave resulting in the highest UK summer temperature of 38.7°C recorded at the Cambridge University Botanic Garden [15]. The wider climate thermal burden is further complicated in urban areas, as the long-established heat island phenomenon adds to this environmental thermal excess. The compounding influence in turn presents potential for causing adverse effects to the health, comfort, and wellbeing of urban populations, where growth and density has long been identified to be on an upward trend [16]. Climate warming and its threat to urban populations is therefore very much an urgent problem requiring multidisciplinary mitigation and adaptation solutions [12,13], with the intention of this thesis to make contribution to this demand.

#### Impact concern: health, comfort, and wellbeing

The most critical impact of climate warming is how it adversely affects the health, comfort, and wellbeing of urban inhabitants [17]. Although lower winter temperatures remain the dominant climate risk to health in the UK (35,000-50,000 excess deaths, with climate warming contributing to a decreasing trend), warmer summer temperatures have received increased attention in light of recent studies establishing strong correlation with increasing morbidity and mortality [12,18,19]. This risk has been acknowledged by public health and epidemiological research as early as the 70s, with significant increase in attention and call for action since the turn of the century [18]. This is particularly pronounced in the European context, where the adverse consequences of the 2003 pan-European heatwave compelled the need for better understanding the association between excess heat and health [19,20]. Recent studies have as a result found exposure to excess heat as a significant public health issue with around 2,000 premature annual deaths in the UK, and predicted climate warming likely to contribute to annual increased mortality of around 7,000 by the 2050s [21]. Such health experts have warned that although physiological, behavioural, cultural, and generational adaptation is expected, the rate at which climate warming is projected to increase the magnitude and variability of future temperatures as unprecedented [21]. Adapting to a warming climate is therefore likely to require the implementation of a range of measures that moderates human interactions with the wider climate.

The epidemiological evidence base has also long acknowledged the greater sensitivity of heat-related morbidity and mortality in urban areas relative to the countryside [22,23]. This is principally attributed to the heat island effect [19,24], although its dynamic nature has made it difficult to quantify specific spatial and temporal significance to resulting health consequences. Observations however suggest that its influence varies geographically and seasonally, with night-time temperatures being a greater threat than higher maximum daytime temperatures [22,25], (i.e., corresponds to the nocturnal heat island peak [26]).

Given the above acknowledged worsening heat-related risk to health in cities, adverse influences on comfort and wellbeing aspects of inhabitants is unsurprising [27]. The favourable news is that even modest reductions in excess heat could be beneficial to safeguarding health, as well as serving to enhance comfort and wellbeing. A recent study for example estimated that a mean air temperature reduction as modest as 0.8 K could contribute to a significant reduction in heat-related health risks [28].

### Impact concern: energy use

How cities respond to the risk to health, comfort, and wellbeing from a warming climate has significant bearing on their energy expenditure. If passive heat mitigation measures are not utilised in inhabited environments such as buildings, the alternative of using active mechanical systems will inevitably increase energy consumption and carbon emissions [29,30]. In American cities for example, higher climate temperatures had been shown to result in net annual increases in energy use, where mechanical air-conditioning has been long considered as the principal strategy for addressing heat-related risks [31]. Although in the European context the use of mechanical cooling is currently less extensive than in the United States, ever-increasing heat vulnerability is expected to increase usage [32]. The likelihood of this happening in the United Kingdom has already been exemplified by summertime cooling demand increases in commercial buildings [33].

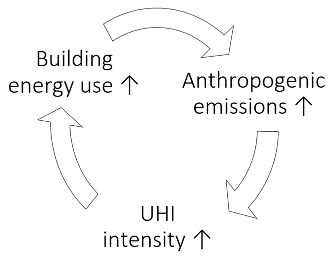


*Fig. 1. Urban energy use positive feedback loop.*

This is further complicated by the nature of the existing building stock in the United Kingdom. Historical emphasis on adapting the built-environment to cold climate loads has led to considerable progress in achieving an energy efficient space-heating dominated building stock [34,35]. This progress however is not evident when considering warmer summertime climate loads as until recently excess heat had not been a leading concern [36]. This lack of adaptation means that indoor environments of many buildings are already overheating in the summer to present risk to occupant health, comfort, and wellbeing [37]. Thus, if passive adaptations are not developed and implemented as a matter of urgency in such buildings, ever-increasing overheating risk could compel widespread adoption of mechanical cooling as a short-term solution, with adverse long-term consequences.

The long-term consequence of increased mechanical cooling is posed by their heat rejection from occupied spaces in buildings back to the climate; which is already a substantial source of anthropogenic emissions in warmer climate cities [31,32,38]. The rejected heat from buildings then serves to worsen outdoor canopy layer comfort, while further exacerbating the thermal loading back on buildings. This inevitable positive feedback loop is likely to lead to the urban climate becoming an unpleasant setting, where migrating from one mechanically cooled space to another becomes the objective of inhabitants seeking to maintain health, comfort, and wellbeing (Fig. 1). Avoiding or reducing air-conditioning use is therefore a primary objective in reducing the energy demand positive feedback loop and enhancing sustainable adaptation, particularly in urban areas where buildings with high-occupancy are increasing as a dominant land-use [29].

### Mitigation strategy: urban greening

There is wide consensus on the response to heat-related risk mitigation prioritising passive approaches where possible, with active (energy consuming) assistance only used where necessary to enhance efficacy [29]. Amongst the range of passive approaches being developed to address this includes greenspace or green infrastructure enhancements, where ecosystem services provided by plants are integrated into built environments to dampen adverse impacts and increase resilience to climate warming [28,39–41]. Many different typologies as a result have been promoted by policymakers and urban planners in recent times, although their specific efficacies have yet to be clarified.

### 1.1.2 Research gaps

As means to identify a focus within the extensive topic of green infrastructure, a two-stage review was conducted at the commencement phase of the project (Fig. 4, p. 23).

*Stage-one:*

This scoping review (discussed in Chapter 2), considered all green infrastructure typologies and their relative contribution to heat-related risk mitigation in urban settings. It sought to examine multidisciplinary literature to answer the following question:

> *A. To what degree of significance do different green infrastructure typologies contribute to heat-related risk mitigation in urban environments?*

Reviewing the various strategies highlighted that to implement enhancements in densely compacted cities, the development of surface greening approaches to be essential. The review identified recent attention to be directed at utilising the typology of vertical greening (Fig. 2, p. 21), although many aspects of such approaches need further investigation and supporting evidence to justify widespread implementation. The outcomes of this stage-one review thus led to the identifying of the focus green infrastructure consideration of this thesis, with material available to date reviewed in stage-two to identify research gaps.

*Stage-two:*

This focused review (discussed in Chapter 3), targeted literature addressing vertical greening strategies to identify evidence shortfalls in the following areas:

- Observational data from temperate climate in-situ installations (i.e., hygrothermal and wind flow modifications);
- Thermal characterisation of installation canopies;
- Installation influence approximation methods (i.e., simulation pathways), at building and urban neighbourhood scales;
- Sustainability of systems in service, including water and nutrient use data, and use of automation (if any); as well as the consideration of adverse plant-related modifications such as toxicity.

The review also identified most of the available evidence base to be focused on outdoor installations, and thus sought to answer the following question:

> *B. Would the already identified outdoor installation ecosystem benefits and risks be similar for applications in indoor environments?*

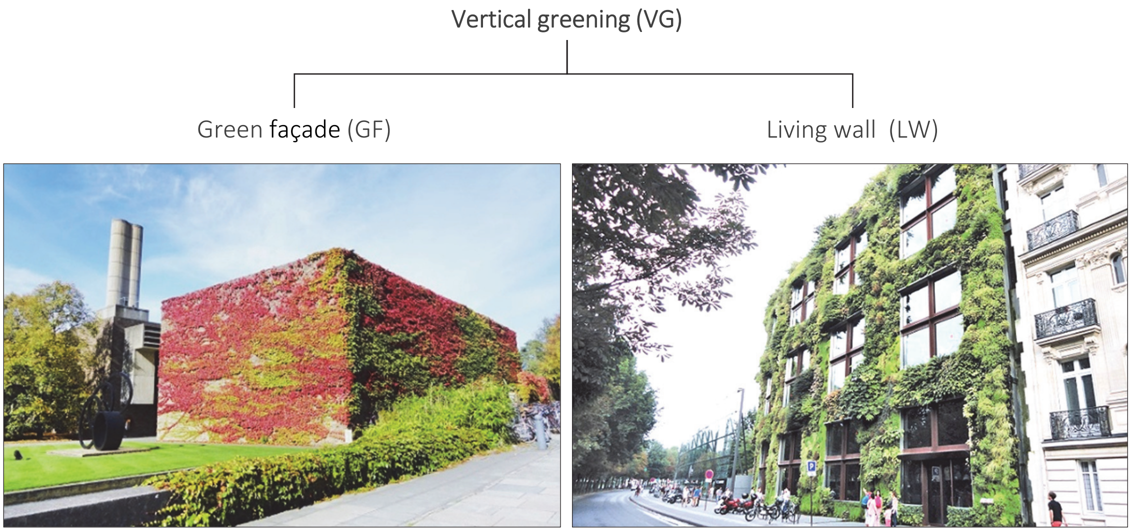


Green façade at Churchill College, Cambridge — Living wall at Quai Branly Museum in Paris, France

*Fig. 2. Principal vertical greening categories and implemented examples.*

### 1.1.3 Aims

a) The overarching aim of the project was to address the call for developing passive climate resilience strategies. In response to a two-stage review, this was focused to consider the influence and effectiveness of vertical greening as a strategy for managing thermal loads of urban buildings and surrounding microclimates. By examining this focus the project aims to improve the design of urban built environments that would in turn lead to health and wellbeing enhancements of their growing populations.

b) The engagement aim of the project was to define the current state of influence and effectiveness of such installations by monitoring real-world applications. The gathered data from such exercises was envisaged to inform the development of the outcomes and enhance the impact of the project.

c) As the principal outcome, the project aim was to deliver analysis pathways that would enable built environment practitioners such as engineers and architects to determine and best integrate the benefits of vertical greening. It is envisaged that this will enable such considerations to be front-loaded to design pathways to offer technically sound reasoning for engaging with vertical greening strategies.

d) Finally, the academic aim of the project was to present findings and developed analysis pathways that has withstood robust peer-reviewed critique. This would in turn contribute to a sound evidence base with far-reaching impact.

### 1.1.4 Objectives

a) Addressing climate resilience requires systematic thinking that brings together multidisciplinary bodies of knowledge. For this project, this included the broader consideration of public health, climate change, urban climatology, city-planning, building physics, and plant science studies; as well as the focussed consideration of the developing body of research concerning vertical greening strategies. The project therefore required the assessment of material from all such knowledge bodies as part of the abovementioned two-stage review to identify interdisciplinary value and research gaps.

e) Following the reviews and gap identification, the project addressed the necessity to define the current state of application influence by engaging with real-world in-situ installations to gather and contribute empirical data. A case-study approach with monitoring exercises was favoured, with installations selected to offer new data from conditions underrepresented by previous research.

b) Addressing the development of analysis pathway outcomes required the consideration of a combined approach of utilising case study monitoring data to inform the simulation of application environments. This demanded the development of two pathways based on the scale and exposure of the application environments considered (Fig. 3, p. 23).

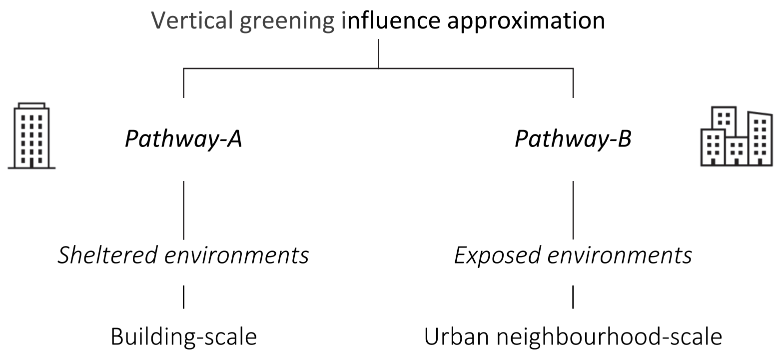


*Fig. 3. Vertical greening assessment pathways proposed.*

c) Finally, addressing the validation of findings required seeking publication in peer-reviewed journals, as well as presenting at relevant international conferences. The thesis presented here is thus a hybrid, which combines such published peer-reviewed material to date with the overarching research narrative.

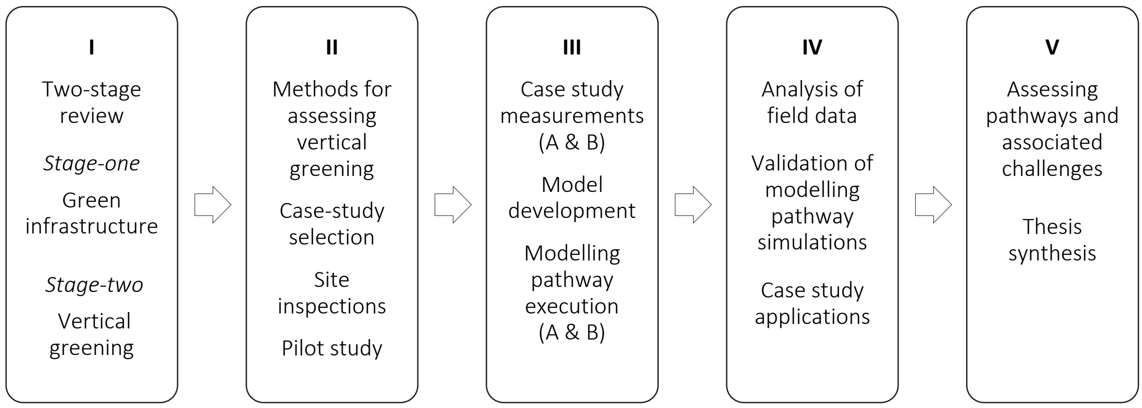


*Fig. 4. Project schematic; structured and implemented as five phases.*

### 1.1.5 Research hypothesis and questions

The principal hypothesis of the project as stated earlier:

> *"Vertical greening enhances heat-related climate resilience in temperate climate urban built environments"*

The principal research question derived from this hypothesis:

> *To what extent does architectural vertical greening enhance heat-related climate resilience in urban built environments, and is there value in advocating for wider application in temperate climates?*

Answering the above principal question was addressed by considering five secondary constituent questions, derived from the earlier identified research gaps from the stage-two review. The first and second of these questions seek to establish the empirical evidence for microclimate influence in underreported in-situ environments. Considering their answers, the third and fourth questions seek the development of influence approximation pathways, for building (Pathway-A) and urban neighbourhood-scale (Pathway-B) applications. Finally, the fifth question seeks to address the challenges of widespread application and its sustainability. These five questions are expressed here as follows:

*Q I.* *To what extent does the presence of a vertical greening installation modify the microclimate of a sheltered environment?*

*Q II.* *How does the plant canopy morphology of a vertical greening installation influence its surface temperature?*

*Q III.* *How can vertical greening influence be approximated for building-scale assessments in a computationally efficient manner?*

*Q IV.* *To what extent would neighbourhood-scale application contribute to enhancing urban climate resilience?*

*Q V.* *What are the key challenges in sustaining the positive contributions of vertical greening installations in temperate climates?*

### 1.1.6 Thesis structure

This thesis consists of three parts (Fig. 5, p. 25): **Part I** representing the two-stage review identifying research gaps; **Part II** representing the five studies that investigate the above constituent research questions; and **Part III** representing the synthesis that answers the aforementioned principal research question.

**PART I:** LITERATURE

**Ch 2.0** URBAN GREEN INFRASTRUCTURE

The chapter represents the first of the two-stage review described above, and examines theoretical material addressing the complexities of urban climates and recent developments in utilising greening approaches to mitigate heat-related risks (the focal climate risk). The content represents an abridged version of the paper by Gunawardena *et al.* [41].

### Ch 3.0 VERTICAL GREENING

The chapter represents the second of the two-stage review, and examines the state-of-the-art of vertical greening strategies. The content represents an abridged version of the published paper by Gunawardena & Steemers [10].

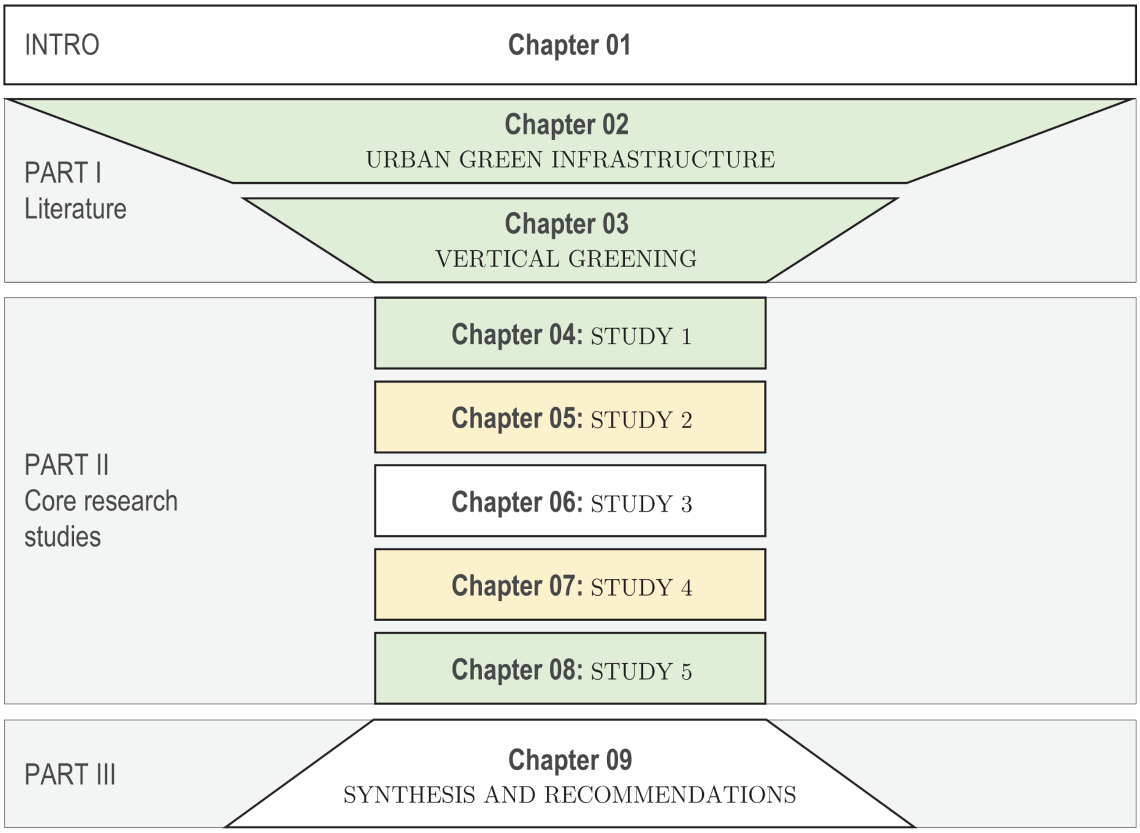


Note: Colour highlight [green] represents published papers; and [yellow] represents partially published material.

*Fig. 5. Thesis structure.*

## **PART II:** CORE RESEARCH STUDIES

### Ch 4.0 STUDY 1: INFLUENCE IN SHELTERED ENVIRONMENTS

The chapter investigates the first-of-five secondary research questions: Q I. It presents living wall monitoring results from two case studies representing indoor and semi-outdoor sheltered environments. The content represents an expanded version of the conference proceedings papers [42,43] and the journal paper [44].

### Ch 5.0 STUDY 2: INFLUENCE OF CANOPY FEATURES

The chapter investigates the second-of-five secondary research questions: Q II. It presents surface temperature monitoring results from living wall canopies, with three urban case studies assessed using thermography (material partly published in [43]).

**Ch 6.0** STUDY 3: BUILDING SIMULATION PATHWAY-A

The chapter investigates the third-of-five secondary research questions: Q III. It presents the development and validation of a novel vertical greening model (VGM) and its integration to simulation Pathway-A, which approximates building-scale installation influence.

**Ch 7.0** STUDY 4: NEIGHBOURHOOD SIMULATION PATHWAY-B

The chapter investigates the fourth-of-five secondary research questions: Q IV. It presents simulation Pathway-B, and simulates urban neighbourhood-scale scenarios to assess potential for wide-scale vertical greening application (material partly published in [45]).

**Ch 8.0** STUDY 5: SITE INSPECTIONS

The chapter investigates the fifth-of-five secondary research questions: Q V. It reports on areas of concern and sustainability aspects highlighted by installation managers associated with ten case study installations inspected. The content represents an abridged version of the paper by Gunawardena & Steemers [46].

**PART III:** SYNTHESIS

**Ch 9.0** SYNTHESIS AND RECOMMENDATIONS

This chapter reconciles the answers from the five core studies to present the synthesised answer to the principal research question. It also highlights the contributions made to the subject, presents recommendations for installation designers, and stresses further developments necessary to achieve added application value.

## 1.2 Methods synopsis

Methodological details of the two-stage review in Part I is described in Chapters 2 and 3, while the secondary constituent research questions in Part II have been investigated as five independent yet associated studies, with each utilising methods specific to answering the said question (Fig. 6, p. 27). Detail descriptions are given in each of the respective study Chapters (4-to-8); while in summary they included case study-based quantitative measurements (Chapters 4 and 5), and computational simulations (Chapters 6 and 7), as well as qualitative interview and observational approaches conducted over an extensive fieldwork campaign in several European countries (Chapter 8).

| PART I | | PART II | | | | |
|---|---|---|---|---|---|---|
| Chapter 2 | Chapter 3 | Chapter 4<br>STUDY 1 | Chapter 5<br>STUDY 2 | Chapter 6<br>STUDY 3 | Chapter 7<br>STUDY 4 | Chapter 8<br>STUDY 5 |
| Standard litereature reviews | | Monitoring of Installation case studies | | Developing simulation pathways for distinct environments | | Site inspections |
| Scoping green infrastrucre | Focused vertical greening | Microclimate parameters | Canopy parameters | Pathway-A Building-scale pathway | Pathway-B Neighbourhood-scale pathway | Maintenance and sustainability |
| Database searchers and interviews | | In-situ deployment of probes and loggers | Qualitative and quantitative thermography application | Building energy model integration of VGM | Urban climate framework integration of VGM | Inspections, direct observations, and interviews |
| Scopus & *iDiscover* results and European installations | | Indoor and semi-outdoor installations | Indoor and outdoor installations | Current climate Indoor and semi-outdoor installations | Current climate Outdoor London canyon installations | European installations |

*Fig. 6. Methods synopsis.*

## 1.3 Scope limitations

Besides achieving the earlier mentioned aims and objectives, the research project was motivated by the desire to present material evidence that would assist urban planners, landscape designers, and architects in improving the design of the urban built environment through green infrastructural enhancements. The synthesis chapter of the thesis addresses this by presenting recommendations based on the findings of the implemented studies, while further areas of investigation required to enhance application are also highlighted.

The necessity to expand as well as contract scope in certain areas while investigating the research questions was expected. Given that it was not always possible to pursue follow-up experiments or seek validation of certain results by means of more detailed modelling and simulations meant that the studies generated several subsidiary hypotheses, which are also presented in the synthesis chapter as suggestions for future research.

# PART I

# Chapter 2

URBAN GREEN INFRASTRUCTURE

## 2.1 Introduction

The hypothesis of green infrastructure or greenspace enhancements contributing to the mitigation of urban climate risks including increasing temperatures, has been extensively examined by both plant and climate scientists. This chapter reviews this diverse evidence base to answer the following research question:

A. *To what degree of significance do different green infrastructure typologies contribute to heat-related risk mitigation in urban environments?*

The chapter represents the first of the two-stage review in Part I, with material representing an abridged version of the published review in Gunawardena *et al.* [41].

### 2.1.1 Urban energy balance and its partitioning

To understand the interactions between vegetation and the urban climate, the uniqueness of the latter must be first clarified. Luke Howard was the first climatologist to hypothesise that the climate of cities and their interactions with the surrounding areas to be determined by the nature of their surface energy exchanges [47]. Sundborg [48] later explained these interactions and in particular the heat island (UHI) phenomenon in terms of the 'urban energy balance', which accounts for the incoming and outgoing energy flux from an urban surface system (Equation 1). The energy absorbed by this urban surface system from solar irradiation and anthropogenic activity, is balanced by warming the air above the surface (convection and radiation), evaporation of moisture, and heat storage in surface materials. The partitioning of this balance defines the nature of the urban climate experienced, which in turn affects the comfort and wellbeing of its citizens, as well as how energy is used [49].

$$\begin{matrix}\mathit{Net} \\ \mathit{radiation}\end{matrix} + \begin{matrix}\mathit{Anthropogenic} \\ \mathit{emissions}\end{matrix} = \begin{matrix}\mathit{Sensible} \\ \mathit{Convection}\end{matrix} + \begin{matrix}\mathit{Latent} \\ \mathit{Convection} \\ (\mathit{Evaporation})\end{matrix} + \begin{matrix}\mathit{Heat} \\ \mathit{storage}\end{matrix} \qquad \text{Equation 1}$$

The increased surface roughness of cities generates different structures or 'layers' in the urban atmosphere (Fig. 7). The planetary boundary-layer (PBL), which is a part of the atmosphere that is influenced by its contact with the planetary surface, is partitioned above urban areas into the urban boundary-layer (UBL) and urban canopy layer (UCL). The UBL is a mesoscale concept referring to the part of the atmosphere that is part of the PBL and overlying the UCL, with its qualities influenced by the presence of an urban area at its lower boundary. The UCL in contrast is a microscale concept that describes the part of the atmosphere between the surface and the tops of buildings and trees, where the local climate is influenced by the materials and geometry of the urban environment (urban roughness), and where people typically inhabit. The UCL therefore represents the part of the atmosphere that is critical for human health, comfort, and wellbeing in cities [50].

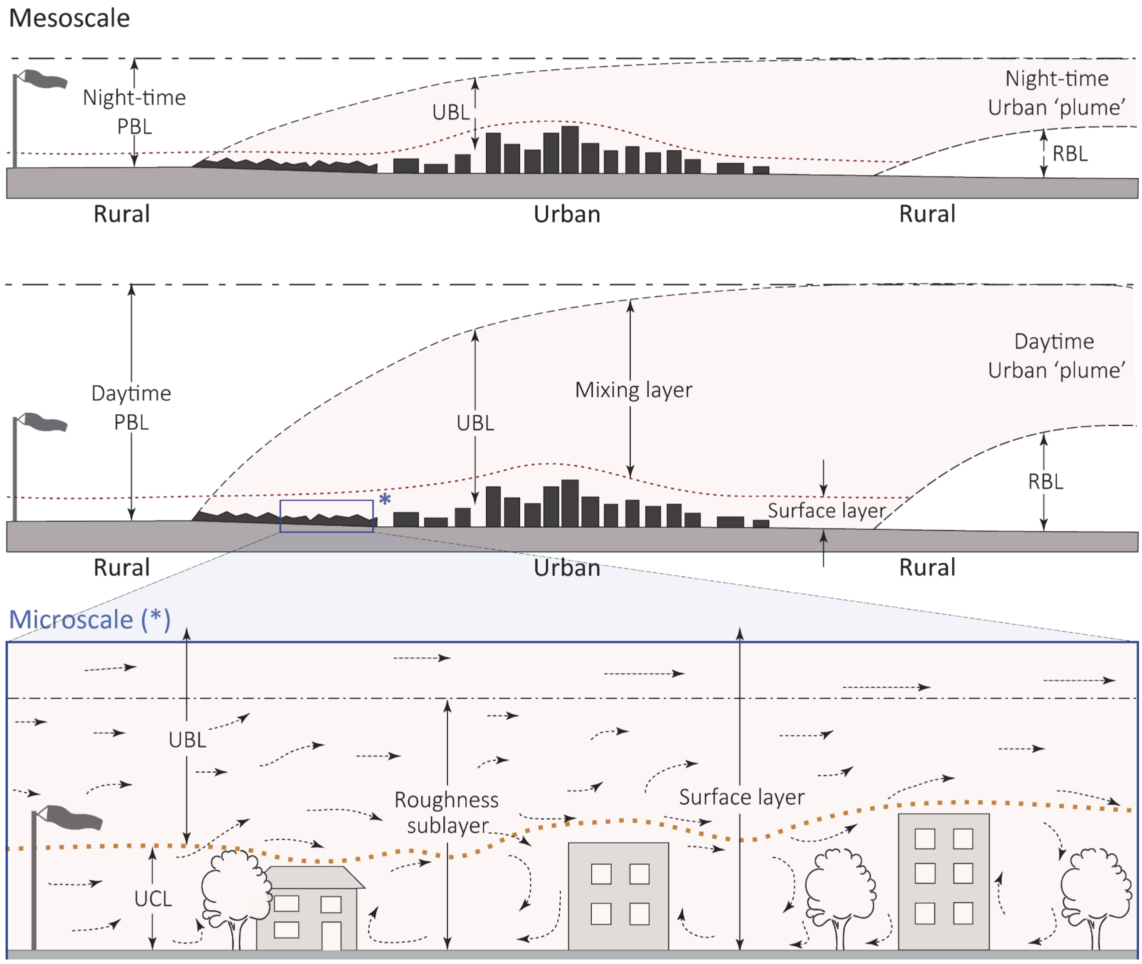


*Fig. 7. Atmospheric boundary-layer structures over a city resulting from increased surface roughness; based on Oke* [2], *published in* [41].

The formation of a heat island is dependent on several climatic processes and described in terms of the phenomena occurring either in the UBL or the UCL. The UBL occurrence is governed by processes relevant at the mesoscale with the higher altitude thermal inversion dominant during the daytime, while the latter UCL occurrence is governed by those at the microscale with the lower altitude inversion dominant during the night-time [50]. Anticyclonic conditions (high atmospheric pressure), with reduced wind velocities and cloud cover provide the ideal circumstances for formation [2,51]. Intensity is observed to be highest during the summer when greater solar radiation incidence increases the energy available within the urban system, while at night-time accumulated heat release from the urban fabric becomes the dominant heat source.

Anthropogenic activity and urban features within the UCL are the main influence on the net positive thermal balance that gives rise to the urban heat island effect [2]. Human activity results in anthropogenic emissions that increases the thermal energy within the urban climate system, while weather and geographical features serve to vary the intensity and distribution of such emissions. The main anthropogenic urban features that modify the surface energy flux relate to the morphology and materiality of the built environment, along with the availability of blue and greenspace features; the latter greenspace features being the focal interest of this chapter (e.g., Fig. 8).

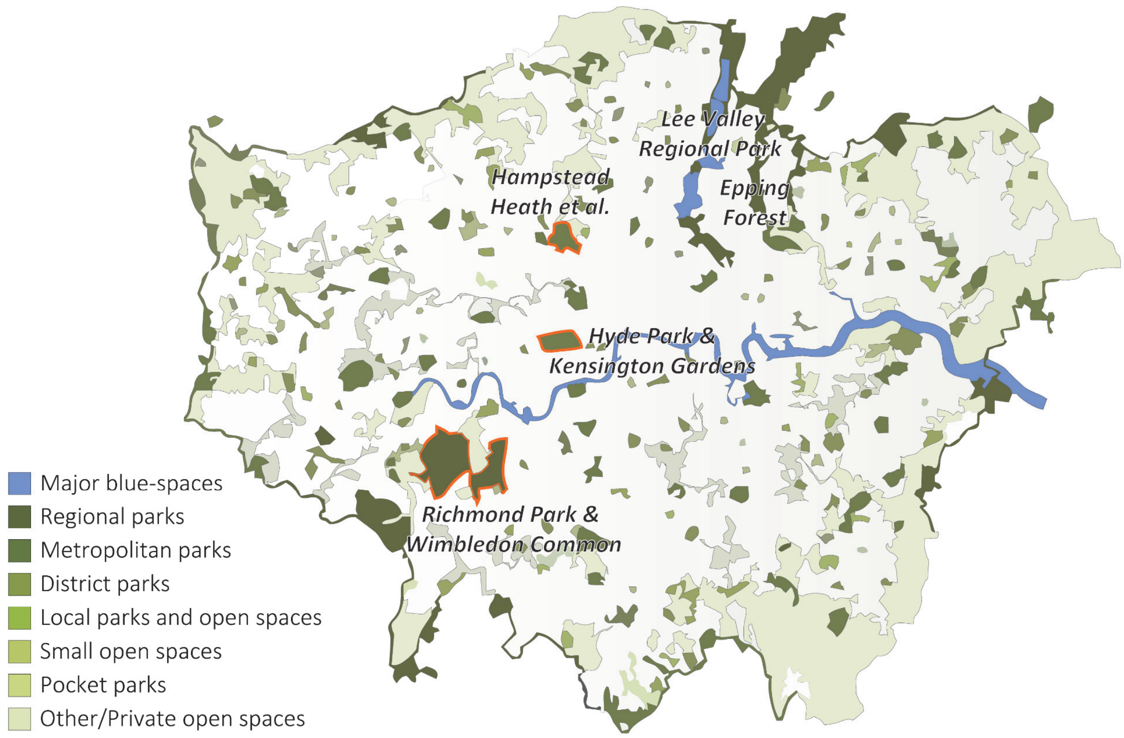


*Fig. 8. Distribution of greenspace features across London.*

## 2.2 Methodology

This standard review considered volumes from climate and plant sciences to address fundamental theory (e.g., [2,52–57]); while peer-reviewed journal articles and reviews, and volume chapters obtained through a database search were used to address the state-of-the-art. The volumes considered were found through Cambridge University Library *iDiscover* searches, while the Scopus database was searched for the keywords ‘green infrastructure’, ‘greenspace’, and ‘urban greening’ (including variant notations), to obtain peer-reviewed material. This Scopus search was revised in 2020 to return 471 results, all dating from 2005 onward to demonstrate a lack of preceding publications (Fig. 9, p. 33). These were then filtered to include those with a primary greenspace focus (criterion 1: #265), and further refined to consider in detail publications that addressed their thermal climate modifications, be it experimental, case study, or simulation-based (criterion 2: #32, Table 1, p. 34). Seven review publications were also referred to discuss identified trends (Table 2, p. 36).

## 2.3 Findings

The review of journal publications highlighted significant interest in greenspace aspects increasing from 2009, with rapid growth from 2013 onward (Fig. 9b). This body of 265 studies is represented in Fig. 10 according to data collection and processing plan; methods used; greening typology; subject area, and climate zones. The breakdown highlighted cross-sectional data collection and processing plans to dominate (46%), along with the use of observational methods (55%). With observational studies, the established practices of remote-sensing had encouraged significant representation (42%), followed by simulation approaches (28%), mainly using computational fluid dynamics (CFD) despite their substantial resource demand (23%). Subject area focus presented clear majority to the thermal influence perspective (74%), while unspecified generic greening dominated greening type in assessments (54%), followed by horizontal greening (15%). Climate representation was dominated by studies in temperate climates (Cfb), followed by humid subtropical (Cfa) and monsoon-influenced hot-summer humid continental (Dwa) zones. This is influenced by the geographical spread of research interest, with East Asia dominant (32%, of which China represented 21%), followed by Europe (24%, UK: 5%), and North America (13%, United States: 10%). Studies from South Asia and Africa were notably sparse (<1%).

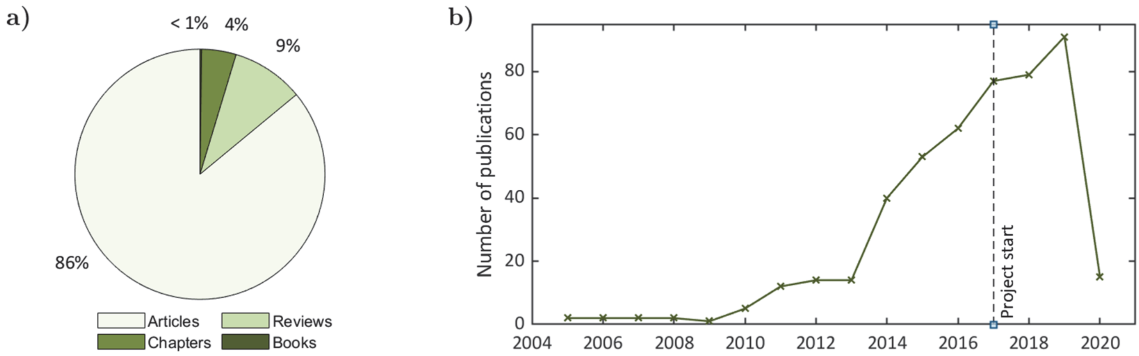


*Fig. 9. Scopus database results by publication type (a), and publications per year (b).*

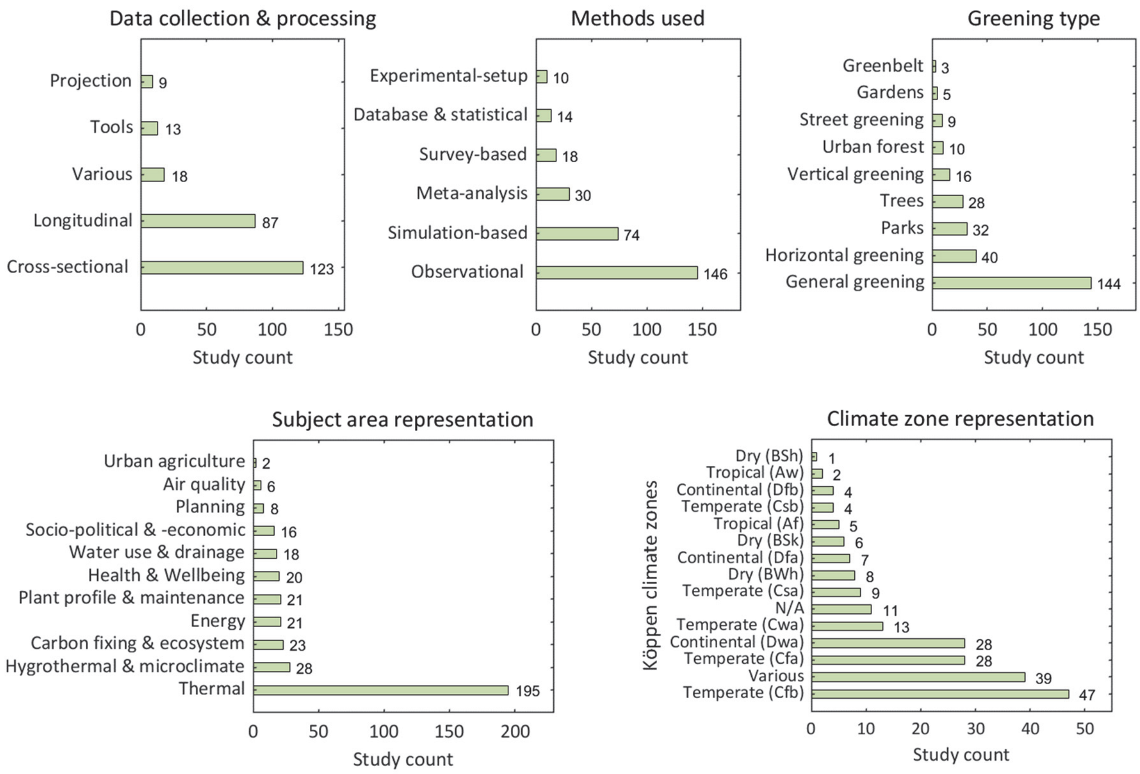


*Fig. 10. Breakdown of 265 studies reviewed (includes multiple counts).*

The update to the review in 2020 highlighted studies with a thermal focus to have remained relatively stable since 2018 (from 74→73%), while a slight increase in those with an energy perspective was noted (8→9%). The data collection and processing profile also remained unchanged, while both observational (55→58%) and simulation (28→31%) methodologies presented increased representation. Greening typology considerations remained mostly stable save for an increase in vertical greening (6→7%), contrasted against a reduction in tree-based assessments (11→9%). Highest climate zone representation was retained by Cfb despite a decrease in studies (18→14%), while Cfa representation had increased (11→12%) attributed to growth in studies from East Asian sources.

Table 1. Summary of urban greening studies reviewed.

| Greening type | Study | Location (Köppen) | Study type | Method (detail) | Key Findings |
|---|---|---|---|---|---|
| **General greening*** | [58] | China, Nanjing (Cfa) | Cross-sectional | Observational (land surface temperature \| $T_{surf}$, monitored with remote-sensing) | Large and regular features have greater cooling distribution. Area increase enhances intensity when feature is <0.1 km$^2$.<br>Reducing shape complexity can enhance cooling intensity when area >0.05 km$^2$. |
| **General greening** | [59] | China, Suzhou (Cfa) | Cross-sectional | Observational (#15 green spaces in Suzhou Industrial Park monitored in the summer) | Large features had obvious and stable cooling and humidification. Small ones had opposite effect, with heat preservation in some cases.<br>Cooling positively correlated with area, and ave. $LAI$ and canopy density; but negatively correlated with perimeter. |
| **General greening** | [60] | European cities (Various) | Longitudinal | Observational (#70 cities with >100,000 residents, using MODIS data) | Greening increases UHI during heatwaves.<br>Cities of cooler climates and with higher shares of greenspaces were more affected. |
| **General greening** | [61] | Hong Kong (Cwa) | Cross-sectional | Simulation (#33 scenarios using ENVI-met) | Green-roofing is ineffective for near-ground thermal comfort in high building-height-to-street-width ratio cities.<br>Trees are more effective than grass surfaces in cooling streets. Tree cover needed to lower pedestrian-level $T_{air}$ by ~**1 K** is ~33% of city. |
| **General greening** | [62] | N/A (N/A) | Cross-sectional | Simulation (two-dimensional numerical model application) | Influence range is a function of scale and interval between features.<br>Smaller features with ~300 m intervals better for effective cooling of surroundings. |
| **General greening** | [63] | North America cities (Various) | Cross-sectional | Simulation (new climate model verified with MODIS data) | Daytime $\Delta T_{UHI}$ mostly explained by efficiency differences in urban and rural convection.<br>This is dependent on background climate, increasing $\Delta T_{UHI}$ by 3.0 K in humid climates, but decreasing it by 1.5 K in dry climates. |
| **General greening** | [64] | UK, Glasgow Clyde Valley Region (Cfb) | Projection | Simulation (#6 scenarios using ENVI-met) | Cover increase of ~20% eliminated a third-to-half of extra UHI expected in 2050, and also led to **2 K** local reductions in $T_{surf}$.<br>Over half of pedestrians considered the 20% increase in cover to be thermally acceptable. |
| **General greening** | [65] | UK, Manchester (Cfb) | Cross-sectional | Simulation (#7 scenarios using ENVI-met for a warm summer's day) | A 5% increase in mature deciduous trees reduced mean hourly $T_{surf}$ by **1 K**.<br>Worst-case scenario of replacing vegetation with asphalt increased midday $T_{air}$ by **3.2 K**. |
| **Greenbelt** | [66,67] | Germany, Frankfurt (Cfb) | Longitudinal | Observational (5 km long and 50-100 m wide greenbelt monitored) | Greenbelt lowered $T_{air}$ by **3-3.5 K** and increased $RH$ by **5-10%**.<br>It ventilates the overheated, dirty, and polluted town centre. |
| **Horizontal greening** (Extensive green-roof) | [68] | Germany, Berlin (Cfb) | Longitudinal | Observational (annual eddy-covariance measurements) | High daytime Bowen ratios prevailed during warm, dry periods.<br>Significant nocturnal cooling potential. Max. daily evapotranspiration of 3.3 mm. |
| **Horizontal greening** (Green-roof) | [69] | UK, Reading (Cfb) | Cross-sectional | Observational (leaf temperature \| $T_{leaf}$, monitored with infrared camera in a range of contrasting genotypes within 3 plant types) | With non-succulents, lighter colour and pubescence lowered $T_{leaf}$; while with succulents, thickness and water loss rate were key regulators.<br>Greatest $T_{leaf}$ reductions associated with higher water loss. Sustainable irrigation and plants with beneficial morphological traits vital for effective cooling. |

| Greening type | Study | Location (Köppen) | Study type | Method (detail) | Key Findings |
|---|---|---|---|---|---|
| **Horizontal greening & general greening** | [70] | France, Paris (Cfb) | Longitudinal | Simulation (using the Town Energy Balance urban canopy model) | Greater the ground greening and tree cover, greater the cooling. Max. cooling during heatwave was **0.5-2 K**.<br>Green-roofs had negligible impact on street level $T_{air}$, but reduced annual energy use. |
| **Parks** | [71] | China, Beijing (Dwa) | Cross-sectional | Observational (using Landsat remote-sensing data) | Park cooling intensity (PCI) defined by cooling distance, $T_{air}$ amplitude difference, and $T_{air}$ gradient.<br>Most parks served as 'cool islands'. Size and shape had opposite effects on PCI. |
| **Parks** | [72] | China, Beijing (Dwa) | Cross-sectional | Observational (mobile traverse monitoring data from 3 summer days with clear skies and low $V_{air}$) | Park **0.6-2.8 K** cooler than surrounding city.<br>Cooling was variable, but could extend ~**1.4 km** beyond the boundary.<br>Large $T_{air}$ differences both in the park and surrounding city, and dependent strongly on land cover features of each site. |
| **Parks** | [73] | Idealised (N/A) | Cross-sectional | Simulation (CFD used to determine $T_{air}$, $RH$, and $V_{air}$ of an ideal 0.02 km$^2$ park) | Possible to normalise cooling effect with a leaf area coefficient ($LAI_{sp}$), including tree density, and size or age.<br>Park cooling up to **4.8 K** at 3.16 $LAI_{sp}$ (4,500 trees per km$^2$, at 50 years); while for a $LAI_{sp}$ of 3, optimal park length was 130 m. |
| **Parks** | [74] | Japan, Tokyo (Cfa) | Longitudinal | Observational (long-term monitoring of 0.2 km$^2$ park with 90% tree cover) | Park **1.5-3 K** cooler than town in summer daytime. Extent of influence greater downwind (**450 m**) than upwind (**65 m**).<br>Park-breeze frequent in calm conditions at night ($V_{air}$ <1.5 m·s$^{-1}$ and after 02:00 hrs). Mean cooling estimated at 39 W·m$^{-2}$. Town cooling equal to 2,600 domestic AC units. |
| **Parks** | [75] | Korea, Seoul (Dwa) | Longitudinal | Observational (street level monitoring with mobile loggers on clear summer days) | Small features reduce $T_{air}$ of an urban block.<br>Polygonal and mixed spaces >2,000 m$^3$ cooled it by **1 K**. Polygonal small features offered better cooling, especially when multi-layered. |
| **Parks** | [76] | Singapore (Af) | | Observational & Simulations (0.1 & 0.4 km$^2$ parks monitored, ENVI-met) | Significant cooling (**1.3 K** max.) on surroundings both day and night.<br>Cooling load reduction of 10% with ideal building energy simulation. |
| **Parks** | [77] | Spain, Madrid (Csa) | Cross-sectional | Observational (mobile monitoring of 1.25 km$^2$ park and questionnaire survey on hot summer days) | Cooling effect at **150 m**; could reduce $T_{air}$ by an ave. **0.63 K** and **1.28 K** for distances **380 m** and **665 m**, respectively.<br>Large-scale parks significant for creating resident perception of thermal comfort. |
| **Parks** | [78] | Sweden, Stockholm (Cfb) | Cross-sectional | Observational (mobile traverse monitoring over 3 summer days) | Built-up area and park $T_{air}$ difference was **0.5-0.8 K** at daytime, and **2 K** max. at sunset.<br>Advection to-and-from the park was strongly indicated (i.e., park-breeze). |
| **Parks** | [79] | UK, London (Cfb) | Longitudinal | Observational (Kensington Gardens monitored from Aug-to-Dec) | Statistical model showed exponential decay in cooling extent with distance. Nocturnal extent from **20-to-440 m**.<br>Mean summer cooling over these distances was 1.1 K, with 4 K max. on some nights. |
| **Parks** | [80] | UK, London (Cfb) | Projection | Simulation (London Olympic Parkland using a neighbourhood-scale model) | Large impermeable features likely to increase $T_{air}$ during the Olympic period.<br>Legacy scenario showed $T_{air}$ reductions from the pre-Olympic period to increase with vegetation coverage growth. |

| Greening type | Study | Location (Köppen) | Study type | Method (detail) | Key Findings |
|---|---|---|---|---|---|
| **Parks & lakes** | [81] | Chongqing, China (Cfa) | Longitudinal | Observational (#6 parks and #3 lakes monitored on calm days between Jul and Aug). | Cooling of parks more obvious than lakes, with **3.6 K** max. for parks and **2.9 K** lakes.<br>Daily variation of parks greater than lakes, 3.8 K max. temperature difference for parks, and for 2.4 K for waterbodies. |
| **Parks & lakes** | [82] | Shanghai, China (Cfa) | Longitudinal | Observational (lake in a park monitored on sunny days in Jul and Aug) | Area 10-20 m from water's edge showed greatest improvement in thermal comfort.<br>Appropriate landscaping in the littoral area can present a synergistic effect. |
| **Trees** | [83] | Switzerland, Basel (Cfb) | Cross-sectional | Observational (using high-resolution thermal camera data, gathered from a helicopter) | Small-leaved tree species remained relatively cooler at high ambient $T_{air}$.<br>*Gleditsia triacanthos* (Honey locust) maintained $T_{leaf}$, even during extreme $T_{air}$ and strong stomatal downregulation. |
| **Trees & general greening** | [84] | UK (Cfb) | Various | Research note (various) | Greenspaces should be a min. 0.005 km$^2$ to achieve cooling at significant distances beyond site boundaries. |
| **Urban forest** (trees) | [85] | China, Changchun (Dwa) | Cross-sectional | Observational (horizontal and vertical $T_{air}$ cooling, soil cooling, shading, and humidifying effects of 605 trees from 152 plots monitored) | Horizontal $T_{air}$ cooling and humidifying change between canopy shade and sunshine was <**4.5 K** and <**9.4%**, respectively.<br>Horizontal cooling, shading, and humidifying stronger in dry, hot, and sunny weather; and in areas with more buildings of lower height.<br>Larger trees present larger cooling area. Vertical canopy cooling was **1.4 K**, with soil cooling in most cases (1.4 K peak). |
| **Urban forest** (Trees) | [86] | Israel, Tel-Aviv (Csa) | Longitudinal | Observational (#11 wooded sites in urban complex monitored, with empirical model developed and applied) | 70% of $T_{air}$ variance explained by partial shaded area under the canopy and $T_{air}$ of non-wooded surroundings.<br>Specific cooling due to feature geometry and tree attributes, and besides shading was ~**0.5 K**, out of an ave. of ~**3 K** at noon.<br>At small sites (~0.001 km$^2$), cooling perceivable up to 100 m in nearby streets. |
| **Vertical greening** (Green façades) | [87] | China, Nanjing (Cfa) | Cross-sectional | Observation & Simulation (novel ENVI-met green façade module validated and applied) | Variations in cooling intensities with different urban forms (30 scenarios), with **0.96 K** max. for the high-rise high-density scenario.<br>Linear relationship between energy-saving rate and greening ratio. |
| **Vertical greening** | [88] | Netherlands, Delft, Rotterdam, Benthuizen (Cfb) | Longitudinal | Observational (1920s green façade, 1970s residential green façade, and a rural living wall monitored from Sep-to-Oct) | No difference in $T_{air}$ and wind profiles 1 m in front of the façades, until inside the foliage.<br>Studied systems are effective sunscreens, with $T_{surf}$ reduction behind the greening, compared to bare façades. |
| **Vertical greening** (Eight systems) | [89] | Singapore (Af) | Cross-sectional | Observational (test rigs monitored on 3 clear days in Feb, Apr, and Jun) | Max. wall $T_{surf}$ reduction of **11.6 K**.<br>Absorbs less heat than a non-greened façade and releases less in the evening and night. |
| **Vertical greening** | [90] | Singapore (Af) | Cross-sectional | Simulation (courtyard surrounded by high-rise buildings, using ENVI-met) | Thermal comfort perception near the façade modified by a category (orientation dependent).<br>Pedestrian thermal benefits provided mainly by lowest levels, (i.e., <6 m). |

Note: * 'General greening' refers to any greenspace that has not been explicitly defined by the paper reviewed as belonging to a commonly identified typology.

Table 2. Summary of referred review studies.

| Greening type | Study | Method (detail) | Key Findings |
|---|---|---|---|
| **General greening** | Saaroni *et al.* [91] | Literature review (review of #89 scientific papers up to 2015) | Similar methods used in different locations and climates, targeting micro to local-scale and limited timespans. Urban parks are the focus of research, while significant cooling of street trees broadly accepted. |
| **General greening** | Su *et al.* [92] | Meta-analysis (analysis of in-situ monitoring data from #77 global sites in 35 cities, using bootstrap sampling and hierarchical partitioning) | Background climate is critical in determining whether vegetation cools or warms $T_{air}$. Key thresholds: vegetation cooling starts when background $T_{air}$ >10°C; evaporative cooling increases when evapotranspiration >62.7 mm per month; and shade cooling increases when vegetated area >0.352 km$^2$. |
| **General greening** | Santamouris *et al.* [93] | Meta-analysis (data from #220 urban rehabilitation projects) | Mean $T_{air}$ reductions at ~**0.74 K**, and ave. peak at ~**2 K**. Almost 31% of projects resulted in a peak $T_{air}$ drop <1 K and 62% <2 K. |
| **General greening** | Bartesaghi Koc *et al.* [94] | Systematic review (identify geographical patterns, theoretical trends, and methodological gaps) | Most studies overlooked the cumulative effects of natural and artificial features. Most studies at microscales. Little is known about optimum types, size, and arrangements. |
| **General greening & horizontal greening** | Santamouris [95] | Meta-analysis (findings from a standard literature review) | Available data mostly from simulation studies using mesoscale models, followed by experimental studies. Decrease in mean ambient $T_{air}$ is ~**0.3 K** per 0.1 rise in albedo, and the corresponding peak decrease was ~**0.9 K**. Green-roof simulations showed city-scale use to reduce mean ambient $T_{air}$ by **0.3-3 K**. |
| **Parks & general greening** | Bowler *et al.* [96] | Meta-analysis (findings from #47 studies representing interventions of interest) | Ave. park **0.94 K** cooler during the day, with effect beyond the boundary supported. Studies of multiple parks showed larger ones to be cooler. Tree-shading is clearly significant, while evaporative cooling is relevant to a lesser extent. |
| **Vertical greening** | Bustami *et al.* [97] | Systematic review (review of #166 papers) | Increasing overall research trend, as well as towards multidisciplinary research. |

## 2.4 Discussion

The literature describes urban greenspace to include a range of features such as forests or woods, parks, street trees and verges, public and private gardens, allotments, and vegetated building envelopes (Fig. 11, p. 38). All such features are acknowledged to offer varying ecosystem services to urban environments including reduced surface runoff, sustainable drainage, and flood relief; increased biodiversity; phytoremediation; modification of local microclimates; and aesthetic and wellbeing enhancements [37]. There is also significant emphasis on their contribution to mitigating heat-related risks presented by urban heat islands, extreme heat events, and climate change. As such they are widely advocated as 'environmental capital' [98], while their strategic deployment as planned interconnected networks offering ecological, social, and economic benefits is supported in contemporary city-planning discourse under the 'green infrastructure' hypernym [99].

*Englische Anlagen* park
Bern, Switzerland

*Stavros Niarchos* garden
Athens, Greece

Street trees
Barcelona, Spain

Private allotments
Bern, Switzerland

*Fig. 11. Examples of urban green infrastructure or greenspace features.*

The scientific foundation for mitigating the adverse effects of heat-related risks is related to vegetation influence on the thermal energy balance. Energy can be transferred from the urban surface to the atmosphere through the evaporation of water, and when vegetation is present this is combined with transpiration to describe ‘evapotranspiration’. The efficacy of this process is influenced by the availability of moisture (vegetation cover, precipitation, irrigation, humidity, etc.) and wind flow [55]. To mitigate heat-related risks, the enhancement of evapotranspiration is encouraged by the addition of vegetation and/or waterbodies to the urban surface, thereby converting ‘sensible heat ($Q_h$) to ‘latent heat’ ($Q_e$), which in turn reduces the ‘Bowen ratio’ (of sensible to latent heat flux) leading to evaporative cooling ($B = Q_h/Q_e < 1$). This is most overtly exemplified in oasis conditions, where the latent heat flux can be larger than the sensible heat flux to create a heat-sink or negative Bowen ratio [31]. Plant contribution to this flux conversion is mainly from transpiration; which describes the process where water transported through the plant (xylem) is evaporated at the aerial parts by absorbing energy from ambient surroundings [52,54,100]. Given the established contribution this process presents to climate modification (e.g., [101]), it is by far the most discussed vegetation-based cooling process represented in the literature.

Climate scientists focus their attention mainly to the assessment of energetic implications, followed by impact on the hydrological cycle. For most vegetated systems, 99% of the water and >50% of the energy absorbed is estimated to be used by transpiration [2]. The efficacy of this transpiration is dependent on the species of vegetation considered; the specifics of which is the focus of plant science studies. Most plants in cool and wet climates are identified to demonstrate ‘C3 photosynthetic metabolism’, which requires regular opening of leaf stomata and the transpiration of significant volumes of water. Plants in warmer climates are found to demonstrate the more efficient 'C4 photosynthetic metabolism', while in drier and harsher conditions some use 'Crassulacean acid metabolism' (CAM) to enable them to retain water by restricting transpiration. The latter CAM plants (e.g., family Crassulaceae) are distinct as they keep their stomata closed during the day (open at night), which in turn provides reduced daytime latent cooling owing to their near negligible transpiration rates [79]. Save for such CAM plants, plant leaf stomatal apertures are typically closed in the absence of solar radiation. Latent cooling from transpiration is therefore mostly relevant for daytime than night-time energy exchanges [55,102]. Transpiration contributions during the day are further dependent on plant physical features including crown area, Leaf Area Index ($LAI$, defined as the single surface leaf area per unit of ground area), canopy elevation, hydraulic resistances of the shoots and roots, and stomatal hygrothermal resistances (or conductances); as well as soil conditions characterised by dryness, compaction, and hydraulic conductivity [54,55,69,103]. Transpiration effectiveness is also influenced by plant responses to the prevailing background climate, with rates controlled through stomatal function (guard cell turgidity requires moisture) to alleviate heat stress and reduce water loss [54,55,92]. The cooling effectiveness of plants have therefore been found to wane subsequent to protracted heatwaves and drought conditions [104].

Next to transpiration, significant attention in the literature is directed at the cooling influence presented by the shading effect of plant canopies. Shading contributes to cooler surroundings by the shading surface acting as a solar radiation interceptor that reflects and absorbs radiant energy, thereby limiting shortwave absorption by urban surfaces and subsequent re-radiation of heat to the UCL atmosphere [55,105]. The reflection component is affected by the albedo of vegetation ($\rho_{veg}$) [31]. In rural vegetated areas for example, grassy fields have been estimated to reflect ~20-25% of incoming shortwave radiation, while for areas with trees with diverse canopy morphologies the value is lower at ~15% [103]. The non-reflected component is absorbed by the plants, with a proportion of this shortwave energy utilised by phyto-active chemicals for photosynthesis, while the residual is stored as heat. The effectiveness of this shading effect is determined by the physical attributes of plants including leaf size, crown area, and $LAI$ of the canopy [95]. Trees, and to lesser extent shrubs, present higher shading effectiveness in comparison to grass types, with larger tree canopies identified to generate their own microclimates beneath them [96].

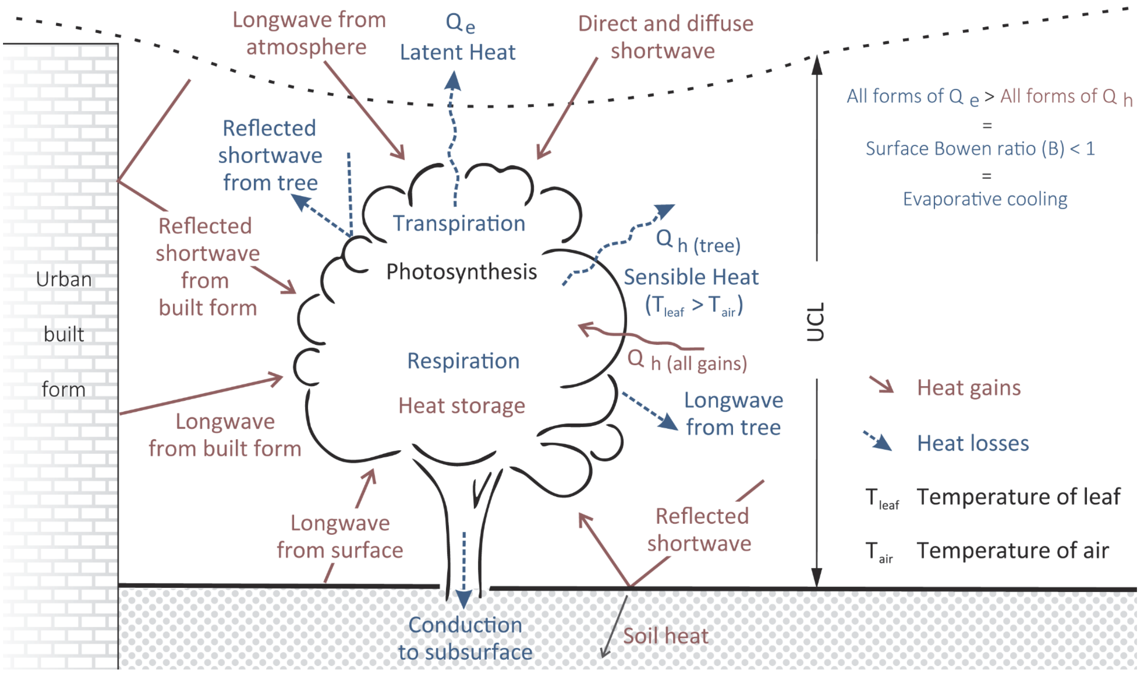


*Fig. 12. Daytime energy exchanges between a solitary tree and urban context; based on* [105], *and published in* [41].

While both climate and plant scientists have paid comparable attention to transpiration and shading aspects, cooling influence from wind flow modification is mostly assessed and discussed in climate studies. These have identified vegetation canopies to modify surface roughness and background wind flow to alter convective heat exchange efficiencies [2,55]. Canopy density and foliage features are significant here, with grasslands identified to provide a barrier of stagnant air nearer to the surface; dense forests found to retain a warm insulated air mass beneath the canopy; while dispersed groves with canopy heterogeneity improve surface roughness to generate mechanical turbulence (eddy diffusion), and thereby enhance convective heat loss [2,63]. Convective heat loss also tends to be greater with isolated plants (e.g., of a tree in Fig. 12), as they protrude into the atmosphere to present greater surface area exposure and increased opportunity for contact with drier air flowing from non-vegetated areas. The three-dimensional morphology and exposure presented by a given plant canopy (individual or community), therefore has significant bearing on its convective heat flux efficiencies and resultant surface cooling contributions [52,55,103].

In addition to the above direct processes of transpiration, solar shading, and modification of wind flow, pollution filtering and runoff reduction are also identified by climate studies to indirectly assist climate cooling. Pollution filtering is largely achieved by dry-deposition (process where pollutants impact upon and adhere to vegetation surfaces such as canopy leaves), followed by gaseous pollutants absorbed directly by leaves [106–108]. The removal of such pollutants reduces atmospheric scattering and absorption of shortwave radiation and longwave infrared radiation, which in turn influences the radiation balance and the rates of atmospheric warming or cooling. Larger canopy trees unsurprisingly filter out more pollutants per unit land area than other types of vegetation. A modelling study for example estimated that the tree cover of the West Midlands (UK) was likely to reduce urban particulate matter ($PM_{10}$) concentrations by ~4% [109]. Vegetation canopies and their characteristics also assist in reducing runoff by the interception of rainfall, while surface root spread characteristics and typical undergrowth reduces runoff to encourage greater absorption; thereby providing increased soil moisture content for evapotranspiration [110].

The effectiveness of the plant-based cooling processes mentioned above are dependent on the background climate of the vegetated area considered. Soil and atmospheric moisture content are critical for the latent flux contribution, with precipitation and/or irrigation providing greater soil water potential for unhindered transpiration, while in contrast high atmospheric humidity suppresses transpiration given the reduced gradient [53,95]. This moisture availability influence is vital to the extent that it often defines the typical vegetation profiles that result, with greater availability resulting in denser growth that generates greater surface roughness relative to drier climates [63]. Ambient air temperature is another critical variable, and determines the sensible heat flux from the vegetated surface. Seasonal sensible heat flux is a minimum in winter, while the maximum occurs during the summer when the vegetation-to-atmosphere temperature gradient is higher [2]. Notably, wind flow is significant for modifying both these climate variables. Higher velocities facilitate greater sensible flux as the convective heat transfer coefficient is primarily dependent on forced convection, thereby encouraging heat loss irrespective of the temperature gradient [55]. Wind flow is also advantageous in high humidity conditions as it assists to advect away accumulated saturated air, while at higher velocities serves to reduce the leaf boundary-layer to enhance the water potential gradient and resulting latent heat flux [53,95]. The background variables of moisture content and ambient air temperature, and their interaction with wind flow therefore influences the typical vegetation profiles that flourish within a given area. This in turn defines the availability and effectiveness of the cooling processes discussed earlier, with distribution of influence discussed next.

### 2.4.1 Extent of UCL cooling provided by greenspace

The spatial extent of the cooling influence provided by greenspace is significant for understanding the likely public health and comfort benefits of urban greening proposals. Urban parks in this regard have been the focus of most available studies, with cooling contributions well-established (e.g., [71,77,91,111]). A meta-analysis of studies for example had identified that on average they are ~1 K cooler during the day, with evidence of this influence extending to their surroundings by varying degrees [96]. The distribution extent therefore seems to demonstrate significant temporal and spatial variance. As examples, an early study of London's Kensington Gardens and Hyde Park found a 3 K cooling influence to extend up to 200 m beyond its boundaries [112], while a longitudinal study of Kensington Gardens recorded a mean summer cooling influence of 1.1 K (4 K max. on certain nights), and nocturnal distribution ranging from 20-440 m with 83% of influence evident 63 m (~half the range) from its boundary [79]. In contrast, a study of a large park in Beijing (Dwa) revealed the 0.6-2.8 K cooling recorded to extend as far as 1.4 km [72]. The variability of such recorded distributions therefore suggests the need for greater examination of the variables and mechanisms that influence horizontal and vertical cooling transport.

Early climate studies had identified the formation and function of wind systems to play a significant role in the distribution of cooling from vegetated spaces. Macro-to-mesoscale prevailing wind flow and direction over the city affects downwind spread, aided by a combination of simple advection along aligned canyon geometries and turbulent mixing above roofs of canyons aligned across the flow [74]. These observations established the urban morphological features defined by sky-view factor, canyon aspect ratio, and orientation as significant variables in modifying cooling distribution [105,112]. Further observations of features such as parks identified the formation of microscale systems to also play a role in horizontal distribution [74]. Under conditions with low wind velocities typical of anticyclonic weather systems, thermals rising from surrounding urban areas generate low-level advection currents that draws air from cooler green areas to characterise 'park-breezes' [78,105]. This park-breeze effect can develop further to form a centripetal thermal system, which completes its cycle with the subsidence of warmer urban air from above into the greenspace (Fig. 15, inset, p. 49). The occurrence of such systems explain why the cooling rate within urban parks is seldom comparable to that of rural areas, but rather is strongly affected by the surrounding urban context [105]. It also explains why parks seldom appear on daytime heat island intensity plots (e.g., Fig. 13, p. 45), as the occurrence of such centripetal systems are likely to hinder the vertical transport of the park cooling plume beyond the UCL. Although this suggests minimal impact on overall heat island mitigation, the greater microscale (UCL) horizontal distribution encouraged could be argued to offer the highest cooling influence when it is most likely to be useful in relieving heat stress in nearby neighbourhoods [79]. However, as these centripetal systems along with heat island formation are buoyancy-driven, their occurrence is strongly reliant on the dynamic stability of the prevailing atmosphere (i.e., occur best under anticyclonic conditions). Higher wind velocities (>5 $m{\cdot}s^{-1}$) tend to impede vertical movement and disrupt buoyancy-driven effects by introducing rapid turbulent mixing [74,105]. With strong winds, greenspace cooling influences are therefore rapidly mixed to present little to no discernible impact [105].

When examining the characteristics of greenspaces and their influence on horizontal cooling transport across urban areas, a higher proportion of cooling is said to be maintained per metre beyond park boundaries of larger scale bodies [58,59,72,79]. This significance of scale could be attributed to the increased potential of the park-breeze system, either due to the increased temperature gradient or else the increased fetch (length of area over which a given flow has contact). There is certainly a minimum effective size to consider, with Doick *et al.* [84] highlighting those smaller than 0.05 $km^2$ as offering negligible contribution. This supports the hypothesis that a certain fetch is required to generate a park-breeze, and that larger parks generate larger breezes allowing for greater cooling transport to the surrounding urban fabric, even for a minimal temperature gradient. The geometry of the park is also significant here, with square or round-shapes providing higher cooling efficiency and distribution [75]. This is explained with reference to the greater opportunity for increased temperature and humidity gradients and fetch between the body and its surrounding landscape [58,113,114]. Finally, the range of distribution experienced is also dependent on the vegetation profile (trees, shrubs, or grass), and its heterogeneity [104].

A modelling study that combined tree age and planting density as a composite Leaf Area Index ($LAI_{sp}$) as means to calculate optimum cooling effect relative to park size [73], confirmed the findings of Shashua-Bar & Hoffman [86] that highlighted networks of smaller 0.2-0.3 $km^2$ greenspaces to also provide effective cooling distribution [73]. A study that considered the scale and interval between greenspaces suggested that such network or cluster arrangements should be spaced <300 m apart in order to provide their collective benefit

[62]. More research however is required to examine if the park-breeze effects can be achieved by such networks of smaller greenspaces, and if so, the necessary size and interval required in relation to surrounding urban surface roughness features.

### 2.4.2 Extent of UBL cooling provided by greenspace

Although many studies of parks have demonstrated the horizontal distribution of their cooling influence, there is little quantitative evidence presented to clarify how such isolated cases affect the overall urban climate [96]. The need for clarity is demonstrated by considering London (~47% greenspace [115]), and its averaged atmospheric heat island simulation for a relatively warm summer (see Fig. 13, p. 45, [116,117]). Accounting for predominant south-westerly winds, the following areas of interest are identified for discussion:

- Although Kensington Gardens and Hyde Park cooling potential is evident at surface level temperatures [115], their significance is not apparent at the atmospheric level.

- Notable atmospheric level cooling contributions are presented by the combined larger greenspaces of Richmond Park and Wimbledon Common, and to a lesser extent and intensity by the cluster of greenspaces that includes Hampstead Heath.

- Contribution from the linear shaped Lee Valley Regional Park is remarkably absent in the atmospheric simulation, despite amounting to ×4 the area of Richmond Park.

From the above observations it can be hypothesised that there is some relationship between the magnitude and geometrical distribution of greenspaces and their citywide (UBL) cooling influence. Reflecting on the findings of studies in section 2.4.1 [79,113,114], the linear geometry and limited fetch of the Lee Valley Regional Park (~1 km width, compared with 5×7.5 km dimensions of Richmond Park and Wimbledon Common) could be suggested to impede the development of strong temperature and humidity gradients necessary to affect citywide cooling. This is also likely to be compounded by a significant proportion of its area being occupied by reservoirs (~22%), which in certain conditions could contribute a counterproductive warming effect [39,41,118]. The observation related to Hampstead Heath and its context on the other hand could be said to conform to the evidence that suggests effective collective influence from clustered greenspaces [73,86].

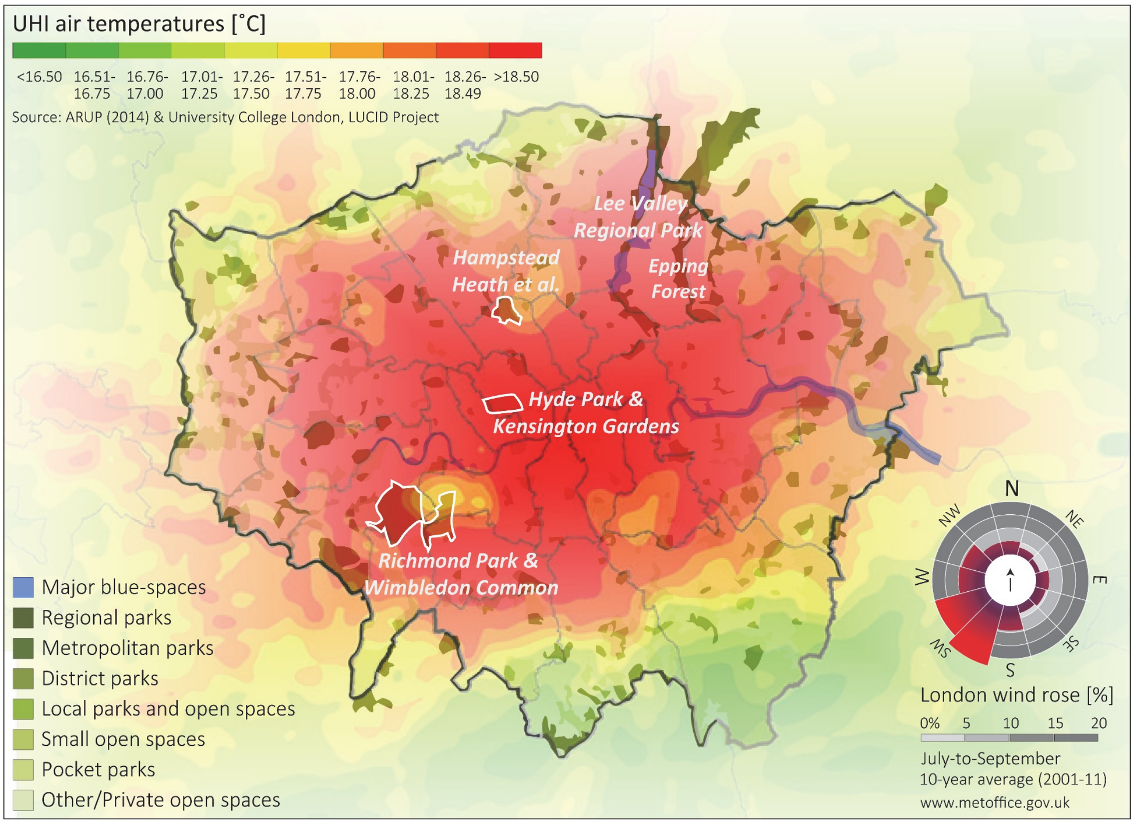


Note: Compiled from [119], [120], and UHI simulation from [115] and University College London, LUCID project.

*Fig. 13. LUCID atmospheric level UHI simulation overlaid over London's greenspaces; in* [41].

Table 3. London greenspaces and approximate extents for comparison with Fig. 13.

| **Greenspace** | **Area ($km^2$)** | **East-west span (km)** | **North-south span (km)** |
|---|---|---|---|
| Hyde Park + Kensington Gardens* | 2.5 | 2.5 | 1.0 |
| Hampstead Heath** | 3.2 | 1.7 | 1.8 |
| Richmond Park* | 9.6 | 4.0 | 4.5 |
| Epping Forest** | 24.8 | 2.7 (widest) | 8.8 (linear) |
| Lee Valley Regional Park*** | 40.5 | 1.4 (widest) | 42.0 (linear) |

Note: Compiled from: *[121]; **[122]; ***[123]; and [124].

While the above explanations could be justified to an extent in relation to evidence from isolated greenspace studies, there is a significant shortfall in available monitored vertical cooling distribution data to affirm associations between geometric parameters and vertical transport within the UBL. This lack of empirical data is attributed to the infrastructural cost necessary to carry out such vertical measurements particularly for longitudinal analyses, which are required to characterise the temporal patterns of vertical transport. Most recent studies therefore present and discuss findings only in relation to UCL cooling, almost exclusively with reference to horizontal distribution.

Until recently, the reduction of evapotranspiration was considered as the dominant contributor towards the daytime UBL heat island [31]. However, a study of cities across the United States argued that the daytime heat island was in fact principally dependent on the relative effectiveness with which urban and rural areas convect heat to the climate, rather than on precipitation and evapotranspiration (heat storage remains the dominant determinant of the night-time heat island), [63]. The modelling study suggested that if urban areas are aerodynamically smoother than surrounding rural areas (due to dense vegetation in the latter and its relative absence in the former), heat dissipation is relatively less efficient to increase potential for warming. Conversely if surface roughness in urban areas is greater, it could potentially lead to a cooling effect. The relative difference in convection efficiency between urban and rural conditions in different cities and parts of the world is dependent on the background climate and its influence on the vegetation cover in rural areas. In humid temperate climates in the United States, Zhao *et al.* [63] found convection to be less efficient at dissipating heat from urban form than from rural land, as the rural areas tended to be aerodynamically coarser than urban areas due to the presence of generally denser and coarser vegetation canopies. The study highlighted urban form in such humid temperate cities in the United States as having a reduced convection efficiency of 58% relative to adjacent rural areas, leading to relative temperature increases of up to 3.0 K dominating their daytime heat island intensity. In drier climates the opposite was observed, as the built environment was coarser relative to the surrounding landscape, where drier conditions typically impeded the growth of denser vegetation types. The study found that in such cities in the United States, a decrease in heat island intensity of ~1.5 K. In certain cities, this decrease even presented a daytime heat sink effect. This phenomenon had previously been explained with reference to the 'oasis effect' resulting from evaporative cooling provided by urban trees and soft landscaping [125]. Zhao *et al.* [63], however argued that based on proportional contributions to overall daytime heat island intensity (as determined by their climate model and verified through remote-sensing surface temperatures), the evaporative cooling contribution to daytime (UBL) heat island reduction was minimal in comparison to the effects of convection.

The above findings suggest that the addition of vegetation with the principal aim of improving evapotranspiration qualities of the urban surface may prove to be less effective in mitigating the daytime heat island than previously understood. At the UBL scale of the urban surface, the presence of vegetation seems to provide greater service to urban cooling by enhancing its surface roughness. This provides another insight into the results presented in Fig. 13 (p. 45), where Richmond Park and Wimbledon Common presents a pronounced heat island reduction effect in contrast to Hyde Park and Kensington Gardens, not only because they are larger in area, but also as their surfaces are significantly coarser. In humid climates where daytime heat island warming is substantial, the addition of vegetation to increase inner-city surface roughness could thus be a feasible strategy [63]. It can be hypothesised that if urban greening is to be undertaken for this purpose, tree planting with species diversity would provide a greater provision of roughness than surface greening. The types of trees to be utilised requires consideration of not only their transpiration potential, but also the surface roughness they deliver in their varied canopy arrangements. Green infrastructure designers will therefore need to take account of this and anticipate likely canopy morphological arrangements when planning urban enhancements.

### 2.4.3 Greenspace in relation to compaction and dispersal urban development

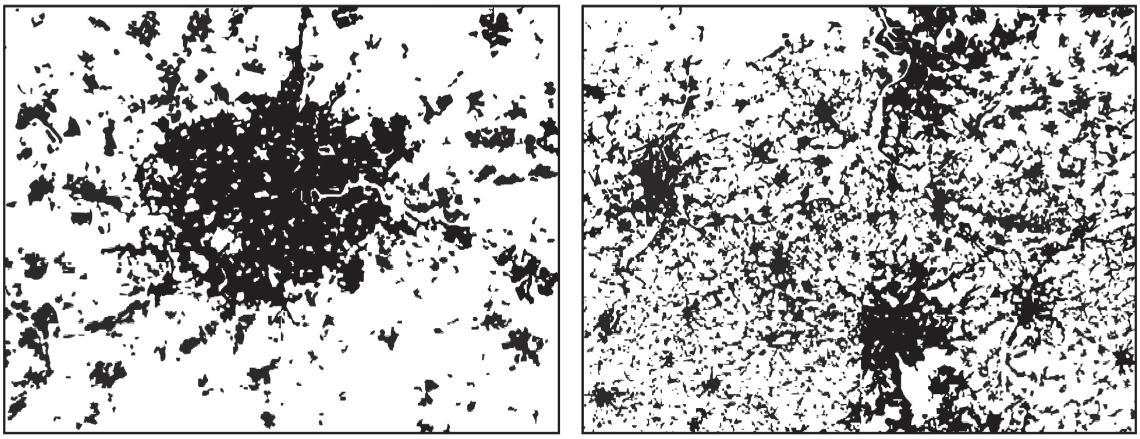

Compact development model Dispersed development model

*Fig. 14. Illustration of diametrically opposed urban development strategies; based on* [126].

Dispersed urban development is typically criticised for increased land usage in comparison to compaction or densification strategies (e.g., Fig. 14), with much of this usage likely to be greenfield land leading to the loss of peripheral greenspace and tree coverage [126]. A study from the United States has shown the rate of rural greenspace loss in the most actively dispersing urban regions to be more than double the rate in the more compact urban regions, with correlation evident between loss of regional vegetative cover and the frequency of extreme heat events experienced [127]. The significance of peripheral greenspace was also demonstrated by a study of the German city of Frankfurt (Cfb) that highlighted its peripheral greenbelt to provide a beneficial cooling influence of 3-3.5 K. The study discussed this cooling influence with reference to the formation of a mesoscale ‘city-country breeze’ (Fig. 15, p. 49), also referred to as heat island flow [66,67]. Under anticyclonic conditions this citywide system develops as thermals at the core of the city rise to the boundary-layer, which then generates advection flows at the canopy-layer level from the cooler surroundings of the greenbelt [2]. Urban growth strategies that expand into such peripheral areas can reduce this beneficial breeze by modifying the surface energy balance in such areas to reduce the city-country temperature gradient and potential of the system, while also preventing the supply of relatively cooler airflow that would otherwise have been provided by the greenbelt vegetation. Notably, compact forms of development that encourage higher heat island intensity by concentrating heat-absorbing material mass, seem to favour the formation of these cooling breezes (i.e., by enhancing the city-country temperature gradient), while dispersed developments tend to weaken their potential.

Table 4. Urban development model influence on greenspace cover and the thermal environment.

| Greenspace | Compaction | Dispersal |
|---|---|---|
| ***Scale*** | Relatively smaller scale features feasible. The substantial scale required to demonstrate mesoscale influence is seldom achievable. | Scale varies, with several medium-to-larger features possible. There is potential for these to function synergistically with existing rural features and context. |
| ***Typical arrangement*** | Planned, ordered, and managed arrangements. | Fragmented with planned and managed arrangements coexisting with undeveloped greenfield land and unplanned development. |
| ***Expansion impact*** | Further compaction may lead to decline in inner-city greenspace. | Loss of rural greenspace, as well as agricultural land. |
| ***Likelihood of coverage loss*** | Loss is more likely given the higher land values and resulting pressure to develop. | Coverage loss is relatively lower, given the lower land values and reduced market interest for high-density living. However, external ‘nodal’ densification could lead to cover loss. |
| ***Surface roughness and impact on convection efficiency*** | Potential reductions from inner-city coverage loss. The significance of this is dependent on other inner-city morphological features. | Reductions from coverage loss at periphery. The significance of this is dependent on the profile/types of vegetation lost). |
| ***Surface permeability reduction from coverage loss*** | Further decreased from default low levels, thereby increasing runoff, and reducing evaporative cooling of the surface. An exception to this would be compaction projects integrating green-roof-based sustainable urban drainage systems (SuDS). | Greater loss of surface permeability at urban peripheries likely to reduce drainage flows and capacity to increase risk of flooding. |

| Greenspace | Compaction | Dispersal |
|---|---|---|
| ***City-country impact on thermal energy gradient*** | Increased compaction (densification) may enhance the gradient leading to a stronger city-country breeze, which advects in cooling from the greenbelt. | Greater spread of the surface balance (i.e., urban sprawl) may lead to a reduced gradient and a resultant diminished city-country breeze. |
| ***Addition of greenspace features*** | Large ground level features unlikely with new projects. Smaller strategically spaced (wind direction) networks viable with regeneration and windfall-site projects. | Smaller strategically spaced (wind direction) networks viable. Opportunity to integrate natural features from existing surroundings to such networks. |
| ***Synergetic arrangement*** | Potential to plan with regeneration schemes. Strategies include enhancing greening with tree planting as a priority, and surface greening as a secondary alternative, whether at ground level or enveloping built form. | Greater potential to plan entire new urban extensions with optimal blue-green ecosystems from the outset. |

The degree of any cooling shortfall expected at the city core from dispersing arrangements into its peripheral greenbelt is dependent on the distribution and typologies of vegetation lost. It is significant to note that while future dispersal growth can be reasonably forecasted in terms of magnitude, its market-driven spatial distribution is less straightforward to anticipate, as demonstrated by a systematic modelling projection of Toulouse, France (Cfb) by Masson *et al.* [128]. Vegetation related cooling shortfalls are therefore more challenging to forecast when dispersed relative to compaction scenarios are considered.

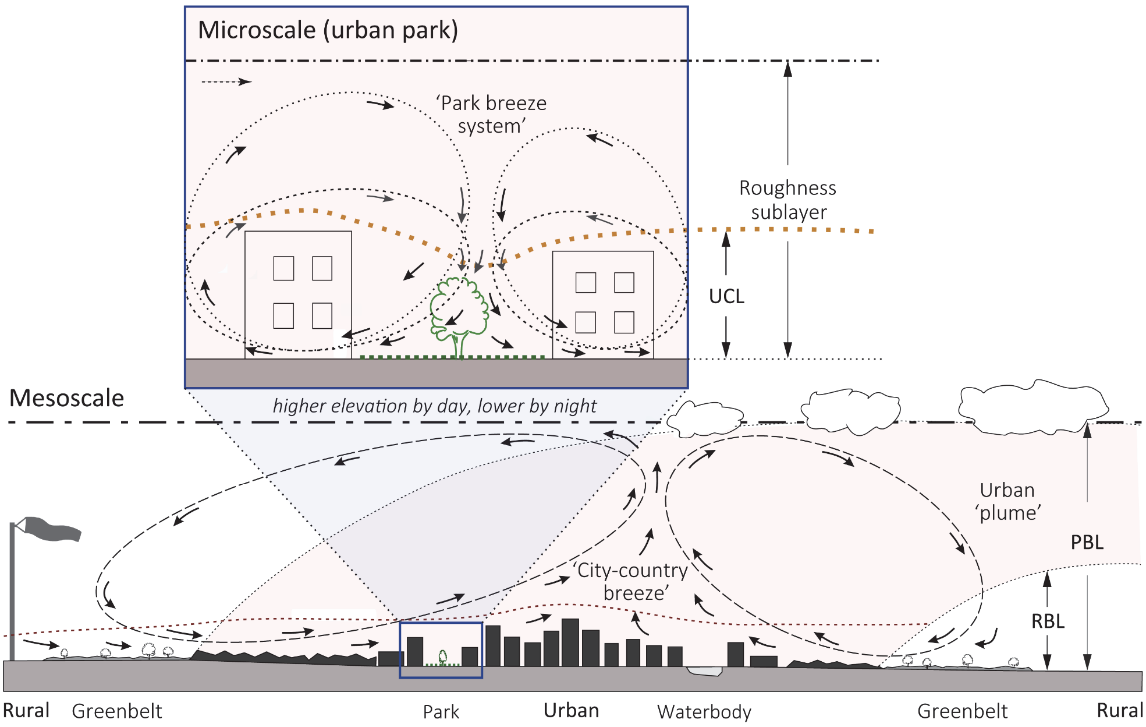


*Fig. 15. Heat island formation flow, also referred to as the city-country breeze; and park-breeze centripetal thermal system (inset); published in* [41].

### 2.4.4 Contribution from vegetated building envelopes

In densified urban areas, tree-planting schemes to create green pockets or corridors in available sites is advocated, subject to effective geometry and width. A study of Hong Kong (Cwa) for example, discussed several effective means to enhance urban greening in compacted arrangements, with tree cover supported as offering greater benefit over grassed surfaces. The study recommended overall coverage (based on Hong Kong morphology) of a third of a given urban area to achieve street level temperature reductions of ~1 K [61]. Similarly, greenspaces planted with trees were considered by Doick *et al.* [79] to be more effective in terms of urban cooling per unit area than grassed surfaces, as they contribute more of the beneficial vegetative cooling processes discussed earlier.

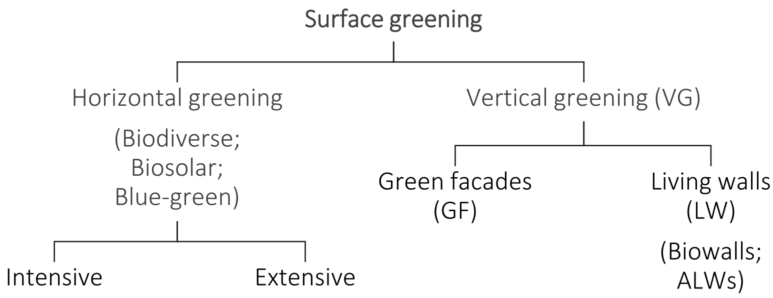


*Fig. 16. Principal surface greening categories (and variants).*

Notwithstanding the above evidence, a systematic modelling assessment of future urban growth had argued that enhanced tree-dominant greening of this nature as unlikely to be achieved in many already compacted urban centres [128]. The Hong Kong study [61] also acknowledged that with extreme urban core densities, and when roof loadbearing capacities limit retrofit options, surface greening solutions such as green-roofs (i.e., horizontal greening, Fig. 16) to present the only viable enhancement option. This acknowledgment has led to the significant popularity of such applications in urban areas, with the corresponding development of an already substantial body of research [91,95]. Such studies have assessed applications to identify microclimate cooling contributions (e.g., [68,69]); although the range of influence is not always characterised. Ng *et al.* [61] for example found green-roof provision to be less effective than street vegetation for street level cooling, particularly when mean urban morphology height exceeds 10 m. In cities with higher average building heights, street level cooling influence of green-roofs is negligible [61,70]. A broader review of green-roofing studies similarly concluded a proximity dependency with limited vertical transport, although there seems to be little empirical evidence to comprehensively quantify the latter as studies tended to avoid considering thermal effects beyond the immediate range [95]. Notwithstanding this ambiguity in effectiveness range, studies have presented ample evidence to suggest discernible cooling benefit to users of urban roof gardens, and thus makes useful contribution to localised thermal relief in densely compacted cities [61].

The influence of green-roof strategies on building energy use is similarly well-supported in the literature [129,130], with heat transfer to-and-from occupied spaces modified to affect cooling or heating loads and resulting heat rejection back to the urban climate. The impact on space-conditioning loads is predominantly assessed by studies in comparison to the alternative strategy of cool-roofing (which alters the albedo of roofs). The William *et al.* [130] study for example demonstrated that both cool and green-roofs provide comfortable indoor temperatures in the summer, with green-roofs offering lower annual energy costs resulting from the insulation uplift contributing a wintertime saving. The overall energy saving potential of green-roofs have also been found to increase with the vegetation $LAI$, and with cooling-dominated building profiles be a critical parameter [131]. Building on this evidence base, green-roofing has been adapted and advanced over the years, with the most recent strategies integrating water features to offer 'blue-green' ecosystems [132].

*Fig. 17. Bosco Verticale (left) and 25-Verde (right), northern Italy; inspected in summer 2019.*

While green-roofing continues to advance as an urban greening strategy, the need to enhance cover beyond such provisions has encouraged alternative approaches to be developed. One school of thought aims to address this challenge by acknowledging the greater benefits offered by trees and shrubs and integrating them into building fabrics. Recent notable examples of such integrated approaches include the *Bosco Verticale* (2014) and *25-Verde* (2012) projects from northern Italy (Fig. 17), both receiving significant public attention given their unique aesthetics [133]. The second school of thought has sought to adapt a traditional form of ‘vertical greening’ to apply vegetation to the most abundant of urban built environment surfaces, building façades. These approaches have gained significant attention over the last decade and a half, the evidence of which is seen in most cities where installations are increasingly introduced to new as well as existing building façades [97]. The aesthetic appeal and interest that such flourishing installations generate have resulted in a significant upward trend in commissions received by specialist installers [132,134]. The assessment of their cooling potential and delivery of other ecosystem services in urban settings however is an emerging area of research interest [94,97], with available studies and research gaps identified in the next chapter.

## 2.5 Summary

This chapter considered observations on how greenspace features contribute to the mitigation of urban heat-related risks. From the meta-analysis of studies from key knowledge bodies, the degree of significance that different green infrastructure typologies contribute towards enhancing urban climate resilience was found to be dependent primarily on the **scale of the feature**, along with associated secondary parameters discussed below. Climatological evidence highlighted that to make mesoscale or city-scale modifications, substantial coverage areas are required, while **microscale thermal relief is achievable with modest, well-arranged features**. The latter is significant for enhancing heat-risk resilience of urban communities, given that greenspace microscale cooling has been found to be greatest during harsher conditions typical of heatwaves and high heat island intensity.

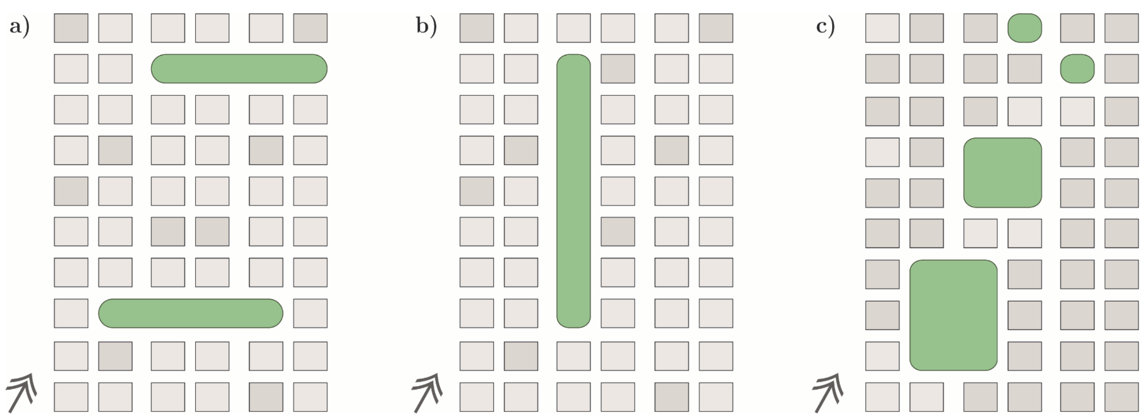


*Fig. 18. Greenspace arrangements: linear features arranged across dominant flow (a); linear feature near parallel to flow (b); and regular features fragmented in dominant flow direction (c).*

The following details key considerations:

- The magnitude and potency of greenspace thermal influence experienced is dependent on their **intrinsic characteristics** such as **scale, geometry, surface roughness and fetch length,** and **spread and interval of features**; as well as **prevailing background conditions** such as **wind flow, morphology and materiality of the context,** and **feature-to-context air temperature and moisture gradients** (Table 5). These characteristics and conditions influence their thermal feedback to the surrounding climate and its horizontal and vertical transport. Horizontal transport evidence provides ample encouragement for utilising greenspace as a significant heat-risk resilience strategy. The review however highlighted **vertical transport aspects to be underrepresented** in previous research, and thus requiring further attention to clarify significance to the urban boundary-layer climate [41].

Table 5. Characteristics and conditions influencing greenspace thermal feedback, as addressed by the literature reviewed.

| **Study** | | **Intrinsic characteristics of feature** | | | | **Prevailing background conditions** | | |
|---|---|---|---|---|---|---|---|---|
| | Köppen climate | Scale/size | Geometry/ shape | Surface roughness & fetch length | Spread and interval between | Wind flow | Context morphology & materiality | Feature-to-context $\boldsymbol{T_{air}}$ & $\boldsymbol{RH}$ gradients |
| Yu & Hien [76] | Af | | | | | ✔ | | ✔ |
| Wong *et al.* [89] | Af | | | | | | | ✔ |
| Acero *et al.* [90] | Af | | | | | | | ✔ |
| Zhou *et al.* [58] | Cfa | ✔ | ✔ | | | | | |
| Xiao *et al.* [59] | Cfa | ✔ | ✔ | | | | | |
| Sugawara *et al.* [74] | Cfa | | | | | ✔ | ✔ | |
| Li & Yu [81] | Cfa | ✔ | ✔ | | | | | ✔ |
| Xu *et al.* [82] | Cfa | | | | | | | ✔ |
| Peng *et al.* [87] | Cfa | ✔ | | | | ✔ | ✔ | ✔ |
| Emmanuel & Loconsole [64] | Cfb | ✔ | | | | | | |
| Skelhorn *et al.* [65] | Cfb | ✔ | ✔ | | | | | |
| Bernatzky [66,67] | Cfb | | | | | ✔ | ✔ | ✔ |
| Heusinger & Weber [68] | Cfb | | | | | | | ✔ |

| **Study** | | **Intrinsic characteristics of feature** | | | | **Prevailing background conditions** | | |
|---|---|---|---|---|---|---|---|---|
| | Köppen climate | Scale/size | Geometry/ shape | Surface roughness & fetch length | Spread and interval between | Wind flow | Context morphology & materiality | Feature-to-context $\boldsymbol{T_{air}}$ & $\boldsymbol{RH}$ gradients |
| Monteiro *et al.* [69] | Cfb | | | | | | | ✔ |
| de Munck *et al.* [70] | Cfb | ✔ | | | | | ✔ | |
| Jansson *et al.* [78] | Cfb | | | | | ✔ | ✔ | ✔ |
| Doick *et al.* [79] | Cfb | ✔ | | | | ✔ | | ✔ |
| Hamilton *et al.* [80] | Cfb | | | | | ✔ | ✔ | ✔ |
| Leuzinger *et al.* [83] | Cfb | | | | | | | ✔ |
| Doick *et al.* [84] | Cfb | ✔ | | | | | | |
| Perini *et al.* [88] | Cfb | | | | | ✔ | | ✔ |
| Aram *et al.* [77] | Csa | ✔ | | | | | | ✔ |
| Shashua-Bar & Hoffman [86] | Csa | ✔ | ✔ | | | ✔ | ✔ | ✔ |
| Ng *et al.* [61] | Cwa | ✔ | | | | ✔ | ✔ | |
| Qiu & Jia [71] | Dwa | ✔ | ✔ | | | | | ✔ |
| Yan *et al.* [72] | Dwa | ✔ | | | | | ✔ | ✔ |
| Park *et al.* [75] | Dwa | ✔ | ✔ | | | | | ✔ |
| Wang *et al.* [85] | Dwa | | | | | | ✔ | ✔ |
| Vidrih & Medved [73] | N/A | ✔ | | | | ✔ | | |
| Honjo & Takakura [62] | N/A | ✔ | | | ✔ | ✔ | | ✔ |
| Ward *et al.* [60] | Various | | ✔ | | ✔ | | | |
| Zhao *et al.* [63] | Various | ✔ | | ✔ | | ✔ | ✔ | ✔ |

- The **addition of multiple smaller features** that take advantage of dominant wind flow patterns (in the summer), offer greater cooling transport across a larger canopy layer area than with a solitary larger feature (Fig. 18, p. 52). This suggests that useful greenspace can still be introduced as infilling features in regeneration strategies, although in existing high-density cities enhancement approaches are likely to necessitate surface greening. Previous research has promoted horizontal greening for this purpose, while **recent attention is directed towards considering vertical greening** [41].

- Greenspace and the environment they occupy are mutually related. The state of the surrounding climate is modified by the latent and sensible heat flux from vegetation, while the vegetation responds to changes in the surrounding climate to modify their heat flux. The review highlighted that although this reciprocal dependency is understood, discussion in studies is often limited to a single direction. The **limitations of protracted heat-related risk mitigation** (i.e., thermal relief provision), **are therefore often understated or overlooked** [41].

- Addressing greenspace loss and enhancing cover at present is discussed and reflected in city-planning policy [99]. Some planning systems already **account for the relative abilities of different greenspace types to deliver cooling and other ecosystem benefits.** The Green Area Ratio (GAR) implemented in Berlin (Germany) and adapted in Malmö (Sweden) for example, assigns weighting factors to greenspace types relative to their climate change mitigation potential [135]. Such planning mechanisms however require periodic assessment against the latest multidisciplinary evidence, with more detailed consideration of vertical greening strategies expected in the future.

As remedying city-wide heat-related impacts with green infrastructure features become progressively more challenging in densely constructed cities, the focus is shifting towards microscale or localised thermal mitigation/relief measures. Reducing thermal loads in such localised settings is expected to reduce demands on health, comfort, and wellbeing, as well as energy used to modify these immediate climates. The study of green infrastructure enables policymakers, city-planners, engineers, and architects to determine appropriate types and their efficient urban arrangements, with the exponential increase in attention received in recent years indicative of the subject's acknowledged value to urban planning.

# Chapter 3

VERTICAL GREENING

## 3.1 Introduction

The previous chapter discussed the heat-related climate risk mitigation contributions of different green infrastructure typologies, with surface greening highlighted as having received increased attention to achieve coverage enhancements in densely built cities. It further identified that although initial efforts had targeted the promotion of horizontal greening measures, vertical greening as having gained significant favour in recent years. This chapter examines the context of this green infrastructure typology, its emerging variants, and available evidence in relation to outdoor and indoor application influences. By reviewing the available literature, the chapter seeks to address the following research question:

> *B. Would the already identified outdoor installation ecosystem benefits and risks be similar for applications in indoor environments?*

The chapter represents the second of the two-stage review belonging to Part I of the project, with material presented representing a revised and abridged version of the published review in Gunawardena & Steemers [10].

### 3.1.1 Unintended growth and the built environment

Plants have evolved to thrive and propagate in diverse environments. The built environment is no exception with many able to takeover structures at the slightest sign of human neglect. The encouragement for unplanned (unaided by human intervention) growth and propagation is provided by the presence of light, moisture, and nutrients. Neglected buildings provide greater opportunities for securing these growth factors, where weathering has surfaced mineral-rich substrate impurities, and rustic finishes and fissures are likely to have collected decomposing matter (humus) and moisture. Envelope fissures are a significant attraction, with colonising plants showing preference for propagating along their course much like the lithophytes that spread along rock fissures in natural environments [136]. The types of vegetation able to colonise built structures vary with the climate. In temperate climates, such species generally include climbers, smaller herbaceous plants, and shrubs. Examples include *Hedera* spp. (ivy), family Poaceae (grasses), family Crassulaceae (succulents), or *Erysimum* spp. (Wallflowers). In tropical climates these include colonising saxicolous flora that demonstrate rapid and aggressive growth, as exemplified by the smaller surface spreading *Desmodium triflorum* (Tick trefoil), as well as the larger *Ficus religiosa* (Sacred fig) often found growing on temple structures in Asia (Fig. 19) [137].

a) b) c)

*Fig. 19. Herbaceous plants growing on a wall in Cambridge (a); a moss carpet over roof tiles also in Cambridge (b); and a mature F. religiosa, countless D. triflorum, and moss growing on an ancient ruin from the Polonnaruwa Kingdom in Sri Lanka (c).*

The spectrum of plant impact on built structures from unplanned growth can vary between superficial, hazardous, or destructive damage caused by physical and chemical processes. Superficial impact on built structures is evident in most climates and generally include the spread of algae, mosses, and ferns. Such plants are often accepted by building inhabitants as ‘natural’ greening features resulting from weathering, with the main complaint raised against their retention of moisture encouraging possible damp-related surface damage. Superficial impact may also result from unintended climbing plant growth. Ivy species are known to colonise built structures where neglect has provided opportunity, at times to the extent that in some areas they are considered as invasive weeds. Recent studies identify this impact however as mostly superficial. Field studies in England had found that ivy acts as a 'blanket' to protect surfaces from heat, frost, and humidity extremes, while also shielding against the harmful deposition of particulate matter. Experiments in Oxford had also revealed ivy roots adhering to stone surfaces to present negligible damage (e.g., Fig. 20, [138,139]). Their adhering mechanism however is a challenge to remove if required, as the biochemical bonding of the adventitious roots tend to leave markings that could compel resurfacing work (Fig. 22 & Fig. 23). There is also some evidence to suggest that root-sap and bonding secretions may modify the pH of the substrate to cause acid-attack (chemical action), although any substantial damage is likely to take many decades to cause hazardous impact [140]. Unrestrained growth of climbers however will become hazardous if allowed to grow into conditions such as gutters, tiled roofs, or masonry cracks or voids, where dislodging of tiles, blockages, or loss of bonding integrity may result with time. Such outcomes in turn may pose a risk to the integrity of the construction assembly concerned and its performance, as well as being a safety risk to inhabitants. Often this degree of hazardous growth is witnessed at structures suffering from severe neglect, over many years.

*Fig. 20. Limestone after extensive ivy growth removed and showing no damage to surface; image from* [139].

*Fig. 21. Ivy damage at Gleaston Castle, Cumbria, resulting from organ growth within a wall void; image from* [139].

*Fig. 22. Markings from adventitious roots left behind by dead and removed ivy.*

*Fig. 23. Tendril adhesion pads left behind by dead Parthenocissus tricuspidata (Boston ivy).*

In tropical climates where colonising species have the advantage of abundant growth factors, severe neglect may rapidly lead to destructive growth [140]. In such instances, construction elements may be separated by growing plant organs to compromise the integrity of an assembly to the extent that it may cause failure (e.g., Fig. 21, p. 58). The discussion on such destructive growth is mainly focused on root development. Plant root growth results from cell division in the apical meristem, and their subsequent expansion with water influx. This then generates the turgor pressure to drive growth in the radial and axial directions [54]. Darwin [141] observed that roots have hydrotropic ability, which enables them to grow towards moisture sources and overcome mechanical impediment presented by the substrate. The persistent mechanical impediment caused by hard barriers such as built structures is treated by the roots as a stress, following which several adaptation measures are actioned (described as thigmomorphogenesis responses). These result in slowing the rate of cell production, stiffening cell walls in the axial direction and enlargement in the radial direction (increases diameter), and the production of finer lateral roots to increase exploratory growth into smaller pores and cracks [142]. The radial expansion of roots that have found their way into such pores and cracks of a barrier can exert significant growth pressure over time to generate new cracks and propagate the existing. The damage to building elements from such action can be substantial and even catastrophic, with woody species causing greater damage from the secondary growth of roots and stems that lead to larger radial sections [140]. The fact that plants find favourable conditions for growth in existing cracks commonly found in neglected buildings (i.e., areas with lower resistance), therefore accelerates their plant-based destruction as a form of 'organic demolition'.

### 3.1.2 Historical context

Early observations of unintended plant growth on built structures are likely to have inspired their eventual inclusion by design. Examples of such integration has ample representation across the many cultural and geographical contexts, with notable references traced back to ancient Egypt, Babylon, and Greco-Roman cities [143]. In drier European climates, the use of creeping *Vitis* spp. (grape vine) to cover sheltering structures and parts of buildings had become traditional practice by the latter part of the middle-ages [144,145]. Examples of such practice is manifested in the literature of the period, with the fourteenth century literary anthology *Decameron* (1358) including a notable description [146]. The reasoning behind the use of such features is not explicitly explained but hypothesised as an intuitive response to a warmer Mediterranean climate, in which shade was simply achieved by encouraging vegetative cover, while the unique and seasonal appearance they generated resulted in their proliferation as a desirable aesthetic adornment. These early representations were soon replicated and elaborated in Renaissance gardens, as represented in the late fifteenth century literary work *Hypnerotomachia Poliphili* (1499); which amongst its many woodcuts of structures exemplifying the Renaissance rediscovery of classical antiquity, presents depictions of vine-covered tunnel arbours and a domed bower (Fig. 24 [147]). While such elaborate features gained recognition as archetypal elements of the Italianate Renaissance garden, simpler representations also gained acceptance across the European continent (e.g., Fig. 25a, p. 61) [143].

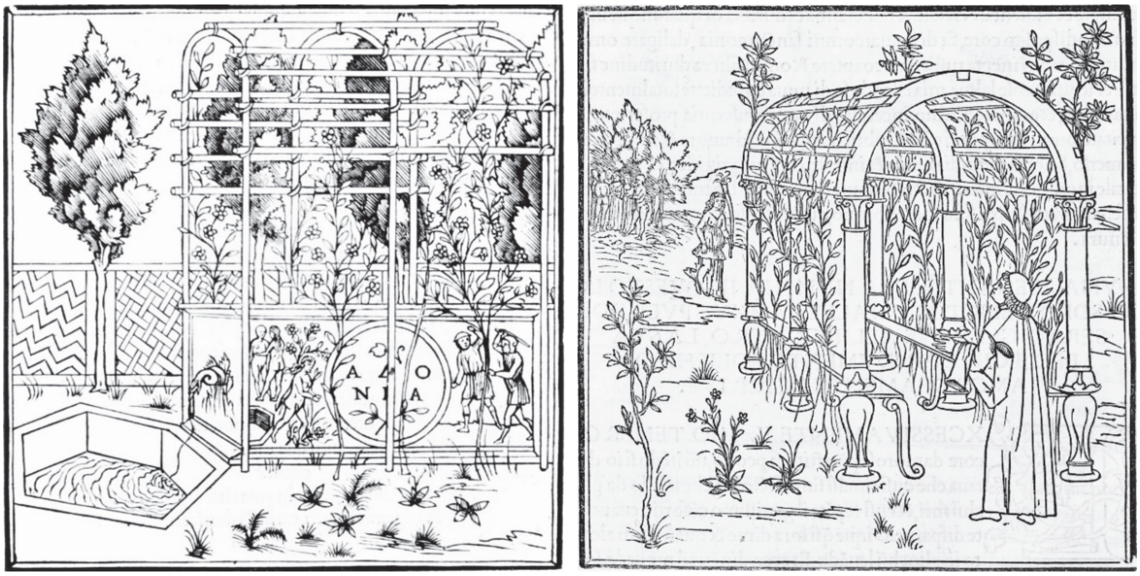

*Fig. 24. Hypnerotomachia Poliphili woodcuts of tunnel arbours, credited to Benedetto Bordone* [147].

In Britain, interest in the architectural use of climbing plants is apparent from the early part of the sixteenth century onward, when associated terminology and descriptions entre the lexicon. The earliest use of the word 'bower' for example was recorded in 1534, which is described by the Oxford English Dictionary as 'a shady recess' [143]. The admiration of Italianate Renaissance gardens sustained interest in such features for several centuries after, while during the nineteenth century a surge in interest marked the onset of a Victorian tradition spanning between 1837 and 1901, and widely popularised from the 1880s to the early 1900s [148]. This was encouraged by the Garden City movement, which introduced a renewed interest in greening to better the city; and the arts and crafts movement, which encouraged the aesthetic integration of vegetal motifs and forms to objects of everyday life, along with a closer and more potent association between house and garden (e.g., Fig. 25b). Hestercombe in Somerset presents an example of such early twentieth century arts and crafts sentiment (1904-09), where an arbour with a canopy of pleached *Ulmus glabra* (Wych Elm) was realised by Sir Edwin Lutyens in collaboration with Gertrude Jekyll [143].

**a)** **b)**

*Dance under the trellis*, 1610-85, by Adriaen van Ostade (Dutch golden age painter).

*Trellis*, designed in 1862 and first produced in 1864, by William Morris.

*Fig. 25. Depictions of structures with climbing plants, from the Metropolitan Museum of Art archive, New York, United States.*

From the mid-to-late-nineteenth century, the use of climbers was introduced to building façades in many European cities and British colonies, including North America and Australia. These practices were mainly encouraged by aesthetic considerations that used such climbers as decorative enhancements or devices of concealment [144]. In colonies such as America however, the ivy-covered aesthetic attained additional significance at prestigious higher educational institutions (e.g., Fig. 27, p. 63). Many colonial-era Colleges including Harvard and Yale began to partake in 'class day ceremonies' associated with academic excellence, where ivy was planted from the mid-1800s onward. This association even led to a prestigious group of such institutions being branded as the 'ivy league', a sports-focused collective including institutions with ivy-covered buildings [149]. Such ivy application could be interpreted as a nostalgic attempt to replicate the aesthetic familiarity and prestige of the ivy-covered institutions of the motherland, which was an agenda also seen at other colonial-era institutions notably in Australia and Canada. With most such examples, ivy was promoted on buildings of a neogothic styling, much like at the many Colleges belonging to Oxford and Cambridge Universities in England (e.g., Fig. 26, p. 62).

*Front Quad of Lincoln College; an Oxford College where the presence of climbing plants has been recorded since the 1860s* [148].

*Front Quad of Merton College; an Oxford College where the presence of climbing plants has been recorded since the 1870s* [148].

*P. quinquefolia (Virginia creeper) at Peterhouse Cambridge, introduced in the 1990s.*

*P. tricuspidata at Churchill College, Cambridge, presence since founding in 1958.*

*P. tricuspidata at rear face of New Court at St. John's College, Cambridge.*

*P. tricuspidata at Gisborne Court, Peterhouse Cambridge.*

*Fig. 26. Climbing plants at Oxford and Cambridge Colleges, photographed between 2017-19.*

*Massachusetts Hall, Harvard University, Cambridge, United States (photographed, circa 1900).*

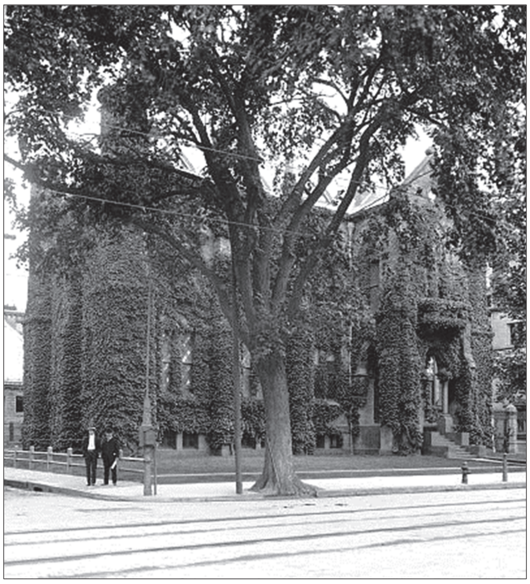

*Yale College, the Art School, Connecticut, United States (photographed between 1890-1910).*

*College Hall, University of Pennsylvania, Philadelphia, United States (photographed between 1900-1910).*

*Ormond College, the University of Melbourne, Australia (photographed in 2003).*

*Fig. 27. Examples of ivy-covered buildings at American (from the Library of Congress Archive, Washington D.C.) and Australian Universities (from Ormond College) with colonial-era founding.*

### 3.1.3 Redefining vertical greening

Contemporary literature describes vertical greening as an intentional effort to cover vertical built surfaces to a significant degree with plant life. Various authors have presented different terminology to describe this principle, and a few have analysed common structures to distinguish categories and derived variants. Presently there is consensus on the presence of two principal categories described as 'green façades' and 'living walls' (Fig. 28, p. 64); predicated principally on the placing of the growth substrate (e.g., [150–152]).

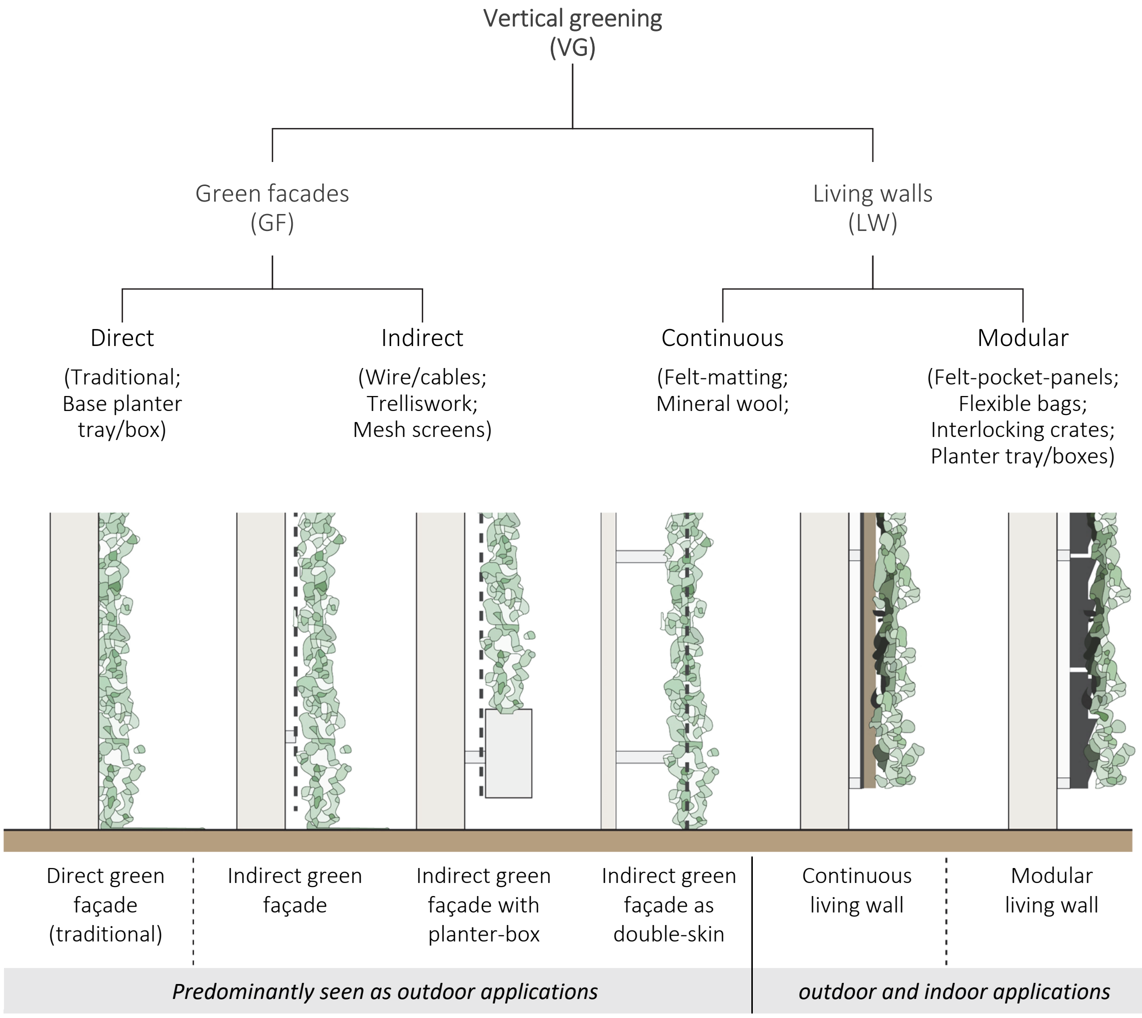


*Fig. 28. Vertical greening categories and some exemplar variants.*

## Green façades (GF)

The most established category of vertical greening is represented by green façades, the earliest examples of which were discussed in section 3.1.2. The growth medium in such features is either a limited ground area or contained within a planter that is placed at the base of a host structure or wall. The plants therefore root at the base and shoots grow up along the surface of the host; which is the reasoning why some authors describe such features as 'ground-based' greening [152]. Typical plants used for this purpose include climbers and wall-shrubs representing a wide range in size, form, and phylogenetic origin. Historical descriptions however have considered climbing traits and mechanisms as the principal means for cataloguing encountered varieties. This is best exemplified by Charles Darwin [153] and his five classes that include: twining plants (e.g., *Dioscorea* spp., *Ipomoea* spp.), leaf-climbers (e.g., *Clematis* spp.), tendril-bearers (e.g., *Vitis* spp.), hook-climbers (e.g., *Uncaria* spp., *Calamus* spp.), and root-climbers (e.g., *Hedera* spp., *Parthenocissus* spp.).

The latter class of root-climbers represents the most common variety of climbers used with green façade applications. These climbers attach to surfaces by growing into irregularities of the host surface and bonding with glandular secretions. The class includes both adventitious root-climbers such as *Hedera helix* (English ivy), and adhesive tendril-climbers such as *P. tricuspidata*. Both types can ascend supports of any form, although require close contact with their surface to adhere. Tendrils of *P. tricuspidata* for example become inflamed at their tips and flatten to form adhesion pads upon contact with the support surface (Fig. 29), which then secretes a bonding substance to achieve a close adhesion. Darwin was particularly interested in such 'viscid fluid' secretions that accumulate at the point of contact and their papillate epidermal cells [153]. Such substances have in recent times been found to include mainly polysaccharides [154], with research examining *H. helix* having identified the presence of uniform nanoparticles that aid the formation of a natural nanocomposite to offer its typically high adhesion strength [155]. It has also been suggested that these adhesive substances lignify with tendril or root senescence to be weather resistant [154]. This lignification in turn contributes to the difficulty in their removal and resultant 'scarring' of support surfaces highlighted earlier.

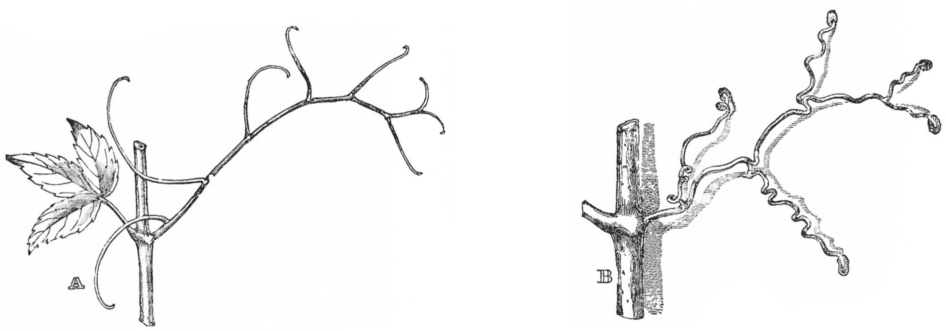


*Fig. 29. Growth of tendril adhesion pads that bond to surfaces; from* [153].

### Living walls (LW)

Living wall approaches are a recent innovation that includes the growth substrate on the vertical face of the host-wall. The approach is referred to by some authors as 'wall-based' greening, and is designed to allow the plants to root into a decoupled substrate carrying support-work that is tied back to a host-wall construction [152]. The systems used allow for water and nutrients to be delivered through embedded closed-loop irrigation and fertigation networks, including automated monitoring and controls [132]. Depending on the application method, such constructions are further differentiated into the two types described as either 'continuous' or 'modular'.

a) b)

*Fig. 30. Mur Vegetal at the Quai Branly Museum in Paris, photographed in September 2014 (a); and being replanted for its tenth anniversary, taken during the November 2017 inspection (b).*

Continuous systems use a bespoke decoupled lightweight support skin, into which plants are individually plugged onsite. The system approaches vary considerably, with some using hydroculture felt or irrigation cloth made from recycled hydrophilic fibres (e.g., *Mur Vegetal* [136], Fig. 30); some that use a deeper zone containing alternative substrates such as clay balls, peat chunks, peat moss, mineral wool, coconut fibres, etc.; and a few that use graded soils [132,156]. Modular wall systems in contrast use offsite manufactured interlocking cassettes or units to build-up a larger vertical surface area. Continuity of the arrangement is ensured by interlocking, which creates a tiled effect initially that mergers with subsequent growth. The units are typically made from lightweight plastic or metal, and filled with either soil or alternative substrates as above. Unlike continuous arrangements, they are transported to site pre-planted and typically include mature plants. This in turn provides rapid assembly, and if need be, disassembly benefit [151].

In recent years, application within indoor environments has encouraged adaptation and innovation. ‘Bio-walls’ for example represent a specialised variant of living walls (continuous or modular) that are adapted to passively enhance air quality aspects in indoor environments [134,151]. The specialist aspect of such systems is represented by the ecosystems cultivated, which include a diverse range of microorganisms and ‘bryophytes’ (non-vascular plants that include liverworts, hornworts, and mosses). Lacking transport and woody tissue to support greater mass, bryophytes have limited growth extents and thrive in moist and reduced sunlight habitats that make them ideally suited for most indoor environments [157]. ‘Active living walls’ (ALW) represents a technical advancement of such walls that enhances air purifying services further by actively forcing air (with mechanical support) through the bio-wall filter [134,158]. They make use of the evaporative cooling potential of plants as well as their phytoremediation capabilities to purify and condition the indoor air supply. This is expected to avoid or reduce the need for other mechanised filtration devices, which in turn could reduce indoor space-conditioning loads [158,159]. Another active soil-less growth approach is 'aeroponics', where plants are grown without a substrate and within a nutrient-rich mist medium. This approach removes the loading burden of a substrate zone and associated support, although includes active misting mechanisms that present specific maintenance requirements. This latter maintenance difficulty together with humidity control concerns have thus far prevented the integration of these approaches as scalable built-environment applications, despite this form of cultivation being used for many years in horticultural and agricultural practice.

Recent developments in living wall approaches have predominantly focused on enhancing system efficiencies. The research and development teams of suppliers have considered alternative growing media, irrigation, fertigation, drainage solutions, and remote monitoring and management systems to deliver efficient technical solutions in terms of performance, along with installation, maintenance, and replacement. Advancements in these areas have led to living walls being considered for a diverse range of building typologies and varying degrees of scale and complexity. Such advancements have meant that these features are now being adopted for retrofit strategies in urban spaces, as well as at building level outdoor and indoor applications [132,134,151,156,160].

## 3.2 Methodology

This study involved a standard review of peer-reviewed papers, reviews, and volume chapters obtained through a database search. The Scopus database was searched for the keywords 'vertical greening', 'green wall', 'green façade', and 'living wall' (including variants); with the 2020 revised search returning 439 results from the 1980s onward to demonstrate a lack of preceding publications (Fig. 31, p. 68). These were first filtered to include those with vertical greening as the principal subject matter (criterion 1: #209), and further refined to consider in detail those that addressed the study of their microclimate modification contributions, be it experimental, case study, or simulation-based (criterion 2: #104). The review was also supplemented by seven unstructured interviews with experts, addressing aspects related to current practice, sustainability concerns, and continuing innovation.

## 3.3 Findings

The earliest research observations of vertical greening are from botanical sources, where authors had considered plant behaviours pertinent for direct and indirect greening applications (e.g., [141,153]). Studies discussing ecosystem service contributions are a recent development first evident from the 1980s [145], while quantitative performance evidence considering green façades is represented from the late-80s onward (e.g., [161]). The revised review highlighted interest in vertical greening aspects increasing rapidly from 2010 onward, with the years since project onset showing steady growth (Fig. 31). Owing to its relative novelty, investigations concerning living walls has only a limited history. The category however represented the dominant focus of recent studies, with the 2020 revision highlighting a relative increase in dominance since 2018 (from 54→69%, including ALWs). This was also stressed in the consultant interview responses, where growth in commissions was reported as exemplified in Fig. 32 by the breakdown of projects provided by a leading UK-based supplier. The most significant observation of the review relates to the dominant representation of outdoor application studies (77%); with the representation profile remaining unchanged since 2018. This contrasted with consultant responses, where most recent enquiries and commissions were said to be for indoor applications [162].

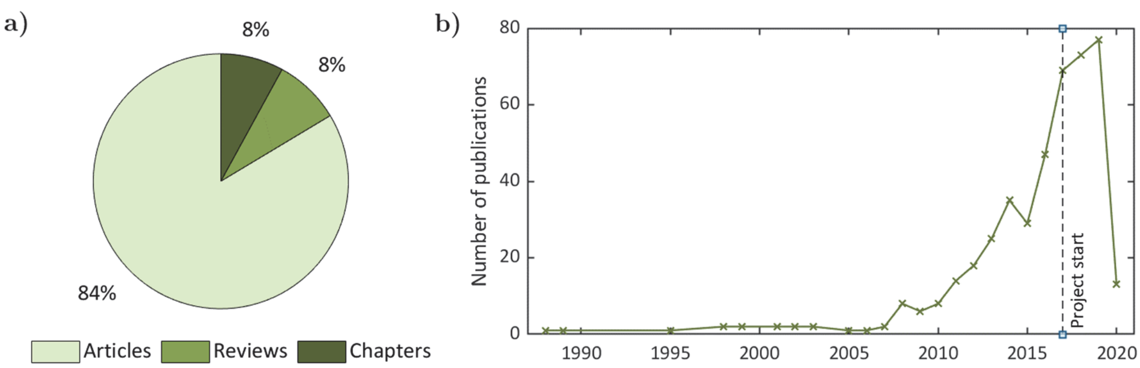


*Fig. 31. Scopus database results by publication type (a), and publications per year (b).*

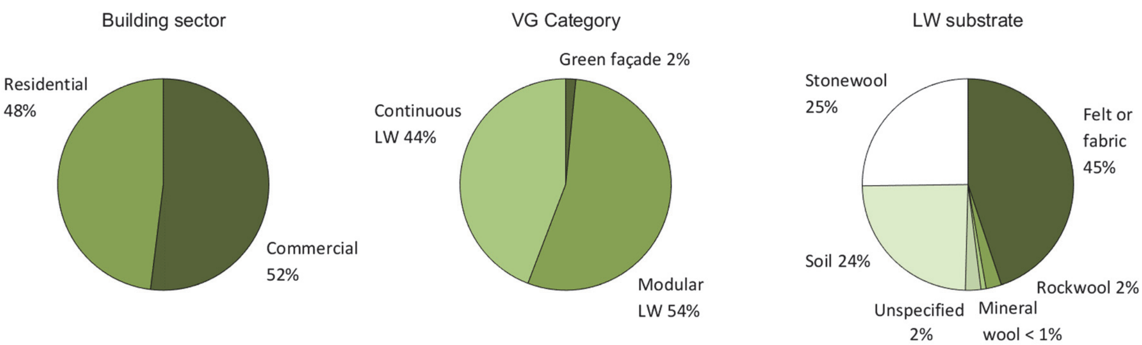


*Fig. 32. Vertical greening workload representation from a UK-based supplier; 2018-19 data* [162].

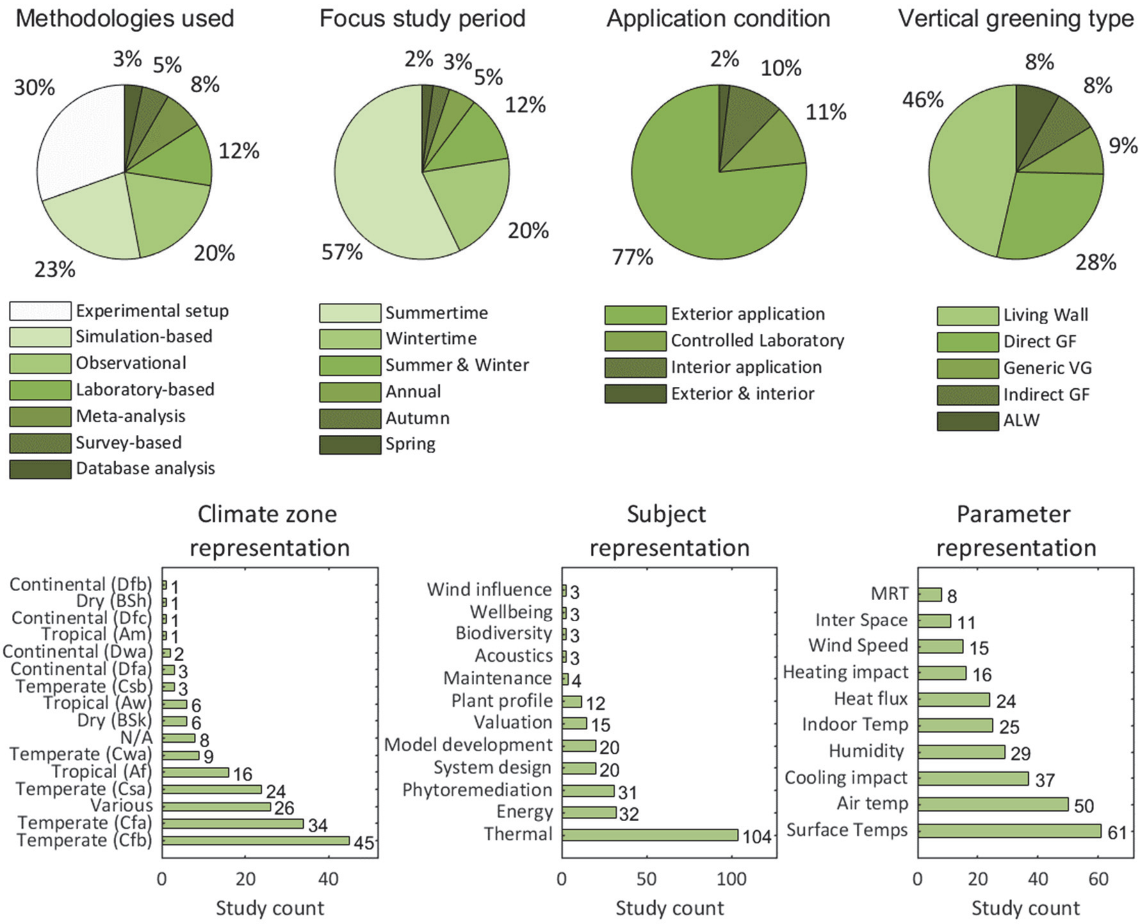


*Fig. 33. Breakdown of 209 studies reviewed (includes multiple counts).*

The updated and distilled body of literature reviewed including 209 studies is represented in Fig. 33 according to methodologies used; focus study period; application condition; vertical greening typology; and representation according to subject, parameter, and climate zone. The breakdown highlighted dominant focus on examining thermal aspects (104 studies, ~50%), with the 2020 update highlighting continued increase since 2018, although with reduced proportional dominance (from ~50→39%); while significant growth in studies concerning phytoremediation (including air quality improvement) was noted (~15→19%). In terms of seasonal bias, summertime assessments dominated (57%), with the update highlighting little change since 2018. Climate zone representation was dominated by 'temperate oceanic' (Cfb) and 'humid subtropical' (Cfa) studies (21.5 and 16.3% respectively). This is influenced by the geographical spread of research interest, with Europe dominant (41%, of which the UK represented 6%), followed by East Asia (15%, China: 9%) and Australasia (12%, Australia: 8%). Studies from North and South America, and Africa were notably sparse (<2%). The 2020 update highlighted Cfa climate representation to have increased to present the highest (~16→21%), mainly credited to greater studies from Chinese sources.

Examining the methodologies of the studies highlighted the majority to have been carried out under experimental conditions at ideal test sites or rigs (30%), limited to short periods of monitoring, and/or limited to a narrow range of plant species [41,152,163,164]. These conditions are mostly unrepresentative of in-situ installations, with the use of single or limited range of species in particular contradicting design guidance [165,166]. Experimental conditions logically contradict such best practice to facilitate the gathering of simplified data necessary to improve transferability between studies. Even with such normalising attempts, the diversity of installation assemblies currently in use makes this transferability a challenge [152,164,167]. Observational studies on the other hand are severely challenged by the absence of generalisable case study sites with controllable conditions, which explains the reluctance to engage with in-situ monitoring, and the resultant reduced representation of studies (20%). Simulation approaches that avoid monitoring difficulties altogether have received greater attention in response (23%), with the 2020 update having highlighted an increase in interest to match experimental design representation.

With policy representation, there is some progress towards including vertical greening in the wider agenda to enhance urban green infrastructure. At the European level this is reflected in the *EU 2030 Biodiversity Strategy*, and is associated with *EU Green Infrastructure Policy* [168,169]. National level recognition in the UK is expressed through a White Paper [170], which is based on the findings of the *National Ecosystem Assessment* [171]. In the European context there is a general lack of national level guidance specifically addressing such features, while certain cities in contrast have dedicated greater attention in their respective metropolitan policies. As examples, the German cities of Munich, Cologne, and Hamburg have enacted subsidy programs, while Berlin has a long history of initiatives with ~250,000 m$^2$ of vegetated façades implemented between 1983-97 [145], and the introduction of the 'Biotope area factor' (BAF) planning parameter to account for all greening strategies [172]. In Sweden, Malmö had developed a similar 'green space factor' [173], while in France, Paris introduced its 2020 surface greening objective ('*Objective 100 hectares*'), and the Italian municipalities of Firenze, Brescia, Carugate, and Genoa have all introduced favourable building codes [174]. In the United Kingdom, decision-making on implementation aspects are made at the local level, with a few Local Planning Authorities having addressed this with generic guidance [175]. London for example is most prominent, with policy included in the London Plan of 2008, and guidance published as part of the All

London Green Grid (ALGG) policy framework [119,176,177]. While such metropolitan policies are gaining ground in implementing some research findings, concerns still hinder widespread support. These stem from the lack of in-situ performance evidence from temperate climates and resulting concern for the sustainability of such systems, with criticism targeted at water, nutrient, and energy use efficiencies [157,178,179]. Valuation has long been identified as one means to counter criticism and justify promotion [175,180,181], with some recent studies having begun to address this demand (e.g., [175,179,182–184]).

## 3.4 Discussion

The published research from predominantly outdoor application assessments initially seek to determine the climates in which vertical greening approaches could generate and sustain flourishing ecosystems, followed by the examination of their feedback responses to the climates they occupy. The latter presents both benefits to human interaction with such features as well as certain risks. Built environment discourse however is at present biased towards emphasising benefits than risks, with the discussion of certain risks still confined to specialist knowledge areas such as plant sciences.

### 3.4.1 Local climate influence

The review of studies considering outdoor vertical greening performance in cities highlights local conditions characterised by light, temperature, moisture, and the wind climate as key determinants in generating and sustaining ecosystem service provision. Significant variance of such parameters determines stress responses, with extremes and exposure determining failure. With indoor installations however, the climate encountered operates within a narrow band of variance relative to outdoors. This is particularly the case for conditioned buildings where indoors are maintained within an occupant comfort band that is equally suitable for the optimal growth of most plants [136]. Temperature related stress risk is therefore limited, with only localised stress from cold or warm draughts likely to cause failures [134]. Indoor humidity conditions in contrast can present a moderate risk to plant health as these are maintained at lower levels to ensure occupant comfort (RH 40-70%). As some plant species selected for such indoor installations (e.g., tropical shade-loving) tend to require high canopy humidity to maintain foliage health (RH 85-95%), comfort level RH may present the risk of foliage water stress. Vertical canopies however have been observed to maintain a self-hydrating microclimate to mitigate this risk to an extent [136].

The most significant indoor climate risk is light availability, which is factored when selecting species for indoor environments and often results in the inclusion of tropical shade-loving plants [132,134,136]. Typical indoor light intensity below 10 $\mu mol \cdot m^{-2} \cdot s^{-1}$ of photosynthetically active radiation (PAR) is likely to result in negligible efficacy in plant ecosystem service provision. It has been observed that horticultural light specifications that are much higher than this are also inadequate to ensure useful ecosystem service provision such as net $CO_2$ removal [185]. This may be overcome by the provision of artificial PAR, although the approach could have a negative effect on energy saving and ecosystem benefits expected. It is also significant to note that low-light tolerant species exhibit lower photosynthesis and respiration rates [185], which in turn influences the beneficial ecosystem feedback that can be reasonably expected.

### 3.4.2 Feedback to local microclimate

Vertical greening feedback to the microclimates they occupy presents their ecosystem benefits as well as risks. Studies characterise feedback influences by mainly examining the parameters of proximate surface temperature (ST | $T_{surf}$), air temperature ($T_{air}$) and relative humidity ($RH$), and to a lesser extent wind flow (predominantly velocity, $V_{air}$).

#### Thermal feedback

Surface temperature is by far the most common parameter measured to assess thermal influences of outdoor applications. Main measurements taken are of either the foliage or substrate relative to a control condition, with some studies extending measurements to interstitial as well as indoor surfaces. In general, research shows good representation across observational, experimental, and modelling approaches taken by studies dating from 1980 onward. Examples of direct green façade studies are represented in: [88,138,157,163,186–201]; indirect green façades in: [88,89,189,190,202–207]; and living walls in: [88,89,189,208–218]. In summary, they highlight significant surface temperature reductions resulting from greening presence (up to 30 K, [218]), with evidence of higher summertime benefit offered by living walls relative to green façades (e.g., [88,89]). The limited wintertime studies available highlight green façades to provide a beneficial warming influence (e.g., [138,199,200]), while living walls provide reduced benefit (e.g., [208]). Across all typologies, these effects seem to be most pronounced on the harshest of days in both summer and winter, with cooling performance during the daytime and a potential warming influence during the night-time likely (e.g., [196,199–201,203–205]). No significant observations or results are presently available for indoor installation applications, save for limited laboratory-based observations that have examined ALWs (e.g., [158]). Reduced penetration of solar radiation however could be hypothesised to present lower surface temperature variance in such indoor environment applications.

As indirect green façades (by default) and most living wall constructions (for buildability) include an interstitial air cavity/gap, studies have also focused on examining this feature's contribution to their overall thermal performance. Examples of indirect green façade studies are represented in: [190,192,203,207,219–222]; and living walls in: [214,217,220]. Such cavity microclimates have been found to be typically cooler than ambient conditions [217], with a comparison study suggesting living walls to present cooler cavities than indirect green façades [220]. Relative humidity on the other hand has been reported to be mostly constant subject to cavity depth [217], with a comparison study finding indirect green façades to present higher values than living walls [220]. Cavity depth is stressed as a critical factor, with smaller cavities performing better thermally, although with increased humidity [217]. Considering diurnal changes had suggested smaller cavities to perform best in the morning, while in the afternoon the converse was observed [214]. These observations are explained by the degree of coupling that is achieved between the transpiration cooling from the vegetation foliage and the building, which is dependent on the cavity depth as well as system arrangement characteristics [223]. Larger cavities present relatively weaker coupling by reducing vegetation proximity with the building envelope, which in turn sacrifices the relative significance of the transpiration cooling benefit to the dominance of the shading effect. This is more apparent with indirect green façade performance given their double-skin arrangement presenting an increased cavity by default. They are thus identified to perform mainly as a solar interceptor with the dominant influence of shading, and with the added secondary influence from evapotranspiration contribute to typically lower cavity temperatures in the summer (with higher humidity), while in winter they perform mainly as a wind barrier [219]. Some double-skin studies have emphasised the summertime advantage of the lower cavity temperatures to advocate further enhancement by introducing inter-cavity vegetation (e.g., [221]). Recent innovations presented by Penaranda-Moren & Korjenic [222] for example utilised this form of enhanced cavity cooling to increase the yield of a photovoltaic integrated double-skin arrangement.

Studies that prioritise the investigation of microclimate modifications use $T_{air}$ proximate to an installation as the essential parameter to be measured. Such measurements are typically taken relative to a control condition, and to a lesser extent with increasing distance from the host surface to assess effective range. The studies ranging from observational studies to model simulations (examples in Table 6), suggest the immediate $T_{air}$ modifications of vertical greening including passive direct, indirect, or living wall approaches to range between 0-3 K, while the effective range seldom exceeds the proximate zone from the wall surface (e.g., [89,157,187,195,197,198,224,225]). Best performance has been demonstrated when conditions are drier and warmer (i.e., in the summer), relative to colder (i.e., autumn and winter) conditions (e.g., [224]). There is however insufficient data amassed at present to suggest relative order of performance between the different typologies.

A secondary parameter considered by a few microclimate studies is mean radiant temperature (MRT), which is necessary to consider when characterising influence on occupant comfort. Direct green façade examples of studies are represented in [167,226]; indirect green façades in: [187]; and living walls in: [225,227]. The general range of values across the different observational-to-modelling approaches and system typologies examined suggests an MRT influence of <4 K, with performance peak demonstrated when conditions are drier, warmer, and considerably sunnier (summer), relative to colder (autumn and winter), overcast conditions (i.e., dependent on solar radiation loading).

Table 6. Vertical greening influence on air temperature ($T_{air}$).

| VG type | Study | Location (climate) | Method (detail) | Plant species (type) | Period (orientation) | Proximate $T_{air}$ cooling influence (K) |
|---|---|---|---|---|---|---|
| Direct green façade | [197] | Greece, Thessaloniki (Cfa) | Observational (five-storey building façade monitored) | *P. tricuspidate* (climber) | Summertime (east) | Foliage zone $T_{air}$ reduction between **1-2 K**. |
| Direct green façade | [157] | UK, Reading (Cfb) | Experimental (brick walls monitored under controlled conditions) | *Jasminum* sp., *Hedera* sp., *Stachys byzantina*, *Fuchsia* sp., *Cupressus macrocarpa* (climbers & shrubs) | Summertime (north and south) | Highest **3 K** $T_{air}$ cooling from *Prunus laurocerasus* during mid- to late-afternoon. |
| Direct green façade | [198] | USA, Chicago (Dfa) | Experimental (#4 campus building façades monitored) | *P. tricuspidate* (climber) | Summertime (facing east, west, north, and south) | Cooling between **0.8-2.1 K** on ave. adjacent to façades. |

| VG type | Study | Location (climate) | Method (detail) | Plant species (type) | Period (orientation) | Proximate $T_{air}$ cooling influence (K) |
|---|---|---|---|---|---|---|
| Direct green façade | [228] | Teheran, Iran (Bsk) | Observational & simulation (wall fronting road monitored and simulated in ENVI-met) | Unspecified (climber) | Summer & wintertime | Summer: **0.4-0.8 K**. Winter: **0.4-1.3 K**. Effective range: **0-0.5 m**. |
| Direct green façade | [191] | China, Guangzhou (Cfa) | Experimental (test rig monitored) | *Pyrostegia venusta* (climber) | Wintertime (west) | Hottest period of day (14:00–17:00), max. **1.9 K** WBGT. |
| Direct green façades (#3) | [188] | Germany, Berlin (Cfb) | Observational (#3 campus façades monitored) | *P. tricuspidata*, *H. helix*, *Fallopia baldschuanica* (climbers) | Summertime (south-west, east, & west) | No $T_{air}$ cooling effect in street canyon. |
| Direct, indirect green façades & Living wall | [88] | Netherlands, Delft, Rotterdam, Benthuizen (Cfb) | Observational (20s façade, 70s residential façade, and a rural LW, monitored) | *H. helix* (climber) Various (herbaceous) | Autumn (north-west) Summer & winter (north-east) (west) | No $T_{air}$ difference within **1 m** zone. |
| Indirect green façade | [89] | Singapore, HortPark (Af) | Experimental (modular trellis test rig monitored) | Unspecified (climber) | Summertime (unspecified) | Negligible $T_{air}$ effect. |
| Indirect green façade | [187] | Japan, Fukuoka (Cfa) | Observational (Kindergarten veranda sunscreen monitored) | *Wisteria sinensis* (climber) | Summer daytime (south-west) | Between **1-3 K** ambient $T_{air}$ cooling. |
| Living wall (ALW) | [158] | Spain, Sevilla (Csa) | Laboratory (ALW test rig in a hall monitored) | Various (herbaceous) | Summertime (indoor) | **4 K** $T_{air}$ cooling near installation. Max. **6 K**. |
| Living wall | [229] | Australia, Canberra (Cfb) | Observational (campus building, monitored pre and post intervention. | Various (herbaceous) | Summertime (indoor, south corridor) | No significant $T_{air}$ change post intervention. |
| Living wall (*MV*) | [224] | Spain, Madrid (Csa) | Observational (CaixaForum case study monitored) | Various (herbaceous) | Summer & autumn (south-east) | Summer cooling max. range between **2.5-2.9 K**. Autumn max. **<1.5 K**. |
| Living walls (#7) | [89] | Singapore, HortPark, (Af) | Experimental (test rigs monitored) | Various (herbaceous) | Summertime (unspecified) | Peat moss substrate: up to **3.3 K** reductions at **0.15 m**; **0.60 m** range. |
| Living walls | [225] | France, La Rochelle (Cfb) | Experimental (monitored reduced-scale canyon rig, at 1:10 scale) | Various (herbaceous) | Summertime (east & west) | **1.5 K** $T_{air}$ reduction in canyon. |

Studies have demonstrated vertical greening application on building exterior wall surfaces to increase their thermal buffering properties and in turn improve indoor comfort; with cooling influence in the summer (e.g., [210,215,230–233]), and heat conservation in winter (e.g., [209]). The studies typically use indoor air or operative temperature to characterise these benefits, with direct green façade examples represented in: [161,191,210,233,234]; indirect green façades in: [189,203,230,231,234,235]; and living walls in: [159,189,209,210,213–215,234,236,237]. The investigation of such influences when vertical greening is applied within an indoor environment is lacking. Few exceptions are presented by laboratory-based studies of ALWs, where cooling efficiency has been found to be at its best when the initial room conditions are drier and warmer [158,159]; broadly in agreement with findings from outdoor application studies. The cooling gained by such specialist applications vary from >0 to ~6 K, with any benefit contributing to energy savings by reducing peak demands from typically energy intensive mechanical cooling systems [159,238,239].

### Moisture feedback

Although relative humidity is monitored in most vertical greening assessments as a background variable, only a few studies focus on its specific characterisation. These present measurements mainly taken relative to a control condition, and to a much lesser extent with increasing distance from the host-wall to assess effective range. The studies generally acknowledge vertical greening to contribute towards a moderation of moisture influence. As examples, a recent pre- and post-intervention study considering an indoor living wall found the addition to reduce humidity variance from 3→1% [229], while an outdoor green façade study found the moderating effect to be less potent than the surface temperature moderation observed [138]. The canopy depth (denoted later as $z_{veg}$), is a significant factor in this moderating function, while higher canopy $LAI$ encourages the greater accumulation of humidity [195,198]. Susorova *et al.* [198] however found the $RH$ increase within the layers to be driven by the cooling of the canopy air temperature, as opposed to increase in absolute humidity ($AH$). The humidity produced by transpiration was suggested to be repurposed by the canopy to maintain foliage health, particularly during warmer summer conditions. This self-generating, bio-protective humid microclimate therefore assists in sustaining good plant health [46,136], which is a significant advantage in indoor climates where humidity is typically maintained at lower levels to facilitate building occupant comfort.

The available studies considering both vertical greening categories present evidence to suggest $RH$ immediately beyond the canopy zone to be typically greater than the ambient value (e.g., [195,229,240]). Beyond this immediate zone however, the influence range or decay is not well characterised at present. An exception was provided by Blanc [136] where $RH$ in a temperate climate was reported to demonstrate decay from 90% at 0.05 m; 80% at 0.1-0.2 m; 70% at 0.3-0.5 m; 60-65% at 1 m; and normalise at 59% ambient humidity around 1.5 m away from the hydroculture felt of a *Mur Vegetal* system. In hot and humid climates however, the decay to ambient levels have been described to occur within a much narrower distance (e.g., <0.15 m [195]). More data however is needed to clarify $RH$ decay, particularly in relation to indoor conditions given the potential for increased levels posing risk to both occupant thermal comfort and health. Influence also needs to be characterised in relation to both $RH$ and $AH$; the latter presenting a better description of the capacity to affect other humidity associated risks to health, such as pathogen and mould growth.

### Wind flow feedback

Greenspace studies discussed in Chapter 2 highlighted the surface roughness enhancement of vegetation canopies to exert mean flow transformation by introducing mechanical turbulence [55]. The introduction of surface greening similarly enhances a building's interaction with mean flow by increasing its micro-scale roughness (Fig. 34, p. 78). The resulting reduction in surface proximate mean flow can improve the thermal resistance of the building envelope to reduce heat losses. Surface roughness induced turbulent eddies in contrast can enhance the sensible and latent flux of surfaces irrespective of temperature and vapour gradients, which could in turn serve to increase heat dissipation. The characterisation of such surface proximate flow regime influences however are underrepresented at present.

When assessed, flow modification is typically characterised by surface proximate flow velocity measurements taken relative to a control condition, and to a much lesser extent with increasing distance from the host-wall to assess effective range. The available observations at present exclusively relate to outdoor applications (Table 7, p. 79), with mean flow reductions demonstrated to vary between vertical greening categories and their variants (e.g., [88,198,211]). Perini *et al.* [88] identified that the lower wind velocities observed in the foliage zone (<0.2 $m \cdot s^{-1}$) could be used to equate exterior surface resistance with interior resistance, which in turn affects the total thermal resistance calculation of the envelope to present potential energy savings. With dense foliage canopies, the reduced mean flow above the canopy is exponentially reduced within the canopy zone [54,88]. As wind velocity has an inverse relationship with boundary-layer thickness, which in turn has an inverse relationship with boundary-layer conductance, leaves within canopies are observed to have lower boundary-layer conductance and thus are poorly coupled with the atmosphere. In such conditions transpiration efficiency will be mostly driven by radiation incidence [54]; which in turn is reflected in the diurnal pattern of cooling observed. This suggests that in indoor conditions where radiation incidence is restricted, thicker canopies are likely to be less effective in delivering the transpiration cooling benefits expected.

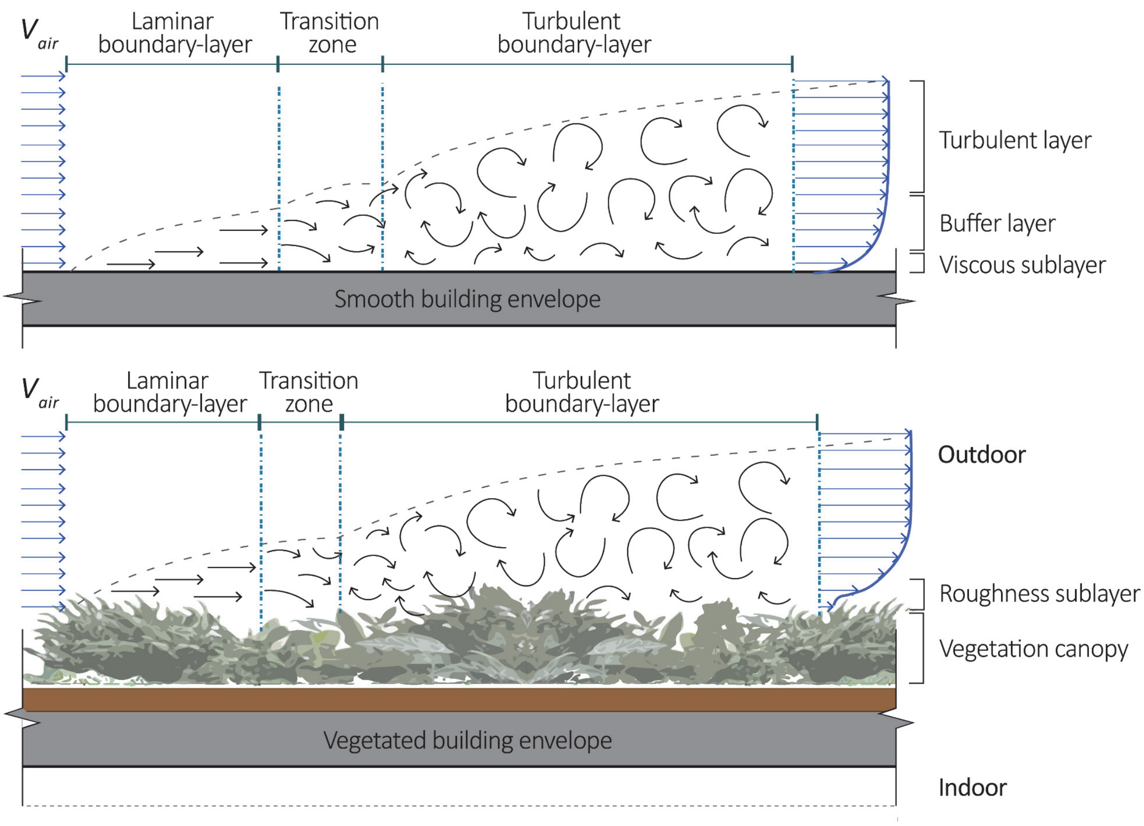


*Fig. 34. Building envelope interaction with mean air flow.*

The relatively cooler surface presented by an installation could be hypothesised to generate cold radiation effects, and the formation of a 'downdraught effect' resulting from natural convective boundary-layer flows along its surface. Such cold surface effects are well-documented in indoor environments, with studies mainly addressing occupant discomfort arising from proximity to cold window surfaces [241]. Manz & Frank [242] found such draughts to be critical for discomfort relative to reduced operative temperatures or radiation asymmetry, while Heiselberg [241] found discomfort to rapidly decrease within the first 2 m off the surface to highlight decay. The potential relevance of such surface temperature influences however have yet to be assessed in relation to vertical greening installations. With outdoor conditions such effects are likely to be detectable only under stable conditions with very low background wind velocities, as at higher velocities turbulent mixing rapidly normalises such microscale effects. Vox *et al.* [194] for example observed green façade cooling influence to rapidly diminish beyond 4 $m \cdot s^{-1}$. Given that in indoor environments flow velocities are considerably lower, the potential for such convective boundary-layer flows to develop could be greater. The magnitude of this influence in turn could either threaten or benefit the building occupant thermal experience. This hypothesised flow influence therefore warrants further investigation, and is examined later in Study 1.

Table 7. Vertical greening influence on surface proximate wind flow.

| **VG type** | **Study** | **Location (climate)** | **Method (detail)** | **Species (type)** | **Period (orientation)** | **Wind flow reductions (% \| $m \cdot s^{-1}$)** |
|---|---|---|---|---|---|---|
| Direct green façade | [88] | Netherlands, Delft (Cfb) | Observational (1920s façade monitored) | *H. helix* (climber) | Summer & wintertime (north-west) | **71%** relative to velocities 1 m in front of façades. |
| Direct green façade | [198] | USA, Chicago (Dfa) | Experimental (#4 campus building façades monitored) | *P. tricuspidata* (climber) | Summertime (east<br>west<br>north<br>south) | <br>**42%**<br>**43%**<br>**0%**<br>**18%** |
| Indirect green façade | [88] | Netherlands, Rotterdam (Cfb) | Observational (70s residential façade monitored) | *H. helix* (climber) | Summer & wintertime (north-east) | **62%** relative to velocities 1 m in front of façades. |
| Living wall (trough) | [88] | Netherlands, Benthuizen (Cfb) | Observational (rural LW monitored) | Various (herbaceous) | Summer & wintertime (west) | **15%** relative to velocities 1 m in front of façades. |
| Living walls (modular) | [211] | UK, London (Cfb) | Observational (#3 sites monitored) | Various (climbers & herbaceous) | Summer (east, north, east) | **0.7 $m \cdot s^{-1}$** relative to 2 m in front of façade. |

### 3.4.3 Building energy use implications

Hygrothermal feedback from plant cover and its influence on building energy use has been well-established by previous horizontal greening studies [95]. Vertical greening studies considering outdoor applications have similarly highlighted the modification of surface temperatures to affect climate thermal load transfer or wall flux into indoor building environments [243]. Such flux reductions have been reported with the application of several vertical greening typologies and variants, exemplified by the green façade study by Susorova *et al.* [198], grass-based living wall study by Cheng *et al.* [212], and the Mazzali *et al.* [216] study of three living wall variants that also measured outgoing flux to identify an enhanced envelope cooling effect. These flux modifications in turn could present substantial changes to indoor space-conditioning loads and resultant energy use [163,235], although the magnitude of change is dependent on envelope constructions and their thermal resistance, as well as background climate conditions [208].

Table 8. Vertical greening influence on summertime cooling energy use.

| **VG type** | **Study** | **Location (climate)** | **Method (detail)** | **Plant species (type)** | **Period (orientation)** | **Cooling energy reduction (% \| kWh)** |
|---|---|---|---|---|---|---|
| Direct green façade | [196] | China, Beijing (Dwa) | Observational (two-story campus building monitored) | *Hedera* sp. (climber) | Summertime (west) | **28%** peak-cooling load for clear summer day. |
| Direct green façade | [233] | Greece, Thessaloniki (Cfa) | Simulation (building zone using a lumped capacitance thermal-network model) | *P. tricuspidata* (climber) | Summertime (west<br>east<br>south<br>north) | Estimated cooling loads:<br>**20.08%**<br>**18.17%**<br>**7.60%**<br>**4.65%** |
| Generic vertical greening | [244] | Daejeon, Korea (Cwa/ Dwa) | Simulation (#3 campus buildings using DesignBuilder) | Unspecified | Summertime:<br>Spring:<br>(north, south, & east) | Overall, **12%**<br>Overall, **33%**<br>(electricity consumption) |
| Indirect green façade | [189] | Spain, Puigverd de Lleida (Csa) | Experimental (cuboid pod monitored) | *P. tricuspidata* (climber) | Summertime (east, west, & south) | **16.7%** (10 days in Aug, with internal loads)<br>**43.4%** (10 days in Jul, without loads) |
| Indirect green façade | [204] | Spain, Lleida (Csa) | Experimental (cuboid pod monitored) | *P. tricuspidata* (climber) | Summertime (east, west, & south) | **33.8%**; or<br>**19.4%** consumption reduction per solar irradiation kWh. |
| Indirect green façade | [203] | Spain, Lleida (Csa) | Experimental (cuboid pod monitored) | *P. tricuspidata* (climber) *LAI* 3.5-4 | Summertime (east, south, & west) | **34%** electricity saving, main contributions from east and west. |
| Indirect interstitial green screen | [221] | Netherlands, Delft (Cfb) | Laboratory (double-skin test rig monitored under controlled conditions) | Unspecified (herbaceous) | Summer simulated (N/A) | **20%** cooling load<br>**10%** ventilation fan operation hours (natural ventilation option). |
| Living wall | [204] | Spain, Lleida (Csa) | Experimental (cuboid pod monitored) | *Rosmarinus officinalis* & *Helichrysum thianschanicum* (shrubs) | Summertime (east, west, & south) | **58.9%**, or<br>**23.4%** consumption reduction per solar irradiation kWh. |

| VG type | Study | Location (climate) | Method (detail) | Plant species (type) | Period (orientation) | Cooling energy reduction (% \| kWh) |
|---|---|---|---|---|---|---|
| Living wall | [245] | Singapore (Af) | Simulation (#3 scenarios of hypothetical 10-storey building, using TAS) | *LAI* specified (various) | Summertime (east, west, & south) | Ranged between **10-32%** cooling savings for scenarios. |
| Living wall | [189] | Spain, Lleida (Csa) | Experimental (cuboid pod monitored) | *R. officinalis* & *H. thianschanicum* (shrubs) | Summertime (east, west, & south) | **27.8%** (10 days in Aug, with internal loads) **50.3%** (10 days in Jul, without loads) |
| Living wall | [246] | Greece, Athens (Csa) | Simulation (street canyon scale-model using TRNSYS) | Various (herbaceous) | Summertime (east & west) | **37%** in street canyon (aspect ratio: 1); **33%** as standalone building. |
| Living wall | [247] | France, La Rochelle (Cfb) Morocco, Casablanca (Csa) | Experimental & simulation (street canyon scale-model using TRNSYS) | Various (herbaceous) | Summertime (east & west) | La Rochelle: **7.8** to **2.5 kWh·m$^{-2}$** Casablanca: **17.6** to **7.4 kWh·m$^{-2}$** |
| Living wall | [248] | Italy, Genoa (Cfb/Csa) | (Observational (office façade monitored) | Various (climbers & shrubs) | Summertime (south) | Calculated saving: Ave. **26.5%** |
| Living wall & Green roof | [249] | Australia, Brisbane (Cfa) | Simulation (parametric study of building zone using EnergyPlus) | *LAI* specified (various) | Summertime (north south west east) | Overall: **18%** **24%** **11%** **19%** **17%** |
| Living wall (modular) | [212] | Hong Kong (Cwa) | Experimental (residential façade setup monitored) | *Zoysia japonica* (grass) | Summertime (south-west) | Reduction of **1.45** ±1.85 **kWh** of daily energy use. |

Space-conditioning impact is mainly discussed in relation to building façade application influence on indoor summertime cooling loads (Table 8, p. 80). This preference is attributed to the evidence discussed earlier in relation to optimal plant-based surface cooling benefits being evident during this period. There is notable preference for this hypothesis to be investigated using simulation approaches, with results having estimated reduced indoor temperatures, improved thermal comfort, and reduced cooling loads (e.g., [233,249–251]). The dominant preference however is for using experimental design, with many examples presented for the different categories and their variants identifying cooling energy savings. As examples, the direct green façade study by Susorova *et al.* [198] reported small savings from the solar shading effect and additional savings from reduced air infiltration; while the double-skin indirect green façade study by Pérez *et al.* [203] reported main savings from east and west orientations to stress solar shading influence; and the grass-based living wall study by Cheng *et al.* [212] attributed savings to the lower and delayed heat transfer of the wall build-up (i.e. enhanced thermal resistance and inertia). From these studies, a strong correlation between solar irradiation and energy savings is generally observed to suggest higher relative cooling energy savings in climates with high irradiance [204].

The relatively fewer studies that have considered the wintertime influence of building façade application (Table 9), have generally observed a moderating effect with colder temperatures to offer thermal benefit [252]. Observational studies by Bolton *et al.* [200] and Cameron *et al.* [199] for example identified the insulating and shielding thermal benefits offered to reduce heating loads, while better performance was highlighted with increased cover and during relatively harsher conditions. The Coma *et al.* [204] comparative study also identified better performance with a living wall relative to a green façade. More evidence however is required for living wall applications as some studies have reported negligible savings (e.g., [189]), while a minority have reported increases in expenditure (e.g., [189,247]). The few studies that have considered the annual impacts of façade application counter this potential shortcoming by stressing net energy use to still offer a saving, given that cooling energy expenditure is relevant for the building profile [247]. The green façade evidence base in contrast broadly concurs with the wintertime insulating benefit of green-cover, and supports their use as an energy saving strategy particularly for retrofitting older buildings, where other options may be unsuitable [157,178,199].

Table 9. Vertical greening influence on wintertime heating energy use.

| **VG type** | **Study** | **Location (climate)** | **Method (detail)** | **Plant species (type)** | **Period (orientation)** | **Heating energy reduction** (%\|$m^2 \cdot K \cdot W^{-1}$) |
|---|---|---|---|---|---|---|
| Direct green façade | [200] | UK, Manchester (Cfb) | Observational (campus façade monitored) | *H. helix* (climber) | Late-winter (north) | ~**8%** |
| Direct green façade | [199] | UK, Reading (Cfb) | Experimental (brick-cuboid monitored) | *H. helix* (climber) | Winter 1<br>Winter 2<br>(south) | **21%**, ave. 1.1 $kWh \cdot wk^{-1}$<br>**37%**, ave. 2.2 $kWh \cdot wk^{-1}$ |
| Direct green façade | [252] | France, Lille (Cfb) | Laboratory & simulation (guarded hotplate for conductivity measurements, and residence modelled in TRNSYS) | *Hedera* sp. & *P. quinquefolia* (climbers) | Wintertime (N/A) | **3%** heating load reduction (50 mm cover depth) |

| VG type | Study | Location (climate) | Method (detail) | Plant species (type) | Period (orientation) | Heating energy reduction (%\|m²·K·W⁻¹) |
|---|---|---|---|---|---|---|
| Generic vertical greening | [244] | Korea, Daejeon, (Cwa/ Dwa) | Simulation (#3 campus buildings, using DesignBuilder) | Unspecified | Wintertime: Autumn: (north, south, east) | Overall, **55%** Overall, **28%** (electricity consumption) |
| Indirect green façade | [189] | Spain, Lleida (Csa) | Experimental (cuboid room monitored) | *P. tricuspidata* (climber) | Wintertime (east, west, & south) | **-9.3%** (13 days in Dec, with internal loads) **-6.2%** (13 days in Jan, without loads) |
| Indirect green façade | [204] | Spain, Lleida (Csa) | Experimental (cuboid room monitored) | *P. tricuspidata* (climber) | Wintertime (east, west, & south) | Ave. **-0.36%** (Dec) & Ave. **1.90%** (Jan-Feb) |
| Indirect green façade | [235] | China, Hunan (Cfa) | Experimental (greened and reference rooms monitored) | Sedum (succulents) | Wintertime (east, south, west, & north) | **18%** (relative to reference room) |
| Indirect interstitial screen | [221] | Netherlands, Delft (Cfb) | Laboratory (double-skin test rig monitored) | Unspecified | Wintertime simulated (N/A) | **2.1%** increase in ventilation fan operation hours. |
| Living wall | [189] | Spain, Lleida (Csa) | Experimental (cuboid room monitored) | *R. officinalis* & *H. thianschanicum* (shrubs) | Wintertime (east, west, & south) | **-9.5%** (13 days in Dec, with internal loads) **-5.9%** (13 days in Jan, without loads) |
| Living wall | [204] | Spain, Lleida (Csa) | Experimental (cuboid room monitored) | *R. officinalis* & *H. thianschanicum* (shrubs) | Wintertime (east, west, & south) | Ave. **2.96%** (Dec) & Ave. **4.20%** (Jan-Feb) |
| Living wall | [247] | France, La Rochelle (Cfb) Morocco, Casablanca (Csa) | Experimental & simulation (street canyon scale-model, using TRNSYS) | Various (herbaceous) | Summertime (east & west) | La Rochelle: 'Negligible' Casablanca: 'Slight increase' |
| Living wall & Green-roof | [249] | Australia, Brisbane (Cfa) | Simulation (parametric study of building zone using EnergyPlus) | *LAI* specified (various) | Wintertime (north, south, west, & east) | Overall **46%** |
| Living wall, planter-box (#2) | [253] | Portugal, Bragança (Csb) | Simulation (building zone in suburbs, using EnergyPlus) | Evergreen (herbaceous and climbers) | Wintertime (north west south east) | Thin wall: **28.6%** **-34.7%** **37.0%** **-81.2%**; Thick wall: **13.3%** **11.2%** **16.8%** **13.9%** |
| Living walls (#2) | [208] | Austria, Vienna (Cfb) | Observational (office and school façades monitored) | Various (herbaceous) | Wintertime (south) | Heat resistance increased Trough: **0.31 m²·K·W⁻¹** Grate: **0.68 m²·K·W⁻¹** |

The review found no studies to quantify energy use implications of passive vertical greening application in building interiors. Indoor environments could be considered as analogous to a greenhouse, where seasonal dependencies are controlled to offer continuous growth and year-round ecosystem service provision. Given the limited influence of radiation incidence in such conditions, the energy saving potential from the canopy shading effect could be assumed to be minimal. The identified $T_{air}$ cooling influence however is likely to have some impact on reducing cooling demands, as suggested by the Pérez-Urrestarazu *et al.* [159] study of an ALW. In winter however, continued growth and resultant cooling from ever-green-cover could present a negative influence on space-conditioning loads as well as condensation risk. Annual expenditure must therefore be assessed to determine net value.

### 3.4.4 Carbon sequestration

The uptake and long-term storage of $CO_2$ is described as carbon sequestration, which represents a significant feedback benefit of plant cover.

*Photosynthesis:*

$$6CO_2 + 6H_2O + Solar\ radiation = C_6H_{12}O_6\ (Glucose) + 6O_2 \qquad \textit{Equation 2}$$

Plants remove atmospheric $CO_2$ by photosynthesis to produce biomass (Equation 2), and thus are natural carbon sinks. Like all greenspace features, vertical greening also provides this valued ecosystem service, although the relative significance of which is not well quantified by current research [199]. The study by Marchi *et al.* [254] presented an exception, where they estimated that for a 98 m$^2$ living wall $CO_2$ capturing was between 13.4 and 97 kg $CO_{2eq}$. Plant selection was identified as significant for this sequestration efficacy, with CAM plants of the genus Sedum showing relatively poor performance compared to C4 grass and C3 herbaceous plants [254]; while a study by Charoenkit & Yiemwattana [215] identified a woody plant to perform better than the evergreen herbaceous plants examined. The latter study also noted performance to be dependent on plant stress, with poor sequestration observed from summertime heat and water stress [215]. In indoor environments where stress conditions are managed, the air purification benefit from $CO_2$ uptake is significant. A study by Tudiwer & Korjenic [240] for example demonstrated how a ~5 m$^2$ living wall in a classroom (~1% of the room volume) accelerated its $CO_2$ decay.

### 3.4.5 Improving air quality

In addition to $CO_2$ uptake, plants have long been observed to capture a variety of pollutants, and even partly metabolise or bio-transform them with the aid of microorganisms that coexist in their microbiome. Plant phyllosphere surfaces such as leaves and stems, adsorb significant amounts of such pollutants. A proportion of this also enters the plant through stomatal pores, while some of the surface residual may be washed down with rainfall and added to the soil below to facilitate contact with the rhizosphere. In both the phyllosphere and rhizosphere, microorganisms such as bacteria and fungi perform the beneficial function of detoxifying pollutants by means of degradation, transformation, and sequestration pathways. The use of plants and their microbiome to remove, detoxify, or immobilise contaminants is described as 'phytoremediation', and has long been used in decontamination practices. Interest in phytoremediation-based air-purification peaked during the 1980s, following several NASA projects considering closed-system applications for space-stations [255]. Many studies have since then replicated findings to suggest potential for wider applicability, with removal action typically assessed with reference to particulate matter (PM), volatile organic compounds (VOCs), and inorganic pollutants [256].

Particulate matter represents a diverse range of airborne solids and liquids that are categorised based on their aerodynamic diameter. They are generated naturally by processes such as erosion, and by various anthropogenic activities such as combustion. The diversity of their origins, forms, and chemical compositions mean that toxicity also varies, although evidence suggests the pollutant in any form to represent one of the most hazardous to human health [257]. In addition to climate conditions such as precipitation and wind, and PM quantity and composition, plant capturing capacity is influenced by species-specific features such as canopy morphology and leaf: size, ultrastructure, thickness, and surface roughness (presence and density of trichomes or pubescence), as well as the chemical composition and structure of epicuticular waxes. Electrostatic forces play a role in attracting particulates [136], while the epicuticular wax layer immobilises and stabilises adsorbed PM [258,259]. Alongside these physical features that assist capturing, microbes associated with the plant microbiome are significant in implementing degradation and metabolic pathways. These are mainly implemented in the rhizosphere, with root endophytes identified to utilise a metal-resistance sequestration system to decrease attached metal toxicity, and enhance tissue bioaccumulation [260]. Similar action on leaf surfaces is expected from phylloplane microbes, although little evidence is available at present to support this hypothesis [108].

With outdoor studies that have examined capturing, greater $PM_{10}$ removal effectiveness has been identified with vertical greening canopies than horizontal greening [261], with variable canopy morphology [262], smaller and complex leaf shapes [259], and higher deposition on leaf topside contributing [139,263]. Indoor studies currently consider potted plants as opposed to the influence of larger canopy extents. A notable example found daily $PM_{10}$ levels in a classroom to be higher than outdoors, with the addition of potted plants observed to reduce these concentrations by up to 30% [264]. These observations broadly support PM capturing as a significant service offered by plants, with effective action in both outdoor and indoor environments [265,266].

VOCs are described by their physical and chemical characteristics such as boiling range and vapour pressure, and carbon number. The most referenced are Toluene, Ethylbenzene, and Xylene (TEX); Benzene; Poly Aromatic Hydrocarbons (PAHs); and formaldehyde [108]. They are produced by anthropogenic activities such as transportation or manufacturing, and by biogenic activities of plants [267]. Various materials and industrially processed products such as carpets, wallpaper, curtains, and electronic equipment emit VOCs, with newer materials emitting the highest concentrations [268]. They are hazardous to human health with recorded short and long-term effects, including contribution to multiple chemical sensitivity and a range of symptoms described as 'sick building syndrome' [269]. Removal action from plants is exemplified mostly by potted plant studies (e.g., [264]), with recent investigations considering ALWs (e.g., [270]). This VOC uptake is mainly achieved through leaf stomata, with the residual contribution from the surface cuticle and rhizosphere. In dry conditions, VOCs penetrate the soil and are degraded by the more efficient degradation system in the rhizosphere [108,255]. Wolverton *et al.* [255] stressed that as the rhizosphere is the most effective removal area, maximising air contact to this zone should be prioritised; while the net effect must be considered when selecting plants for phytoremediation, given that they are also a source of VOCs (see plant review in [271]).

The most common inorganic air pollutants are Carbon dioxide ($CO_2$), Carbon monoxide (CO), Sulphur dioxide ($SO_2$), Nitrogen oxides ($NO_x$), and Ozone ($O_3$); (Table 10, p. 87). Ozone is formed when solar radiation (ultraviolet) induces photochemical reactions between

$NO_x$, VOCs, and CO, while the rest are mainly added to the atmosphere from combustion processes. In high concentrations such inorganic air pollutants cause adverse effects to plants, although some species are more tolerant and sink these by bioaccumulation in tissue. The Weyens *et al.* [108] review stresses that less is known about the significance of the plant-associated microbiome in inorganic phytoremediation. With carbon sequestration, it is known that the microbiome affects humus formation, although the potential contribution of mycorrhizal fungi is not well-addressed. They hypothesise that the microbiome could be involved in some $NO_x$ and $SO_2$ capturing, although little evidence is currently available. Ozone in contrast is a known antimicrobial agent, thus any contribution of the microbiome is likely to be associated with toxicity moderation [108].

Table 10. Inorganic pollutant removal action from plants.

| Pollutant | Removal action |
|---|---|
| **$CO_2$** | Removal from photosynthesis (Equation 2). For example, Pegas *et al.* [264] observed potted plants to reduce indoor mean $CO_2$ concentration by 44%. |
| **CO** | Plants metabolise CO by oxidation into $CO_2$ or by reduction and assimilation into the amino acid Serine. Bidwell & Bebee [272] experiments identified CO as showing mixed influence on photosynthesis, ranging from inhibition at low concentrations, increased net fixation at very high concentrations, and no influence in some cases. This means that in urban areas where high CO concentrations are typical, plant uptake of CO could be significant [272]. |
| **$SO_2$** | Modest concentrations can be a sulphur source. After entering through stomata following the same pathway as $CO_2$, it may be utilised in a 'reductive sulphur cycle' to form amino acids needed for growth and development [273]. |
| **$NO_2$** | Removal occurs mainly by stomatal uptake to the apoplast, and secondly by adsorption to leaf and root surfaces. Mostly metabolised through the nitrate assimilation pathway into compounds such as amino acids [108]. |
| **$O_3$** | Removal achieved mainly by absorption through stomatal apertures, and secondly by cuticle adsorption when surface moisture is available. Readily decomposes when reacting in the gaseous-phase or when impacted by cuticle or apoplastic compounds, although less is known about what occurs after stomatal entry [108]. |

A key advantage of living walls over other greening strategies is the enhanced coverage and planting density offered, which maximises the provision of vegetation related ecosystem services for a given footprint. This is illustrated by a study considering $CO_2$ removal with *Dypsis lutescens* (Bamboo palm), where it was shown to require the impractical use of 249 potted plants to offset the respiration output generated by an average human occupant in an unventilated room (average exhalation of 34.5 $CO_2$ $mg{\cdot}h^{-1}$). It was estimated that to offset this output would require around 57 $m^2$ of leaf area, which could be addressed by around 5 $m^2$ of living wall coverage [274]. A key requirement for maintaining the efficiency of this purification ecosystem service is good plant health. A laboratory study by Rondeau *et al.* [275] for example highlighted that although a planted biofilter was able to remove low concentrations of pollutants, the addition of nutrient solution was essential for maintaining this pollutant degradation efficiency. Indoor bio-walls are therefore likely to require greater attention to ensure effective and sustained air-purification services.

### 3.4.6 Acoustics

Plants attenuate noise by absorbing, diffracting, and reflecting sound. Vegetated installations have as a result been widely used as means to improve outdoor and indoor sound environments [152,276]. Experimental vertical greening studies by Wong *et al.* [277] found stronger attenuation at low-to-middle frequencies attributed to substrate absorption, while a lesser attenuation at higher frequencies was attributed to foliage scattering. The systems examined also exhibited the highest sound absorption coefficients relative to other materials, with coefficients positively correlated with frequencies and plant coverage [277]. Laboratory studies by Davis *et al.* [278] identified that living walls correspond to the behaviour of porous absorbers, with low absorption evident at lower frequencies and the converse at higher frequencies. To improve their acoustic performance, parameters such as mass (thickness and composition of substrate and plants), impenetrability (sealing joints, e.g., [279]), and structural insulation are highlighted as requiring greater attention [276]; while performance is also dependent on plant maturity and health [280].

### 3.4.7 Biodiversity

From the few available urban biodiversity studies that address surface greening, the majority have examined green-roofs to identify enhancements in diversity and population abundance of flora and fauna [281–283]. Notable earlier work on green façades include a study by Benedict & McMahon [284] that found greater presence of birds, and the thesis by Matt [285] that found greater collections of diverse arthropods. A study of thirty-three sites in Paris by Madre *et al.* [286] characterised such green façades as 'xerothermophilous' habitats comparable to cliffs, while continuous felt and modular substrate-filled living wall types were characterised as cool damp habitats analogous to vegetated waterfalls. Of the two categories examined, the latter modular living wall system with its increased substrate depth was found to offer the highest diversity and abundance of species [286].

Such surveys are currently available only for outdoor applications, where the ecosystems are exposed to migration influences and interactions with the wider context. Biodiversity at indoor applications in contrast is likely to be significantly limited owing to the near-closed ecosystems created, with introductions most likely at planting or replanting stages [132]. Further attention is needed to identify the diversity present and sustained at such installations, as well as the nature of their interactions with building occupants (favourable or otherwise). Biodiversity potential at both outdoor and indoor installations must also be considered in relation to other associated services including pollination, biological control, and decomposition (sustaining microbial diversity).

### 3.4.8 Wellbeing and restorative impact

The natural environment including plant life is identified to increase positive distractions and emotions, enhance the sociocultural climate, and promote restoration from illness and stress [287–289]. The contribution of plants to the aesthetic and wellbeing enhancement of cities is acknowledged in built environment discourse as 'biophilic design', which gathered interest and momentum in response to the need to alleviate symptoms of sick-building syndrome [281]. One school of thought have based their argument on plant ecosystem services offering physiological benefits to building occupants, particularly in relation to their ability to purify air and enhance microbial diversity (e.g., [290,291]). The alternative school have based their argument on the psychological associations made by building occupants in relation to natural environments. This latter school was established by early health restorative studies from Ulrich [287,292], as well as 'attention restoration theory' by Kaplan & Kaplan [293] that promoted exposure to natural environments including plants as having a restorative effect on attention, wellbeing, and health.

Following early work by Ulrich [287] and others, recent health restorative studies present supporting evidence for plants to be used in healthcare facilities as a supplementary healing incentive (e.g., [288,294,295]), with Dijkstra *et al.* [295] notably identifying the perception of attractiveness offered by plants as a key influence. Kaplan & Kaplan [293] argued the presence of a natural setting with plants to offer stimulation that does not demand exhaustive directed or focused attention, but in contrast to trigger undirected attention or 'soft fascination' to encourage the restoration of attention capacity. Raanaas *et al.* [296] for example found significant participant performance improvements following exposure to potted plants, while a study of classrooms by van den Berg *et al.* [297] presented one of the first studies to have considered an indoor living wall, with results of better scores for selective attention and classroom evaluations positively influenced.

Examining such plant influences has progressed significantly with the greater understanding of biochemical processes of human physiological and psychological responses. A body of studies as a result has branched-off to combine the assessment of physiological indicators and their association to psychological responses. In such studies, physiological indicators such as heart rate and pulse variability; blood pressure; skin moisture conductivity; hormone concentrations such as cortisol and cortisone; oxyhaemoglobin concentrations in the prefrontal cortex; and brain activity are quantified to characterise participant anxiety or stress. These are then related to psychological responses characterised by their answers to Semantic Differential, Profile of Mood State (POMS), or bespoke questionnaires (e.g., [298–301]). Notably, such a study by Yin *et al.* [300] validated the Dijkstra *et al.* [295] findings to stress the primacy of visual perception in affecting positive psychological responses.

The consideration of the visual perception of vertical greening installations using such experimental approaches is very much an emerging area of research interest. A recent outdoor green façade study by Elsadek *et al.* [301] for example found its visual perception to increase participant alpha relative waves in the frontal and occipital lobes, increase parasympathetic activity, decrease skin conductance, and enhance feelings of comfort, relaxation, and mood state. While living walls present significant potential for greater visual and physical interaction influence owing to their unavoidable vertical presence, and with proximity and interaction likely to be greater with indoor installations, no studies specifically relating to such installations have been identified by this review.

### 3.4.9 Potential risks

While most biogenic processes of plant life could be considered as beneficial influences, some could present challenges to human comfort and health. These include plant VOC emissions discussed earlier, $CO_2$ emissions from respiration, humidity increases from transpiration, and release of pathogens, allergens, and toxins.

*Respiration:*

$$C_6H_{12}O_6 + 6O_2 = 6CO_2 + 6H_2O + Combustion\ energy \qquad \text{Equation 3}$$

As discussed earlier, $CO_2$ is an essential ingredient of photosynthesis and plants reduce atmospheric concentrations to provide an air purification service that is particularly useful in indoor environments. The Irga *et al.* [274] study for example, recorded a concentration reduction of 214 $mg \cdot m^{-2} \cdot h^{-1}$ from the houseplant *Nephthytis* sp., while the Torpy *et al.* [185] study measured the highest reduction to be around 657 $mg \cdot m^{-2} \cdot h^{-1}$ from *Dypsis lutescens*. These removal rates are dependent on species-specific photosynthesis rates and efficiency, as well as light levels and climate temperatures experienced. Low light level conditions reduce photosynthesis rates and the resulting net effect of removal [302]. In certain situations (i.e., below the light compensation point), this could lead to net increases in concentrations that are exacerbated by contributions from continuous respiratory emissions from non-photosynthetic plant organs and the microbiome (Equation 3), as well as photorespiration resulting from photosynthesis inefficiencies [274]. As plants do not photosynthesise in darkness, continuous plant respiration dominates at night to add $CO_2$ to the atmosphere [303]. This in turn could become an air pollutant that affects the nocturnal comfort and health of inhabitants in very poorly ventilated spaces (i.e., acts as a mild narcotic). However, the concentrations involved in most indoor environments including plant life as potted plants are likely to be dissipated by the presence of some degree of background air infiltration and ventilation to mitigate this risk. A rare laboratory study considering nocturnal emissions nevertheless suggested a preference for using CAM plants indoors, as they present net $CO_2$ absorption during the night to best mitigate the risk [303].

As discussed earlier, humidity from evapotranspiration is a significant microclimate influence generated by plant feedback. Increases can have an adverse effect on human health by promoting the growth of adverse microbial activity, and by hindering efficient thermoregulation to cause discomfort [304]. Previous studies examining indoor environments have demonstrated humidity levels to increase with the addition of potted houseplants, although with substantially less capacity than amounts generated by other devices to present risk to comfort or health [291,305,306]. Potted plant humidity influence on pathogenic microbial growth has also been identified to fall short of the concentrations necessary for colony forming units (CFU), with their microbiome potentially preventing airborne pathogenic colony growth by releasing inhibiting allelochemicals [306]. These findings however must now be reassessed in relation to the greater plant coverage presented by living walls.

Pollen, spores, and other plant matter are significant allergens that can cause individual-specific reactions. The limited allergy studies available highlight allergen concentrations in outdoor environments to be much greater than indoors, although increased indoor occupation increases exposure risk. Studies assessing this indoor risk have thus far considered only typical houseplants (e.g., [307]). Although increased risk from indoor living walls may be expected owing to the increased abundance and diversity introduced, the topic is sparsely addressed in vertical greening research at present. An exception presented by a recent classroom experiment with a ~5 $m^2$ living wall however found concentrations of spores to be of insufficient capacity to promote mould growth [240]. A unique risk is also presented with building façade installations located adjacent to ventilation inlets or windows. As plant allergens have been found to readily transport across vast distances [307], such circumstances present the potential for allergens entering indoor air circulation. This infiltration risk however is yet to be investigated.

Plants also produce various toxic compounds that can be distinguished as either relevant for plant metabolism or residuals. It is hypothesised that during the evolution of metabolic pathways such compounds may have been produced as by-products, and the failure to expel these from their system had resulted in these existing as toxic residuals; with some species repurposing this toxicity as defence mechanisms against herbivorous attack [308]. Examples of toxic compounds found in typical houseplants include Alkaloids, Cardiac Glycosides, Colchicine, Diterpene Esters, Grayanotoxins, Oxalates, Polyacetylenes, Protoanemonin, and Tannins [309]. These may have adverse physiological impact on both humans and domesticated animals. The effects usually result from ingestion of significant quantities, or dermal or ocular contact for significant durations. The human reactions that arise from such toxins range from dermatitis following dermal contact, gastrointestinal upset from ingestion, and more acute reactions including cardiac or respiratory failure that could lead to death. Children and smaller domesticated animals in particular show higher vulnerability to such adverse toxicity reactions [309]. Acknowledging these vulnerabilities and high-exposure risk to building occupants has encouraged plant toxicity research to focus attention on well-known houseplants. However, the potential risks from indoor living wall presence are not currently addressed. This is significant to consider given the prevalent desire to include exotic shade-loving tropical plants at such installations, and the potential for their resulting adverse reactions being unfamiliar to attending medical practitioners.

Various studies from plant sciences have examined the above discussed adverse modifications to identify some degree of risk to inhabitants from including plant life in the built environment. It is significant to note that most built environment focused studies advocating plant inclusion at present seem to discuss such risks cursorily, with research addressing risks in relation to specific applications such as indoor living walls as notably lacking.

## 3.5 Summary

This chapter considered the context of vertical greening, its emerging variants, and available research evidence in relation to outdoor and indoor applications. From the review of available studies, the concise answer to the research question raised at the onset is that the relatability of observations derived from outdoor installation studies in relation to indoor installations has yet to be established by research evidence. Although it is hypothesised for thermal (as well as other ecosystem services) performance to be relatively lower in indoor or sheltered environments, there is currently little evidence available (particularly from in-situ observations) to conclude as such.

The following details key considerations:

- The review highlighted the vertical greening category of green façades to present a rich application history, with technical research development from the 1980s onward. Vertical greening interest from the 2000s however has been taken over by the newer category of **living walls to currently dominate both application and research**. Within the developing body of research, the current **dominant interest is for considering outdoor applications** given the greater availability of installations to carryout studies. Consultants however stress a recent shift in attention to implement indoor installations, which will eventually translate to a significant body of installations to warrant an increase in research interest [10].

- Outdoor application studies present evidence to suggest vertical greening belonging to both categories to offer significant thermal benefit, with **cooling influence during the summer and on occasion a warming insulating effect in winter**; along with improved performance when conditions are at their harshest. There is some evidence to suggest better performance in drier, warmer climates, with more evidence required to justify claims for cooler temperate climates. These thermal enhancements in return have been established to offer summer cooling and winter heating energy use benefits to buildings, although the body of evidence is biased towards emphasising summertime benefits. This is explained by the acknowledgment of preceding plant science observations that validate optimal vegetation ecosystem service provision to be **pronounced during the summer** (including carbon sequestration, air purification, biodiversity, and wellbeing and restoration enhancements) [10].

- Given that outdoor application studies attribute radiation incidence and associated plant canopy shading to significantly contribute to their enhanced thermal performance, suggests that in indoor climates their thermal performance is likely to be represented greater by the less potent contributions from evapotranspiration. The limited studies available suggests that this contribution is still beneficial for reducing cooling loads in the summer, although no evidence is available for winter performance and how this might influence net annual space-conditioning. The **assessment of annual performance is highlighted as significant** as the plants used in indoor applications are typically shade-loving, tropical, evergreen, and able to provide ecosystem services throughout the year. This annual consideration is also applicable to the examination of other ecosystem services including carbon sequestration, air purification, acoustic, biodiversity, and wellbeing and restoration influence, where more evidence is necessary to assess the **relative significance of introducing greater plant coverage and diversity in the form of indoor living walls** [10].

- Although the outdoor application-based evidence base can be related to indoor applications to a certain degree, the specific study of indoor applications is required to justify the value of ecosystem services they generate. This call for further study is pertinent given that much of human habitation in cities occurs within indoor environments, thereby providing greater opportunity to enhance building occupant health, comfort, and wellbeing. Some of this **attention should also be directed at examining potentially adverse plant-related modifications such as toxicity**, which to date has received little attention from built-environment-focused studies [10].

# PART II

# Chapter 4

## STUDY 1: INFLUENCE IN SHELTERED ENVIRONMENTS

### 4.1 Introduction

The body of research examining living walls (LW) reviewed in Chapter 3 highlighted significant recent interest in quantifying their ecosystem benefits. The chapter also identified this developing body to be mostly concerned with outdoor installations (e.g., [230,310]), while the few that have examined indoor installations had favoured laboratory conditions to best characterise influence (e.g., [158,159,311]). In-situ application performance data particularly from sheltered conditions is scarce (i.e., conditions not well-coupled with the background climate), with increasing necessity to present data to clarify and quantify the extents of influence on such inhabited environments. To address this research shortfall, and the first-of-five secondary research questions introduced in Chapter 1:

> *Q I.* *To what extent does the presence of a vertical greening installation modify the microclimate of a sheltered environment?*

…this study utilised a case study approach with two urban morphological conditions selected for longitudinal monitoring campaigns. These represented living wall installations of comparable evergreen coverage (>90 m$^2$), located in the sheltered urban conditions of an indoor atrium and a semi-outdoor court, respectively described in section 4.1.1.

This monitoring study also addressed the principal learning objective of the project of engaging with real-world conditions and resolving associated challenges in data gathering, with the chapter presenting material published in Gunawardena & Steemers [42–44].

### 4.1.1 Case studies selected

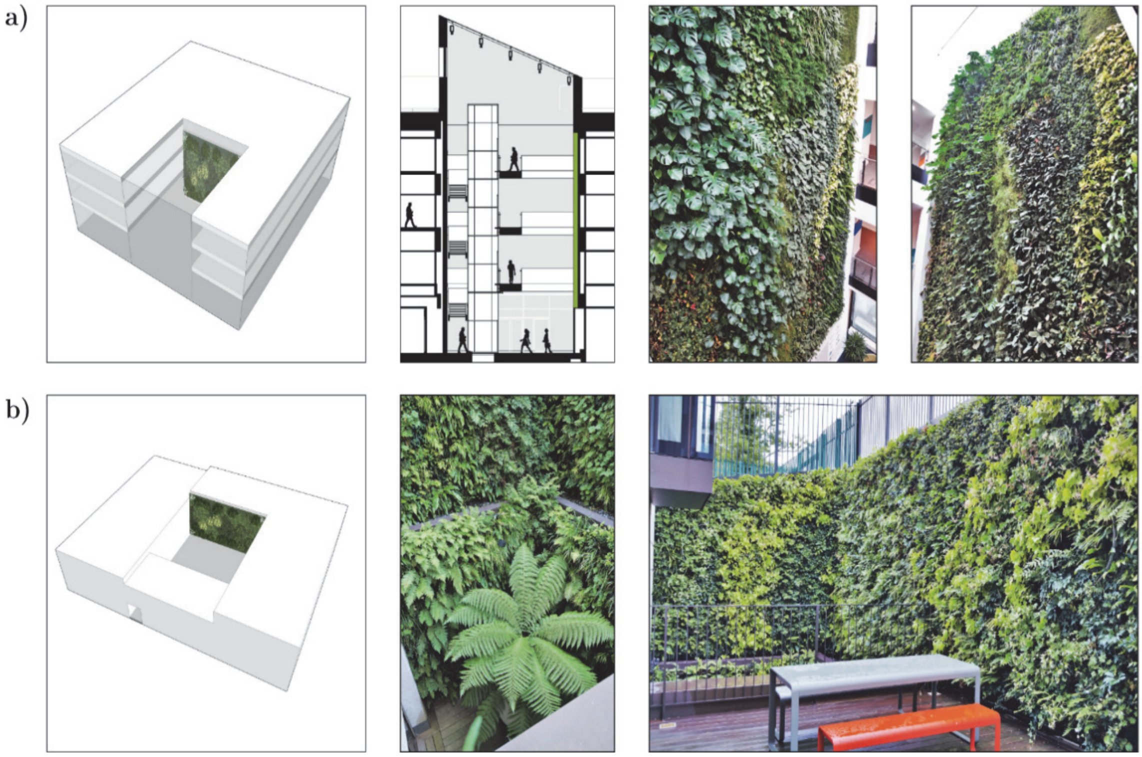


*Fig. 35. Diagram of an indoor atrium installation, with building section extract showing the DAB atrium and its living wall (a); and a diagram of a semi-outdoor court installation, with the SET basement level court and east- and south-facing walls (b).*

#### a) Indoor atrium

Within larger urban buildings the general arrangement typically includes a large atrium situated off the main entrance (Fig. 35a). This creates a transitional volume where a controlled coupling is maintained between the indoor building environment and the outdoor climate [312–314]. An example of such an atrium is presented at the David Attenborough Building (DAB) in Cambridge (Cfb). In this building, the northeast and southwest facing surfaces bounding the five-storey high atrium volume are either building façades or internal partitions, while the southeast surface is host to a circulation core, and the remaining northwest surface is host to a three-storey living wall, believed to be one of the largest in the UK (Fig. 35a, [134]). At the atrium top is a southeast sloping skylight that floods the space with daylight, while the volume is naturally ventilated (entrance heaters are no longer utilised in winter [315]). The living wall installation is 13 m-high and 91 $m^2$ in area, with ~8,750 evergreen plants from 24 species representing eleven global regions and countries planted onto a soil-based, modular interlocking crate system. Nearly all species were observed to be in good health over the course of the monitoring campaign [134,162].

### b) Semi-outdoor court

In densely built urban fabrics, vacant spaces are represented by street canyons and numerous polygonal voids. The latter presents a central void space by joining the vertical façades of surrounding buildings to provide a degree of peripheral shelter, although remain open and exposed to the urban atmosphere from above (Fig. 35b, p. 97). Such spatial conditions are referred to as courts, with the degree of shelter presented determined by the scale of the void and its bounding morphological context. Whatever the degree of shelter provided by each instance, they can be described to be relatively 'better coupled' to the background climate than the earlier mentioned atrium condition. The most expansive representation of such an arrangement is the urban square, while the most intimate would be a residential court. The vertical building façades that face such a sheltered court provide ample opportunity for vertical greening application, with historical preference for cultivating green façades, and implementing living wall installations in more recent times (see Chapter 3).

The resources necessary to carry out a monitoring exercise within a large urban square was not available to this project. An intimate-scaled residential court was therefore selected in consultation with a living wall designer and installer [134]. The selected St. Edmund's Terrace court (SET) in Primrose Hill, London has living walls installed on three bounding surfaces of the court, while the remaining north-facing surface is represented by the Portland stone and glazed façade of the residential building. The arrangement also includes a lower-level court which continues the living walls at the northwest corner down to form a basement pit/court (Fig. 35b). The flourishing installations observed have an average height of ~4 m (~7.5 m at the basement court) and a total area of 102 m$^2$; with ~5,000 plants representing 14 species planted onto a soil-based, modular felt-pocket system [162].

## 4.2 Methodology

The monitoring of the indoor DAB case study included the measurement of soil ($T_{soil}$), surface ($T_{surf}$ and $T_{leaf}$), and air ($T_{air}$) temperatures; relative humidity ($RH$); and air velocity ($V_{air}$) and direction (Table 11, p. 99; Fig. 37a & b, p. 101); while absolute humidity ($AH$) was calculated from measured variables (Equation 4, [53,55]):

$$AH = \frac{e_a\, M_w}{R\, \boldsymbol{T_a}}, \qquad \textit{Equation 4}$$

where,

| | |
|---|---|
| $AH$ | Absolute humidity expressed as vapour density [g·m$^{-3}$]; |
| $e_a$ | Partial vapour pressure of air = $e_s(T)\ rH$ [kPa]; |
| $e_s(T)$ | Vapour pressure of air at saturation (from Tetens formula, [53]), $= 0.611 \cdot \exp(17.502 \cdot T_{air}/T_{air} + 240.97)$ [kPa]; |
| $rH$ | Humidity ratio = (0-1); |
| $M_w$ | Molecular weight of water = 18.015 [g·mol$^{-1}$]; |
| $R$ | Molar gas constant = 8.31 [J·mol$^{-1}$·K$^{-1}$]; and |
| $\boldsymbol{T_a}$ | Absolute temperature of air = $T_{air} + 273.15$ [K]. |

The hygrothermal and air velocity observations were recorded between June 2018 and March 2019, with the period from June-to-September 2018 considered as summer, and October 2018 to March 2019 as winter (i.e., heating period). The datasets were differentiated between day (i.e., when transpiration is active) and night-time hours, with daytime commencing at sunrise +01:00 hrs and ending at sunset -01:00 hrs, while the active building operation hours from 07:00 to 19:00 hrs were treated as daylight hours by default (light levels maintained to facilitate growth by natural and/or artificial means). Surface air movement monitoring was carried out from October-to-December 2018 (summer monitoring was not possible due to equipment unavailability). This dataset was also differentiated between day and night-time based on standard building operation hours, seven days a week.

Table 11. Probe and logger deployment at the DAB atrium.

| **Parameter measured** | **Measurement objective** | **Placing within atrium** | **Logger and probe used** |
|---|---|---|---|
| $T_{air}$ and $RH$ | Vertical distribution | Suspended at each level, 0.05 m off the LW surface and at 1.1 m AFFL (floor levels *L01-* \| *L02-* \| *L03-0.05 m*). | HOBO MX2302 $T_{air}$ and $RH$ logger with external probes (×03) |
| $T_{air}$ and $RH$ | Horizontal distribution (including *L02-0.05 m*) | Suspended at L02, 1.2 m off the LW surface and at 1.1 m AFFL (*L02-1.20 m*). | As above (×01) |
| Ambient $T_{air}$ and $RH$ | Ambient control (and horizontal distribution) | In atrium at L02, 6.00 m off the LW surface and at 1.1 m AFFL (*Control*, also notated as *'Ctrl'* or *L02-6.00 m*). | HOBO MX2301 $T_{air}$ and $RH$ logger with internal probe (×01) |
| Wall $T_{surf}$ and $T_{leaf}$ | Vertical $T_{surf}$ distribution and representative $T_{leaf}$ data | Atrium northwest surface without LW, at L00 (~3 m AFFL) and L02 (1.1 m AFFL, approx. vertical centre-point of installation). $T_{leaf}$ of L02 canopy area. | HOBO U12-008 logger with external TMC6-HE $T_{surf}$ probe (×03) |
| $T_{soil}$ | Typical substrate temperature | Atrium LW at L02, embedded in soil substrate (approx. vertical centre-point of installation). | U12-008 logger with TMC6-HD external temp. probe (×01) |
| $V_{air}$ and direction | Omnidirectional ambient velocity | Omnidirectional probe mounted in atrium at L01. | TSI M8475 $V_{air}$ transducer (×01) |
| | Directional air movement off canopy surface | 2D-ultrasonic sensor mounted perpendicular to the LW at its base on L00 at ~3.2 m AFFL. For practical reasons, 'Northpoint' or 0/360° was directed down, with alignment correction. | Gill WindSonic-1 $V_{air}$ and direction sensor (×01) |

Table 12. Probe and logger deployment at the SET court.

| Parameter measured | Measurement objective | Placing within court | Logger and probe used |
|---|---|---|---|
| $T_{air}$ and $RH$ | Vertical distribution | Fixed within canopy centred to the east-facing wall at basement (*EF-C Basement*) and ground floor terrace level (*EF-C Terrace*), at ~2 m AFFL, and sheltered from direct radiation incidence. | Tinytag Plus 2 TGP-4020 $T_{air}$ and HOBO MX2302 (×02) |
| $T_{air}$ and $RH$ | Horizontal distribution | Fixed within canopy centred to the south-facing wall at ~2 m AFFL (*SF-C Canopy*). | HOBO MX2302 (×01) |
| | | Suspended at 1.0 m off the installation surface and at 0.9 m AFFL (*IP01*); sheltered from direct radiation incidence. | HOBO MX2302 (×01) |
| | | Placed at 2.0 m off the installation surface and at 0.05 m AFFL (*IP02*). | HOBO MX2302, in a radiation shield (×01) |
| | | Suspended at 2.5 m off the installation surface and at 0.9 m AFFL (*IP03*); sheltered from direct radiation incidence. | HOBO MX2301 $T_{air}$ and $RH$ logger with internal probe (×01) |
| Ambient $T_{air}$ and $RH$ | Ambient control, and Horizontal distribution | Placed 4.0 m off the LW surface (furthest point from installation), at 0.05 m AFFL (*Control*, also notated as *'Ctrl'*). | HOBO MX2302 in a radiation shield (×01) |
| $T_{sub}$ | Irradiance influence on surface temperatures | Probe fixed to felt surface, one centred to west-facing wall (*WF-C*); and the other ~2 m from the south-facing wall-return edge (*SF-E*); both at ~2 m AFFL. | Tinytag Plus 2 TGP-4020 loggers with external probes (×02) |

Note: Suffix *'-C'* refers to 'centred to surface/wall'; and *'-E'* to 'from surface/wall edge'.

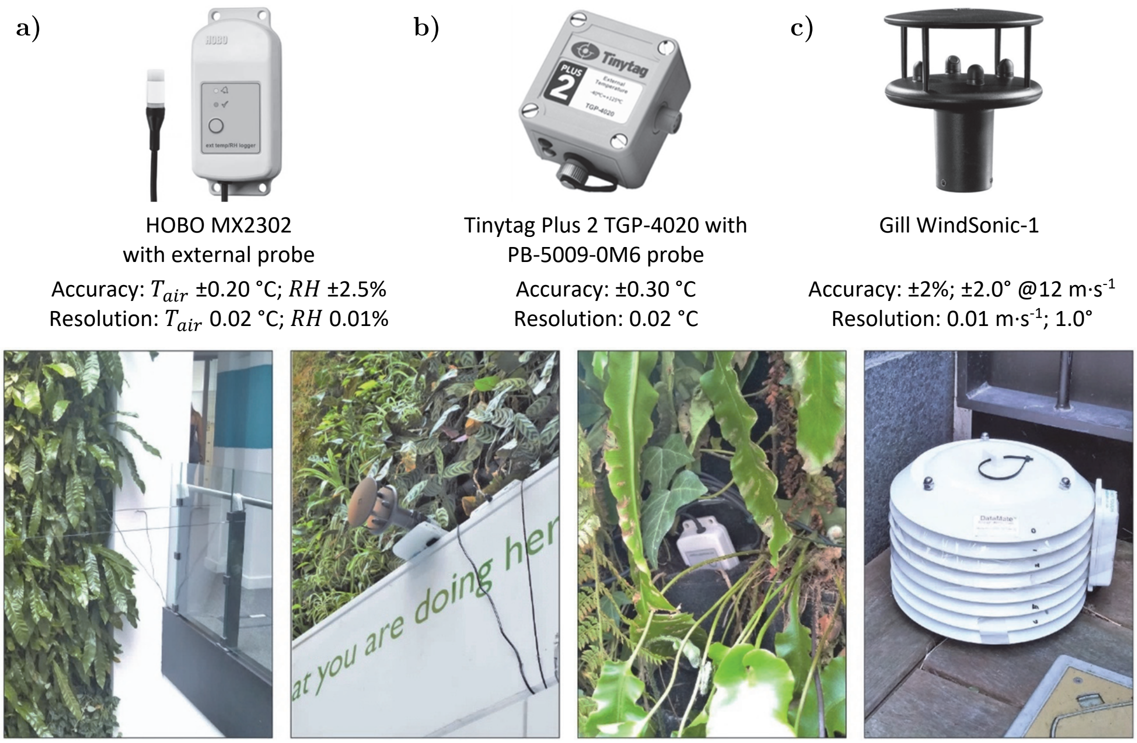


*Fig. 36. Apparatus used: HOBO $T_{air}$ and $RH$ logger (a); Tinytag $T_{air}$ logger (b); WindSonic $V_{air}$ sensor (c); and from left-to-right: HOBO and WindSonic sensor deployed at the DAB; and HOBO's deployed within canopy zone and radiation shield at SET.*

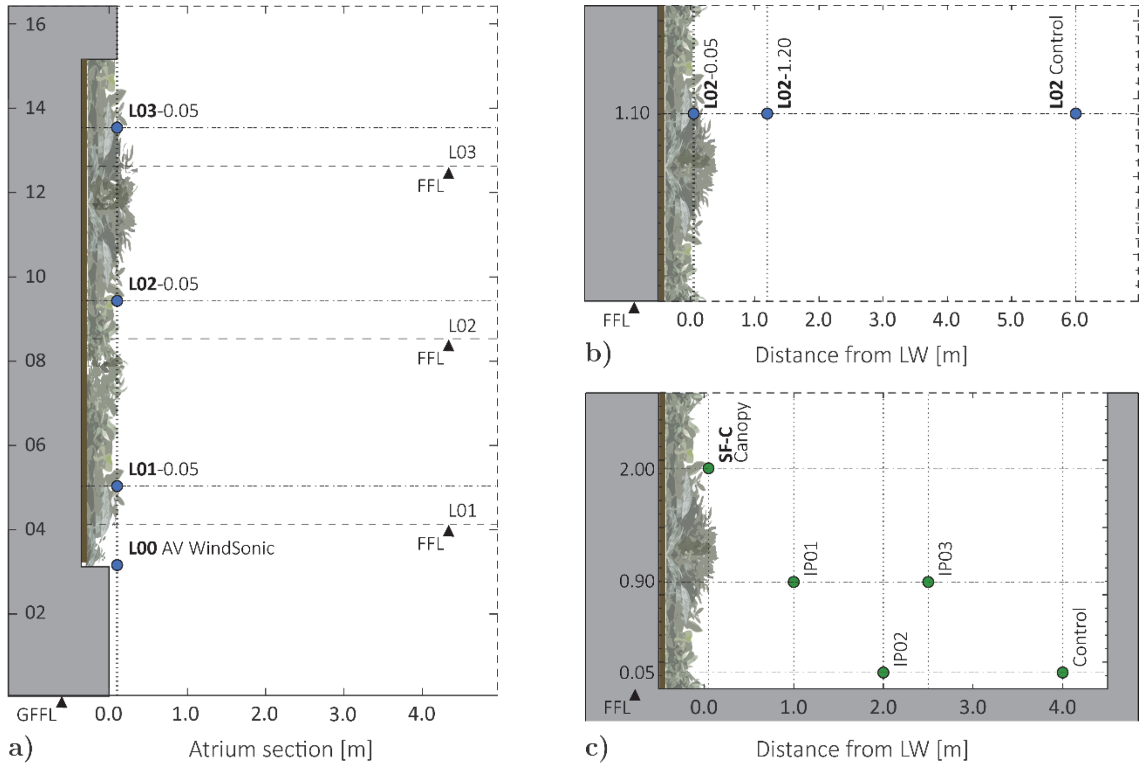


*Fig. 37. Probe deployment at the DAB showing vertical layout in section (a), and L02 section extract showing horizontal layout (b); and deployment at SET showing horizontal layout (c).*

The monitoring of the semi-outdoor SET study included the measurement of $T_{air}$, $T_{sub}$, and $RH$ (Table 12, p. 100; Fig. 37c), with $AH$ calculated. The hygrothermal observations were recorded from August 2018 to December 2019, with May-to-September considered as summer, and October-to-April as winter. The datasets were again differentiated between day and night-time hours as earlier. They were then filtered to exclude readings when background $V_{air}$ exceeded 5.0 m·s$^{-1}$ (from the Hampstead weather station, [316]), as convective heat loss from higher $V_{air}$ reduces reliability of readings [317]. As a result, 1,800, five-minute interval readings from summer and 5,124 from winter datasets were removed.

The apparatus used for the monitoring exercises included calibrated HOBO (Onset Computer Corporation, Bourne, MA, USA) and Tinytag (Gemini Data Loggers, Chichester, West Sussex, UK) probes detailed in Table 11 and Table 12; an Environmental Meter with hygrothermal probes (PCE Instruments UK Ltd., Southampton, UK); a TSI M8475 Air Velocity Transducer (TSI Inc., Minneapolis, MN, USA); and a WindSonic ultrasonic wind sensor (Gill Instruments, Lymington, Hampshire, UK); (Fig. 36, p. 100). The HOBO and TSI sensors were purchased new with manufacturer calibration, while a HOBO sensor was used to calibrate the existing Tinytag sensors, and the WindSonic loaned from the Cambridge Department of Chemistry had recent calibration from an ongoing project.

All datasets were processed and analysed using MATLAB R2019b software (MathWorks, Natick, MA, USA). The results were principally considered using correlation analysis, with shared variance ($r^2$) nearer to one highlighting most of the variability in the dependent dataset to be explained by the independent (i.e., stronger association). For large datasets (N >300), normality was determined with reference to skewness and kurtosis thresholds (see [318]), with failures assessed with nonparametric tests. Given that mean value datasets and their relation to probe positioning parameters were limited (N <5), the relationships were plotted as profiles to facilitate discussion.

## 4.3 Findings

### a) Indoor atrium

The results presented below characterises the hygrothermal microclimate modifications at the DAB atrium, along with living wall surface thermal and air movement observations.

*Wider climate association:*

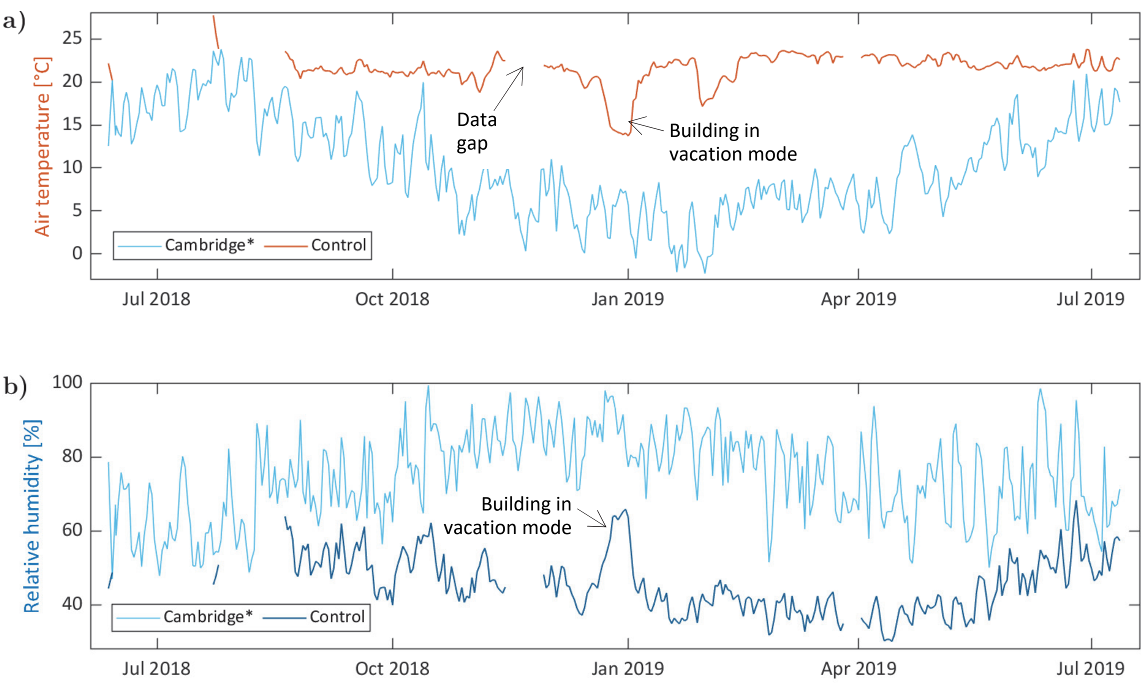


Note: *Cambridge University weather station [319]; ~2 km from the DAB site.

*Fig. 38. DAB Control daily mean $T_{air}$ (a) and RH (b) profiles relative to outdoor Cambridge climate.*

The *L02-6.00 m* probe was considered as the *'Control'* for the campaign following an analysis of spot measurements that demonstrated negligible deviation relative to readings at atrium extents (<1%). Its annual $T_{air}$ (daily mean) dataset demonstrated 'weak' correlation with the outdoor climate (Spearman's rank-order $r_s$ (311, N = 313) = 0.140, $p$ = 0.013), while the summer mean was warmer than in winter by 0.95, ±0.2 K during the daytime and 0.21, ±0.2 K during the night-time (see Fig. 38, p. 102 for profiles). The weak climate association and modest seasonal variation in means is unsurprising given that the atrium is a regulated near-closed system, despite being naturally ventilated. The *Control* $T_{air}$ (5-minute interval) relationships with other atrium probe datasets on the other hand were 'very strong', and strongest with horizontal (across the level to indicate stratification) than vertical distribution probes. The weakest of these relationships was notably during the summer daytime, which suggested interference from other sources that are enhanced with warmer conditions (i.e., rising stack and resulting lateral infiltration flows).

The annual *Control RH* dataset also presented a 'weak' correlation with the outdoor climate (Pearson $r$ = 0.27, $p$ <0.01); while the *AH* dataset in contrast presented a 'very strong' correlation ($r_s$ = 0.92, $p$ <0.01). The latter confirmed the dominant humidity source for the atrium as the background outdoor climate. Seasonal variation was evident with summer *RH* means greater than winter by 5.03, ±0.4% during the daytime and 6.35, ±0.5% during the night-time; while *AH* presented greater summer means than winter by 1.51, ±0.1 g·m$^{-3}$ during the daytime and 1.34, ±0.1 g·m$^{-3}$ during the night-time. These modest differences again are expected (from natural ventilation and infiltration), with *RH* variation notably explained mostly by *AH* ($r^2$ = 66%) variance than $T_{air}$ (17%).

*Horizontal distribution:*

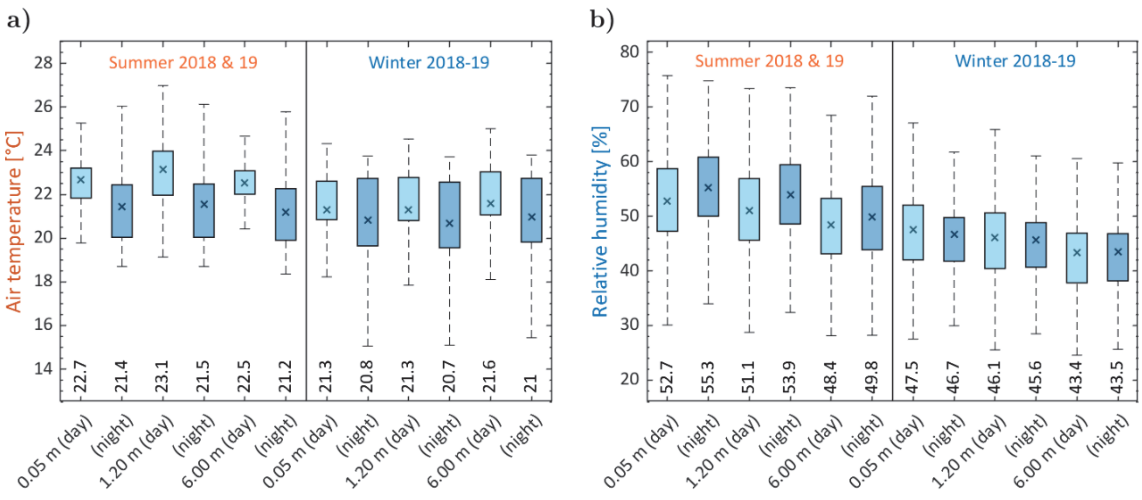


Note: In all boxplots from hereafter the symbol '×' represents mean value for datasets (also represented to one decimal point above the $x$-axis); while 'NaN' or blank spaces represent absence of data.

*Fig. 39. DAB, L02 horizontal $T_{air}$ (a) and RH (b) distribution datasets.*

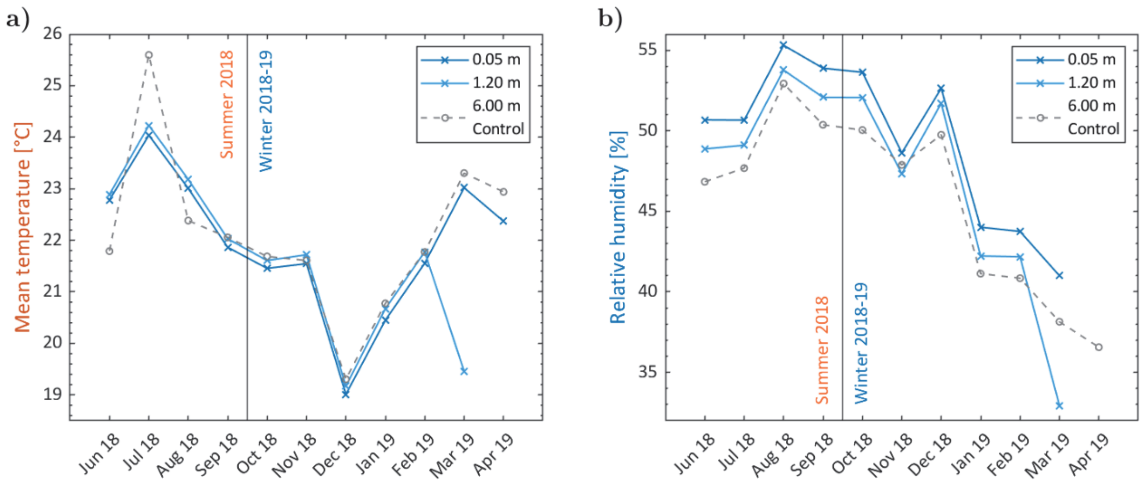


*Fig. 40. Monthly breakdowns of daytime horizontal distribution of $T_{air}$ (a) and RH (b) means.*

Table 13. DAB, horizontal $T_{air}$, $RH$, and $AH$ distribution mean influence.

| | SUMMER 2018 & 19 | | WINTER 2018-19 | |
|---|---|---|---|---|
| | ***0.05 - 1.20 m*** | ***1.2 - 6.00 m*** | ***0.05 - 1.20 m*** | ***1.20 - 6.00 m*** |
| $\boldsymbol{T_{air}}$ (°C) | | | | |
| **Daytime** | ↑0.46 (±0.02)<br>↑2.04% | ↓0.61 (±0.02)<br>↓2.62% | ↑0.01 (±0.02)<br>↑0.05% | ↑0.27 (±0.02)<br>↑1.27% |
| {6.00 m *Ctrl*: 100%} | {*0.05 m*: 100.6%} | {*1.20 m*: 102.7%} | {*0.05 m*: 98.69%} | {*1.20 m*: 98.74%} |
| **Night-time** | ↑0.13 (±0.02)<br>↑0.60% | ↓0.37 (±0.02)<br>↓1.70% | ↓0.14 (±0.02)<br>↓0.67% | ↑0.30 (±0.02)<br>↑1.44% |
| {*Ctrl*: 100%} | {*0.05 m*: 101.1%} | {*1.20 m*: 101.7%} | {*0.05 m*: 99.2%} | {*1.20 m*: 98.6%} |
| ***RH*** (%) | | | | |
| **Daytime** | ↓1.67 (±0.10)<br>↓3.2% | ↓2.67 (±0.09)<br>↓5.2% | ↓1.46 (±0.07)<br>↓3.1% | ↓2.71 (±0.07)<br>↓5.9% |
| {*Ctrl*: 100%} | {*0.05 m*: 109.0%} | {*1.20 m*: 105.5%} | {*0.05 m*: 109.6%} | {*1.20 m*: 106.3%} |
| **Night-time** | ↓1.40 (±0.09)<br>↓2.5% | ↓4.07 (±0.10)<br>↓7.6% | ↓1.02 (±0.07)<br>↓2.2% | ↓2.17 (±0.07)<br>↓4.8% |
| {*Ctrl*: 100%} | {*0.05 m*: 111.0%} | {*1.20 m*: 108.2%} | {*0.05 m*: 107.3%} | {*1.20 m*: 105.0%} |
| ***AH*** (g·m⁻³) | | | | |
| **Daytime** | ↓0.24 (±0.02)<br>↓2.2% | ↓0.87 (±0.02)<br>↓8.3% | ↓0.18 (±0.01)<br>↓2.1% | ↓0.39 (±0.01)<br>↓4.5% |
| {*Ctrl*: 100%} | {*0.05 m*: 111.5%} | {*1.20 m*: 109.0%} | {*0.05 m*: 107.0%} | {*1.20 m*: 104.7%} |
| **Night-time** | ↓0.23 (±0.02)<br>↓2.2% | ↓0.98 (±0.02)<br>↓9.6% | ↓0.14 (±0.01)<br>↓1.7% | ↓0.26 (±0.01)<br>↓3.2% |
| {*Ctrl*: 100%} | {*0.05 m*: 113.0%} | {*1.20 m*: 110.6%} | {*0.05 m*: 105.1%} | {*1.20 m*: 103.3%} |

Notes: Values in (brackets) hereafter refer to relative mean difference SD; signs '↑' and '↓' hereafter indicate relative increase and decrease respectively; and {brackets} refer to value relative to *Control/Ctrl* 6.00 m: 100%.

The relationships between horizontal $T_{air}$ distribution datasets (Fig. 39a, p. 103; and Fig. 40a, p. 104), presented 'very strong' correlations/$r^2$ for summer and winter daytime ($r_s$ >0.94 and >0.98, $p$ <0.01 respectively) and night-time ($r^2$ >96 and >98%). Owing to the abovementioned stack-flow interference at the *Control* probe, horizontal distribution influence is best limited to the discussion between the *L02-0.05* and *L02-1.20 m* datasets, where the latter demonstrated >99% shared variability with the former. When mean profiles were examined (Fig. 43a, p. 107), the summer day and night-time, and winter daytime profiles presented increased means at the *L02-1.20 m* probe (2.0, 0.1, and 0.05% respectively). Save for the winter night-time profile, all others therefore presented cooler $T_{air}$ values nearer to the installation surface (highest reduction during summer daytime, M ~0.5, ±0.23 K).

Horizontal ***RH*** (Fig. 39b and Fig. 40b) and ***AH*** distribution datasets, also presented significant 'very strong' correlations/$r^2$ (>91 and 92% respectively), while correlations/$r^2$ for the *Control* were marginally weaker, with summer daytime presenting the relative weakest. The mean ***RH*** distribution profile from the installation to the *Control* decreased in winter and summer, and both day and night-time, with steeper gradients between the *L02-0.05* and *L02-1.20 m* probes (Fig. 43c). The highest ***RH*** was therefore always nearer to the canopy (5.5, ±0.6%, L02 mean increase relative to the *Control* for the summer night-time). Absolute humidity profiles complemented this trend (Fig. 43d), with the maximum summer night-time mean increase for L02 relative to the *Control* at 1.20, ±0.1 g·m$^{-3}$ or 13.0%. The summer daytime difference between the *L02-0.05* and *L02-1.20 m* probes however was notably modest (0.24, ±0.1 g·m$^{-3}$ or 2.5%), which highlighted slower decay.

### *Vertical distribution:*

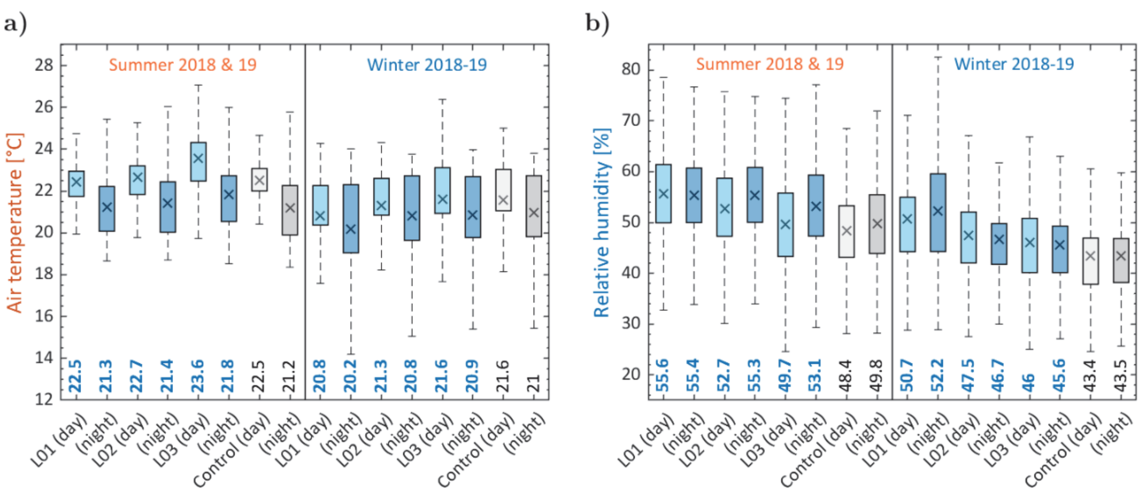


*Fig. 41. DAB, vertical $T_{air}$ (a) and RH (b) distribution datasets, relative to the Control.*

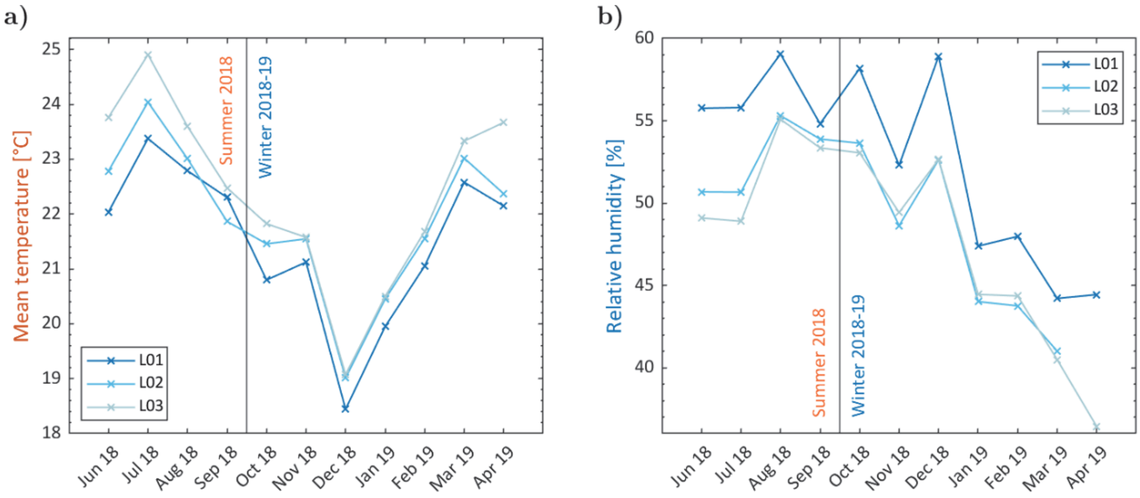


*Fig. 42. Monthly breakdowns of daytime vertical distribution of $T_{air}$ (a) and RH (b) means.*

Table 14. DAB, vertical $T_{air}$, $RH$, and $AH$ distribution mean influence.

| | SUMMER 2018 & 19 | | WINTER 2018-19 | |
|---|---|---|---|---|
| | ***L01 - L02*** | ***L02 - L03*** | ***L01 - L02*** | ***L02 - L03*** |
| $T_{air}$ **(°C)** | | | | |
| **Daytime** | ↑0.22 (±0.01), ↑1.0% | ↑0.90 (±0.01), ↑4.0% | ↑0.48 (±0.02), ↑2.3% | ↑0.32 (±0.02), ↑1.5% |
| {*Ctrl*: 100%} | {*L01*: 99.7%} \| {*L02*: 100.6%} \| {*L03*: 104.7%} | | {*L01*: 96.5%} \| {*L02*: 98.7%} \| {*L03*: 100.2%} | |
| **Night-time** | ↑0.17 (±0.02), ↑0.8% | ↑0.40 (±0.02), ↑1.9% | ↑0.62 (±0.02), ↑3.1% | ↑0.06 (±0.02), ↑0.3% |
| {*Ctrl*: 100%} | {*L01*: 100.3%} \| {*L02*: 101.1%} \| {*L03*: 103%} | | {*L01*: 96.3%} \| {*L02*: 99.2%} \| {*L03*: 99.5%} | |
| ***RH*** **(%)** | | | | |
| **Daytime** | ↓2.89 (±0.08), ↓5.2% | ↓3.06 (±0.09), ↓5.8% | ↓3.19 (±0.08), ↓6.3% | ↓1.49 (±0.07), ↓3.1% |
| {*Ctrl*: 100%} | {*L01*: 114.9%} \| {*L02*: 109%} \| {*L03*: 102.6%} | | {*L01*: 117%} \| {*L02*: 109.6%} \| {*L03*: 106.2%} | |
| **Night-time** | ↓0.09 (±0.09), ↓0.2% | ↓2.16 (±0.09), ↓3.9% | ↓5.57 (±0.08), ↓10.7% | ↓1.12 (±0.07), ↓2.4% |
| {*Ctrl*: 100%} | {*L01*: 111.2%} \| {*L02*: 111%} \| {*L03*: 106.6%} | | {*L01*: 120.1%} \| {*L02*: 107.3%} \| {*L03*: 104.8%} | |
| ***AH*** **(g·m⁻³)** | | | | |
| **Daytime** | ↓0.29 (±0.02), ↓2.7% | ↓0.27 (±0.02), ↓2.5% | ↓0.40 (±0.01), ↓4.3% | ↓0.04 (±0.01), ↓0.5% |
| {*Ctrl*: 100%} | {*L01*: 114.5%} \| {*L02*: 111.5%} \| {*L03*: 108.7%} | | {*L01*: 111.8%} \| {*L02*: 107.0%} \| {*L03*: 106.5%} | |
| **Night-time** | ↑0.12 (±0.02), ↑1.1% | ↓0.22 (±0.02), ↓2.1% | ↓0.73 (±0.01), ↓8.1% | ↓0.06 (±0.01), ↓0.7% |
| {*Ctrl*: 100%} | {*L01*: 111.7%:} \| {*L02*: 113.0%} \| {*L03*: 110.6%} | | {*L01*: 114.3%} \| {*L02*: 105.1%} \| {*L03*: 104.3%} | |

Note: {brackets} refer to value relative to *Control/Ctrl* 6.00 m: 100%.

The relationships between vertical distribution probe datasets from floor levels L01-to-L03 (Fig. 41a, p. 105; and Fig. 42a), presented significant 'very strong' correlations/$r^2$ for the summer night-time, and winter day and night-time (>88%); while the summer daytime[I] presented 'moderate-to-strong' correlations to highlight the influence of moderate

[I] *L02* $T_{air}$ summer daytime dataset not normally distributed (skewness: 1.39; kurtosis: 10.30).

interference and disruption ($r_s$ >0.62, $p$<0.01). The *L01-0.05 m* probe notably presented relatively weaker relationships, with only 63% of L02 and 38% of L03's variability explained by L01. This suggested *L02-* and *L03-0.05 m* variation to be influenced by lateral thermal contributions and mixing from the respective floor levels, as well as from living wall modifications. The mean $T_{air}$ profiles nevertheless always maintained a vertical thermal gradient with increasing means from floor levels L01-to-L03 (Fig. 43b). The *L03-0.05 m* probe therefore presented the warmest canopy proximate values, with the summer presenting the highest means. This gradient confirmed the sustained presence of thermal stratification, and with it the occurrence of a buoyancy-driven stack-effect in the atrium. Although such flow is typically considered to be weak, it had sufficient potency in the summer to cause the abovementioned interference and reduced associations at the DAB atrium.

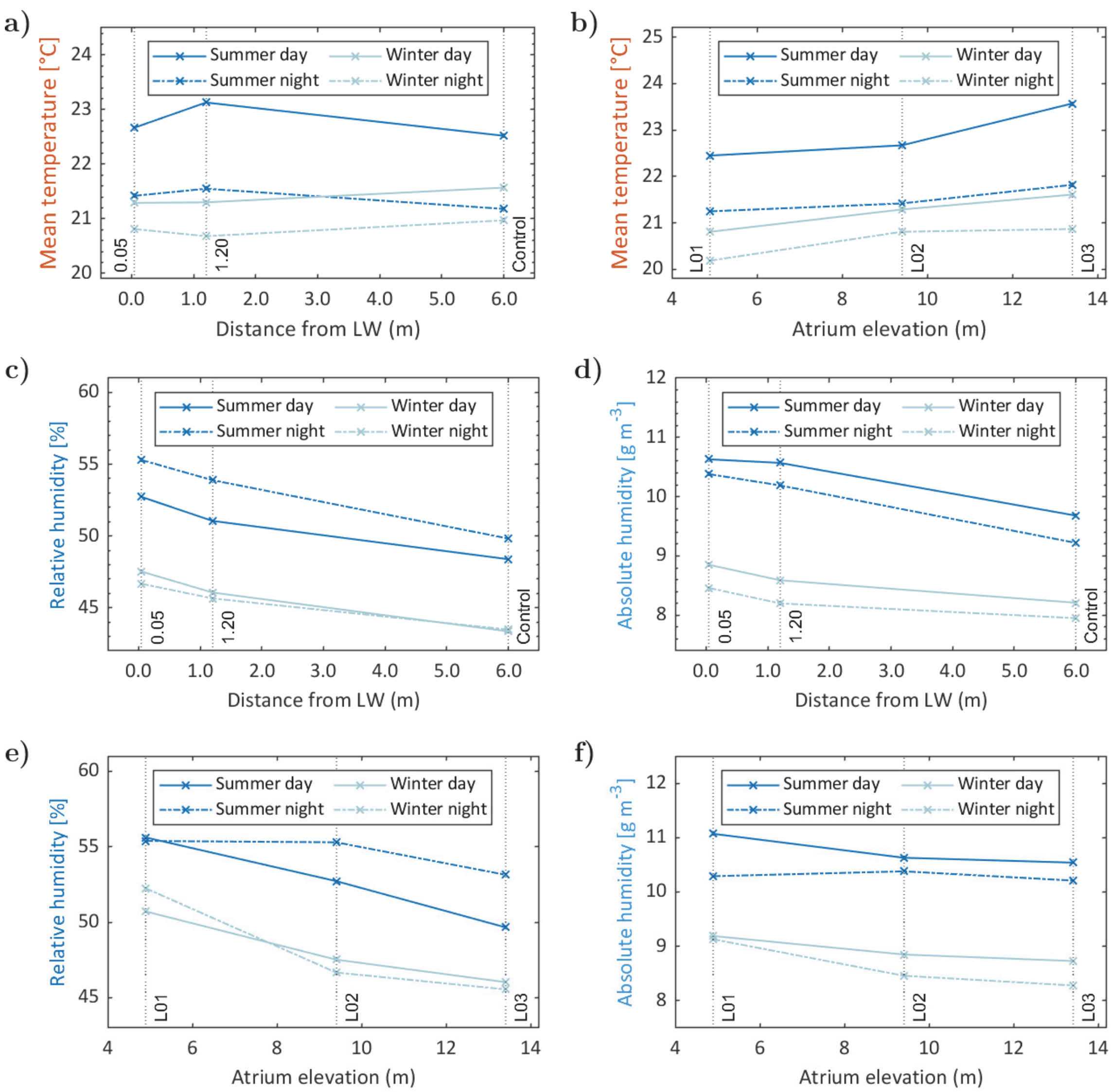


*Fig. 43. DAB, mean $T_{air}$ horizontal (a) and vertical (b) distribution profiles; and mean RH and AH horizontal (c & d) and vertical (e & f) distribution profiles.*

Vertical $RH$ (Fig. 41b, p. 105; and Fig. 42b, p. 106) and $AH$ distribution dataset correlations/$r^2$ were higher for the summer night-time and winter daytime ($RH$: $r^2$ >80 and >82%; and $AH$: 89 and 84% respectively), than for the summer daytime and winter night-time ($RH$: >59 and >65%; and $AH$: 71 and 65%). The *L01-0.05 m* probe again presented relatively weaker relationships to L02 and L03 datasets, while distribution profiles presented an inverted gradient with means decreasing from L01-to-L03 to confirm humidity stratification (Fig. 43e & f, p. 107). L01 therefore presented the highest surface proximate $RH$ (8.8, ±0.4% increase relative to the *Control* for the winter night-time), as well as $AH$ means for the atrium (1.4, ±0.3 g·m$^{-3}$ or 14.5% increase for the summer daytime).

### *Surface temperatures and airflow:*

The *L02* $T_{leaf}$ data collected was for the validation purposes of Study 3, and is not assessed here (see Chapter 6). The living wall adjacent bare wall $T_{surf}$ datasets represented by L00 (at installation base) and L02 (at vertical mid-point; Fig. 44a, p. 109), presented 'very strong' correlations/$r^2$ for the summer and winter, both day and night-time ($r$ >0.83, $p$ <0.01). From these, the summer day and night-time correlations/$r^2$ were notably less (both $r^2$ ~78%) than winter (97 and 94% respectively). The relatively stronger correlations presented with wintertime data (as well as higher means) suggested greater association with the atrium $T_{air}$ gradient, which was clarified by the marginally stronger correlations ($r_s$ >0.97) between L02 surface proximate $T_{air}$ and corresponding $T_{surf}$.

Relationships between *L02* $T_{soil}$, installation adjacent wall *L02* $T_{surf}$, and proximate *L02* $T_{air}$ datasets (Fig. 44a), presented 'strong' to 'very strong' correlations/$r^2$ [II] ($r$ >0.74, $p$ <0.01). From these, *L02* $T_{soil}$ correlations/$r^2$ were notably weaker for the corresponding $T_{surf}$ and $T_{air}$ (slightly higher for the former), during the summer day ($T_{surf}$: 61% and $T_{air}$: 60%) and night-time (57 and 54%), as well as during the winter night-time (76 and 73%). For the winter daytime however, the correlations were stronger (*L02* $T_{surf}$: $r_s$ (29,934, N = 29,934) = 0.86, $p$ <0.01; and *L02* $T_{air}$: $r_s$ = 0.82). *L02* $T_{soil}$ means were notably lower than the corresponding $T_{surf}$ and $T_{air}$, both day and night-time, and in the summer and winter. The lower association as well as means of the soil substrate could be attributed here to its saturated status and resultant influence from surface evaporation.

---

[II] *L02* $T_{air}$ winter daytime dataset not normally distributed (skewness: -2.01; kurtosis: 7.2).

Table 15. DAB, surface temperature influences.

| Temp. (°C) | SUMMER 2018 & 19 | | | WINTER 2018-19 | | |
|---|---|---|---|---|---|---|
| | $T_{surf}$ *L00 - L02* | *L02* $T_{surf}$ - $T_{soil}$ | *L02* $T_{surf}$ - $T_{air}$ | $T_{surf}$ *L00 - L02* | *L02* $T_{surf}$ - $T_{soil}$ | *L02* $T_{surf}$ - $T_{air}$ |
| **Daytime** | $\uparrow$0.93 (±0.01), $\uparrow$4.2% | $\downarrow$1.95 (±0.01), $\downarrow$8.6% | $\downarrow$0.11 (±0.21), $\downarrow$0.5% | $\uparrow$1.09 (±0.02), $\uparrow$5.4% | $\downarrow$2.48 (±0.02), $\downarrow$11.6% | $\downarrow$0.12 (±0.17), $\downarrow$0.5% |
| {*L00* $T_{surf}$} | {*L02*: 104.2%} | | | {*L02*: 105.4%} | | |
| {*L02* $T_{surf}$} | | {*L02* $T_{soil}$: 91.4%} | {*L02* $T_{air}$: 99.5%} | | {*L02* $T_{soil}$: 88.4%} | {*L02* $T_{air}$: 99.5%} |
| {*L02* $T_{air}$} | | {*L02* $T_{soil}$: 91.9%} | {*L02* $T_{surf}$: 100.5%} | | {*L02* $T_{soil}$: 88.9%} | {*L02* $T_{surf}$: 100.5%} |
| **Night-time** | $\uparrow$0.38 (±0.02), $\uparrow$1.8% | $\downarrow$0.76 (±0.01), $\downarrow$3.5% | $\downarrow$0.32 (±0.22), $\downarrow$1.5% | $\uparrow$1.08 (±0.02), $\uparrow$5.4% | $\downarrow$2.23 (±0.02), $\downarrow$10.6% | $\downarrow$0.30 (±0.17), $\downarrow$1.4% |
| {*L00* $T_{surf}$} | {*L02*: 101.8%} | | | {*L02*: 105.4%} | | |
| {*L02* $T_{surf}$} | | {*L02* $T_{soil}$: 96.5%} | {*L02* $T_{air}$: 98.5%} | | {*L02* $T_{soil}$: 89.4%} | {*L02* $T_{air}$: 98.6%} |
| {*L02* $T_{air}$} | | {*L02* $T_{soil}$: 97.9%} | {*L02* $T_{surf}$: 101.5%} | | {*L02* $T_{soil}$: 90.7%} | {*L02* $T_{surf}$: 101.4%} |

Notes: {brackets} refer to values relative to base *L00* $T_{surf}$: 100%; *L02* $T_{surf}$: 100%; or *L02* $T_{air}$: 100%.

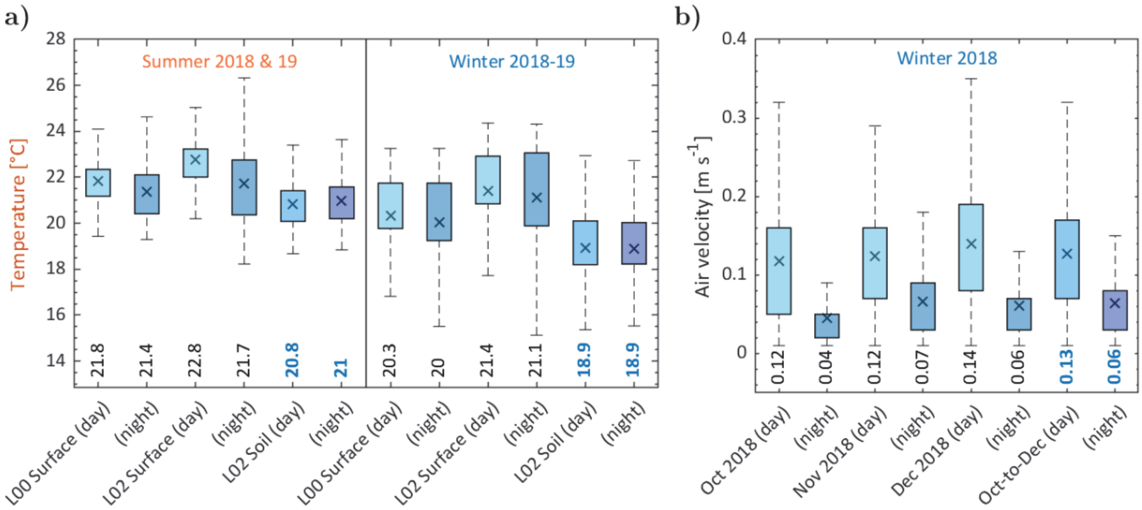


*Fig. 44. DAB, living wall* $T_{soil}$ *and adjacent wall* $T_{surf}$ *(a); and omnidirectional* $V_{air}$ *(b) datasets.*

Ambient omnidirectional $V_{air}$ and its variability within the atrium was moderate, with the summer mean at 0.096, ±0.05 m·s$^{-1}$ and winter at 0.116, ±0.06 m·s$^{-1}$. The latter winter mean being marginally higher than the summer is attributed to unavoidable contamination flow arising from greater entrance door operation during this period (i.e., building occupancy profile dependent). The $V_{air}$ means were nevertheless in the expected range for the building use with sedentary occupants in normal indoor clothing (0.12 m·s$^{-1}$ during cooling and 0.10 m·s$^{-1}$ during heating season for offices; [320]). Any adverse influence of airflow is also yet to be reported, partly for the reason that the atrium is mainly experienced by building occupants as a transitional space (i.e., minimal exposure) [315].

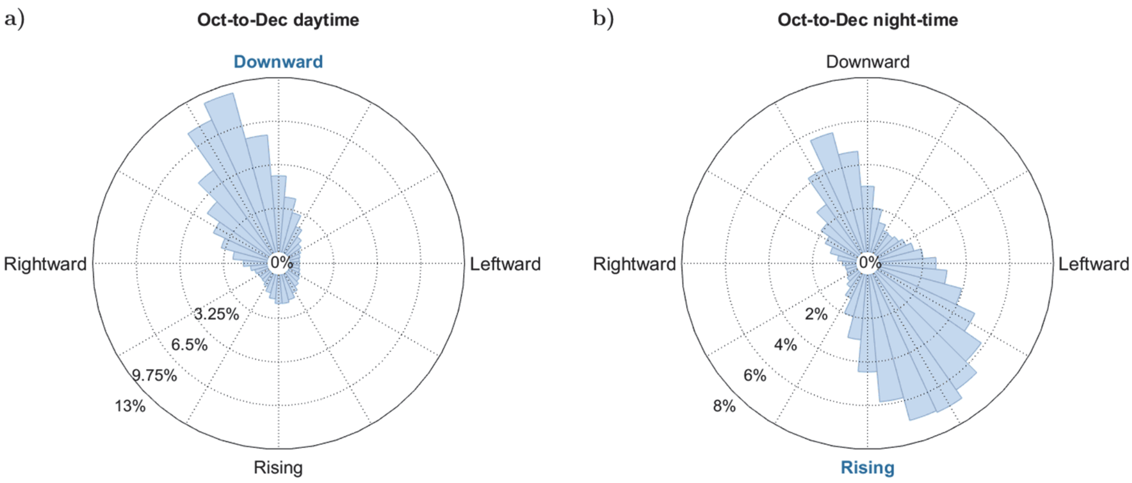


*Fig. 45. Oct-to-Dec surface air movement vertical wind roses for daytime (a); and night-time (b).*

Localised living wall surface air movement for the monitored wintertime period also demonstrated moderate omnidirectional $V_{air}$ values, with 0.13, ±0.08 m·s$^{-1}$ daytime mean, and night-time air movement at M = 0.06, ±0.06 m·s$^{-1}$ (Fig. 44b, p. 109). Daytime surface proximate flow was therefore significantly more potent than during the night. The $V_{air}$ data showed 'very weak' negative correlations with proximate L01 $T_{air}$ ($r$ = -0.10, N = 2,604 [5-minute intervals], $p$<0.01) and proximate L01 $RH$ ($r_s$ = -0.05, $p$ <0.01) for the daytime, while for the night-time the correlation was positive and 'weak' for L01 $T_{air}$ ($r$ = 0.34, N = 2,243, $p$ <0.01) and negative and 'weak' for L01 $RH$ ($r_s$ = -0.30, $p$ <0.01). Daytime shared $V_{air}$ variance with proximate $T_{air}$ and $RH$ was therefore minimal ($r^2$ = 1.0 and 0.3% respectively), while at night-time it was relatively higher (11.4 and 9%). This suggested installation proximate air movement potency and its variance to be explained mostly by the variance of other factors, particularly during the daytime.

Table 16. DAB, surface airflow by quadrant; monthly, day and night breakdown.

| **Quadrant flow** | October Day | October Night | November Day | November Night | December Day | December Night |
|---|---|---|---|---|---|---|
| Vertical, rising | **41.9%** | 20.0% | 12.7% | **37.9%** | 8.9% | **44.1%** |
| Vertical, downward | 28.6% | 24.3% | **56.6%** | 28.0% | **64.8%** | 21.2% |
| Lateral, rightward | 18.1% | 10.3% | 22.5% | 9.7% | 21.5% | 5.2% |
| Lateral, leftward | 11.4% | **45.4%** | 8.2% | 24.5% | 4.8% | 29.5% |
| #hrs recorded | ~17 | ~12 | ~154 | ~132 | ~46 | ~43 |
| Mean $T_{air}$* (°C) | 19.9, ±1.1 | 18.3, ±0.8 | 21.3, ±0.9 | 20.5, ±1.1 | 21.5, ±0.3 | 20.5, ±0.6 |

Note: * During monitored periods at L01 (proximate to wind sensor).

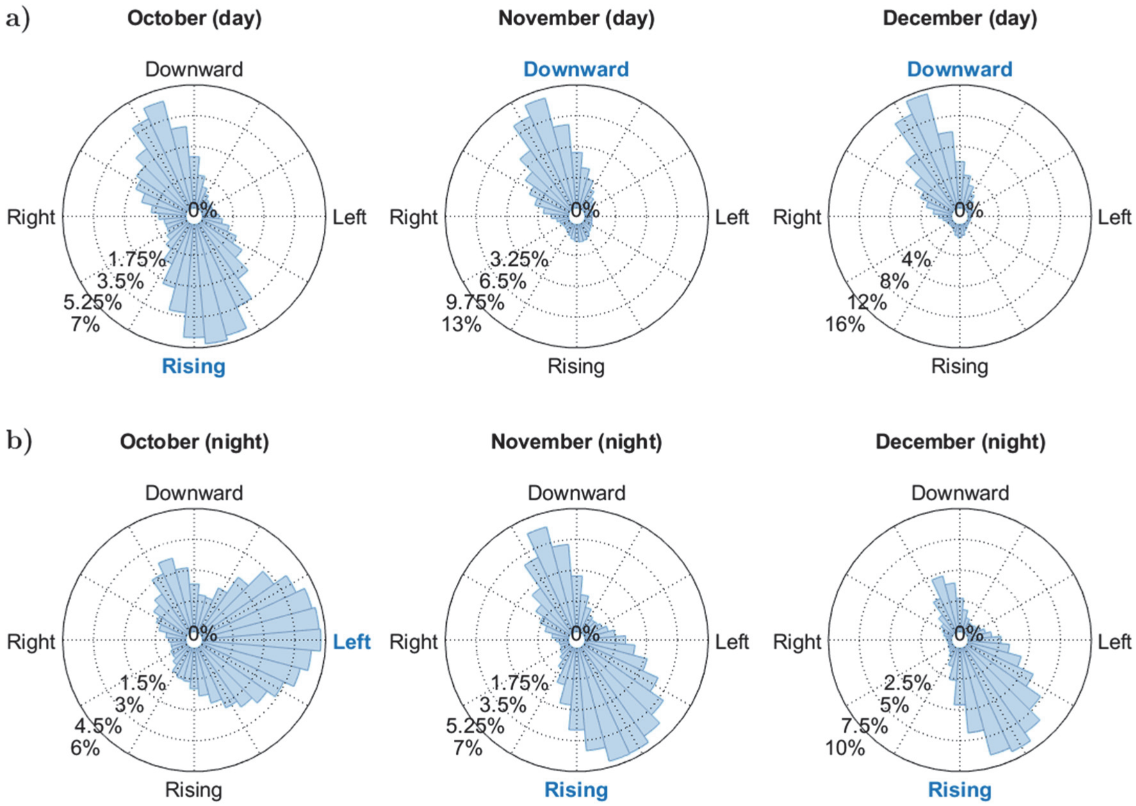


*Fig. 46. Surface air movement monthly vertical wind roses for day (a), and night-time (b).*

When flow directional data for this period was examined, contrasting conditions were revealed for the day and night-time (Fig. 45, p. 110; Fig. 46; Table 16, p. 110; and Table 17). During the daytime, dominant flow was directed down the living wall surface (56.1%), while at night this was inverted (38.2% rising). Examining the monthly breakdown showed that save for October (shorter duration of data collected), November and December datasets agreed with this trend. Notably, lateral flow had the highest velocities/potency, which confirms contamination from cross-infiltration or draughts (e.g., from greater entrance door or occupant window operation). This contamination could be a contributing factor to the weaker correlations noted earlier with surface proximate $T_{air}$ and $RH$.

Table 17. DAB, surface airflow quadrant means, by day and night-time.

| **Quadrant flow*** | **Quadrant definition (Degrees)** | **Daytime** | | | **Night-time** | | |
|---|---|---|---|---|---|---|---|
| | | Relative flow % | Mean Direction † (Degrees) | Mean velocity (m·s$^{-1}$) | Relative flow % | Mean Direction † (Degrees) | Mean velocity (m·s$^{-1}$) |
| Upward | <045°, >315° | 14.2% | 354° | 0.168 | **38.1%** | **346°** | **0.094** |
| Downward | >135°, <225° | **56.1%** | **164°** | **0.171** | 26.2% | 165° | 0.105 |
| Rightward | >045°, <135° | 21.9% | 112° | 0.221 | 8.7% | 113° | 0.142 |
| Leftward | >225°, <315° | 7.7% | 272° | 0.221 | 27.0% | 286° | 0.135 |

Note: * Meteorological wind direction inverted; † using Mardia's [321] method of averaging unity direction vectors.

## b) Semi-outdoor court

The results presented below characterises the hygrothermal microclimate modifications at the SET court for the monitored duration.

### *Wider climate association:*

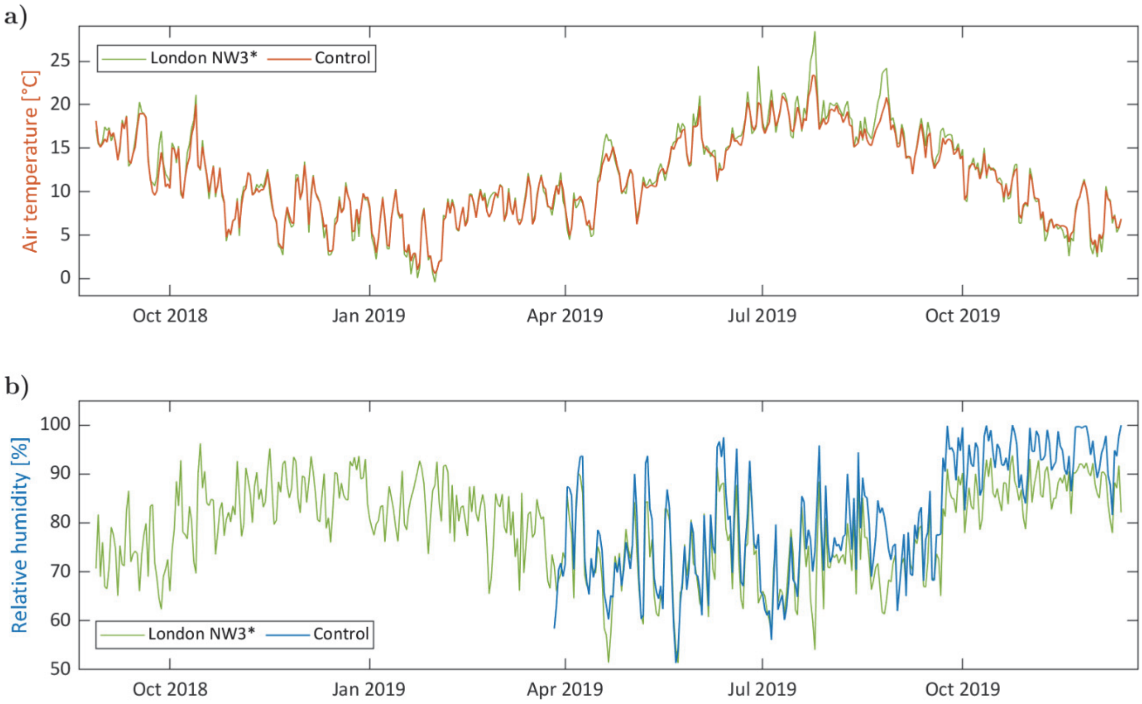


Note: *Hampstead, north London weather station data [316].

*Fig. 47. SET Control daily mean $T_{air}$ (a) and RH (b) profiles relative to NW3 Hampstead climate.*

The probe at 4.00 m was considered as the *'Control'* for the monitoring campaign as it was at the physical limit of the court, and thus the furthest distance from the living wall. Its $T_{air}$ dataset presented 'very strong' correlation/$r^2$ with the outdoor climate (98.2%), and seasonal variance with the summer means warmer than winter by 7.3, ±0.1 K during the daytime and 6.7, ±0.1 K during the night-time (see Fig. 47 for profiles). The greater seasonal variation relative to the indoor study is expected given the court's exposure as an open system, despite its sheltering bounds. Notably, *Control* readings presented lower means for both the day and night-time than the intermediate horizontal distribution probes within the court (i.e., *IP01-to-IP03*, Fig. 52a, p. 116). This suggested influence from the proximate building façade's thermal properties (i.e., Portland stone), as well as possible contamination influence from the operation of the nearby terrace door. The *Control* $T_{air}$ means were nevertheless greater than the *SF-C Canopy* probe at the living wall surface.

The *Control* $RH$ and $AH$ datasets also presented 'very strong' correlations/$r^2$ with the outdoor climate (87% and 97%, slightly weaker than with $T_{air}$). Mean $RH$ as a result varied seasonally, with the summer means lesser than winter by 10.2, ±0.9% during the daytime and 9.4, ±0.9% during the night-time; while $AH$ presented summer means greater than winter by 2.6, ±0.1 g·m$^{-3}$ during both day and night-time. These relatively larger variations are again expected owing to the court's exposure to the wider climate. Absolute humidity means however highlighted humidity in the court to have been only ~9% (<0.9 g·m$^{-3}$) greater than at the atrium study over the summer, while in winter was ~7% (<0.6 g·m$^{-3}$) lesser. In contrast to the atrium, $RH$ variation at the court was better explained by $T_{air}$ variance ($r^2$ = 18%) than $AH$ (1.4%).

*Horizontal distribution:*

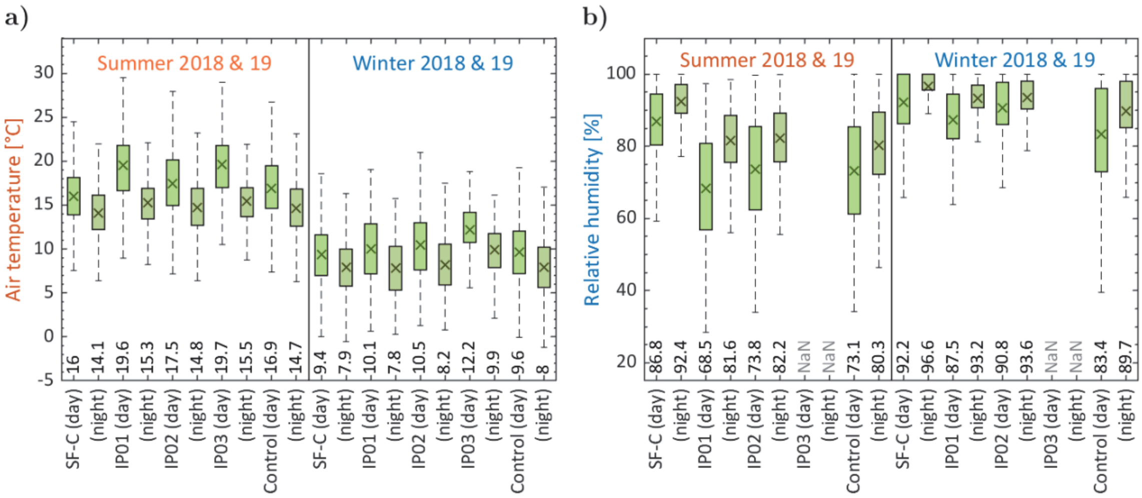


*Fig. 48. SET, horizontal* $T_{air}$ *(a) and RH (b) distribution datasets.*

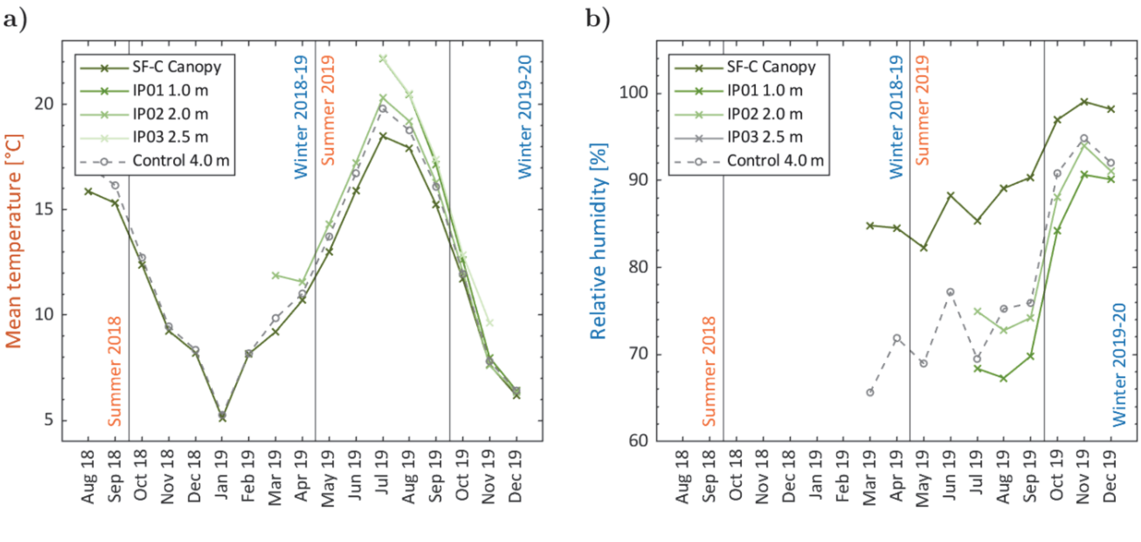


*Fig. 49. Monthly breakdowns of daytime horizontal distribution of* $T_{air}$ *(a) and RH (b) means.*

Table 18. SET, horizontal $T_{air}$, $RH$, and $AH$ distribution influence.

| | SUMMER 2018 & 19 | | | | WINTER 2018 &19 | | | |
|---|---|---|---|---|---|---|---|---|
| | ***SF-C - IP01*** | ***IP01 - IP02*** | ***IP02 - IP03*** | ***IP03 - Ctrl*** | ***SF-C - IP01*** | ***IP01 - IP02*** | ***IP02 - IP03*** | ***IP03 - Ctrl*** |
| **$T_{air}$ (°C)** | | | | | | | | |
| **Daytime** | ↑3.55 (±0.05) ↑22.1% | ↓2.07 (±0.05) ↓10.6% | ↑2.18 (±0.05) ↑12.4% | ↓2.74 (±0.04) ↓13.9% | ↑0.69 (±0.05) ↑7.4% | ↑0.42 (±0.06) ↑4.2% | ↑1.71 (±0.06) ↑16.3% | ↓2.56 (±0.05) ↓21.0% |
| {*Ctrl*: 100%} | {*SF-C*: 94.6%} | {*IP01*: 115.5%} | {*IP02*: 103.3%} | {*IP03*: 116.2%} | {*SF-C*: 97.3%} | {*IP01*: 104.51%} | {*IP02*: 108.9%} | {*IP03*: 126.7%} |
| **Night-time** | ↑1.20 (±0.03) ↑8.5% | ↓0.51 (±0.04) ↓3.3% | ↑0.68 (±0.04) ↑4.6% | ↓0.80 (±0.03) ↓5.2% | ↓0.11 (±0.03) ↓1.4% | ↑0.42 (±0.04) ↑5.4% | ↑1.70 (±0.04) ↑20.6% | ↓1.96 (±0.04) ↓19.8% |
| {*Ctrl*: 100%} | {*SF-C*: 96.0%} | {*IP01*: 104.3%} | {*IP02*: 100.8%} | {*IP03*: 105.4%} | {*SF-C*: 99.4%} | {*IP01*: 98.0%} | {*IP02*: 103.3%} | {*IP03*: 124.6%} |
| ***RH* (%)** | | | | | | | | |
| **Daytime** | ↓18.35 (±0.16) ↓21.1% | ↑5.29 (±0.21) ↑7.7% | NaN | NaN | ↓4.72 (±0.14) ↓5.1% | ↑3.30 (±0.15) ↑3.8% | NaN | NaN |
| {*Ctrl*: 100%} | {*SF-C*: 118.7%} | {*IP01*: 93.6%} | {*IP02*: 100.9%} | | {*SF-C*: 110.6%} | {*IP01*: 104.9%} | {*IP02*: 108.9%} | |
| **Night-time** | ↓10.79 (±0.10) ↓11.7% | ↑0.61 (±0.13) ↑0.7% | NaN | NaN | ↓3.41 (±0.06) ↓3.5% | ↑0.41 (±0.06) ↑0.4% | NaN | NaN |
| {*Ctrl*: 100%} | {*SF-C*: 115.0%} | {*IP01*: 101.6%} | {*IP02*: 102.3%} | | {*SF-C*: 107.7%} | {*IP01*: 103.9%} | {*IP02*: 104.3%} | |
| ***AH* (g·m$^{-3}$)** | | | | | | | | |
| **Daytime** | ↓0.64 (±0.03) ↓5.3% | ↑0.19 (±0.03) ↑1.7% | NaN | NaN | ↓0.36 (±0.03) ↓4.2% | ↑0.09 (±0.03) ↑1.02% | NaN | NaN |
| {*Ctrl*: 100%} | {*SF-C*: 113.5%} | {*IP01*: 107.5%} | {*IP02*: 109.3%} | | {*SF-C*: 109.2%} | {*IP01*: 104.6%} | {*IP02*: 105.7%} | |
| **Night-time** | ↓0.76 (±0.02) ↓6.6% | ↑0.36 (±0.03) ↑3.4% | NaN | NaN | ↓0.53 (±0.02) ↓6.4% | ↑0.18 (±0.02) ↑2.3% | NaN | NaN |
| {*Ctrl*: 100%} | {*SF-C*: 110.9%} | {*IP01*: 103.6%} | {*IP02*: 107.1%} | | {*SF-C*: 106.9%} | {*IP01*: 100.02%} | {*IP02*: 102.3%} | |

Notes: {brackets} refer to value relative to base *Control/Ctrl* 4.00 m: 100%.

The horizontal distribution $T_{air}$ datasets presented 'very strong' correlations/$r^2$ for the summer and winter, both day and night-time ($r$ >0.8, $p$<0.01). The daytime presented greater range in both the summer (>81%) and winter (>90%) than night-time (>95 and >96% respectively). The *SF-C Canopy* probe presented the lowest or coolest means (highest M = 0.9, ±0.14 K for the summer daytime relative to the *Control*), while the lowest was for the winter night-time (M = 0.05, ±0.05 K). Influence distribution notably showed summer irregularity, with the intermediate probes (*IPs*) presenting relatively higher means save for a daytime dip at *IP02* (Fig. 48a, p. 113; and Fig. 52a, p. 116). The reason for this dip is unclear, and is hypothesised as mixing introduced from an unidentified source.

With $RH$, the correlation/$r^2$ range of the datasets was lowest for the summer daytime (>86%), while wintertime ranges were higher for the daytime (>69%) and night-time[III] ($r_s$ >0.79). In agreement with the atrium study, the highest means were at the *SF-C Canopy* probe (13.7, ±0.75%, highest increase relative to the *Control* for the summer daytime). Distribution showed greatest reduction between the *SF-C Canopy* and *IP01-1.0 m* probes (18.4, ±0.16%, for the summer daytime), while at *IP02-2.0 m* $RH$ showed a relative increase analogous to the mean $T_{air}$ dip discussed above (pronounced for the summer, Fig. 48b, p. 113 and Fig. 52c, p. 116). Absolute humidity data presented the highest correlation/$r^2$ range for the summer daytime (>83%) than others (>90%), with the summertime mean profiles clarifying the $RH$ increase to be influenced by the fall in $T_{air}$. In the wintertime, *IP02* demonstrated an increase in $AH$ to disrupt linear decay, as observed with summertime decay (Fig. 52d). This again highlighted interference from an unidentified source.

### *Vertical distribution:*

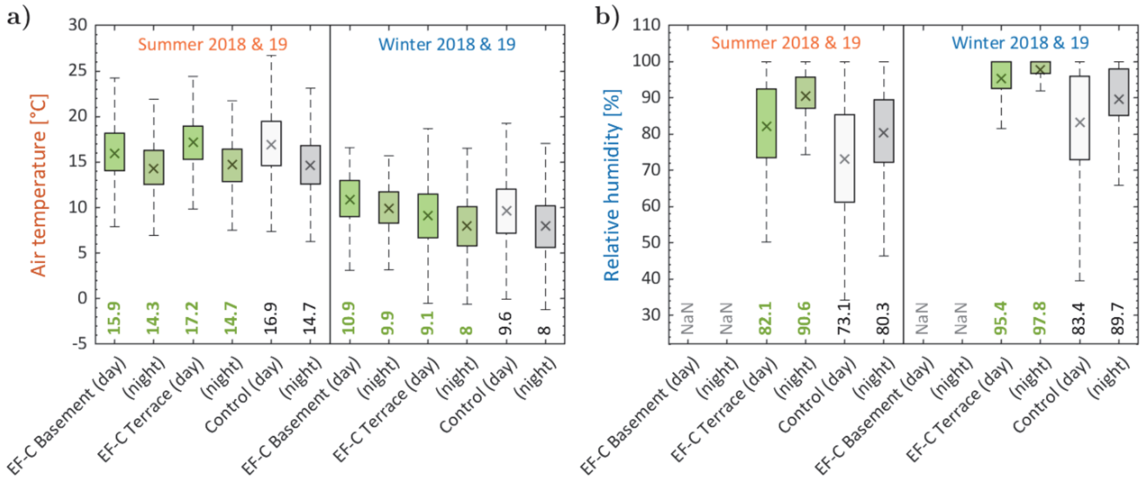


*Fig. 50. SET, vertical $T_{air}$ (a) and $RH$ (b) distribution datasets.*

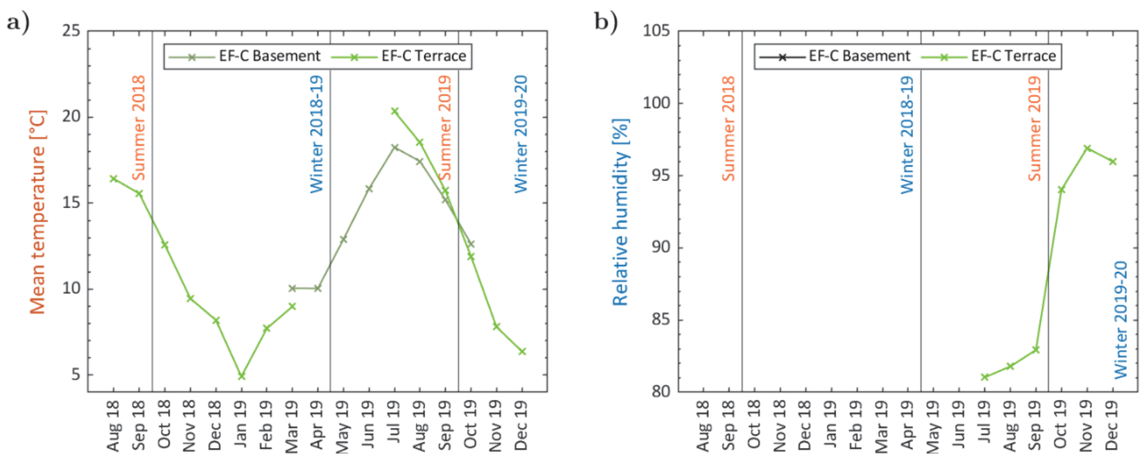


*Fig. 51. Monthly breakdowns of daytime vertical distribution of $T_{air}$ (a) and $RH$ (b) means.*

---

III *SF-C* winter night-time $RH$ dataset not normally distributed, skewness: -3.15; kurtosis: 16.18.

Table 19. SET, vertical $T_{air}$ distribution influence.

| | SUMMER 2018 & 19 *EF-C (Basement - Terrace)* | WINTER 2018 & 19 *EF-C (Basement - Terrace)* |
|---|---|---|
| ***$T_{air}$*** (°C) | | |
| **Daytime** {*Ctrl*: 100%} | ↑1.29 (±0.03); ↑8.1% {*Basement*: 94.1%} \| {*Terrace*: 101.7%} | ↓1.79 (±0.04); ↓16.4% {*Basement*: 113.2%} \| {*Terrace*: 94.6%} |
| **Night-time** {*Ctrl*: 100%} | ↑0.40 (±0.03); ↑2.8% {*Basement*: 97.6%} \| {*Terrace*: 100.3%} | ↓1.96 (±0.03); ↓19.7% {*Basement*: 124.9%} \| {*Terrace*: 100.3%} |
| ***RH*** (%) | | |
| **Daytime** {*Ctrl*: 100%} | NaN {*Basement*: NaN} \| {*Terrace*: 112.2%} | NaN {*Basement*: NaN} \| {*Terrace*: 114.5%} |
| **Night-time** {*Ctrl*: 100%} | NaN {*Basement*: NaN} \| {*Terrace*: 112.8%} | NaN {*Basement*: NaN} \| {*Terrace*: 108.9%} |

Notes: {brackets} refer to value relative to *Control/Ctrl* 4.00 m: 100%.

The relationship between vertical distribution datasets also presented 'very strong' correlations for the summer and winter, both day and night-time ($r$ >0.93, $p$<0.01). The daytime data correlations/$r^2$ in both the summer (86%) and winter (93%) were marginally weaker than the night-time (97 and 98% respectively). Given that only two vertical points were monitored (with ~3 m difference, Fig. 52b), a clear thermal disparity was evident with the *EF-C Terrace* presenting warmer day (1.29, ±0.03 K) and night-time (0.40, ±0.03 K) means relative to the *EF-C Basement* in the summer, while in winter this was inverted (cooler by 1.79, ±0.04 K and 1.96, ±0.03 K respectively).

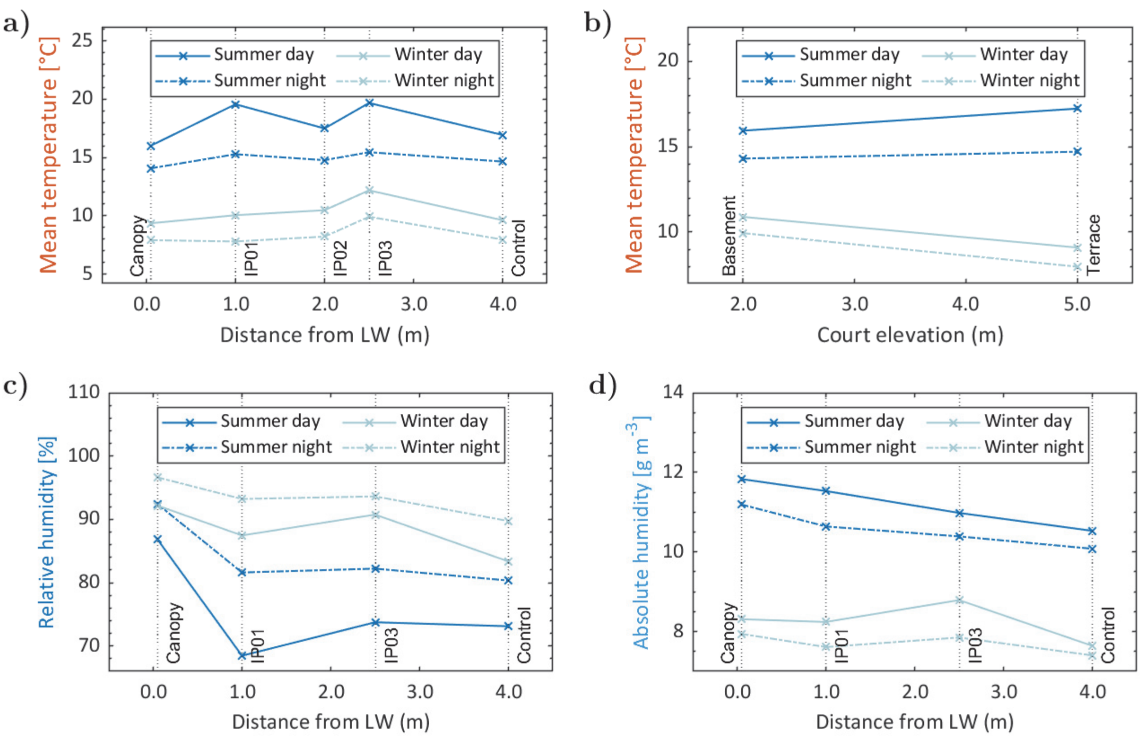


*Fig. 52. SET, mean $T_{air}$ horizontal (a) and vertical (b) distribution profiles; and RH and AH horizontal (c & d) distribution profiles.*

### *Surface temperatures at wall-return:*

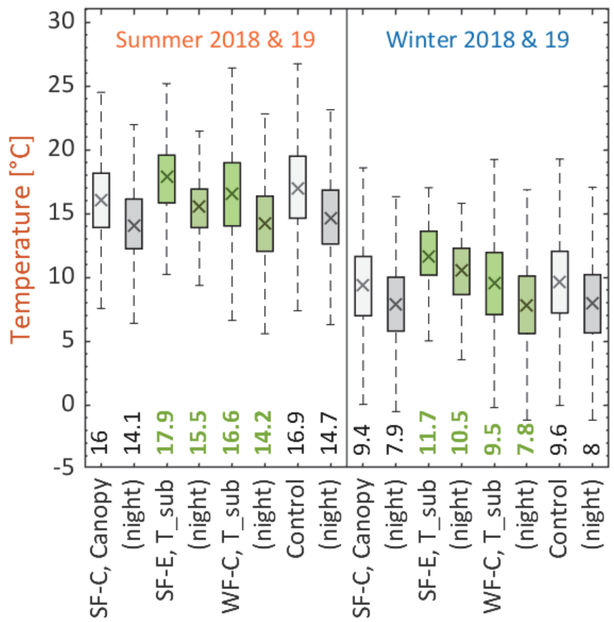


*Fig. 53. SET, wall-return condition $T_{sub}$ datasets relative to the SF-C Canopy and Control datasets.*

Table 20. SET, wall-return condition mean temperature influences.

| Temps (°C) | SUMMER 2018 & 19 *SF-C - SF-E* | *SF-E - WF-C* | WINTER 2018 & 19 *SF-C - SF-E* | *SF-E - WF-C* |
|---|---|---|---|---|
| **Daytime** | ↑1.86 (±0.02) ↑11.6% | **↓1.30** (±0.02) ↓7.3% | ↑2.29 (±0.02) ↑24.5% | **↓2.11** (±0.02) ↓18.1% |
| {*SF-C*: 100%} | {*SF-E*: 111.6%} | {*WF-C*: 103.5%} | {*SF-E*: 124.5%} | {*WF-C*: 102%} |
| **Night-time** | ↑1.44 (±0.02) ↑10.3% | **↓1.35** (±0.02) ↓8.7% | ↑2.61 (±0.02) ↑32.9% | **↓2.72** (±0.02) ↓25.9% |
| {*SF-C*: 100%} | {*SF-E*: 110.3%} | {*WF-C*: 100.7%} | {*SF-E*: 132.9%} | {*WF-C*: 98.5%} |

Notes: {brackets} refer to value relative to base *SF-C Canopy*: 100%.

The wall-return surface temperature probes *SF-E* and *WF-C* were mounted on the outer face of the felt-pocket system, shielded from direct solar exposure by the plant canopy. Their ST data is therefore analogous to substrate temperatures ($T_{sub}$), and were measured to characterise radiation incidence influence[IV] (Fig. 53). The *Control* presented 'very strong' correlations/$r^2$ with *SF-E*, and *WF-C* datasets for the yearly night-time (>99%); while for the yearly daytime *SF-E* presented higher $r^2$ (96 and 99% respectively) relative to the *WF-C* dataset (93 and 99%) to suggest modest influence from building shading.

The relationship between *SF-C Canopy* $T_{air}$ and *SF-E* $T_{sub}$, as well as *SF-E* $T_{sub}$ and *WF-C* $T_{sub}$ datasets presented 'very strong' correlations/$r^2$ (>98%) for all periods. Notably, correlations between *SF-C Canopy* $T_{air}$ and *WF-C* $T_{sub}$ were marginally weaker than between *SF-C Canopy* $T_{air}$ and *SF-E* $T_{sub}$, and SF-E and *WF-C* $T_{sub}$, while means highlighted the south-facing *SF-E* probe to present higher $T_{sub}$ relative to *WF-C* for all periods (pronounced during the winter, Table 20). These observations suggested the influence of irradiance disparities, with the west-facing wall of the court (i.e., the *WF-C* probe) subjected to greater shading burden from the main building mass to result in the modest divergences identified, the effect of which was pronounced with lower winter solar altitudes.

[IV] *WF-C* dataset was also utilised for model validation in Study 3.

## 4.4 Discussion

The investigation of installations sited in sheltered environments is represented in current research by laboratory-based studies of active living walls (ALWs), with microclimate cooling typically found to contribute to energy savings [158,159]. The purpose of this study was to broaden the evidence base by presenting monitoring findings from underrepresented in-situ passive applications with substantial and similar evergreen coverage. Although the two case studies monitored were broadly categorised as sheltered environments (semi-closed or semi-open systems), the microclimates they generate are distinct. This must be emphasised when interpreting comparisons, as the findings are not from controlled experiments.

Atriums are nearer to closed systems, with the Cambridge case study utilising a natural ventilation strategy to maintain occupant comfort. This approach influences the environmental comfort factors of $T_{air}$, $RH$, $V_{air}$, and $MRT$, with the latter influenced by $T_{surf}$ values (given the personal factors of clothing insulation and metabolic rate are constant). The addition of plant coverage to such a system is expected to influence $T_{air}$, $RH$, and $T_{surf}$ mostly, while some modification of $V_{air}$ values is hypothesised. Sheltered courts on the other hand are relatively nearer to open systems, with the background climate having greater influence on environmental comfort factors (irradiation and wind exposure). The height-to-volume ratio of the court influences the degree of exposure, with the London case study's single-storey height enhancing, and compactness limiting [322]. The geometry or compactness of the court greatly influences exposure to wind dynamics [323], which in turn affects the efficacy and distribution of vegetation-related $T_{air}$ and $RH$ influences.

### 4.4.1 Air temperature influence

Given the distinct spatial and exposure conditions of the two studies, relatable performance was apparent only with $T_{air}$ influence distribution. Most horizontal distribution profiles (Fig. 54a & c, p. 119) demonstrated coolest $T_{air}$ values proximate to the installation, and increasing means with distance away from the surface; broadly in agreement with previous studies [10,159]. The winter night-time profiles however were highlighted as exceptions, with the semi-outdoor study having presented the weakest relative cooling, and a slight warming influence at the indoor study. This markedly reduced contribution from the evergreen-cover is not surprising given that photosynthesis and transpiration is negligible during nocturnal hours (see Chapter 2); which is exacerbated further by typical evergreen efficiencies in general being lower in winter [324]. Mean vertical distribution profiles also highlighted an increasing $T_{air}$ trend with height (Fig. 54b & d), which was influenced by the specific properties of the installation environments. This was most modified by solar radiation penetration into the sheltered conditions (accounts for the increased disruption presented during the summer daytime), followed by thermal contributions from other sources. The latter was also responsible for disrupting horizontal distribution gradients, with contribution from the stack-flow at the indoor study and mixing from an unidentified source at the semi-outdoor study observed as the main sources.

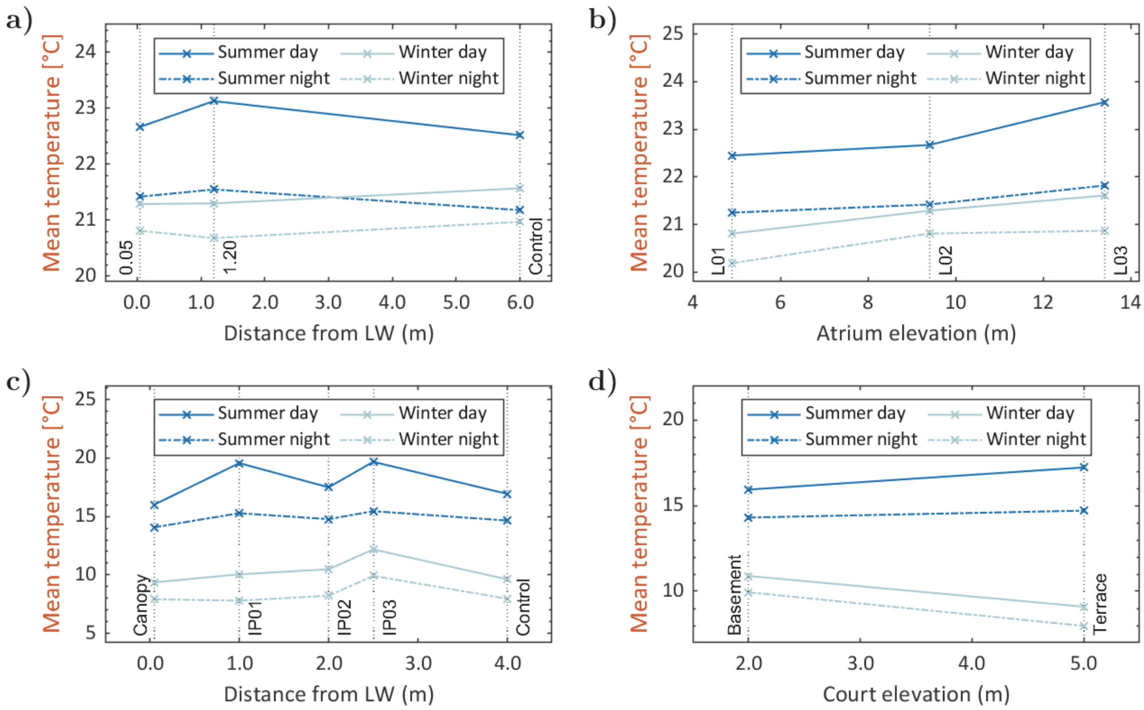


*Fig. 54. DAB, mean $T_{air}$ horizontal (a) and vertical (b) distribution profiles; and SET, semi-outdoor mean horizontal (c) and vertical (d) distribution profiles.*

Distinction between the two case study environments was highlighted by the magnitudes of influence recorded. The maximum surface proximate cooling of M = 0.3, ±0.8 K presented at the indoor study contrasted against the greater influence of M = 0.9, ±0.14 K at the semi-outdoor study. Outdoor living wall observations have demonstrated influence to range from 0.0-3.5 K (e.g., [89,224]), while ALWs in laboratory studies have highlighted much greater effects up to ~6 K [158,159]. There is however little evidence available for passive installations in indoor environments to compare results. The Ghazalli *et al.* [229] pre- and post-intervention study offered an exception, where they found the introduction of a rather modest installation (3.25 m$^2$) to have no significant $T_{air}$ effect. This in turn presents some relatable reasoning for the modest influence of the atrium installation, with relative enhancement attributed to its greater coverage area (~91 m$^2$). The semi-outdoor court on the other hand performed relatively better, although at the lower half of the spectrum of influence reported for more exposed outdoor installations. Distinction was also highlighted in relation to contributions from unique installation features, which is a given consideration with in-situ assessments. At the atrium study this was characterised by the observed stack-effect and thermal loading from intermediate floor level gains, which is to be expected from such atrium arrangements [312–314]. At the semi-outdoor court, radiation penetration had greater influence (exemplified by wall-return data, Table 20, p. 117) given its reduced height [322], while the basement court also introduced greater conduction exchanges with the subsurface and adjoining occupied spaces that in turn contributed to an inverted vertical distribution profile in contrast to the indoor study (Fig. 54b & d, p. 119).

### 4.4.2 Humidity influence

Relatable performance between the distinct exposure conditions was again only apparent with the distribution of humidity influence. The decrease or decay in horizontal $RH$ distribution with increasing distance from the living wall surface was observed at both studies (Fig. 55, p. 121), in broad agreement with previous vertical greening observations (e.g., [158,198]). Although the $AH$ profiles complemented this $RH$ trend, the marginal difference between installation-proximate probes suggested the increased $RH$ nearer to the canopy during the summer daytime to be mostly affected by $T_{air}$ cooling, rather than by an increase in humidity. A similar minimal mean difference was noted between elevational levels, highlighting $T_{air}$ influence on the vertical $RH$ profile (e.g., DAB, L02→L03 summer daytime profile, Fig. 55c & d). This $T_{air}$ dependence on $RH$ as opposed to substantial increases in humidity is in agreement with the findings of Susorova *et al.* [198], where a significant proportion of the humidity produced by transpiration was said to be repurposed to maintain foliage health during warm summertime conditions. This is particularly useful for installation plant health in indoor environments, where ambient $RH$ is maintained at much lower values (40-60%, [325]) than would be required for the good health of typical evergreen plants used (85-95%); while in general clarifies the common criticism of increased summertime humidifying risk to occupant comfort in sheltered environments as overstated.

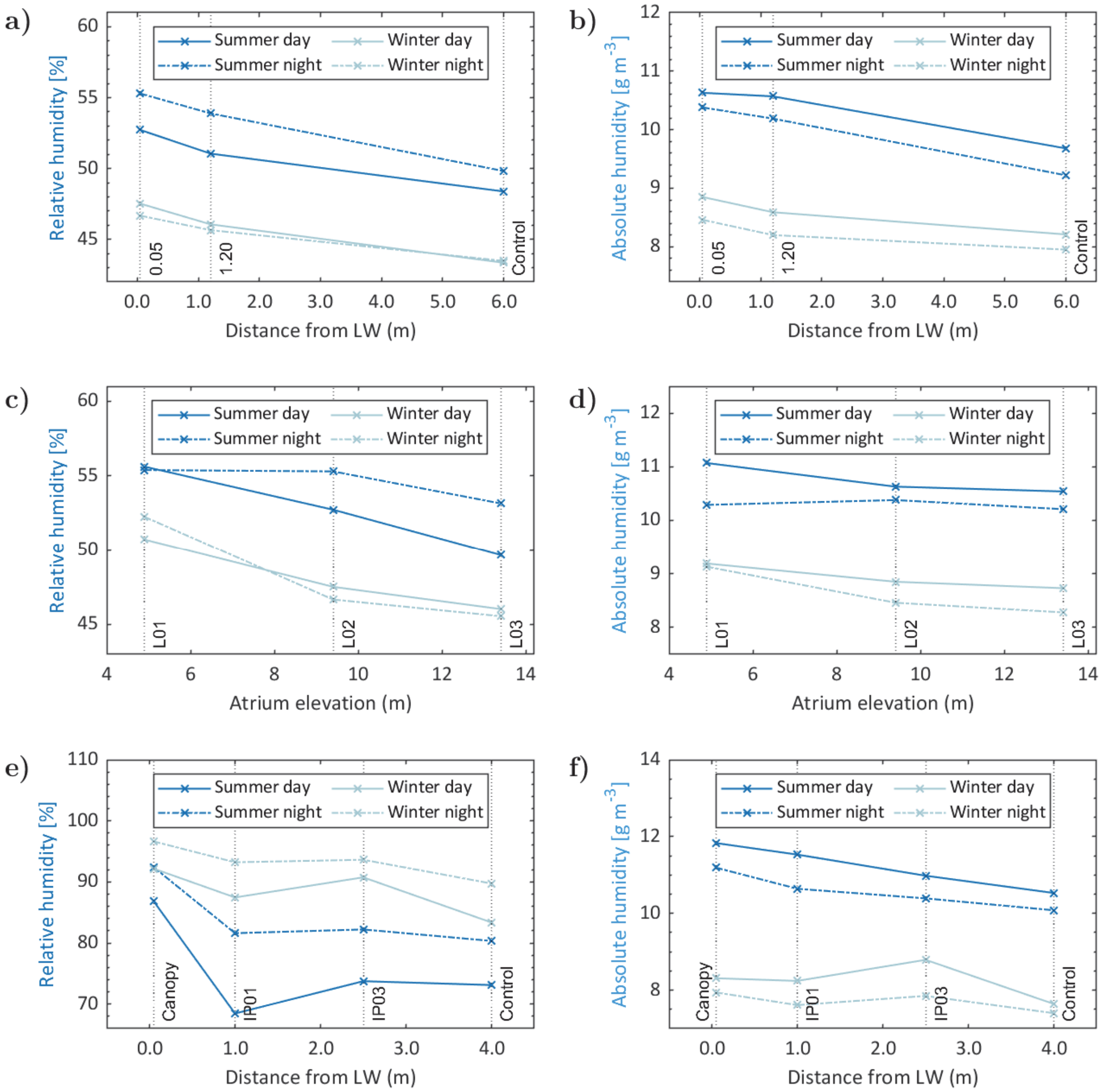


*Fig. 55. Mean $RH$ and $AH$ profiles for horizontal (a & b) and vertical (c & d) distribution at the DAB indoor study; and for horizontal distribution at the SET semi-outdoor study (e & f).*

The distinction between the two case study environments was again highlighted by the magnitude of influence. The relatively greater exposure to the wider background climate meant that all $RH$ means were significantly higher at the semi-outdoor court (68-97%), than at the indoor atrium (43-56%). The latter environment's natural ventilation strategy managed to maintain $RH$ at moderate levels within the comfort band, while the maximum installation proximate mean increase was relatively modest at 5.5, ±0.6%. In contrast, the semi-outdoor court's means often exceeded the 70% comfort upper limit particularly in winter, while the maximum installation proximate mean increase was much higher at 13.7, ±0.75%. It is significant to note that the absolute difference in humidity levels at the court was minimal, which again highlights greater $T_{air}$ significance to the $RH$ values recorded.

The concerning aspect however is that $AH$ levels in the summer showed substantial enduring influence within the most frequented zone of the court to suggest greater risk to occupant comfort. This is supported by the compactness of the court, where restricted exposure to mean climate airflow reduces opportunity for efficient humidity advection, and in turn encourages accumulation. Notwithstanding this potential risk, summertime discomfort is yet to be reported by the case study's residential occupants.

### 4.4.3 Surface temperature and airflow modification

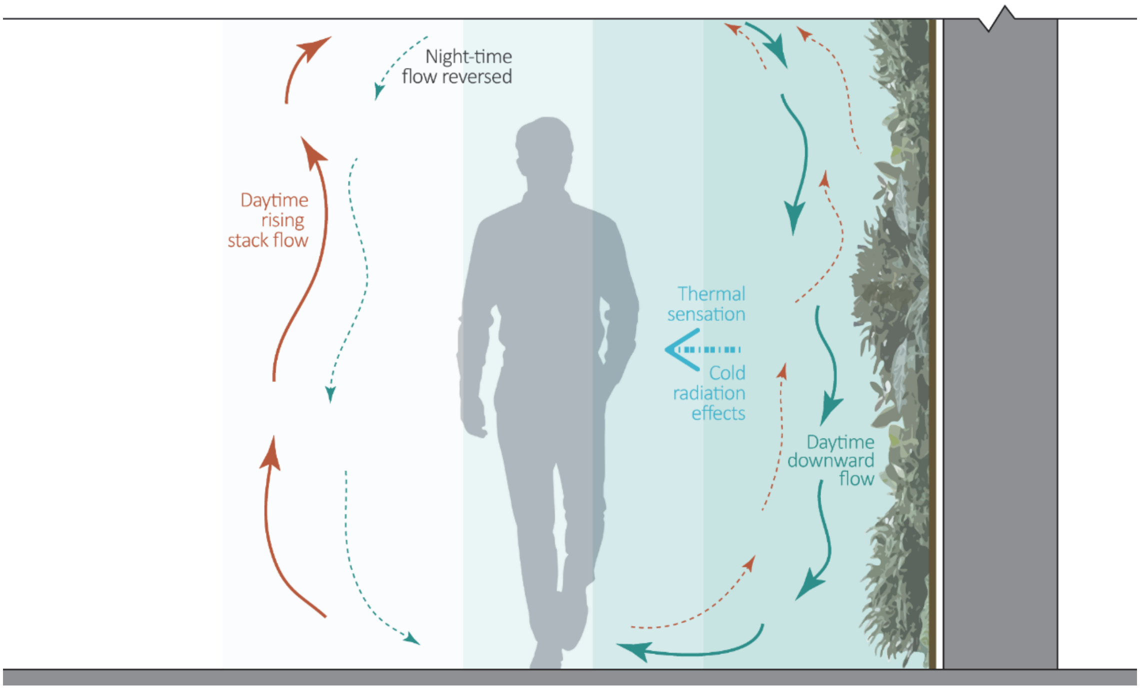


*Fig. 56. Proximity influence and microscale flow system.*

Documented cold surface effects in indoor environments relate mainly to investigations of glazed surfaces or active cool-walls (e.g., [241,326]). These have typically identified such effects as a source of occupant discomfort in winter, with draughts identified to be more critical than reduced air temperatures or radiation asymmetry [242]. There is also strong dependency on proximity, with discomfort determined by the predicted percentage of dissatisfied (PPD) persons found to rapidly decrease within the immediate 2 m-zone from the surface [241]. While the cooler surface presented by vegetation and the substrate could be hypothesised to result in radiation effects or generate a downdraught, no observations have thus far been presented to describe relevance or impact at living walls. The occurrence of such effects could be a risk to occupant comfort in winter, while in the summer provide a beneficial cooling effect. The rapid decay of influence however means that the detectability of such observations to be more likely in highly sheltered conditions, while in outdoors is only likely under dynamically stable conditions (i.e., negligible $V_{air}$). At higher $V_{air}$ turbulent mixing rapidly normalises microscale effects, which explains why some studies have failed to record $T_{air}$ influence even within the immediate zone (e.g., [188]). Given these prior observations, the project prioritised resources to examine living wall canopy surface temperature ($ST_{leaf}$) and surface air movement only at the indoor study.

The recorded $T_{soil}$ means were notably lower than the corresponding $ST_{leaf}$ and proximate $T_{air}$. This could be attributed to the moisture retention properties (increase in heat capacity) and continued evaporation from exposed soil surfaces. Qualitative thermography confirmed this soil substrate to be the coolest surface in the atrium, while quantitative assessment highlighted some areas to be cooler by as much as ~6 K (see Study 2). Considerable $ST_{leaf}$ differences between areas could in theory result in radiation asymmetry associated discomfort, with cooler vertical surfaces found to present greater risk than warmer ones. As mentioned above, the maximum differences recorded at the installation however were less than the >10 K threshold required to adversely affect comfort (Fig. 57a), although fell within the range where localised thermal sensation could be reported by nearby occupants (>45%) [326]. The presence of the living wall could therefore result in occupants experiencing thermal diversity (alliesthesia) and resultant enhancement in wellbeing [8], which highlights an area that requires further investigation including occupant participation.

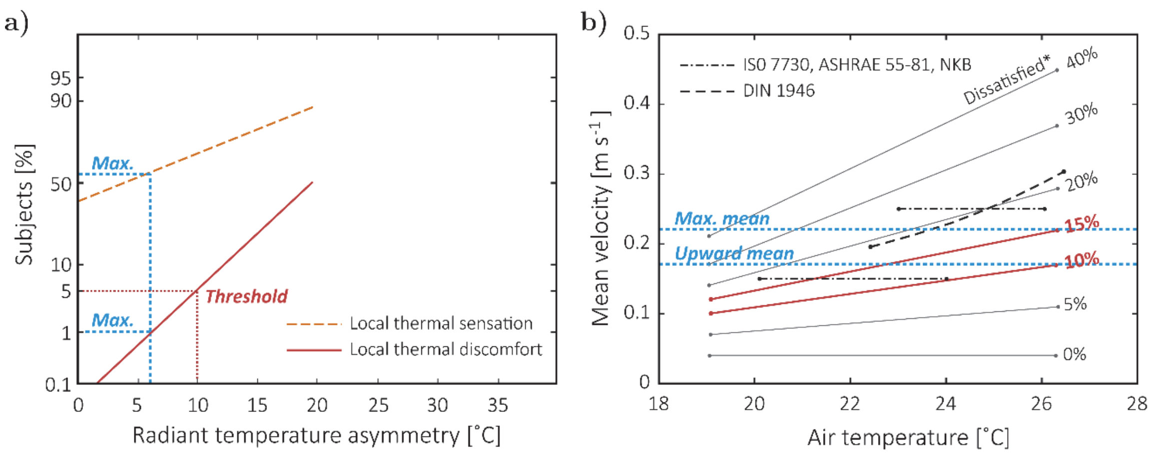


Notes: *Applies to sedentary persons wearing normal indoor clothing, exposed to $V_{air}$ in the occupied zone of ventilated spaces at turbulence intensity of 0.346. Fanger & Christensen [327] recommended a higher PPD threshold of 10-15% to qualify draught-related discomfort.

*Fig. 57. Cool-wall subjective responses concerning local thermal sensation and thermal discomfort* [326]*, with max. difference from atrium study (a); and Fanger & Christensen* [327] *draught chart and comparison between standard limits, with max. mean and upward flow mean from study (b).*

The surface air movement results were significant as they highlighted the presence of a dominant downward flow during daylight hours, when vegetation ecosystem provision (photosynthesis and transpiration) is at its peak, while the nocturnal reversal of this flow occurred when ecosystem provision is at its lowest (respiration is dominant). This observed surface flow could be contributing and even accelerating the function of a localised microscale centripetal thermal system within the atrium volume. Settling flow along the wall could thus be joining rising flow from the atrium's stack-effect during the daytime, while at night-time the cycle is reversed (Fig. 56, p. 122). This evidence encourages the further investigation of the possible occurrence and relevance of such systems at larger sheltered installations, and to identify the contribution extent of the living wall itself, given that the velocity correlations in this study highlighted variance to be explained mostly by other parameters than surface proximate $T_{air}$ or $RH$.

The generated maximum mean velocities of the isolated downward flow was marginally above the maximum recommended wintertime indoor velocities for offices [320], with PPD between 10-15% given that Fanger & Christensen [307] recommended this threshold to qualify draught-related discomfort (Fig. 57b, p. 123). The likelihood of building occupants encountering this isolated flow as an uncomfortable draught however is low, given the disruption from other directional flows, as well as the atrium being used by occupants predominantly as a transitional space as opposed to one where prolonged periods of presence is necessary (i.e., minimal exposure). Furthermore, encountering this airflow as well as any radiation asymmetry influence at higher floor levels is restricted by the installation's default arrangement (i.e., facing a void), which prevents proximity and contact. The ability of building occupants to experience thermal sensation and diversity from such effects is therefore impeded at this installation by its design arrangement.

## 4.5 Summary

Previous studies had presented evidence to suggest significant thermal benefit from outdoor living wall applications. This study presented in-situ monitoring results from an indoor atrium and semi-outdoor court including living walls of comparable coverage to characterise influence in underreported sheltered conditions. The results highlighted only a modest surface proximate cooling and humidifying influence at the **indoor study (maximum**

**$T_{air}$: M = 0.3 K and $RH$: M = 5.5%)**, in contrast to relatively higher influence at the **semi-outdoor study (maximum $T_{air}$: M = 0.9 K and $RH$: M = 13.7%)**. These modifications were therefore less potent than those reported for outdoor installations in the available literature. The potency of hygrothermal modifications characterised by horizontal distribution was most apparent within the 1-2 m zone from installation surfaces, in broad agreement with previous studies reviewed in Chapter 3. Beyond this range other phenomena such as the stack-flow at the indoor atrium study, caused interference and mixing to disrupt distribution. Hygrothermal gradation with installation height was also observed, although the semi-outdoor court presented a wintertime inversion explained by its unique arrangement and resultant thermal exchanges. Examining absolute humidity levels revealed **moisture generated from transpiration to be mostly repurposed** to maintain good foliage health in the summer, which is significant at the indoor condition where ambient $RH$ is maintained within the occupant comfort band, as opposed to typical requirements of evergreen plant cover.

Air movement data gathered off the surface over the autumn-to-winter months at the indoor study presented a **dominant daytime downward flow**. This could be the result of a modest downdraught effect influenced by the cooler surface of the living wall (mainly the moist substrate), which in turn could be contributing to rising thermals from the stack-flow to encourage a microscale centripetal thermal system in the atrium. The potency of this flow when combined with other flows, has insufficient capacity to cause significant discomfort. Such surface effects are likely to present thermal sensation and diversity to occupants, although the design and current arrangements of the installation at the indoor study precludes such benefits from being experienced by its building occupants. This in turn highlights the necessity for installation designers to take account of the proximity influence and increase building occupant access at future installations (e.g., Fig. 56, p. 122).

# Chapter 5

## STUDY 2: INFLUENCE OF CANOPY FEATURES

## 5.1 Introduction

Progressing from the in-situ monitoring results of Study 1, this study addresses the second-of-five secondary research questions introduced in Chapter 1.

> *Q II. How does the plant canopy morphology of a vertical greening installation influence its surface temperature?*

This is addressed by measuring canopy surface temperatures at in-situ living wall installations ($ST_{leaf}$, i.e., determinant of installation surface flux), to characterise associations with key canopy morphological features. To achieve this non-destructively at the selected indoor and outdoor urban installations, thermography has been utilised.

This chapter includes material extracts from the published conference paper by Gunawardena & Steemers [43].

### 5.1.1 Thermography application

As in Study 1, characterising plant canopy surface temperatures in plant science studies has been predominantly achieved using thermocouple arrangements (e.g., [328]). The use of the methodology however has been criticised for the limited number of point readings relied upon, which overlooks the heterogeneity of $ST_{leaf}$ distributions identified by detailed studies [329]. As an alternative approach that captures higher-resolution data arrays, thermography has gained significant favour in recent times with studies presenting application in both agricultural (e.g., [330]) and natural ecosystem contexts (e.g., [331–333]). The method has also been used for assessing soil moisture content (e.g., [334]) and levels of microbial activity (e.g., [335]), both significant for identifying abiotic and biotic plant stressors [317]. It has been applied in such studies as either aerial remote-sensing to capture data covering large extents of canopy, or as ground-based in-situ applications to consider individual canopies as well as leaf-specific features. The non-contact and non-destructive methodology is therefore well-recognised in contemporary plant sciences for the monitoring of physiological functions of a variety of vegetation canopies [336–338].

Thermography also has an established history in building research, and since the 1980s has gained significant prominence as a diagnostic tool in the drive to reduce building energy consumption [339]. It is typically utilised for qualitative 'passive' diagnostics, including the identification of building envelope defects such as insulation gaps, thermal-bridging, cracks, voids, infiltration, and moisture issues; as well as to locate thermal anomalies in mechanical and electrical systems [317,340]. The commonly used passive assessment methodology is described in British Standard BS EN 13187 [341], and involves the thermographer examining external and internal building components for anomalies, and then recording thermograms for subsequent qualitative analysis [342]. In addition to such qualitative applications, quantitative application is increasingly utilised for determining in-situ U-values during façade construction, as well as during the upgrade of existing building fabrics [343]. This study seeks to merge such application experiences from building research with those from plant sciences to offer an assessment approach that can qualitatively and quantitatively consider the relatively novel building façade solution presented by vertical greening (VG).

*Stefan-Boltzmann law:*

$$Q_{R_{lw}} = \varepsilon_{obj}\, \sigma\, \boldsymbol{T}_{surf}{}^{4} \qquad \textit{Equation 5}$$

Thermography characterises surface temperatures by capturing the radiant infrared energy distribution emitted by a target object (e.g., vertical greening surface). Planck's radiation law states that every object with a temperature above absolute zero (-273.15°C or 0 K) emits electromagnetic radiation $\boldsymbol{Q}_{\boldsymbol{R}_{lw}}$ [W·m$^{-2}$] in the infrared spectrum (wavelengths 0.78-1000 µm); while the Stefan-Boltzmann law (Equation 5) states that the extent emitted to be dependent on its emissivity ($\varepsilon_{obj}$) and absolute surface temperature ($\boldsymbol{T}_{surf}$, [K]).

Thermography captures this emitted infrared radiation (IR) by utilising camera optics to focus it onto a detector focal plane array (FPA), with the resulting electrical response signal converted and output as a thermogram. Typical infrared cameras capture radiation in the longwave wavelengths between 7.5 and 13.5 µm known as the 'atmospheric window', where neither water vapour nor $CO_2$ interferes with infrared transmission [344,345]. In practice, the radiation flux captured by the detector FPA ($Q_{R_{lw_{tot}}}$) includes radiation from the target object surface ($Q_{R_{lw_{obj}}}$); radiation first emitted by the background and then reflected by the object ($Q_{R_{lw_{ref}}}$); and atmospheric influence, where the atmosphere between the object and sensor attenuates both the former radiation components by absorption, and adds by atmospheric emission ($Q_{R_{lw_{air}}}$). The contributions from $Q_{R_{lw_{ref}}}$ and $Q_{R_{lw_{air}}}$ sources in Equation 6 are compensated automatically by onboard processing, which assumes solar scattering in the atmosphere or stray radiation from intense radiation sources beyond the camera's field-of-view (FOV) as negligible.

$$Q_{R_{lw_{tot}}} = Q_{R_{lw_{obj}}} + Q_{R_{lw_{ref}}} + Q_{R_{lw_{air}}}, \qquad \textit{Equation 6}$$

$$Q_{R_{lw_{tot}}} = \tau_{atm}\, \varepsilon_{obj}\, \sigma\, \boldsymbol{T}_{obj}{}^{4} + \tau_{atm}\left(1-\varepsilon_{obj}\right) \varepsilon_{sky}\, \sigma\, \boldsymbol{T}_{ref}{}^{4} + \left(1-\tau_{atm}\right) \sigma\, \boldsymbol{T}_{air}{}^{4}, \qquad \textit{Equation 7}$$

where,

| | |
|---|---|
| $\boldsymbol{T}_{obj}$ | Absolute surface temperature of target object [K]; |
| $\boldsymbol{T}_{ref}$ | Absolute reflected temperature ($\boldsymbol{T}_{sky}$ for outdoors) [K]; |
| $\boldsymbol{T}_{air}$ | Absolute atmospheric temperature (or ambient $\boldsymbol{T}_{air}$) [K]; |
| $\tau_{atm}$ | Atmospheric transmissivity, calculated from $T_{air}$, $RH$, and $D_{IR}$; |
| $D_{IR}$ | Distance between target object and infrared sensor [m]; and |
| $\sigma$ | Stefan-Boltzmann constant = $5.67 \cdot 10^{-8}$ [$W{\cdot}m^{-2}{\cdot}K^{-4}$]. |

With qualitative studies the application of thermography is 'passive' (Fig. 58), as the temperature differences of the target object are captured under conditions not modified by the assessor (i.e., thermographer). The approach typically locates an anomaly with a qualitative indication of severity expressed depending on the experience of the interpreting expert [339]. Quantitative studies require infrared cameras with higher accuracy that may be used under either passive or 'active' conditions; with the latter involving the use of an external thermal stimulus to generate target object temperature differences [317]. In this study, passive qualitative and quantitative approaches are used as the living wall canopies selected presented distinct surface temperatures relative to adjacent façade elements. An active approach is in any event unsuitable to examine an ecosystem such as vertical greening, given the likelihood of causing plant stress and injury from an external thermal stimulus.

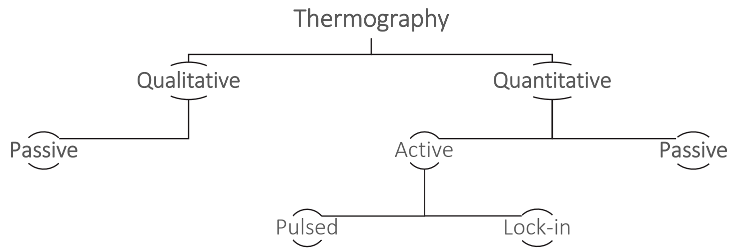


*Fig. 58. Thermography application approaches.*

## 5.2 Methodology

The study utilised thermography to assess living walls (given their greater canopy diversity). An indoor installation was selected to assess characterisation in a sheltered environment, while outdoor installations were selected from Mediterranean and temperate climates to assess climate dependencies (Fig. 59). These are identified here as the indoor installation at the David Attenborough Building (DAB) in Cambridge, UK (Cfb), with a soil substrate-based system (13 m-high, 91 m$^2$); the outdoor south-facing installation at the CaixaForum Museum (CF) in Madrid, Spain (Csa), with a felt-based hydroculture system (24 m-high, 460 m$^2$); and the outdoor northwest-facing installation at the Quai Branly Museum (QB) in Paris, France (Cfb), also with a felt-based hydroculture system (12 m-high, 800 m$^2$).


*Fig. 59. Living wall case studies assessed.*

The apparatus used for the exercises included FLIR T640 and C2 infrared cameras[V], with key specifications described in Table 21, p. 130 (FLIR Systems Inc., Wilsonville, Oregon, USA); a PCE Instruments Environmental Meter with hygrothermal probes; HOBO surface temperature probes and logger; and a TSI M8475 Air Velocity Transducer. All analyses were carried out using FLIR Tools V6.4 and ResearchIR V4.40, MATLAB R2019a, and SPSS V25 (IBM SPSS Statistics, Chicago, Illinois, USA) software.

[V] As the University fieldwork insurance policy did not include cover for the substantial value of the T640, the affordable and portable C2 had to be utilised at the CaixaForum and Quai Branly sites in Europe.

Table 21. FLIR infrared camera specifications.

| **Specification** | **FLIR T640**<br>(*used at the DAB site*) | **FLIR C2**<br>(*used at the Quai Branly and CaixaForum sites*) |
|---|---|---|
| |  |  |
| **Detector focal plane array (FPA)** | Uncooled microbolometer | = T640 |
| **Spectral range** | 7.5-14.0 µm (within atmospheric window) | = T640 |
| **Infrared resolution** | 640×480 (307,200 measurement points) | 80×60 (4,800) |
| **Standard temperature range** | -40 to 2000°C | -10 to 150°C |
| **Sensitivity** | 0.03 K at 30°C | <0.10°C |
| **Accuracy** | ±2°C or 2%, whichever is greater at 25°C | = T640 |
| **Visible image** | Integrated 5.0-megapixel camera | 0.3-megapixel camera |
| **Lens focal length** | 13.0 mm | 1.54 mm |
| **Field-of-view (FOV)** | 45×34° | 41×31° |

The prerequisite inputs $\varepsilon_{obj}$, $\boldsymbol{T_{ref}}$, and the parameters for calculating $\tau_{atm}$, must be recorded prior to thermogram capture. The values used for this study included: $\varepsilon_{obj}$ of 0.95 (typical for vegetation between 0.91-0.99 [52,338,346]); $\boldsymbol{T_{ref}}$ both calculated ($\boldsymbol{T_{sky}}$ from Berdahl & Martin model used for outdoor sites [347,348]) and measured (using the crumpled aluminium reflector method in indoor atrium); $\tau_{atm}$ calculated from $T_{air}$ and $RH$ measured with the Environmental Meter; and $D_{IR}$ measured with a measuring tape.

The CaixaForum and Quai Branly thermograms were taken over seven and five-day summertime campaigns respectively, while the DAB thermograms were taken during a single wintertime inspection (as the climate variability within an indoor system and over a limited campaign is minimal). At all sites, the thermograms were taken at ~2 m AGL (at the Quai Branly and CaixaForum) or AFFL (at the DAB), and in conditions with no interference from overshadowing or intense irradiation from surrounding objects. The thermography also followed best practice guidelines of allowing for an adjustment period prior to capture; avoiding framing the target at acute angles (perpendicular to surface where possible); and capture in focus. With the outdoor sites, capture was avoided when $V_{air}$ was >5 m·s$^{-1}$, as higher values enhance convective heat losses to underestimate surface temperatures [317].

The captured thermograms were then subjected to pre-, as well as post-processing tasks such as segmentation and region-of-interest (ROI) extraction. An example of this processing algorithm for a single thermogram is presented in Fig. 60. Pre-processing tasks prepared the captured thermograms for data extraction, which involved enhancement, calibration adjustment, and cropping using FLIR Tools software. Post-processing was achieved using image processing tools included in FLIR ResearchIR software. Segmentation tasks involved partitioning the thermogram into simplified segments for analysis, with the thresholding method used to segment the histogram into temperature ranges of interest [317]. The background including the cooler substrate was accordingly removed to segment-out only canopy $ST_{leaf}$ of interest. These were refined using user-prescribed ROIs to extract specific plant canopies of interest. As demonstrated by the Kim *et al.* [331] study, the ROI pixel temperatures were then averaged to characterise $ST_{leaf}$ for each canopy. Care must be taken when selecting canopy ROIs for averaging, with distinction made between illuminated and self-shaded areas [349]. In this study, self-shaded areas were thresholded-out during the segmentation step of post-processing to include only illuminated canopy regions.

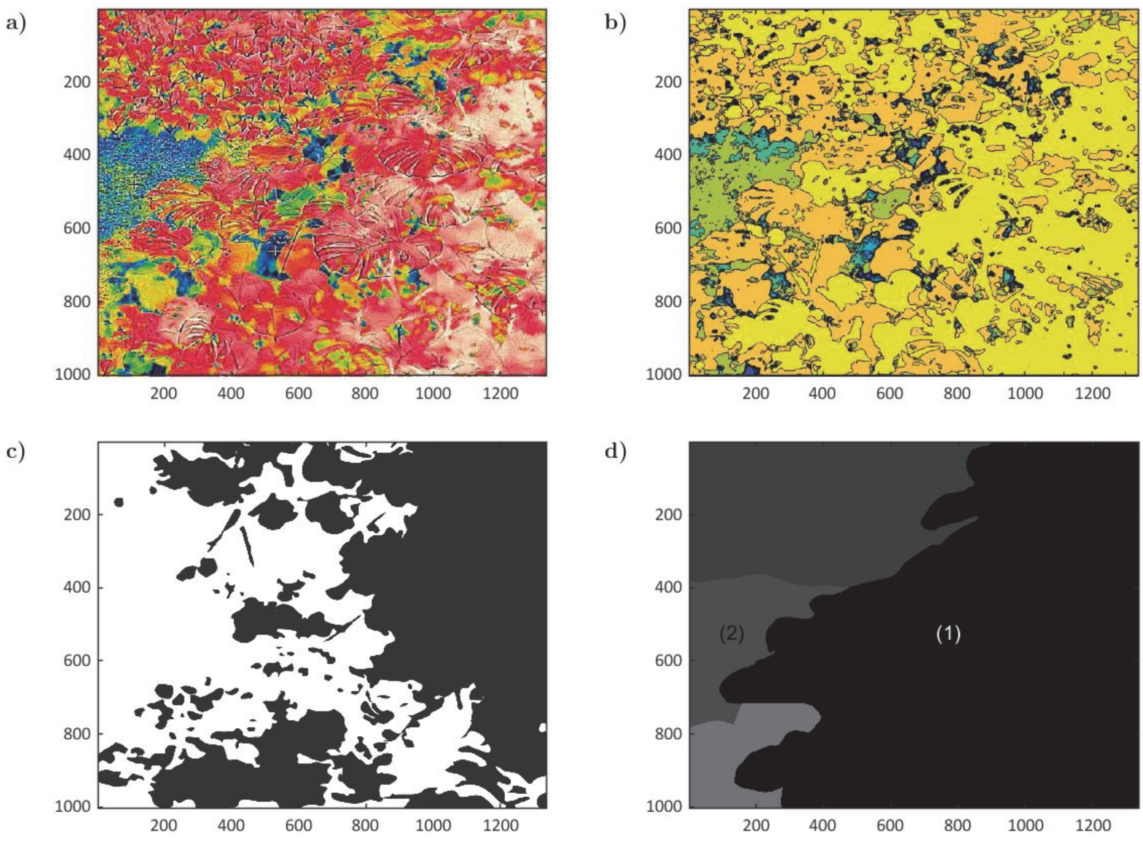


*Fig. 60. Pre-processed thermogram of the DAB LW, level 3, first-of-three sectors (a); thermogram after threshold segmentation (b); segmented canopy data of interest (c); user-defined ROI template for data extraction (d), with e.g., Monstera deliciosa (1) and Soleirolia soleirolii (2) canopy ROIs.*

The literature in Part I (section 3.4.2), described the key morphological canopy features that influence vertical greening climate interactions to include their $LAI$ and 'percentage-cover'; as well as their depth ($z_{veg}$) or protuberance (projection off the surface), and leaf size (analogous to leaf-width, $W_{leaf}$). The $LAI$ is not accurately quantifiable without destructive measurement, particularly when the values are patently >1 (typically involves the removal of leaves of a representative 1 m$^2$ area to be scanned by a leaf-scanner). Destructive measurement was also precluded given the prominence of the selected in-situ case studies. Canopy percentage-cover in contrast was predefined as 1.0 or 100%, as the study's focus was only the canopy cover. The target variables to investigate therefore included only the non-destructively measurable canopy morphological parameters of $z_{veg}$ and $W_{leaf}$.


*Fig. 61. Plant species examined at the DAB (a; also includes S. soleirolii); CaixaForum (b); and the Quai Branly (c) installations, including leaf size and canopy protuberance categorisation.*

The plants selected for analysis included six, nine, and five canopies from the DAB, CaixaForum, and Quai Branly installations respectively; all grouped according to equivalent planting elevational height (between 1.0 and 2.0 m AGL or AFFL) to address comparable irradiation. These are represented in Fig. 61, p. 132; with canopy protuberance ($z_{veg}$) defined by: 'prostrate/**P**' (<0.15 m), 'medium extension/**ME**' (>0.15 and <0.50 m), and 'extensive extension/**EE**' (>0.50 m) ordinal categories; and the broadleaf canopies distinguished by leaf sizes ($W_{leaf}$): 'very small/**VS**' (<0.025 m width), 'small/**S**' (>0.025 and <0.075 m), 'medium/**M**' (>0.075 and <0.15 m), 'large/**L**' (>0.15 and <0.25 m), and 'extra-large/**EL**' (>0.40 m) ordinal categories. The $z_{veg}$ categorising was based on dry-canopy, non-destructive random sample measurements and resultant data means, while the random sample measurements of $W_{leaf}$ considered the means of the largest dimension perpendicular to a mature leaf petiole when laid flat on a rigid surface (all measured using a measuring tape). The analysis of grassy canopies with their narrow blade or $W_{leaf}$, as well as the fern with broad pinnated fronds were considered separately given their distinct leaf morphologies (see Fig. 61, insets).

## 5.3 Findings

### 5.3.1 Passive qualitative assessment

Using the FLIR T640 infrared camera, single inspection thermography was carried out at the Quai Branly in Paris and the DAB in Cambridge in late 2017.

The DAB exercise was carried out on the morning of 29 November 2017, with all plants at a mature stage of growth. Three thermograms were taken perpendicular to the wall, across the atrium void from floor levels 1-3 (nine sectors or thermograms in total). As examples, thermograms from level 3 (a) and level 2 (b), from the left-hand third sectors of the installation are represented in Table 22, p. 134, with corresponding qualitative observations.

The Quai Branly exercise was carried out on 25 November 2017, afternoon. Due to felt replacement and replanting works in progress, only half the installation had plants at a mature stage of growth, while the other had exposed felt and some young plant-plugs in place. As examples, thermograms from each half of the installation are represented in Table 23, p. 135, with corresponding qualitative observations.

Table 22. David Attenborough Building (DAB) thermogram examples and observations.

| | | |
|---|---|---|
| Conditions | Outdoor weather conditions | Cloudy with scattered rain; $T_{air}$: 4°C; $RH$: 7%; and moderately windy: $V_{air}$ ~7.6 m·s$^{-1}$ |
| | Indoor wall surface conditions | Vegetation leaves visibly dry |
| | $\boldsymbol{D_{IR}}$ | ~6 m (Horizontal FOV: 5.00 m; Vertical FOV: 3.75 m; IFOV: 7.79 mm) |
| | $\boldsymbol{T_{air}}$ | a) 21.1°C; b) 21.6°C |
| | $\boldsymbol{T_{ref}}$ | 21.5°C (measured) |
| | $\boldsymbol{RH}$ | a): 55.0%; b): 53.9% |
| | $\boldsymbol{V_{air}}$ | 0.13 m·s$^{-1}$ |
| | Colour image | Composite thermogram |
| Level 3, top-sector - (a) | 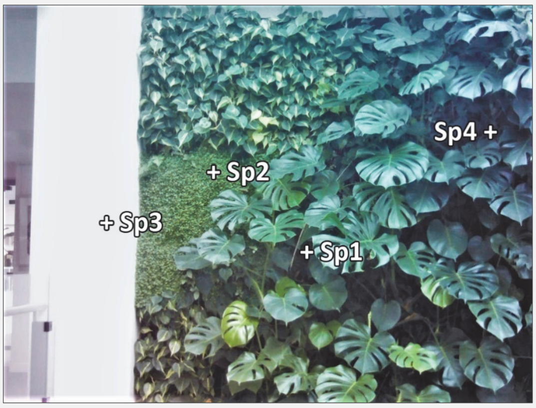  | 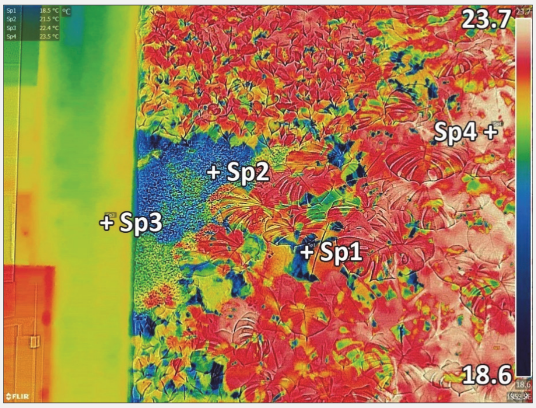  |
| Level 2, mid-sector - (b) |   | 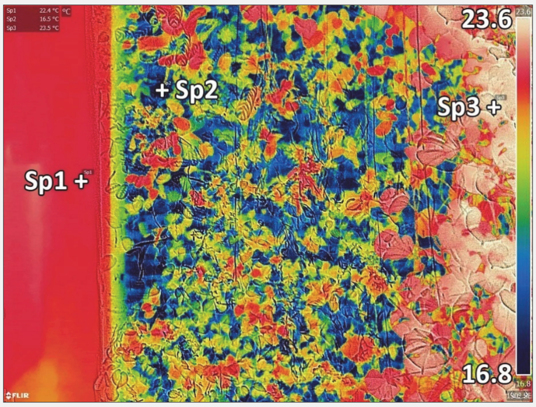  |
| Observations | ▪ Substrate was the coolest surface (a & b).<br>▪ Foliage warmest at the top (e.g., a-Sp4), and where the canopy appears dense and protuberant (e.g., b-Sp3).<br>▪ Thermogram (b) highlights an area with poor plant health with dieback exposing the cooler substrate surface.<br>▪ The large-leaved *M. deliciosa* (a & b, right) presented warmer canopy $ST_{leaf}$, while within the canopy $T_{leaf}$ was cooler to demonstrate the canopy overshadowing effect (e.g., a-Sp1). | a-Sp1: 18.58°C (canopy overshadowing)<br>a-Sp2: 21.52°C (relatively cooler foliage)<br>a-Sp3: 22.42°C (bare side-column surface)<br>a-Sp4: 23.52°C (warmest foliage)<br><br>b-Sp1: 22.41°C (bare side-column surface)<br>b-Sp2: 16.55°C (cooler substrate)<br>b-Sp3: 23.48°C (warmest foliage) |

Table 23. Quai Branly (QB) museum installation thermogram examples and observations.

| | | |
|---|---|---|
| Conditions | Outdoor weather conditions | Cloudy with intermittent sunny skies; and moderately windy: $V_{air}$ ~4.18 m·s$^{-1}$ |
| | Outdoor wall surface conditions | Morning rain had left surroundings damp |
| | $D_{IR}$ | ~3 m (Horizontal FOV: 2.50 m; Vertical FOV: 1.90 m; and Instantaneous FOV/IFOV: 3.89 mm) |
| | $T_{air}$ | 5.4°C |
| | $T_{ref} = T_{sky}$ | -16°C (calculated for 0.5 cloudiness [347]) |
| | $RH$ | 80.6% |
| | Colour Image | Composite thermogram |
| Replanted half, mid-area - (a) | 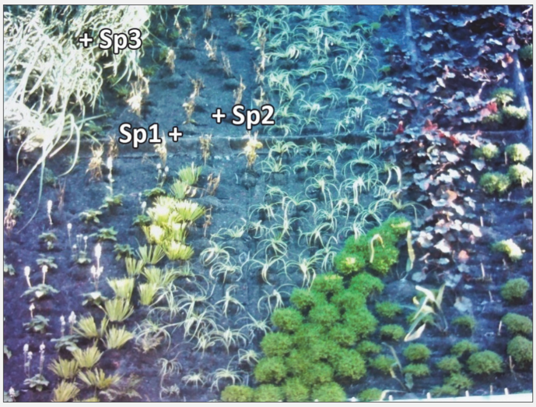 | 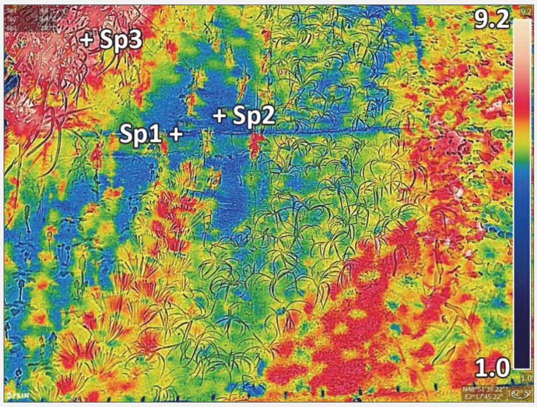 |
| Mature half, base-area - (b) | 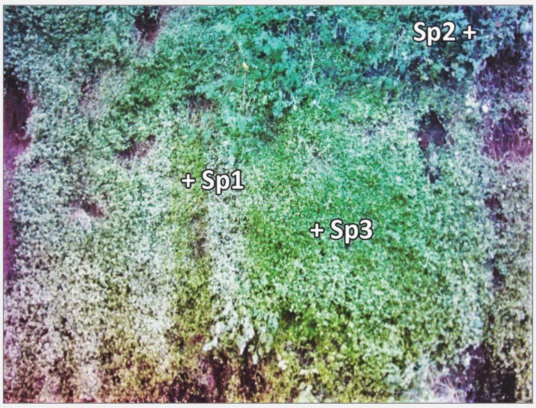 | 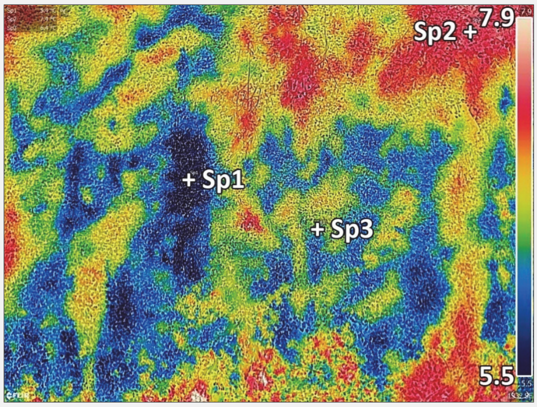 |
| Observations | ▪ Vegetation generally showed cooler canopy $ST_{leaf}$ relative to other surrounding building façade elements.<br>▪ The exposed felt (a) was significantly cooler (e.g., a-Sp2) relative to the surrounding canopy foliage.<br>▪ The dark blue horizontal and vertical lines evident with (a) highlight significantly cooler irrigation pipework embedded in the felt (e.g., a-Sp1).<br>▪ Some areas with mature foliage (e.g., b-Sp1) demonstrated ~2 K cooler $ST_{leaf}$. | a-Sp1: 4.77°C (cooler irrigation pipe below felt)<br>a-Sp2: 5.38°C (exposed moist felt)<br>a-Sp3: 7.80°C (warmest young foliage)<br><br>b-Sp1: 5.41°C (coolest mature foliage)<br>b-Sp2: 7.44°C (warmest mature foliage)<br>b-Sp3: 6.37°C (relatively cooler mature foliage) |

### 5.3.2 Passive quantitative assessment

The following presents the quantitative analysis of canopy $ST_{leaf}$ captured at all three case studies. This included the processing of ~7.5 million datapoints covering nine sectors at the DAB installation (Fig. 62); ~1.8 million datapoints at the Quai Branly installation (Fig. 63a, p. 137); and ~8.5 million datapoints at the CaixaForum installation (Fig. 63b).

With the DAB installation, canopy $ST_{leaf}$ along the height of the installation demonstrated an increasing gradient (Fig. 62a), with the highest mean (23.0, ±0.7°C) for Level 3 or top-third section of the installation, relative to Level 1 or bottom-third (21.1, ±1.7°C). This gradient was also evident with individual species canopies, with the notable example presented by the large-leaved *M. deliciosa* canopy that spans all three floor levels (Fig. 62b).

No elevational mean differences however could be reported for the outdoor Quai Branly and CaixaForum installations, as only a single elevational level was considered due to restricted accessibility to higher levels.

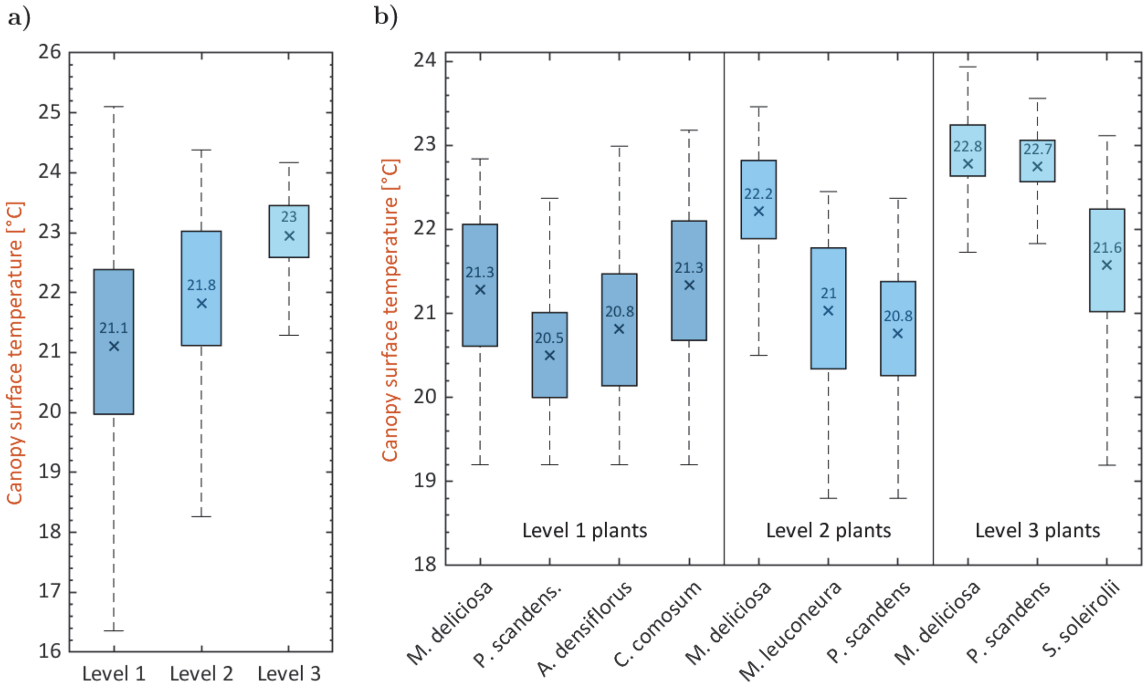


| Background means | Air temperature ($T_{air}$) | Relative humidity ($RH$) | Air velocity ($V_{air}$) |
|---|---|---|---|
| Level 3 | 21.4°C | 57.0% | 0.08 m·s$^{-1}$ |
| Level 2 | 21.5°C | 55.5% | 0.08 m·s$^{-1}$ |
| Level 1 | 21.2°C | 59.4% | 0.09 m·s$^{-1}$ |

Note: Symbol '×' in boxplots represent dataset mean (with value above symbol, or above $x$-axis).

*Fig. 62. DAB, daytime canopy $ST_{leaf}$ datasets by atrium level (a); and by plants at each level (b).*

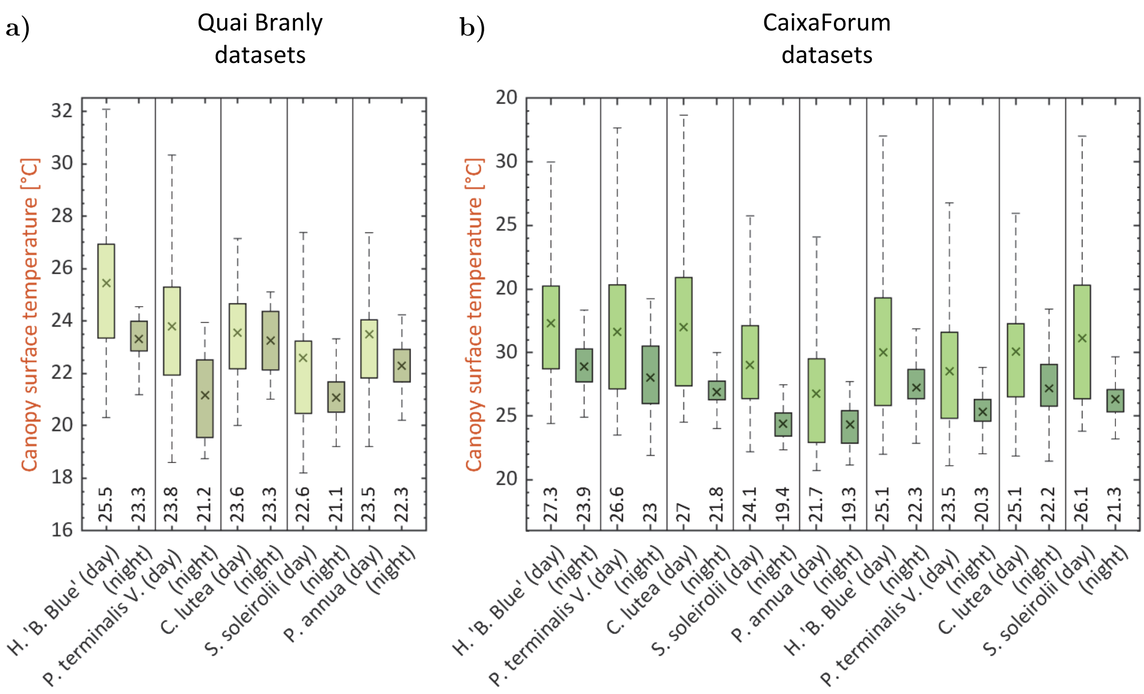


Quai Branly background means:

| | $T_{air}$ | $RH$ | $V_{air}$ |
|---|---|---|---|
| Daytime: | 24.9°C | 50.2% | 4.2 m·s$^{-1}$ |
| Night-time: | 26.4°C | 51.3% | 2.2 m·s$^{-1}$ |

CaixaForum background means:

| | $T_{air}$ | $RH$ | $V_{air}$ |
|---|---|---|---|
| Daytime: | 25.5°C | 41.8% | 2.7 m·s$^{-1}$ |
| Night-time: | 27.5°C | 35.9% | 2.8 m·s$^{-1}$ |

*Fig. 63. Day and night-time canopy $ST_{leaf}$ datasets by plant species at the Quai Branly (a) and CaixaForum (b) installations.*

To assess canopy $ST_{leaf}$ values across the three different case study conditions, the plant leaf-to-air temperature difference metric was utilised ($ST_{leaf} - T_{air} = \Delta T_{\text{veg}}$). In previous studies it has been used to identify canopy thermal stress, with positive values indicating $ST_{leaf}$ warmer than the surrounding air ($T_{air}$). High $\Delta T_{\text{veg}}$ values are typically indicative of heat stress, stomatal closure, and reduced $CO_2$ exchange [331,333]. It therefore presents an indication of canopy performance, while accounting for local climate variations.

When $\Delta T_{\text{veg}}$ for the three studies were considered, the overall night-time mean was negative to indicate cooler canopies (M = -5.25, ±1.65 K; max. -8.10 K), while during the daytime the mean was marginally negative (M = -0.10, ±1.32 K) to indicate relatively warmer $ST_{leaf}$. Canopies with 'medium' to 'large' leaves such as *Hosta* spp. presented higher positive daytime and higher negative night-time $\Delta T_{\text{veg}}$ to indicate warmer $ST_{leaf}$, while the converse was presented by smaller-leaved plants (Fig. 64a, p. 138). At the warmer climate CaixaForum installation this spectrum was represented by *H. sieboldiana* (daytime max. 2.14 | night-time -3.52 K) and *V. minor* (-3.47 | -8.10 K), while at the temperate climate

Quai Branly installation the spectrum range was lower to represent *H. 'Bressingham Blue'* (0.90 | -2.97 K) and *S. soleirolii* (-1.96 | -5.23 K). At the DAB temperate climate indoor study, the daytime range was represented by higher positive $\Delta T_{\mathrm{veg}}$ from the large-leaved *M. deliciosa* (1.42 K), although the converse was represented by the medium-leaved *P. scandens 'Brasil'* (-0.72 K), as opposed to the smaller-leaved *S. soleirolii* (0.21 K) to present an anomaly. Diurnal changes in $\Delta T_{\mathrm{veg}}$ considered at the south-facing CaixaForum installation on the other hand confirmed peak values recorded to be around midday, when solar irradiance was at its highest (Fig. 64b).

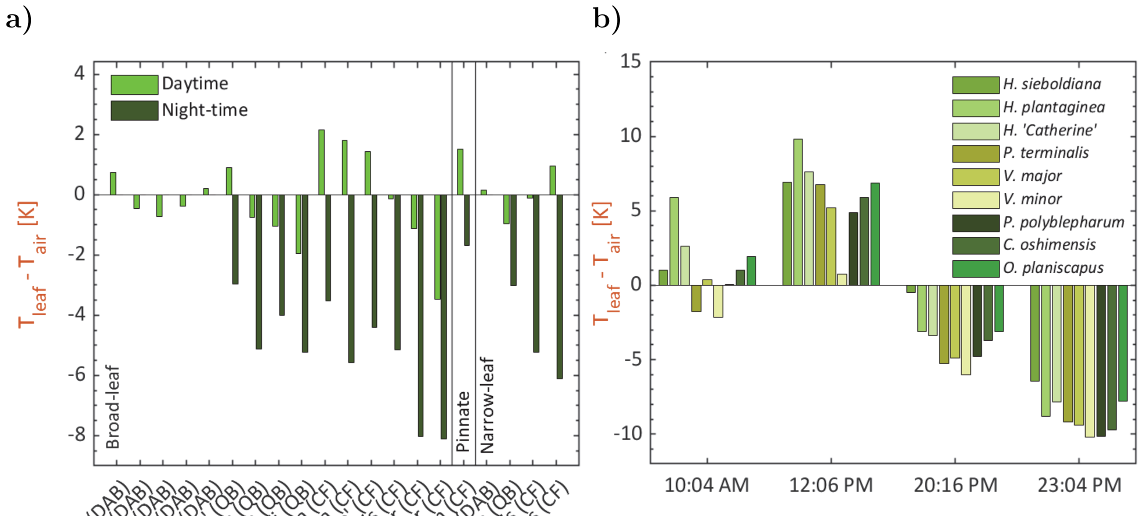


CaixaForum background means (at above times):

| | | | | |
|---|---|---|---|---|
| $T_{air}$: | 23.5°C | 24.9°C | 23.9°C | 27.9°C |
| $RH$: | 59.5% | 42.0% | 33.9% | 28.8% |
| $V_{air}$: | 2.2 m·s$^{-1}$ | 3.9 m·s$^{-1}$ | 4.4 m·s$^{-1}$ | 2.2 m·s$^{-1}$ |

*Fig. 64. $\Delta T_{veg}$ means for all plant canopies reviewed (a); and $\Delta T_{veg}$ for plants at the CaixaForum in Madrid at different times of the day on 13 August 2018 (b).*

The fern *P. polyblepharum* from the CaixaForum has distinct canopy features (Fig. 64a). Although it presented a 'large' leaf and a positive daytime $\Delta T_{\mathrm{veg}}$, it had lower canopy $ST_{leaf}$ means comparable to 'small' or 'very small' leaved canopies (23.5, ±4.2°C for the day, and 20.3, ±1.5°C for the night). When mean $\Delta T_{\mathrm{veg}}$ for the grass types with their narrow blades were considered, both *C. oshimensis* (at the CaixaForum) and *P. annua* (at the Quai Branly) presented cooler foliage $ST_{leaf}$ means during the daytime ($\Delta T_{\mathrm{veg}}$ = -0.1 and -1.0 K respectively), with even cooler values at night (-5.3 and -3.0 K). In contrast, the canopies of *O. planiscapus* (at the outdoor CaixaForum) and *C. comosum* (indoor DAB), presented positive $\Delta T_{\mathrm{veg}}$ during the day (0.94 and 0.15 K), while at night the former presented the coolest for the grass types (-6.12 K).

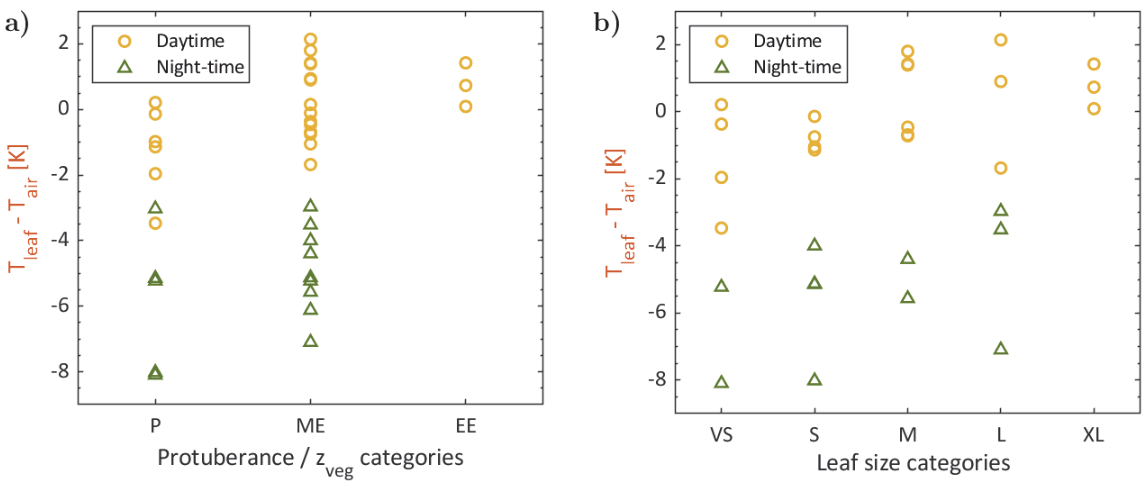


*Fig. 65. $\Delta T_{veg}$ plotted against canopy morphology features.*

Table 24. $\Delta T_{veg}$ means relative to canopy morphological features.

| | **Protuberance / $z_{veg}$ categories** | | | **Leaf size / $W_{leaf}$ categories** | | | | |
|---|---|---|---|---|---|---|---|---|
| | **P** | **ME** | **EE** | **VS** | **S** | **M** | **L** | **XL** |
| **Daytime** | -1.24 (±1.34) | 0.19 (±1.16) | **0.75** (±0.66) | -1.40 (±1.66) | -0.77 (±0.45) | 0.46 (±1.20) | 0.45 (±1.95) | **0.75** (±0.66) |
| **Night-time** | -5.90 (±2.16) | **-4.89** (±1.31) | N/A | -6.66 ±2.03 | -5.57 (±1.72) | -4.99 (±0.83) | **-4.53** (±2.25) | N/A |

When $\Delta T_{veg}$ means from all studies were considered against the ordinal categories of canopy morphological features (Fig. 65 and Table 24), $z_{veg}$ presented a significant 'moderate' positive correlation for the daytime means (Spearman's rank-order $r_s(22,\ n = 24) = 0.50$, $p = 0.01$), while for the night-time presented an insignificant 'weak' correlation ($r_s(12,\ n = 14) = 0.26$, $p = 0.37$). With $W_{leaf}$, a significant 'moderate' positive correlation was presented for the daytime ($r = 0.55$, $N = 20$, $p = 0.01$), while the positive night-time correlation was insignificant ($r = 0.44$, $N = 11$, $p = 0.18$).

## 5.4 Discussion

Chapter 3 identified $T_{surf}$ as the most common parameter measured to assess the thermal influence of vertical greening installations. The measurements in these have included canopy $ST_{leaf}$, as well as $T_{leaf}$ within the canopy and $T_{surf}$ immediately behind; while the methodologies utilised have predominantly taken readings from either point or limited array thermocouple arrangements (e.g., [88,89]). The use of thermography for the same purpose is a novel consideration, limited to only a few recent studies to note (e.g., [311]). The offer of higher-resolution arrays of quantitative data, non-invasive and non-destructive capture, and near instantaneous qualitative summaries are all advantageous for considering vertical greening assessments. These potential benefits have also gained greater relevance for living wall studies, where the focus is now shifting from laboratory-based work to consider in-situ assessments to identify applied performance and maintenance issues [10,42].

Qualitative thermography has a proven record in performance and maintenance diagnostics in building research. In this study, this application experience was extended to consider the same at living wall installations. The application demonstrated that it provides the experienced assessor with the opportunity to visually identify canopy $ST_{leaf}$ and irrigation aspects to qualitatively diagnose plant stress. It also demonstrated from a systems maintenance point of view, the opportunity to identify and locate irrigation and fertigation network routes and flow distribution, as well as any disruptions (e.g., [311]). It is worth noting that such detection is best achieved with thin-substrate living wall systems (e.g., *Mur Vegetal* installations at the Quai Branly and CaixaForum), as opposed to those with deeper substrates (e.g., the DAB). Substrate properties can also be assessed to determine their contribution to system hygrothermal performance. This is attributed to substrate moisture retention affecting the medium's thermal resistance (increased conductivity and heat capacity) and increasing evaporation to cool the surface [252,253,311]. In this study, the coolest $T_{surf}$ values (~6 K) were captured where the substrate was exposed to highlight its evaporative cooling influence and function as a moisture-rich medium. The latter aspect is critical for hydroculture or felt-based systems as they rely on maintaining a saturated medium to facilitate growth, and the detection of warmer $T_{sub}$ could be indicative of an irrigation fault requiring attention. Although such qualitative detection is useful from a maintenance point of view, accurate diagnosis is dependent on the assessor's experience. Detailed stress detection relevant for automated responses therefore require more accurate quantitative approaches to be implemented.

### 5.4.1 Characterising canopy feature influence

The principal aim of this study was to present a quantitative understanding of the canopy morphological features that affect a vertical greening installation's surface temperature, which in turn affects their surface flux and thus vital for accurately simulating their performance (considered in Study 3). Canopy density is characterised in vegetation studies by their $LAI$ value (between 0-10), the definition of which is modified for vertical greening applications to consider the ratio of total leaf area relative to the exposed vertical wall area [157]; and followed by the extent of the canopy characterised by percentage-cover (between 0-1). In this study, the focus was the canopy itself with the background wall and substrate segmented out to isolate only the target canopies. The percentage-cover was therefore ~1.0 (subject to 1-6% segmentation error, with greatest for smaller leaved canopies than larger); while the vertical $LAIs$ were all >1. As the aims of the study also included the non-destructive assessment of in-situ installations belonging to the more diverse living wall category, the typically destructive measurement of $LAI$ was precluded. The study therefore limited consideration only to the non-destructively measurable canopy morphological features of protuberance ($z_{veg}$) and leaf size ($W_{leaf}$). The former characterises the extent of a canopy's coupling with the bulk atmosphere, while the latter describes its nature.

The results showed that plant canopy surfaces across the case studies presented cooler $ST_{leaf}$ means during the night than daytime, which is expected given the absence of solar irradiance. The preliminary qualitative assessment had suggested that broad and large-leaf canopies that project off the wall surface (i.e., protuberant, or $\uparrow z_{veg}$) to present much warmer surface temperatures relative to small-leaf canopies that are more surface spreading (i.e., prostrate, or $\downarrow z_{veg}$), both in indoor and outdoor environments. The following quantitative assessment confirmed this, while presenting positive correlations for the canopies examined[VI]. The three-dimensional protuberance of the canopy morphology was approximated by defining three categorical levels. Higher protuberance represented conditions where canopies are decoupled from the wall substrate and increasingly coupled with the ambient $T_{air}$, while prostrate canopies are well-coupled with the substrate and its moisture-richness. With the outdoor case studies, prostrate canopies at the same elevational height presented the coolest $\Delta T_{\mathrm{veg}}$ (e.g., *S. soleirolii*: -1.96 and -5.23 K at the Quai Branly, and *V. minor*: -3.47 and -8.10 K at the CaixaForum, for day and night-time means respectively), while with the most protuberant canopies for the corresponding presented the warmest $\Delta T_{\mathrm{veg}}$ (e.g., *H. 'Bressingham Blue'*: 0.90 and -2.97 K at the Quai Branly, and *H. sieboldiana*: 2.14 and -3.52 K at the CaixaForum, for day and night means). With the indoor study the same observations remained mostly valid, although was dependent on the elevational height of the installation owing to the vertical thermal stratification present in

[VI] The ordinal categorisation of data meant that the limited datasets presented weaker significance.

the atrium (see Study 1). It must be noted that the canopy $ST_{leaf}$ discussed here does not reflect the entire canopy's $T_{leaf}$. The former is expected to be higher given that the surface of any canopy acts as a radiation interceptor, which inevitably leads to higher energy absorption and resultant $ST_{leaf}$. Greater protuberance only enhances this interception function to increase canopy $ST_{leaf}$, whereas in the canopy interior $T_{leaf}$ could be lower, (e.g., Table 22, p. 134, 'a-Sp1'). This in turn presents a shortcoming of using thermography, where $ST_{leaf}$ acquired presents an overestimation of the installation's actual canopy $T_{leaf}$ (Study 3 later highlights $\uparrow z_{veg}$ to reduce $\downarrow T_{leaf}$).

As components of the canopy, the two-dimensional proportions of leaves also influence canopy $ST_{leaf}$. This is explained by the way individual leaves aid the coupling of the canopy to the surrounding atmosphere [349]. Leaf size ($W_{leaf}$) and morphology, together with prevailing $V_{air}$ determine the leaf boundary-layer depth, with the latter inversely related to the leaf boundary-layer conductance. High boundary-layer conductance allows for leaves to be well-coupled with the atmosphere to facilitate efficient latent and sensible convective heat dissipation that results in relatively cooler leaves [55]. Smaller (e.g., *S. soleirolii*), or pinnated (e.g., *P. polyblepharum*), compound, or dissected leaves, stay cooler in similar conditions as their boundary-layer conductance is increased from a shallower boundary-layer depth [54]. The rate of heat convection per unit area is therefore greater between leaf and air for smaller leaves than larger [329]. This is exemplified by the fern *P. polyblepharum*, where its pinnated fronds helped to present lower canopy $ST_{leaf}$ means comparable to 'small' or 'very small' leaved plants, despite giving the appearance of an overall broad, 'large' leaf canopy with 'medium extension'. Pinnation therefore helps its canopy to function as if it were composed of a multitude of smaller leaves that are well-coupled to the bulk atmosphere. This smaller-leaf benefit is evident in species climate adaptation, with such leaves commonly seen on plants from hot and dry climates where adaptations to minimise high transpiration mean that they must instead rely on enhanced sensible convection to dissipate higher daytime irradiation [350].

Larger leaves in contrast generate a larger boundary-layer depth and resulting reduced conductance, which leads to higher $ST_{leaf}$. With the outdoor installations, mean $\Delta T_{\mathrm{veg}}$ during the day was a positive value for all $W_{leaf}$ over 'medium' and with canopy $z_{veg}$ beyond 'medium extension'. At the CaixaForum for example, both *H. sieboldiana* and

*H. plantaginea* canopies presented the highest mean $\Delta T_{\mathrm{veg}}$, while leaf-edge browning was observed to indicate symptoms of heat stress (Fig. 61, p. 132). The lower convection efficiency of larger leaves means that they must rely on transpirational evaporation for cooling. The increased $ST_{leaf}$ that results also increase the saturation vapour pressure within the leaf, which in turn increases the vapour gradient with the ambient atmosphere. This gives rise to a higher rate of transpiration and resultant latent heat loss, provided there is no water deficit or irradiance stress. Larger leaves can therefore cool more rapidly through transpiration and maintain lower temperatures than smaller leaves [329,351], which is a characteristic species adaptation from hot, humid climates with ample availability of water and growth factors (e.g., the tropical epiphyte *M. deliciosa*) [352]. Larger leaves however are complex, with their size and weight resulting in them distorting to present a convex geometry for irradiation that leads to heterogeneous absorption. This together with the heterogeneity of hydraulic and stomatal function can result in larger range of $ST_{leaf}$ distribution [352]. Leigh *et al.* [329] for example found a positive correlation between leaf size and $ST_{leaf}$ range per leaf. This suggests that single-point thermocouple measurement of such leaves present nonrepresentative canopy $ST_{leaf}$, while the higher resolution of thermography allows for this heterogeneity to be captured.

Previous vegetation studies generally support observations of warmer $T_{leaf}$ for larger leaves relative to smaller [329,331,352]. As examples, Smith & Carter [353] found needle leaves to typically remain within 4-8 K of $T_{air}$; Jones [354] had shown irradiated broadleaves to be 10-15 K warmer than $T_{air}$; while Leuzinger & Körner [333] found coniferous species to have cooler $T_{leaf}$ than comparably sized broadleaved species. With reference to vertical greening studies, Cameron *et al.* [157] found the effective cooling observed with *Jasminum officinale* to be influenced by its pinnated leaves, while the Charoenkit & Yiemwattana [215] study observed the smaller leaves of *Cuphea hyssopifolia* to provide higher cooling efficiency relative to the large-leaved *Excoecaria cochinchinensis*. It is worth noting that the significance of a leaf's convective boundary-layer influence on heat dissipation reduces at very low $V_{air}$ (0.1-0.25 $\mathrm{m{\cdot}s^{-1}}$). In such near still conditions, forced convection gives way to the dominance of the less efficient dissipation from natural convection [329]. At the DAB case study where indoor $V_{air}$ for the study was recorded at ~0.1 $\mathrm{m{\cdot}s^{-1}}$ (summer M = 0.096, ±0.05 $\mathrm{m{\cdot}s^{-1}}$, and winter M = 0.12, ±0.06 $\mathrm{m{\cdot}s^{-1}}$, see Study 1), the dominant canopy cooling influence will be from transpiration. This partly explains the moderate daytime correlations between canopy

$ST_{leaf}$ and its characterisation by $z_{veg}$ and $W_{leaf}$. The dominance of transpirational cooling in such conditions also suggests that the typically higher summertime watering demand of tropical broadleaved plants will be further pronounced. Increasing summertime water supply to address this could encourage beneficial transpirational microclimate cooling (which could reduce indoor space-cooling loads); although this would also encourage aggressive growth that in turn would require frequent maintenance trimming to prevent root push-back and canopy dominance (e.g., as experienced with *M. deliciosa* at the DAB case study).

Beyond the above discussion pertaining to broadleaved canopies, grass types can be described to present distinct behaviour in outdoor settings with higher wind flow. Although grass leaves individually seem smaller due to their narrow-blade morphology, they generate a deeper canopy boundary-layer as the blades are 'streamlined' when wind stress is encountered to present the longest available dimension of the blade to be in contact with prevailing wind flow (i.e., greatest fetch/characteristic dimension, $D$). This in turn reduces the canopy surface roughness to increase the depth of the leaf and canopy boundary-layer to present a lower boundary-layer conductance. The effect is enhanced with increasing length of leaves as streamlining reduces canopy heterogeneity and increases bulk-action. In this study, this form of reduced coupling with the atmosphere was exemplified at the CaixaForum, with *C. oshimensis* and *O. planiscapus* presenting moderately higher day and night-time $ST_{leaf}$ means comparable to other 'small' to 'medium' canopies. This result is in common with *P. annua* at the Quai Branly, although the $ST_{leaf}$ means are much closer to 'very small' leaf canopy day and night-time values given its prostrate canopy extension. The latter aspect could also be associated to blade length, where *P. annua* presents a much smaller length than the other two grasses. When considering $\Delta T_{\mathrm{veg}}$ for *O. planiscapus,* it presented a warmer mean difference during the day and the coolest at night (for all grass types), in contrast to the other two that presented cooler means for the daytime and even cooler means for the night-time like other 'small' leaf canopies. This daytime anomaly is explained by its higher emissivity ($\varepsilon_{leaf}$: 0.99), given the blackish foliage pigmentation.

The physical property of leaf reflectivity or albedo ($\rho_{leaf}$), affects its radiation absorptivity ($\alpha_{leaf} = 1 - \rho_{leaf}$, where transmissivity, $\tau_{leaf} = 0$) [53]. Most plant leaves have relatively low $\rho_{leaf}$ ranging between 0.1-0.3, with single-leaf values typically higher than for canopies ($\rho_{leaf} > \rho_{veg}$, given that multiple reflections between adjacent leaves and stems lead to radiation trapping and resultant increase in $\alpha_{veg}$, [52,338,346]). With certain species, the presence of cuticle wax layers, trichomes, or salt crystal secretions may increase $\rho_{leaf}$. Generally, reflective and pubescent leaves have been observed to increase values and thereby reduce $T_{leaf}$, while non-reflective hairs reduce boundary-layer conductance to result in increased $T_{leaf}$ [54]. Given this influence on $T_{leaf}$, either $\rho_{leaf} \mid \rho_{veg}$ or $\alpha_{leaf} \mid \alpha_{veg}$ must be a known parameter when determining leaf and canopy energy balances, and thus is a key input in vegetation simulation approaches (see Study 3).

### 5.4.2 Thermography application limitations

Before applying thermography, it is significant to consider typical sources of error and accuracy limitations. One principal source is the inaccurate characterisation of relevant environmental variables at the time of capture. These include solar radiation intensity ($Q_{R_{sw}}$), $T_{air}$, $RH$, $V_{air}$, and background pollution [317,336,355]. Atmospheric attenuation or the $Q_{R_{lw}{}_{air}}$ component has been identified to lead to significant errors with increased $D_{IR}$, particularly with largescale aerial remote-sensing applications [345,356]. The $Q_{R_{lw}{}_{air}}$ compensation in cameras may also need to be adjusted in highly polluted outdoor environments, as atmospheric attenuation varies with air density ($\dot{\rho}_{air}$), and the onboard compensation typically accounts only for standard $\dot{\rho}_{air}$ [317]. With ground-based studies (significant for this study), sensitivity analyses had revealed the parameters of $RH$ and $D_{IR}$ as the least sensitive, while $\varepsilon_{obj}$, $\boldsymbol{T_{ref}}$, and $\boldsymbol{T_{air}}$ have been identified to be the most significant particularly for quantitative applications [331,357]. From these three parameters, target $\varepsilon_{obj}$ has the greatest influence [331,332,345], and is a common source of error when very low values are considered [317]. The FLIR infrared camera manufacturer therefore recommends values >0.5 as a minimum to obtain accurate results [340]. With high target $\varepsilon_{obj}$ values (>0.9), as with typical vegetation surfaces, the $Q_{R_{lw}{}_{ref}}$ component and implicit $\boldsymbol{T_{ref}}$ is less significant. This reflected component's compensation and associated error could also be reduced in outdoor environments by carrying out thermography under cloudy conditions, when $\boldsymbol{T_{Sky}}$ is much warmer relative to a clear sky [341].

Another major source of error is contributed by the thermographer's application approach. When framing the target object, it is significant to avoid too shorter $D_{IR}$ as this is likely to add the reflection of the thermographer onto the resulting thermograms [317]. The $D_{IR}$

also affects the FOV and thermogram resolution. Greater distances reduce resolution (increases the IFOV), which reduces detail by averaging a greater area of temperatures per pixel [340]. Furthermore, attention should be paid to how the camera's FOV is targeted. If water status quantification is the principal objective of application, the FOV should be directed to cover the vegetation canopy as much as possible, or else readings would have to be compensated for partial canopy cover [337]. This is significant for living wall assessment as it adds the task of having to segment-out substrate $T_{sub}$ during post-processing, while this may not be straightforward as surface spreading plant canopies with smaller leaves could remain closer or even equal to $T_{sub}$, thereby increasing segmentation errors. Typically, thermograms taken with a narrow FOV, moderate $D_{IR}$, perpendicular to the target object, and in focus, captures the most detailed and accurate information [317,340].

The accuracy of infrared cameras is constantly improving, with typical cameras presenting an accuracy of ±2% (used in this study), while advanced models have an accuracy of ±1% for a defined temperature range. Quantitative research requires a high degree of accuracy, although it must be stressed that no available camera has been validated to be as accurate as a contact temperature measurement method [317]. Another consideration is the spot-size-ratio (SSR), which describes the ratio between the FPA of detectors and the FOV of the camera optics. The highest FPA and narrowest FOV offers the best infrared capture resolution for a given target, which in turn presents the highest detail typically necessary for quantitative research assessments [340]. The infrared camera spectral range must also be assessed to ensure that detection is within the earlier mentioned 'atmospheric window', which is necessary for interference-free capture.

Thermography application accuracy and validation in relation to measuring plant $ST_{leaf}$ requires further attention, particularly in relation to the overestimation of actual canopy $T_{leaf}$ highlighted. The measurement error with applications should ideally be within 1-2 K, given that $\Delta T_{veg}$ gradients in many environments are between 0-5 K (gradients could get as high as 10-15 K, [331]). The accuracy correction measures considered by researchers have already identified to be critical when measuring in extreme cold and hot ambient environments (e.g., [331]). In temperate climates this means that it could be used for critical summertime water status monitoring, while less critical wintertime readings are likely to require some adjustment prior to interpretation. When utilising this methodology for stress detection, it must also be understood that the potency of the stressor must lead to detectable canopy $ST_{leaf}$ changes, which may not be the case with minor shortfalls or for early stages of stress development. Diagnosis of the causal agent stressor is also not consistently evident from temperature related observations alone, as a combination of stressors can affect the potency of $ST_{leaf}$ changes [336,358].

## 5.5 Summary

In this study, the influence of the living wall canopy morphological features of protuberance ($z_{veg}$) and leaf size ($W_{leaf}$) on its $ST_{leaf}$ was assessed using qualitative and quantitative thermography. The preliminary qualitative assessment suggested that **large and broadleaf canopies with substantial protuberance to present much warmer $\boldsymbol{ST_{leaf}}$** relative to small-leaf canopies that are more surface spreading. The subsequent quantitative assessment confirmed this, while presenting positive correlations for the plant canopies examined. This means that both these **canopy morphological parameters are significant and must be input accurately for the reasonable approximation of $\boldsymbol{T_{leaf}}$**; which is the objective of Study 3.

The study also presented **thermography as an alternative and practical methodology for assessing indoor and outdoor living wall installations**, which in turn could inform plant selection considerations for designers and highlight service-life maintenance considerations for installation managers. Despite the limitations of camera accuracy, risk of usage errors, and interpretation cautions, quantitative thermography presents itself as a reasonably accurate, non-contact, and non-invasive means of canopy data harvesting. Coupling such real-time data with a vegetation model (as the one presented in the next chapter), could present the opportunity to automate the maintenance of future installations to reduce costs and enhance their sustainability.

# Chapter 6

## STUDY 3: BUILDING SIMULATION PATHWAY-A

## 6.1 Introduction

Progressing from Studies 1 and 2, this chapter presents Study 3, which addresses the third-of-five secondary research questions introduced in Chapter 1.

> *Q III. How can vertical greening influence be approximated for building-scale assessments in a computationally efficient manner?*

The chapter addresses this question by developing a one-dimensional vertical greening model (VGM), which can be coupled by any built environment analyst familiar with the TRNSYS building energy modeller (referred to as simulation Pathway-A). The following presents the development of this model, its validation results, and application to consider vertical greening influence at the two building environments introduced in Study 1: namely the semi-outdoor court at SET, London, and the indoor atrium at the DAB in Cambridge.

### 6.1.1 Modelling vertical greening

Earliest vertical greening modelling exercises adapted existing vegetation canopy models to consider idealised scenarios. These typically utilised empirical priming data, as exemplified by the approaches in: [161,196,233]. An alternative approach is to consider priming using a reference plant community. The latent flux in such models is calculated for a reference horizontal plant canopy free from water stress, utilising the FAO adaptation of the Penman-Monteith model [359], and then multiplied by a factor that accounts for species-specific vegetation characteristics such as canopy height, roughness, and stomatal responses to environmental loading. The resulting application studies have predominantly utilised published FAO crop-factors either directly, or as a close approximation to what it would be for the vegetation community assessed (e.g., [223,239,360,361]). This reliance on empirically derived crop-factors relating to horizontal canopies means that the method is best suited for considering monoculture systems with uniform coverage. This is a challenging limitation for considering green façades given their inconsistent coverage, as well as for living walls given the canopy diversity of typically implemented plant communities.

The most common modelling attempts to date have considered the adaptation of existing horizontal greening (green-roof) models, given their development preceded interest in vertical greening. Dynamic models developed by Alexandri & Jones [362] and Sailor [363] for example were integrated as a module in the building energy model EnergyPlus [364]; followed by a number of application studies (e.g., [249–251,365]). Djedjig *et al.* [246,366] similarly adapted their own green-roof model to present a series of studies where they coupled it with a mass flow model and the building energy model TRNSYS [367]. The principal issue with these adaptation approaches is that they remain as either specific research exercises or black-boxed pathways, with the code developed not readily available for adaptation and further research development.

The development of a vertical greening model from first principles has also been pursued by researchers. A notable example is the Susorova *et al.* model [163], which simulates the one-dimensional horizontal heat flux through a vertical plant layer. The principal limitation of this simplified model is that it only provides opportunity to consider direct green façades (in addition to using several assumed inputs). The Grabowiecki *et al.* [368] model presented a progression to this Susorova *et al.* model including some accountability of plant stress influence. This 'Vertical Foliage Component' (VFC) however is only available commercially as a black-box TRNSYS add-on (Fortran), and thus was not adaptable to address the research objectives of this project[VII].

From the preceding simulation pathways mentioned above, both EnergyPlus and TRNSYS building energy models have offered the flexibility necessary to introduce coupled components to perform a subset of calculations. This built-in flexibility is useful for developing components to resolve specific problems such as vertical greening approximation, with opportunity for independent development and integration of revisions without need for major modifications to the building energy model's simulation engine. This study utilises this

[VII] The VFC component was provided free-of-charge to the author for assessment, but code sharing was refused.

established advantage of TRNSYS (e.g., [246,368]), to couple a MATLAB coded VGM component and present a computationally efficient simulation pathway for building-scale vertical greening assessments (referred to in this thesis as simulation Pathway-A).

### 6.1.2 Vertical Greening Model (VGM)

The inclusion of a vertical greening system could be considered as the addition of a 'layer(s)' to the face of a new or existing host-wall construction. For direct green façades this takes the form of a 'plant layer' with a certain $LAI$, while for living walls a saturated 'substrate layer' is also included between the plant layer and host structure. This simplified layered representation was modelled in this study as the VGM to calculate one-dimensional flux from vegetated façade constructions.

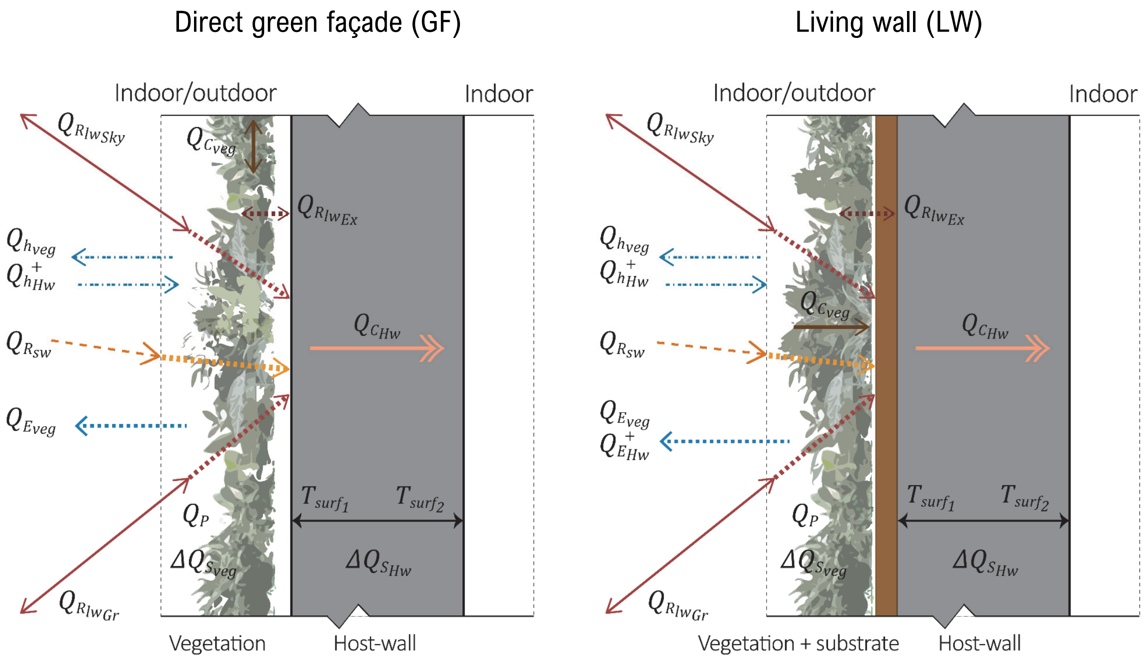


*Fig. 66. Vertical greening (direct green façade and living wall) energy interactions.*

Given the above arrangement in outdoor environments (Fig. 66), the vertical plant canopy intercepts both direct and diffused shortwave radiation received during daylight hours ($Q_{R_{sw}}$); as well as longwave ($Q_{R_{lw}}$) gain from the ground ($Q_{R_{lw_{Gr}}}$), sky ($Q_{R_{lw_{Sky}}}$), and any contextual surfaces present ($Q_{R_{lw_{CS}}}$); (gain from the atmosphere is disregarded). A partition of this absorbed radiation is then emitted as longwave emissions ($Q_{R_{lw_{veg}}}$), to present its net radiation budget. This differs in indoor environments with radiation sources typically including an attenuated transmission of $Q_{R_{sw}}$ (e.g., from a rooflight) and/or artificial PAR lighting, while longwave gain ($Q_{R_{lw}}$) is dominated by exchanges with contextual bounding surfaces. In both environments, partitions of the radiation energy surplus are transferred to the atmosphere by means of sensible convection ($Q_{h_{veg}}$) and latent convection from evapotranspiration ($Q_{E_{veg}}$). A partition is also converted to biochemical storage from plant photosynthesis ($Q_P$), although this is relatively insignificant and disregarded [2,52,55]. Conduction ($Q_{C_{veg}}$) through stems to the supporting host layer (with living walls) or ground (with green façades), and storage in plant matter ($\Delta Q_{s_{veg}}$) is similarly disregarded given the nature of typical vertical greening plant communities considered (mostly herbaceous).

The addition of a vertical vegetation layer makes it the foremost surface exposed to radiation incidence. As with any material, a partition of this intercepted radiation is reflected dependent on the canopy's reflectivity ($\rho_{leaf}$), while the porosity of the layer means that a partition is also transmitted through to the layer behind, of which a partition is reflected by that layer (dependent on its reflectivity, $\rho_{Hw}$) back into the vertical canopy. The transmission of radiation through the plant layer is defined by its transmissivity coefficient ($\tau_{veg}$), which is calculated with reference to the attenuation coefficient ($k$) and $LAI$ of the canopy [52]. While $k$ can be defined by detailed consideration of canopy geometry and resulting leaf-angle ($\theta_{leaf}$) distribution (e.g., spherical, ellipsoidala, or diaheliotropic), as a simplification this model considers a distribution that assumes a mean $\theta_{leaf}$ [52,55].

$$Q_{leaf} = Q_{R_{sw}} + \left( \overbrace{\left(Q_{R_{lw_{Gr}}} + Q_{R_{lw_{Sky}}} + Q_{R_{lw_{CS}}}\right)}^{Q_{R_{lw}}\ gain} - Q_{R_{lw_{veg}}} \right), \qquad \textit{Equation 8}$$

$$Q_{leaf} = \alpha_{leaf}\, I_{tot} + \overbrace{\varepsilon_{leaf}\, \sigma \left[F_{Sky}\left(\boldsymbol{T}_{Sky}^4 - \boldsymbol{T}_{air}^4\right) + F_{Gr}\left(\boldsymbol{T}_{Gr}^4 - \boldsymbol{T}_{air}^4\right) + F_{CS_i}\left(\boldsymbol{T}_{CS_i}^4 - \boldsymbol{T}_{air}^4\right)\right]}^{\text{Longwave balance as exchanges}}, \qquad \textit{Equation 9}$$

where,

| | |
|---|---|
| $k$ | Coefficient, canopy attenuation = (0-1), between 0.3 and 0.5 for $\theta_{leaf}$<45°, and 0.7 and 1.0 for $\theta_{leaf}$>45° [369]; |
| $\tau_{veg}$ | Coefficient, canopy transmissivity = $\exp(-k\, LAI)$; |
| $\sigma$ | Constant, Stefan-Boltzmann = $5.67 \cdot 10^{-8}$ [W·m$^{-2}$·K$^{-4}$]; |
| $\alpha_{leaf}$ | Leaf absorptivity = $\left(1 - \tau_{veg} - \rho_{leaf}\right)$, (0-1), with deciduous broadleaves is between 0.34 and 0.44 for low solar angles, and 0.48 and 0.56 for high solar angles, the typical range is thus between 0.3 and 0.6 [53]; |
| $\varepsilon_{leaf}$ | Leaf emissivity = (0-1), typically between 0.91 and 0.99 [52,338,346]; |
| $\rho_{leaf}$ | Leaf reflectivity = (0-1), typically between 0.1 and 0.3 [52,338,346]; |
| $I_{tot}$ | Irradiation, direct and diffused solar radiation incident on vertical surface [W·m$^{-2}$]; |
| $\mathbf{T}_{Sky}$ | Absolute temperature, of clear sky $= T_{air}\ (0.8 + T_{dew}/250)^{0.25} + 273.15$ [K], [370]; |
| $\mathbf{T}_{dew}$ | Absolute temperature, dewpoint [K]; |
| $\mathbf{T}_{Gr}$ | Absolute temperature, of ground [K]; and |
| $F_{Sky} \mid F_{Gr} \mid F_{CS_i}$ | View-factors, for vertical façade tilt angle $\theta = 90°$, with sky $F_{Sky} = 0.5\ (1 + \cos\theta)$, ground $F_{Gr} = 0.5\ (1 - \cos\theta)$, and contextual surface(s) $F_{CS_i}$, where $i$ = contextual surface, ..., $j$. $\sum_{i=1}^{j} F_i = 1$. |

The net radiation budget for the plant layer $Q_{leaf}$ [W·m$^{-2}$], is calculated from Equation 9. The initial assumption is that $T_{leaf} = T_{Hw} = T_{air}$, which is used for the plant layer longwave exchange calculations, and also nullifies exchanges between plant leaves and the atmosphere, as well as leaves and the host-wall or substrate (i.e., $Q_{R_{lw_{Ex}}}$) [163].

The convection partitions to the climate from $Q_{h_{veg}}$ and $Q_{E_{veg}}$ are determined by the resistances or conductances (inverse of former) to heat and vapour transfer. These are defined as a coupling between leaf and canopy conductances, which describes the principle of a 'big-leaf' model [52,53,55]. Vertical canopy temperature is calculated in this model from the following big-leaf expression presented by Campbell & Norman [53]:

$$T_{leaf} = T_{air} + \frac{\gamma'}{\Delta/P_{air} + \gamma'}\left[\frac{Q_{leaf}}{g_c\, c_{p_{air}}} - \frac{e_s(T) - e_a}{P_{air}\,\gamma'}\right], \qquad \textit{Equation 10}$$

where,

| | |
|---|---|
| $\gamma$ | Constant, psychrometric = $c_{p_{air}}/\lambda$ [K$^{-1}$]; |
| $\gamma^*$ | Apparent value of psychrometric constant = $\gamma\, g_c/g_v$ [K$^{-1}$]; |
| $\lambda$ | Latent heat of vaporisation of water = 44,000 [J·mol$^{-1}$]; |
| $g_c$ | Conductance, of heat through the air $= g_r + g_{bh}$ [mol·m$^{-2}$·s$^{-1}$]; |
| $g_v$ | Conductance, of vapour through the air $= g_{as} + g_{bh}$ [mol·m$^{-2}$·s$^{-1}$]; |
| $e_s(T)$ | Vapour pressure of air at saturation (from Tetens formula), $= 0.611 \cdot \exp(17.502 \cdot T_{air}/T_{air} + 240.97)$ [kPa]; |
| $e_a$ | Partial vapour pressure of air = $e_s(T)\, rH$ [kPa]; |
| $\Delta$ | Slope of the saturation vapour pressure function, $= 17.502 \cdot 240.97 \cdot e_s(T)/(240.97 + T_{air})^2$ [kPa·K$^{-1}$]; |
| $P_{air}$ | Atmospheric pressure [kPa]; |
| $c_{p_{air}}$ | Specific heat of air at constant pressure, 29.3 [J·mol$^{-1}$·K$^{-1}$]; |
| $T_{air}$ | Temperature, of air [°C]; and |
| $T_{leaf}$ | Temperature, of leaf surface [°C]. |

The heat conductance of the canopy ($g_c$) is the sum of its radiative conductance ($g_r$) and convective boundary-layer conductance to heat ($g_{bh}$); while vapour conductance of the canopy ($g_v$) is the sum of the actual stomatal conductance ($g_{as}$) and convective boundary-layer conductance to vapour ($g_{bv}$) [53]. With $g_v$, two principal aspects impact on actual values. The first is irradiance influence on stomatal function (provided that plants are not water stressed); addressed by Equation 11 [163]. The second is the stomatal distribution of leaves (dominant for the plant community), with 'amphistomatous' describing stomata located on both surfaces (adaxial and abaxial) or 'hypostomatous' describing only on the lower surface (abaxial); addressed by Equation 12 [53].

$$g_{as} = g_{asul} = g_{asll} = 1 \Big/ \left[ \frac{1}{g_s} \left( \frac{I_{max}}{0.03 \cdot I_{max} + I_t} + \left( \frac{\eta_{wilt}}{\eta_{root}} \right)^2 \right) \right], \quad \text{Equation 11}$$

$$g_v = \left[ \frac{0.5 \cdot g_{asul}\ g_{bv}}{g_{asul} + g_{bv}} + \frac{0.5 \cdot g_{asll}\ g_{bv}}{g_{asll} + g_{bv}} \right], \quad \text{Equation 12}$$

where,

| | |
|---|---|
| $I_{max}$ | Irradiation, maximum total solar radiation incident on leaves [W·m$^{-2}$]; |
| $\eta_{wilt}$ | Soil moisture, level below which permanent wilting occurs; |
| $\eta_{root}$ | Soil moisture, minimum value in the rhizosphere; |
| $g_s$ | Conductance, stomatal [mol·m$^{-2}$·s$^{-1}$]; |
| $g_{asul} \mid g_{asll}$ | Conductance, actual stomatal for upper \| lower leaf surface [mol·m$^{-2}$·s$^{-1}$]; and |
| $g_r$ | Conductance, radiative $= 4 \cdot \sigma\ (T_{air} + 273.15)^3 / c_{p_{air}}$ [mol·m$^{-2}$·s$^{-1}$]. |

The canopy conductance calculations applied depend on the relevant wind regime for the environment. These are distinguished as conditions where natural convection, forced convection, or eddy diffusion is likely to be dominant (Equation 13 to Equation 17, [53]). A forced convection regime is likely to be dominant in sheltered environments where some crossflow is prevalent, while eddy diffusion is relevant for exposed outdoor environments such as street canyons (considered in Study 4). Observational evidence from Study 1 highlighted airflow in the indoor case study to be modest, with natural convection as the dominant regime. However, Equation 13 and Equation 14 cannot be applied for such conditions here as $T_{leaf}$ is initially unknown. In this model, Equation 15 and Equation 16 are instead applied for indoor simulations, with the exterior forced convection factor ($F_{ext}$) omitted.

Natural convection:

$$g_{bh} = 0.050\,(T_{leaf} - T_{air}/D)^{1/4}, \quad \text{Equation 13}$$

$$g_{bv} = 0.055\,(T_{leaf} - T_{air}/D)^{1/4}, \quad \text{Equation 14}$$

Forced convection:

$$g_{bh} = F_{ext}\,(0.135 \cdot \sqrt{V_{air}/D}), \quad \text{Equation 15}$$

$$g_{bv} = F_{ext}\,(0.147 \cdot \sqrt{V_{air}/D}), \quad \text{Equation 16}$$

Eddy diffusion:

$$g_{bh} = g_{bv} = \frac{vk^2\,\hat{\rho}_{air}\,V_{air}}{[ln(z_{veg} - d_0/z_m) + \psi_m]\ [ln(z_{veg} - d_0/z_h) + \psi_h]}, \quad \text{Equation 17}$$

where,

| | |
|---|---|
| $V_{air}$ | Air velocity [m·s$^{-1}$]; |
| $\hat{\rho}_{air}$ | Molar density of air = $P_{air}\,R\,(T_{air} + 273.15)$ [mol·m$^{-3}$]; |
| $R$ | Molar gas constant = 8.31 [J·mol$^{-1}$·K$^{-1}$]; |
| $D$ | Leaf characteristic dimension in wind direction = $W_{leaf}$ · 0.72 [m]; |
| $W_{leaf}$ | Leaf-width [m]; |
| $F_{ext}$ | Factor, for exterior forced convection conditions = 1.40 [53]; |
| $vk$ | Constant, Von Karman = 0.40; |
| $z_{veg}$ | Canopy depth [m]; |
| $d_0$ | Displacement depth $= 0.701 \cdot z_{veg}^{0.975}$ [m]; |
| $z_m \mid z_h$ | Roughness lengths, $z_m = 0.131 \cdot z_{veg}^{0.997}$ [m]; and |
| $\psi_m \mid \psi_h$ | Stability correction factors for momentum and heat. |

With eddy diffusion dominant applications (considered later in Study 4), several previous studies had identified the inclusion of the stability factors $\psi_m \mid \psi_h$ to have presented little improvement of $g_{bh} \mid g_{bv}$ estimation [53]. As a simplification, these factors have therefore been disregarded in this model.

$$Q_{h_{veg}} = c_{p_{air}}\, g_c\, (T_{leaf} - T_{air}), \qquad \textit{Equation 18}$$

$$Q_{E_{veg}} = \lambda\, g_v \left(\frac{e_s(T_{leaf}) - e_a}{P_{air}}\right). \qquad \textit{Equation 19}$$

The $T_{leaf}$ calculated from the big-leaf model is then used to calculate $Q_{h_{veg}}$ and $Q_{E_{veg}}$ flux (Equation 18 and Equation 19, [53]); while $T_{leaf}$ is input to the energy balance for the host-wall to calculate its surface ($T_{Hw}$ if green façade) or substrate temperature ($T_{sub}$ if living wall). The addition of the plant layer modifies the energy balance of this existing host-wall. The radiation balance is modified to include both daytime direct and diffused shortwave radiation transmitted ($\tau_{veg}$) through the plant canopy ($Q_{R_{sw}}$); longwave ($Q_{R_{lw}}$) energy transmitted from the ground ($Q_{R_{lw_{Gr}}}$), sky ($Q_{R_{lw_{Sky}}}$), and any contextual surfaces if present ($Q_{R_{lw_{CS}}}$); as well as longwave exchanges between plant layer leaves and the host-wall surface or substrate ($Q_{R_{lw_{Ex}}}$). Partitions of this net absorbed radiation is then transferred away from the host surface by means of convection (sensible flux $Q_{H_{Hw}}$ for green façades, while living walls include both sensible and latent flux: $Q_{h_{Hw}} + Q_{E_{Hw}}$); conducted into the interior of the building ($Q_{C_{Hw}}$); and stored in the bulk of the wall material ($\Delta Q_{S_{Hw}}$). The resulting energy balance for the host-wall is represented in Equation 21 [53].

$$\Delta Q_{S_{Hw}} = Q_{R_{sw}} + \left(Q_{R_{lw}} + Q_{R_{lw_{Ex}}}\right) - \overbrace{Q_{h_{Hw}} + Q_{E_{Hw}}}^{for\ GF\ =\ Q_{H_{Hw}}} - Q_{C_{Hw}}, \qquad \textit{Equation 20}$$

$$\frac{dT_{Hw}}{dt} = \frac{Q_{R_{sw}} + \left(Q_{R_{lw}} + Q_{R_{lw_{Ex}}}\right) - \overbrace{Q_{h_{Hw}} + Q_{E_{Hw}}}^{for\ GF\ =\ Q_{H_{Hw}}} - Q_{C_{Hw}}}{Q_{S_{Hw}}}, \qquad \textit{Equation 21}$$

where,

| | |
|---|---|
| $Q_{R_{sw}}$ | Radiation, shortwave absorbed [W·m$^{-2}$]; |
| $Q_{R_{lw}}$ | Radiation, longwave absorbed, $Q_{R_{lw_{Gr}}} + Q_{R_{lw_{Sky}}} + Q_{R_{lw_{CS}}}$ [W·m$^{-2}$]; |
| $Q_{R_{lw_{Ex}}}$ | Radiation, foliage-to-host/substrate exchange [W·m$^{-2}$]; |
| $Q_{C_{Hw}}$ | Conduction, flux through the vegetated façade [W·m$^{-2}$]; |
| $Q_{H_{Hw}}$ | Convection, sensible flux (when green façade) [W·m$^{-2}$]; |
| $Q_{h_{Hw}}$ | Convection, sensible flux (when living wall) [W·m$^{-2}$]; |
| $Q_{E_{Hw}}$ | Convection, latent flux (when living wall) [W·m$^{-2}$]; |
| $\Delta Q_{S_{Hw}}$ | Net heat storage of the vegetated façade [W·m$^{-2}$]; |
| $Q_{S_{Hw}}$ | Heat storage constant of the host-wall [J·m$^{-2}$·K$^{-1}$]; and |
| $T_{Hw}$ | Temperature, of host surface including vegetation [°C], corresponds to substrate temperature ($T_{sub}$) of living walls. |

Where the substrate layer is relevant with living walls, the heat conductance ($g_c$) is the sum of heat conductance between the substrate surface and air within the canopy ($g_{c_{sub}}$) and the boundary-layer conductance to heat ($g_{bh}$); while vapour conductance ($g_v$) is the sum of vapour conductance between the substrate surface and air within the leaf canopy ($g_{sub}$) and boundary-layer conductance to vapour ($g_{bv}$). Where a green façade is relevant, an empirically derived convective heat transfer coefficient ($h_{Hw}$) is applied[VIII] [163].

Green façade: $$h_{Hw} = \acute{a} + \acute{b}\, V_{air} + \acute{c}\, {V_{air}}^2, \qquad \textit{Equation 22}$$

Living wall: $$g_{c_{sub}} = a + b\, V_{air_C}, \qquad \textit{Equation 23}$$

$$g_{v_{sub}} = c_0 + c_1\, (\omega_g/\omega_g^{sat})^{c_2}, \qquad \textit{Equation 24}$$

where,

| | |
|---|---|
| $V_{air_C}$ | Air velocity within canopy = $V_{air_{Cz}} \cdot \exp[-\ddot{a}(1 - 0.05/z)]$ [m·s-1], where, $V_{air_{Cz}} = V_{air}\left[ln(z_{veg} - d_0/z_m)/\left(ln\left(z_{Vair,h} - d_0/z_m\right) - \psi_m\right)\right]$, $\ddot{a} = \sqrt{0.28 \cdot LAI\, z_{veg}\, d_0}$; |
| a \| b | Coefficients, $a \approx 0.004 \cdot \hat{\rho}$ \| $b \approx 0.012 \cdot \hat{\rho}$ [mol·m-2·s-1]; |
| $c_0$ \| $c_1$ \| $c_2$ | Coefficients, based on reference experimental data: 0.0 \| 34.5 \| -3.3 [371]; |
| $\omega_g/\omega_g^{sat}$ | Saturation ratio of substrate; |
| $h_{Hw}$ | Coefficient, of convective surface heat transfer [W·m2·K-1]; and |
| $\acute{a}$ \| $\acute{b}$ \| $\grave{c}$ | Coefficients, of material roughness, for medium-rough surface: 10.79 \| 4.192 \| 0.0. |

The $\Delta T_{HW}$ | $\Delta T_{sub}$ initial value problem of the ordinary differential Equation 21 is numerically solved using the MATLAB *ode45* solver[IX], which is commonly used in general scientific computation and recommended by MATLAB documentation as the first solver to attempt [372]. The output $T_{Hw}$ | $T_{sub}$ solution from the solver is then used to calculate sensible and latent flux from the substrate layer of a living wall, or just the sensible flux for a green façade host-wall (Equation 25 to Equation 27, [53]). The joint flux from this host-wall and vertical greening vegetation represents the surface convective flux for the installation (Equation 28 and Equation 29). This is then combined with the modified net radiation load (i.e., modified $Q_{R_{lw}}$ flux) to present the revised surface gain ($Q_{VG_{gain}}$), which can then be introduced to the host-wall's energy balance (Equation 30).

---

[VIII] The $h_{Hw}$ material roughness coefficients applied here are based on standard wind-height $V_{air}$ measurements and not immediately in front/above the vertical greening canopy (i.e., not $V_{air_{Cz}}$). At present, coefficients based on the latter are unavailable.

[IX] Solver code based on explicit Runge-Kutta formulas appropriate for non-stiff differential equations.

Green façade: $$Q_{H_{Hw}} = h_{Hw}\,(T_{Hw} - T_{air}),$$ *Equation 25*

Living wall: $$Q_{H_{sub}} = c_{p_{air}}\, g_c\,(T_{sub} - T_{air}),$$ *Equation 26*

$$Q_{E_{sub}} = \lambda\, g_v \left(\frac{(e_s(T_{sub}) - e_a)}{P_{air}}\right).$$ *Equation 27*

Façade convective surface flux:

Green façade: $$Q_{GF} = \overbrace{Q_{H_{veg}} + Q_{H_{Hw}}}^{Q_{H_{GF}}} + Q_{E_{veg}}\,,$$ *Equation 28*

Living wall: $$Q_{LW} = \overbrace{Q_{H_{veg}} + Q_{H_{sub}}}^{Q_{H_{LW}}} + \overbrace{Q_{E_{veg}} + Q_{E_{sub}}}^{Q_{E_{LW}}}\,,$$ *Equation 29*

VG surface gain: $$Q_{VG_{gain}} = \overbrace{Q_{R_{sw}} + Q_{R_{lw}}}^{modified\ net\ radiative\ gains} + \overbrace{(Q_{GF}\mid Q_{LW})}^{surface\ convective\ flux}.$$ *Equation 30*

In summary, the algorithm of the VGM is represented in Fig. 67:

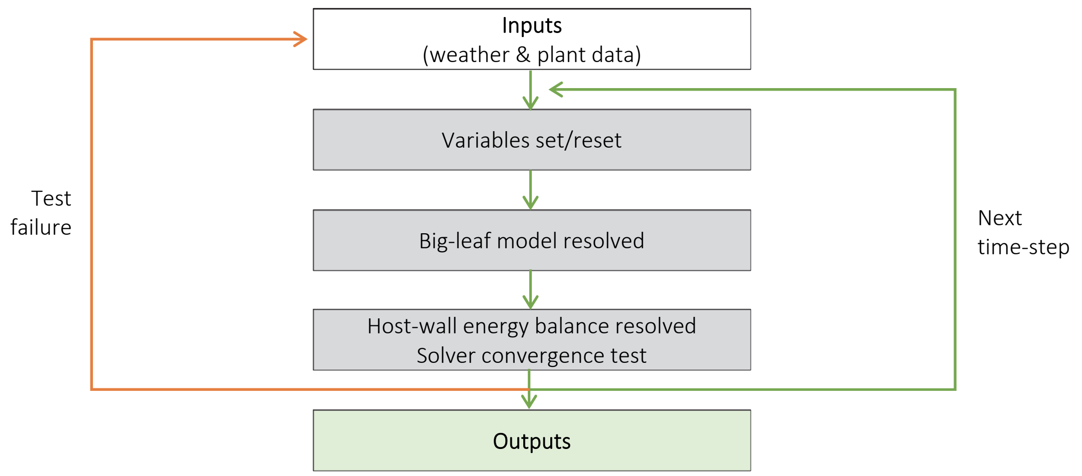


*Fig. 67. VGM algorithm.*

## Key assumptions and limitations

In addition to the assumptions mentioned earlier, the VGM also makes several more to reduce user-specified input burden and maintain computational efficiency.

- The dimensional limitation restricts consideration to one-dimensional horizontal heat flux through the vegetated façade. This means that best approximations are for a limited vertical span, where elevational height dependent parameters such as windspeed can be assumed as constant (typically assumed to be a building storey-height - relevant most for outdoor environment applications).

- To reduce user specified input burden, the model assumes several plant and substrate-related parameter simplifications. These include:
  - Plant thermal resistance, $W_{leaf}$, $LAI$, $\alpha_{leaf}$, $k$, and $g_s$ are constant for the active season defined, while $\theta_{leaf}$, canopy distribution, and orientation are static.
  - Air proximate to stomatal pores is unsaturated, and substrate moisture at roots is a defined constant (i.e., no water stress and constant water use rate), while diffusion variance and precipitation contribution is also not included.

## 6.2 Methodology

The above developed VGM was first implemented in isolation in MATLAB for a hypothetical configuration to ascertain parameter sensitivity to the principal final outputs of $T_{leaf}$ and the vegetated façade's revised surface gain ($Q_{VG_{gain}}$). The one-at-a-time (OAT) parametric approach was used with the effect of a single parameter considered against the output at a time, while keeping the other parameters constant. With the results, higher correlation coefficients indicated greater influence on final output, and thus demonstrated the necessity to input appropriate data to ensure reasonable approximations.

The second implementation considered validation exercises for the indoor and semi-outdoor background environments, where the VGM is proposed for application. In both instances the VGM was coupled with Type 56 TRNSYS Multi-Zone Building models of the defined case study configurations, including appropriate building construction information, thermal properties, and boundary conditions. The MATLAB VGM was directly coupled for these studies using TRNSYS Type 155. This coupling presents the application limitations of requiring a compatible MATLAB engine to be preinstalled[X], as well as the iterative calls to MATLAB at each timestep presenting an increased simulation clock-time. Both these shortcomings were deemed acceptable given the development phase of the model.

The input ⇌ output connections for the coupling of the two application configurations are described in Fig. 68 and Table 25, p. 158. Given that the coupling method involves disconnecting TRNSYS Type 56 $Q_{R_{sw}}$ and $Q_{R_{lw}}$ gains for the target host surface and then replacing them following their modification by the VGM, some base values must either be calculated or generated from a priming simulation and then input to the VGM (see Table 25).

[X] In this study, TRNSYS V17.02 used required MATLAB 2014a engine to be preinstalled.

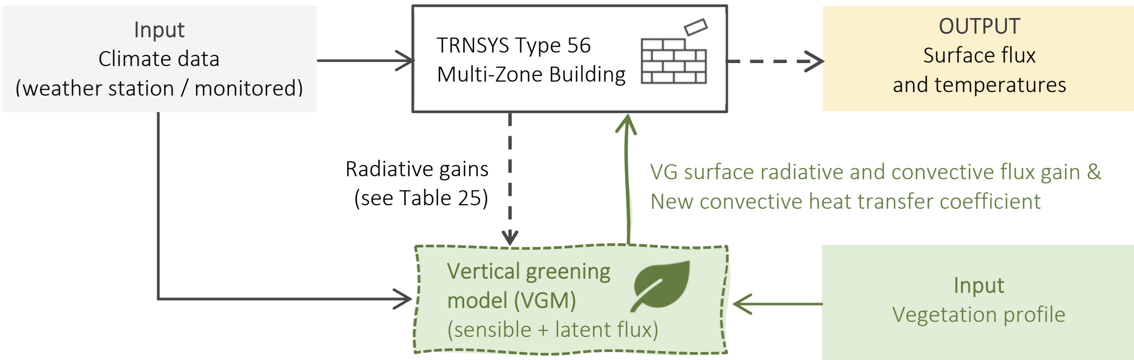


*Fig. 68. TRNSYS-based input and output diagram.*

Table 25. Radiative gains input to VGM.

| **Context** | **Indoor application** | **Semi-outdoor \| outdoor application** |
|---|---|---|
| Standalone (e.g., wall) | N/A | $Q_{R_{sw}}$ incidence (direct and diffused) input directly from weather file or Type 56.<br>$Q_{R_{lw_{Gr}}}$, $Q_{R_{lw_{Sky}}}$ and $Q_{R_{lw_{CS}}}$ calculated by VGM. |
| In context (e.g., building) | $Q_{R_{sw}}$ after shading and transmission is input from priming simulation output[XI].<br>$Q_{R_{lw_{CS}}}$ is input from priming simulation output[XII].<br>Other radiative gains and radiant heating gains (if present), must be added together using a TRNSYS calculator Type and input as a single value. | $Q_{R_{sw}}$ incidence (direct and diffused) after shading is input from Type 56.<br>$Q_{R_{lw_{Gr}}}$, $Q_{R_{lw_{Sky}}}$ and $Q_{R_{lw_{CS}}}$ calculated by VGM. |

To validate the accuracy of VGM simulations when applied for green façade configurations, the simulation results of the defined case study configuration was compared against those from a previously validated model for the same configuration (given the lack of representative green façade monitoring data from this defined study). The previously validated model used here was the Grabowiecki *et al.* [368] Vertical Foliage Component (VFC) discussed earlier, which is also designed to be coupled within a TRNSYS environment as a component Type. The workings of this model are based on an adaptation of the validated model by Susorova *et al.* [163], and as a compiled Type (black-box) only presents defined outputs. It must be noted that the green façade validation exercise is most appropriate for the semi-

[XI] There is no specific output 'NTYPE' for incident $Q_{R_{sw}}$ after shading and penetration in TRNSYS V17.02. This must be derived from absorbed $Q_{R_{sw}}$ from the indoor study's priming simulation output.

[XII] Type 56 calculates this using the host wall's ST (i.e., not VG ST). Given that the indoor study included four scenarios, $Q_{R_{lw}}$ from surrounding indoor walls was derived from the corresponding priming simulations.

outdoor configuration, as the VFC has thus far been validated only for outdoor environment simulations. The case study configuration most relevant for this VGM validation was therefore the SET case study in London; simulated assuming a full-coverage (i.e., 100% of the 15.2 m$^2$ area) of *H. helix* (common ivy) on the west-facing wall of the rear garden court (see Study 1 for details of this case study).

To validate the accuracy of VGM simulations when applied for living wall configurations, simulated temperatures of the defined case study configurations were compared against living wall monitoring data gathered from the corresponding study. Both indoor and semi-outdoor sheltered environments were considered, and relate to the respective configurations of the DAB atrium (northwest-facing wall) in Cambridge, and the SET court (west-facing wall) in London (see Study 1 for case study context).

The DAB study monitoring data was gathered in parallel to the exercises detailed in Study 1, between December 2018 and September 2019. The selected 28.4 m$^2$ midlevel section (L02[XIII]) of the northwest-facing living wall included seven species in total. Local monitoring however was carried out where the most accessible species with substantial coverage, *Phyllitis / Asplenium scolopendrium* ('Hart's tongue' fern) was planted (given the accessibility limitation resulting from the presence of the atrium void). The surface temperature probe (Fig. 69a, p. 160), was mounted on the underside of a sheltered leaf (as the support crate system did not present a dry mountable surface). The monitored temperature data is therefore considered analogous to the leaf temperature ($T_{leaf}$) of simulations.

The SET study monitoring data was gathered in parallel to the exercises detailed in Study 1, between July and December 2019. Although the 15.2 m$^2$ west-facing living wall[XIV] of the study included twelve species in total, local monitoring for validation was carried out where the dominant species *Pachysandra terminalis* was planted (~20% of coverage). The ST probe (Fig. 69b), was mounted on the outer face of the felt-pocket system, well-shielded from direct solar exposure by the plant canopy. The monitored temperature data is therefore considered analogous to the substrate surface temperature ($T_{sub}$) of simulations.

---

[XIII] Level 01 and 03 were excluded for validation monitoring as the former presented intermittent airflow contamination risk from the ground floor entrance doors, and the latter owing to the disproportionate and higher radiation loading received from the atrium skylight.

[XIV] The west-facing wall was selected for validation monitoring as it was mostly sheltered from direct solar radiation incidence (mostly receives evening sun).

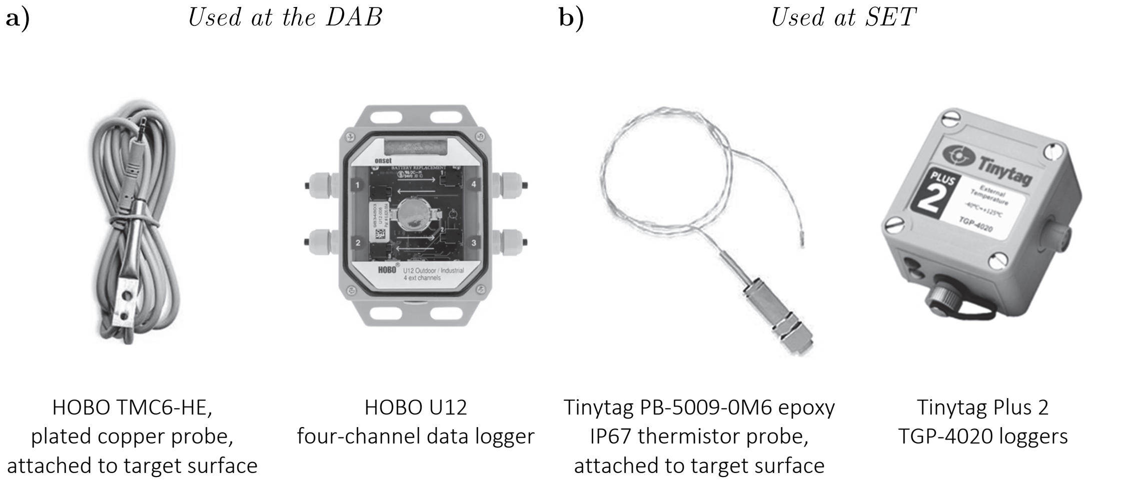


*Fig. 69. Apparatus used for monitoring surface temperatures.*

The validation results were assessed for agreement principally using correlation analysis[XV], with correlation coefficients of determination ($r^2$) nearer to one suggesting good agreement between results. As a secondary measure, Euclidean '*norm*' (normalised relative distance between two vectors; Equation 31) and 'inner product' or '*cosine*' (angular difference between the resultant vectors; Equation 32) analysis was used to evaluate the similarity of magnitude and shape between resultant curves. For good agreement, the *norm* value should be closer to zero and *cosine* value should be closer to one [373].

$$\text{Norm} = \frac{\sqrt{\sum_{i=1}^{n_{tot}} (M_i - S_i)^2}}{\sqrt{\sum_{i=1}^{n_{tot}} (M_i)^2}}, \qquad \textit{Equation 31}$$

$$\text{Cosine} = \frac{\sum_{i=2}^{n_{tot}} (M_i - M_{i-sm})\,(S_i - S_{i-sm})/sm^2(t_i - t_{i-1})}{\sqrt{\sum_{i=2}^{n_{tot}} (M_i - M_{i-sm})^2/sm^2(t_i - t_{i-1}) \quad \sum_{i=1}^{n_{tot}} (S_i - S_{i-sm})^2/sm^2(t_i - t_{i-1})}}, \qquad \textit{Equation 32}$$

where,

| | |
|---|---|
| $M_i$ | Measured $(t_i, M_i)$; |
| $S_i$ | Simulated $(t_i, S_i)$; |
| $sm$ | Datapoints used to smoothen curve; |
| $n_{tot}$ | Total datapoints; and |
| $t_i$ | Time intervals $t_i$, $i = 1, \ldots, n_{tot}$. |

[XV] For large correlation analysis datasets (N >300), normality was determined with reference to skewness and kurtosis thresholds [318], with failures assessed with nonparametric tests.

The third implementation of the model was carried out to assess and quantify the application impact of vertical greening interventions on the case study configurations. Impact was quantified as vertical greening surface flux modifications at the SET semi-outdoor study, while space-conditioning energy consumption impact was also included for the DAB indoor study. With both studies, configurations were simulated in TRNSYS with and without vertical greening interventions applied, as described in Table 26.

Table 26. Simulated case study scenarios.

| **Scenario** | | **Status** | **Conditioning** | |
|---|---|---|---|---|
| **DAB indoor study** | | | *Atrium* | *Adjoining room*† |
| *Bw-Nv* | Bare wall in atrium | Hypothetical | *Nv* | Heating only |
| *Bw-AC* | | Hypothetical | *AC* | Heating + cooling/air-conditioned (AC) |
| *GF-VGM-Nv* | Green façade* | Hypothetical | *Nv* | Heating only |
| *GF-VGM-AC* | | Hypothetical | *AC* | Heating + cooling |
| *LW-VGM-Nv* | Living wall | Existing | *Nv* | Heating only |
| *LW-VGM-AC* | | Hypothetical | *AC* | Heating + cooling |
| **SET semi-outdoor study** | | | *Court* | |
| *Bw-Nv* | Bare walls in court | Hypothetical | *Nv* | |
| *GF-VGM-Nv* | Green façade* | Hypothetical | *Nv* | |
| *LW-VGM-Nv* | Living wall | Existing | *Nv* | |

Notes: * Contribution from substrate containers at the base not included. † Room directly behind vertical greening installation. Abbreviations and suffixes '*Nv*' = natural ventilation; and '*AC*' = cooling added/air-conditioned.

For both studies, default building construction and services inputs were informed by site inspection observations (see Table 27, p. 162)[XVI]. The plant parameters of *A. scolopendrium*[XVII] were assumed for 100% of wall-coverage in simulations for the DAB study, while *P. terminalis* parameters were assumed for the SET study (Table 28, p. 163). The DAB atrium volume was modelled in TRNSYS (TRNBuild) as five vertically coupled zones (×5 airnodes), of which four were connected to occupied building storeys, while the SET court was modelled by adding bounding geometry with relevant boundary wall exteriors. As highlighted in Study 1 (and later in Study 5), atrium heating at the DAB was ceased after a year or so of operation owing to identified localised plant heat stress. Atrium heating was therefore not considered for any of the scenarios (i.e., naturally ventilated volume), while the adjoining room behind the installation was heated for all (existing state).

[XVI] DAB building information was provided by the Cambridge Conservation Initiative, Campus Facilities Manager: B. Walbanke-Taylor (2018-19) and extracted from information authored by the retrofit architect for the DAB refurbishment project (2013-15).

[XVII] 'Middle' habitat data ($T_{air}$: 21.3, ±0.4°C, and $RH$: 71, ±4%), [427].

Table 27. Case study building parameters used for simulations.

| | Parameter | DAB | SET |
|---|---|---|---|
| **Model** | Geometric arrangement | Atrium has ×5 stacked coupled zones, of which ×4 are on occupied floor levels | Bounding geometry for the ×3 garden walls of the court, and ×3 building room zones bounding the 4th, on two levels |
| **Simplified base constructions** | **Building exterior façade**<br>Wall material and thickness: | Type: fairfaced concrete<br>Concrete \| metal studs & mineral wool \| plasterboard<br><br>Thickness: 0.20 \| 0.25 \| 0.02 m<br>U-value: 0.185 $W \cdot m^{-2} \cdot K^{-1}$<br>Albedo, $\rho_{surf}$: 0.50<br>Emissivity, $\varepsilon_{surf}$: 0.90 | Type: Portland limestone<br>Portland cladding \| cavity \| insulation \| concrete \| metal stud & plasterboard<br><br>Thickness: 0.075 \| 0.05 \| 0.1 \| 0.15 \| 0.03 m<br>U-value: 0.365 $W \cdot m^{-2} \cdot K^{-1}$<br>Albedo, $\rho_{surf}$: 0.60<br>Emissivity, $\varepsilon_{surf}$: 0.90 |
| | Glazing | Ratio (GR): 0.4 (40%)<br>Unite U-value: 1.06 $W \cdot m^{-2} \cdot K^{-1}$ | Ratio (GR): 0.5 (50%)<br>U-value: 1.06 $W \cdot m^{-2} \cdot K^{-1}$ |
| | **Installation host-wall**<br>Material and thickness (excluding vertical greening): | Type: atrium partywall<br>Plasterboard \| cavity \| concrete \| plasterboard<br><br>Thickness: 0.02 \| 0.01 \| 0.15 \| 0.02 m | Type: garden wall<br>Concrete<br><br>Thickness: 0.15 m |
| | Wall vegetation coverage ratio: | 1.0 of target wall | 1.0 of target wall |
| | **Building floor slab**<br>Material and thickness: | Type: atrium circulation<br>Carpet & underlay \| metal pads \| concrete slab \| metal hangers & ceiling tiles<br><br>Thickness: 0.02 \| 0.15 \| 0.30 \| 0.01 \| 0.10 m<br>U-value: 0.63 $W \cdot m^{-2} \cdot K^{-1}$ | Type: flat floor<br>Timber \| concrete \| metal studs \| plasterboard<br>Thickness: 0.025 \| 0.15 \| 0.10 \| 0.02 m<br>U-value: 0.62 $W \cdot m^{-2} \cdot K^{-1}$<br><br>Type: terrace floor<br>Timber deck \| waterproofing membrane \| concrete \| metal studs \| plasterboard<br><br>Thickness: 0.025 \| 0.01 \| 0.15 \| 0.10 \| 0.02 m<br>U-value: 0.60 $W \cdot m^{-2} \cdot K^{-1}$ |
| | **Building roof**<br>Material and thickness: | Type: flat green roof<br>Sedum plants \| saturated soil \| insulation \| waterproof membrane \| concrete slab \| metal stud & plasterboard<br><br>Thickness: 0.06 \| 0.10 \| 0.01 \| 0.01 \| 0.30 \| 0.05 m<br>U-value: 0.34 $W \cdot m^{-2} \cdot K^{-1}$ (excluding plant matter) | Type: flat roof<br>Gravel \| insulation \| concrete \| metal stud & plasterboard<br><br>Thickness: 0.07 \| 0.1 \| 0.3 \| 0.05 m<br>U-value: 0.24 $W \cdot m^{-2} \cdot K^{-1}$ |
| **Gains** | Lighting and equipment: | Per level, 5 $W \cdot m^{-2}$ & 100 W | Per room, 5 $W \cdot m^{-2}$ & 50 W |
| | Occupancy: | Per lobby level, 4 persons | Per room, 2 persons |
| | Gains profile used: | Weekdays: 00:00-08:00 @0.2 load \| 08:00-18:00 @1.0 \| 18:00-20:00 @0.5 \| and 18:00-20:00 @0.2. | Weekdays: 00:00-06:00 @0.1 load \| 06:00-18:00 @0.6 \| and 18:00-24:00 @1.0. |

| | Parameter | DAB | SET |
|---|---|---|---|
| | | Weekend: 00:00-09:00 @0.2 \| 09:00-18:00 @0.5 \| and 18:00-24:00 @0.2. | Weekend: 00:00-09:00 @0.1 \| 09:00-18:00 @0.4 \| 18:00-22:00 @0.8 \| and 22:00-24:00 @0.2. |
| **Space-conditioning** | Infiltration: | 1.00 ach | 0.25 ach |
| | Ventilation: | 0.70 ach | |
| | Heating & cooling system power: | Unlimited | |
| | Heating efficiency: | 0.80 | |
| | Heating setpoint: | 19°C | |
| | Cooling setpoint (if applicable): | 24°C | |
| **Priming** | Initial $T_{air}$ and $RH$ of zones: | 20°C and 50% | |
| **Reference weather files** | File location | CU Computer Laboratory, Cambridge | Hampstead Heath, London NW3 |
| | File source | [319] | [316] |
| | Latitude, longitude, & elevation | 52.211, 0.092, +28 m (ASL) | 51.556, -0.155, +57 m (ASL) |
| | Distance to study site | ~2.11 km due northwest | ~2.12 km due northeast |

Table 28. Construction parameters of vertical greening additions.

| | Parameter | Green façade (GF) | Living wall (LW) |
|---|---|---|---|
| **Vertical greening construction** (hypothetical) | Material and thickness: | Evergreen climbing plants \| host-wall | Herbaceous evergreens \| saturated soil (substrate) \| host-wall |
| | | Thickness: | Thickness: |
| | @SET: | $z_{veg}$: 0.2 m \| Table 27 | $z_{veg}$: 0.25 \| 0.1 m \| Table 27 |
| | @DAB: | $z_{veg}$: 0.2 m \| Table 27 | $z_{veg}$: 0.40 \| 0.1 m \| Table 27 |
| | U-value[XVIII] (excluding host-wall): | 1.49 W·m$^{-2}$·K$^{-1}$ | 0.46 W·m$^{-2}$·K$^{-1}$ |
| **Vegetation** | Plant species @SET: | *H. helix* | *P. terminalis* |
| | @DAB: | *H. helix* | *A. scolopendrium* |
| | $LAI$ | 1.5 | 2.0 |
| | Leaf-width ($W_{leaf}$) @SET: | 0.075 m | 0.050 m |
| | @DAB: | 0.075 m | 0.065 m |
| | Stomatal conductance ($g_s$)[XIX] @SET: | 0.30 mol·m$^{-2}$·s$^{-1}$ | 0.20 mol·m$^{-2}$·s$^{-1}$ |
| | @DAB: | 0.30 mol·m$^{-2}$·s$^{-1}$ | 0.15 mol·m$^{-2}$·s$^{-1}$ |
| | Closed $g_s$ | 0.01 mol·m$^{-2}$·s$^{-1}$ | 0.01 mol·m$^{-2}$·s$^{-1}$ |
| | Stomatal arrangement: | Hypostomatous | Amphistomatous (assumed) |
| | Canopy absorptivity ($\alpha_{veg}$) | $(1-\rho_{leaf}-\tau_{veg})$ | |
| | Canopy albedo ($\rho_{veg}$): | 0.20 | |
| | Canopy emissivity ($\varepsilon_{veg}$): | 0.95 | |
| | Leaf-angle ($\theta_{leaf}$): | 45° (assumed) | |
| | Radiation attenuation coefficient ($k$): | 0.5 (assumed) | |
| **Substrate** (LW only) | Density ($\dot{\rho}_{sub}$): | N/A | 1,230 kg·m$^{-3}$ |
| | Specific heat capacity ($c_{p_{sub}}$): | N/A | 1,140 J·kg$^{-1}$·K$^{-1}$ |
| | Volumetric heat capacity: | N/A | 2,310,000 J·m$^{-3}$·K$^{-1}$ |
| | Albedo ($\rho_{sub}$): | N/A | 0.4 |
| | Emissivity ($\varepsilon_{sub}$): | N/A | 0.9 |
| | Soil moisture, permanent wilting threshold ($\eta_{wilt}$): | N/A | 0.39 (for peaty soil) |
| | Soil moisture, root zone mini. ($\eta_{root}$): | N/A | 0.70 (assumed [163]) |

[XVIII] Mean thermal resistance of plant matter ~0.5 K·m$^{2}$·W$^{-1}$ used for calculation [428].

[XIX] Typical mean values for most species is ~0.3 when stomata are open, and ~0.01 mol·m$^{-2}$·s$^{-1}$ when closed [53].

## 6.3 Findings

### 6.3.1 Parameter sensitivity

Parameter sensitivity results from 2,087 green façade simulations demonstrated that surface flux gain ($Q_{VG_{gain}}$) variance was directly dependent on the variance of climate parameters $T_{air}$, $rH$, and $Q_{R_{sw}}$ (Fig. 70a). Notably, $rH$ presented negative influence (i.e., $rH \uparrow \Rightarrow Q_{VG_{gain}} \downarrow$), while $P_{air}$ had negative influence only in outdoor background environments. Both $V_{air}$ and $P_{air}$ had relatively lower influence overall. The highest $V_{air}$ dependence on $Q_{VG_{gain}}$ for example was with the semi-outdoor environment ($r^2$ = 59%), and the relative lowest was with the outdoor environment (31%); while its dependence on $T_{leaf}$ followed a similar trend only with negative values. These green façade climate parameter sensitivity trends were broadly similar for living wall simulations (Fig. 71a, p. 165), save for $V_{air}$ dependence on $Q_{VG_{gain}}$ being marginally lower.

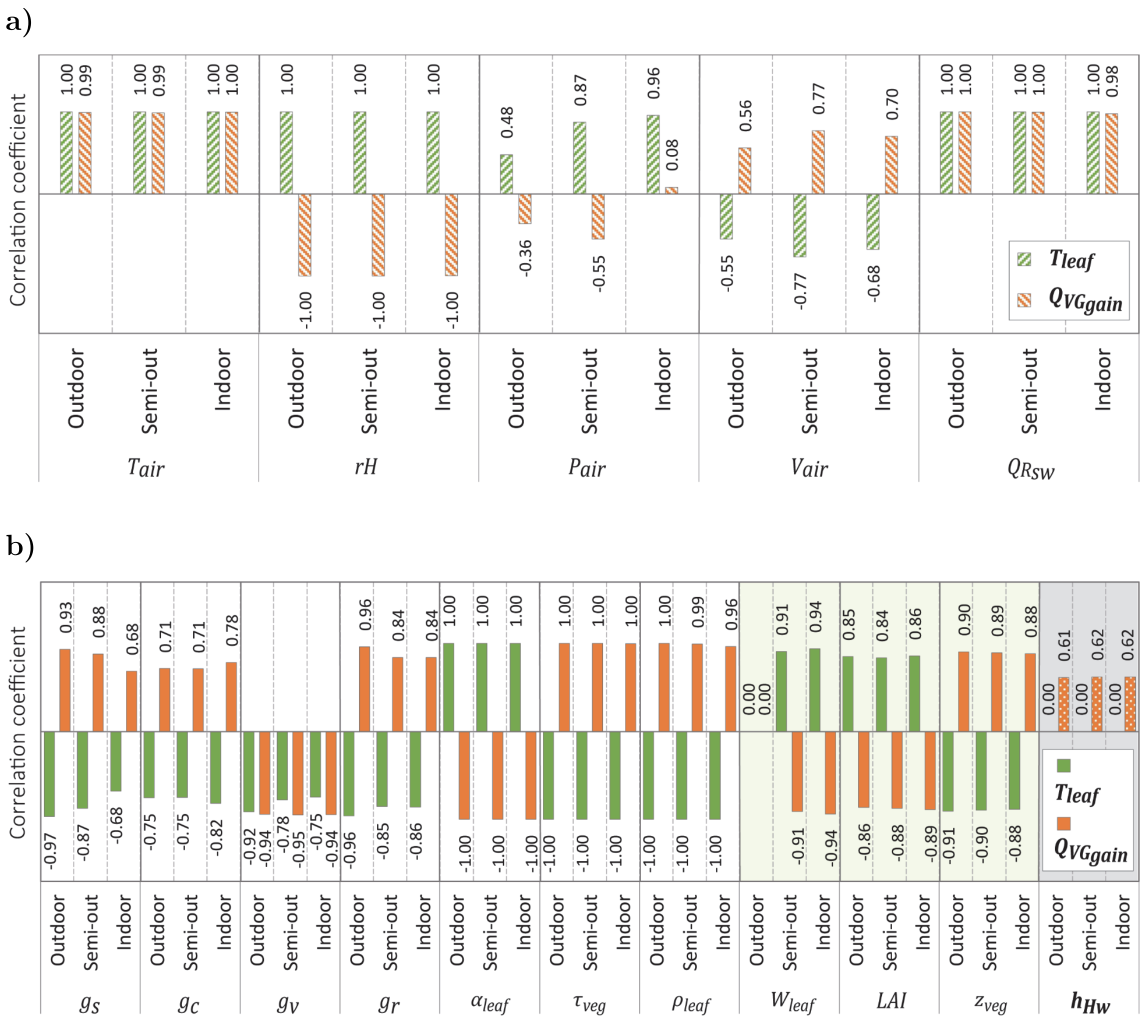


*Fig. 70. Green façade sensitivity correlations for climate (a) and installation (b) parameters.*

With green façade simulations, the host-wall sensible convective flux was calculated using a defined convective heat transfer coefficient ($h_{Hw}$). The variation of this coefficient had only a moderate influence on $Q_{VG_{gain}}$ ($r^2$ = 37-39%). This influence however still highlights the significance of applying better estimates of material roughness coefficients in its determining. The utilised $h_{Hw}$ material roughness coefficients in this study (based on standard wind-height $V_{air}$ measurement as opposed to $V_{air_{Cz}}$ immediately above/front of the canopy), will therefore require revisiting in subsequent revisions to the VGM.


*Fig. 71. Living wall sensitivity correlations for climate (a) and installation (b) parameters.*

Green façade simulation plant parameters $\alpha_{leaf}$, $\tau_{veg}$, and $\rho_{leaf}$ had direct influence on $T_{leaf}$ and $Q_{VG_{gain}}$ variance. All conductances ($g_s$, $g_c$, $g_v$, and $g_r$), as well as $\tau_{veg}$, $\rho_{leaf}$, and $z_{veg}$ parameters had negative influence on $T_{leaf}$ (to contradict the $z_{veg}$ relationship observed in Study 2), while $g_v$, $\alpha_{leaf}$, $W_{leaf}$ and $LAI$ were the only to have negative influence on $Q_{VG_{gain}}$ variance. From the canopy morphological parameters, $W_{leaf}$ presented the strongest influence on $T_{leaf}$ and $Q_{VG_{gain}}$, closely followed by $z_{veg}$, and $LAI$. Given their higher influence (refer to Study 2), applying accurate values for these parameters is of significance. The advantage with $W_{leaf}$ and $z_{veg}$ is that they can be non-destructively measured with relative ease, while the $LAI$ could either be estimated or referenced from literature. With living wall simulations (3,037 in total), the plant parameters $\alpha_{leaf}$, $\tau_{veg}$, and $\rho_{leaf}$ again had direct influence on $T_{leaf}$ and $Q_{VG_{gain}}$ variance, while all conductances (except for $g_s$ negative influence on $Q_{VG_{gain}}$), $\tau_{veg}$, and $\rho_{leaf}$, as well as the morphological parameters $LAI$, $W_{leaf}$, and $z_{veg}$, mostly reflected green façade simulations (Fig. 71b, p. 165). Notably, the living wall substrate conductance parameters to heat ($g_{c_{Sub}}$) and vapour ($g_{v_{Sub}}$) had low significance to $Q_{VG_{gain}}$ variance in all environments ($r^2$ <19%).

### 6.3.2 VGM validation exercises

#### Green façade configuration

Although the VFC has not been validated yet for indoor environments, green façade simulation results of the DAB indoor configuration when compared against VFC simulation results for the same presented good agreement; detailed in Table 29. Notably when the summer period was isolated, agreement was marginally weaker than with annual datasets.

Table 29. Model agreement correlation coefficients, and *norm*, and *cosine* values for the DAB, Cambridge indoor green façade, L02 simulations.

| **DAB** | **Annual data** | | | | **Summer data** | | | |
|---|---|---|---|---|---|---|---|---|
| **STs** | *r** | $r^2$ | *Norm* | *Cosine* | *r** | $r^2$ | *Norm* | *Cosine* |
| $T_{surf_1}$ all-day | 0.99 | 98% | 0.06 | 0.83 | 0.98 | 96% | 0.04 | 0.75 |
| Daytime | 0.99 | 98% | 0.06 | 0.89 | 0.97 | 94% | 0.05 | 0.84 |
| Night-time | 0.99 | 98% | 0.06 | 0.98 | 0.99 | 98% | 0.03 | 0.98 |
| $T_{Hw}$ all-day | 0.99 | 98% | 0.02 | 0.94 | 0.99 | 98% | 0.02 | 0.94 |
| Daytime | 0.99 | 98% | 0.02 | 0.93 | 0.99 | 98% | 0.03 | 0.93 |
| Night-time | 0.99 | 98% | 0.02 | 0.95 | 0.99 | 98% | 0.02 | 0.99 |
| $T_{leaf}$ all-day | 0.99 | 98% | 0.06 | 0.89 | 0.96 | 92% | 0.03 | 0.89 |
| Daytime | 0.99 | 98% | 0.04 | 0.91 | 0.96 | 92% | 0.03 | 0.89 |
| Night-time | 0.99 | 98% | 0.07 | 0.93 | 0.98 | 96% | 0.04 | 0.96 |

Notes: Day and night-time hours correspond to daylight durations for each day in Cambridge. * All *p*-values <0.01.

The green façade simulation results of the SET semi-outdoor configuration in comparison to its VFC simulation results presented the agreement outcomes detailed in Table 30, p. 167. The correlation coefficients calculated for all datasets were >0.99 ($r^2$ >98%) to demonstrate strong agreement between the simulation results. Furthermore, when Euclidean *norm* and *cosine* values were considered, the former values were nearer to zero, while the latter were nearer to one to also indicate good agreement between the two result curves.

Table 30. Model agreement correlation coefficients, *norm*, and *cosine* values for SET, London semi-outdoor green façade, west-facing wall simulations.

| **SET** | **Annual data** | | | | **Summer data** | | | |
|---|---|---|---|---|---|---|---|---|
| **STs** | *r** | $r^2$ | *Norm* | *Cosine* | *r** | $r^2$ | *Norm* | *Cosine* |
| $T_{surf_1}$ all-day | 0.99 | 98% | 0.010 | 0.995 | 0.99 | 98% | 0.009 | 0.994 |
| Daytime | 0.99 | 98% | 0.011 | 0.998 | 0.99 | 98% | 0.011 | 0.997 |
| Night-time | 0.99 | 98% | 0.006 | 0.999 | 0.99 | 98% | 0.005 | 0.999 |
| $T_{Hw}$ all-day | 0.99 | 98% | 0.003 | 0.999 | 0.99 | 98% | 0.003 | 0.999 |
| Daytime | 0.99 | 98% | 0.004 | 0.999 | 0.99 | 98% | 0.003 | 0.999 |
| Night-time | 0.99 | 98% | 0.003 | 0.999 | 0.99 | 98% | 0.002 | 0.999 |
| $T_{leaf}$ all-day | 0.99 | 98% | 0.027 | 0.983 | 0.99 | 98% | 0.023 | 0.983 |
| Daytime | 0.99 | 98% | 0.033 | 0.991 | 0.99 | 98% | 0.028 | 0.991 |
| Night-time | 0.99 | 98% | 0.010 | 0.999 | 0.99 | 98% | 0.006 | 0.999 |

Note: Day and night-time hours correspond to daylight durations for each day in London.

The comparison between agreement results of the two green façade application environments highlighted the indoor case study (i.e., the DAB) to offer marginally weaker agreement (summer period in particular) than the semi-outdoor study (i.e., SET).

### Living wall configurations

The living wall simulations of the indoor case study at the DAB, Cambridge when compared against the experimental data for the same configuration presented the agreement results detailed in Table 31, p. 168. The correlation coefficients ranged from weak-to-moderate, with the Euclidean *norm* and *cosine* values broadly reflecting this trend. This initial comparison however was based on simulation results that utilised TRNSYS simulated air-node $T_{air}$ and $RH$ input to the VGM. Given that the sensitivity study had stressed both these parameters to affect outcome accuracy, a separate simulation including the input of measured installation proximate $T_{air}$ and $RH$ was also carried out. The results of this presented much stronger correlations (>0.85, $r^2$ >72%), as well as *norm* and *cosine* agreement (Table 31). The common trend with both comparisons however was that the relative strongest agreement was observed for the winter than summer, and night than daytime.

The living wall simulations of the semi-outdoor case study at SET, London when compared against monitoring data for the same configuration presented the agreement results detailed in Table 32, p. 168. The monthly datasets from July-to-December presented correlation coefficients >0.87 ($r^2$ >76%) to demonstrate good agreement. The coefficients however were marginally lower for the daytime than night, while the best agreement was presented for the wintertime datasets from October-to-December.

Table 31. Model agreement correlation coefficients, *norm*, and *cosine* values for the DAB, Cambridge indoor living wall, L02 simulations.

| $T_{leaf}$ datasets | | Simulated $T_{air}$ and $RH$ input | | | | Measured $T_{air}$ and $RH$ input | | | |
|---|---|---|---|---|---|---|---|---|---|
| | | $r^*$ | $r^2$ | *Norm* | *Cosine* | $r^*$ | $r^2$ | *Norm* | *Cosine* |
| **All-day** | | | | | | | | | |
| Winter | December† | 0.53 | 28% | 0.41 | 0.62 | 0.99 | 98% | 0.14 | 0.75 |
| | January | 0.53 | 28% | 0.50 | 0.67 | 0.99 | 98% | 0.15 | 0.76 |
| | February | 0.43 | 18% | 0.51 | 0.72 | 0.97 | 94% | 0.16 | 0.78 |
| Summer | August | 0.38 | 14% | 0.08 | 0.50 | 0.93 | 86% | 0.11 | 0.80 |
| | September | 0.28 | 8% | 0.11 | 0.64 | 0.85 | 72% | 0.12 | 0.72 |
| **Daytime** | | | | | | | | | |
| Winter | December† | 0.49 | 24% | 0.44 | 0.78 | 0.99 | 98% | 0.13 | 0.92 |
| | January | 0.39 | 15% | 0.52 | 0.75 | 0.99 | 98% | 0.14 | 0.83 |
| | February | 0.30 | 9% | 0.52 | 0.78 | 0.97 | 94% | 0.15 | 0.86 |
| Summer | August | 0.35 | 12% | 0.08 | 0.65 | 0.94 | 88% | 0.10 | 0.90 |
| | September | 0.31 | 10% | 0.12 | 0.63 | 0.80 | 64% | 0.11 | 0.74 |
| **Night-time** | | | | | | | | | |
| Winter | December† | 0.57 | 32% | 0.40 | 0.74 | 0.99 | 98% | 0.14 | 0.94 |
| | January | 0.63 | 40% | 0.50 | 0.84 | 0.99 | 98% | 0.16 | 0.95 |
| | February | 0.50 | 25% | 0.49 | 0.87 | 0.98 | 96% | 0.16 | 0.91 |
| Summer | August | 0.28 | 8% | 0.08 | 0.69 | 0.94 | 88% | 0.13 | 0.96 |
| | September | 0.18 | 3% | 0.33 | 0.10 | 0.84 | 71% | 0.14 | 0.88 |

Note: † December of 2018, remaining months in 2019.

The comparison between agreement results of the two living wall application environments again highlighted the indoor case study (i.e., the DAB) to offer weaker agreement than the semi-outdoor study (i.e., SET). This disparity however was significantly pronounced than with the green façade configuration results considered earlier, while the indoor study required the input of installation proximate $T_{air}$ and $RH$ to present meaningful agreement.

Table 32. Model agreement correlation coefficients, *norm*, and *cosine* values for SET, London semi-outdoor living wall, west-facing simulations.

| Host-wall ST ($T_{sub}$) | | All-day | | | | Daytime | | | | Night-time | | | |
|---|---|---|---|---|---|---|---|---|---|---|---|---|---|
| | | $r^*$ | $r^2$ | *Norm* | *Cosine* | $r^*$ | $r^2$ | *Norm* | *Cosine* | $r^*$ | $r^2$ | *Norm* | *Cosine* |
| Summer | July | 0.87 | 76% | 0.15 | 0.79 | 0.87 | 76% | 0.15 | 0.86 | 0.86 | 74% | 0.15 | 0.80 |
| | August | 0.92 | 85% | 0.12 | 0.82 | 0.90 | 81% | 0.12 | 0.86 | 0.93 | 86% | 0.10 | 0.86 |
| | September | 0.88 | 77% | 0.13 | 0.72 | 0.83 | 69% | 0.13 | 0.83 | 0.93 | 86% | 0.11 | 0.94 |
| Winter | October | 0.96 | 92% | 0.07 | 0.77 | 0.93 | 86% | 0.08 | 0.87 | 0.99 | 98% | 0.05 | 0.97 |
| | November | 0.98 | 96% | 0.07 | 0.85 | 0.97 | 94% | 0.09 | 0.97 | 0.99 | 98% | 0.04 | 0.97 |
| | December | 0.98 | 96% | 0.11 | 0.77 | 0.97 | 94% | 0.11 | 0.93 | 0.99 | 98% | 0.11 | 0.93 |

### 6.3.3 Scenario simulations

#### DAB, Cambridge case study

The simulated microclimate modification and energy use results for the defined DAB vertical greening application scenarios (in Table 26, p. 161) are detailed below.

#### *Surface temperatures*

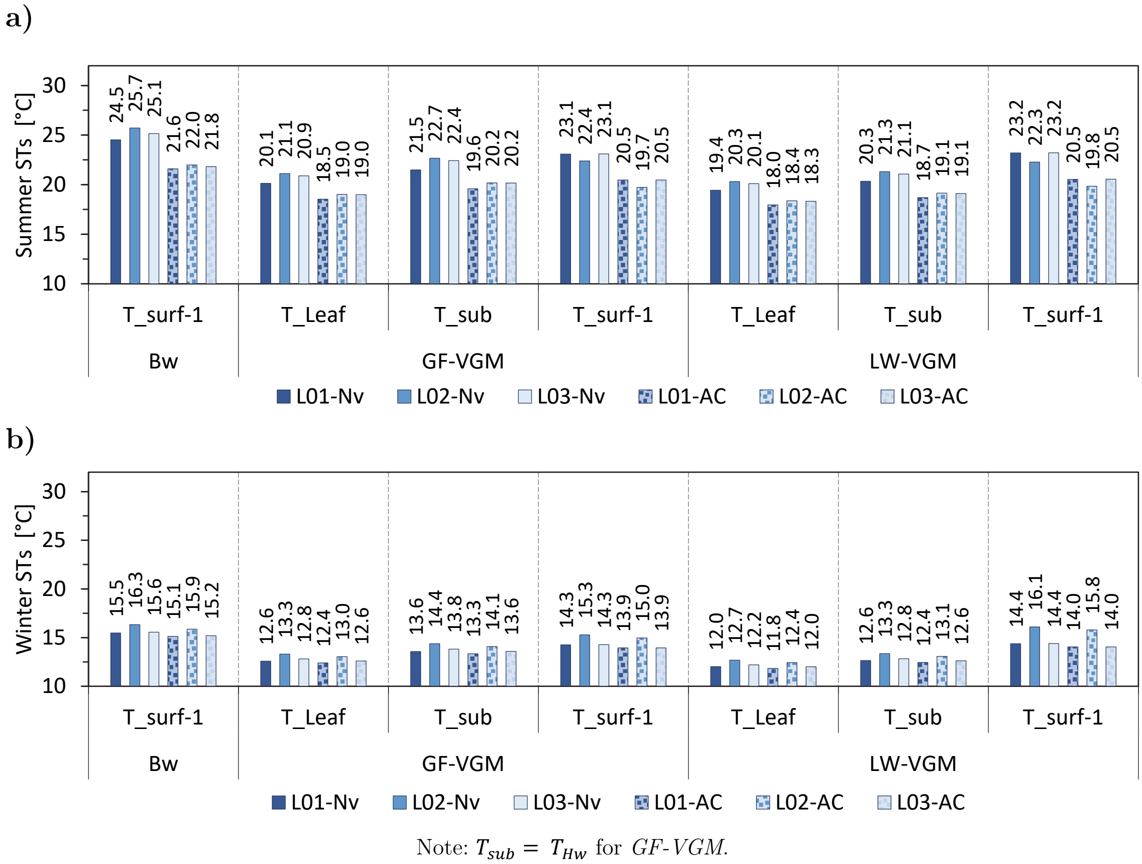


*Fig. 72. DAB, summer (a) and winter (b) mean surface temperatures for floor levels and scenarios.*

Surface temperature modifications were assessed with reference to mean $T_{leaf}$ and $T_{Hw} \mid T_{sub}$ (where simulated for vertical greening scenarios), and $T_{surf_1}$ that represented the TRNSYS output surface temperature for the host-wall surface facing the atrium volume (Fig. 72). As expected, the summertime data presented much warmer surface temperature means than winter for all levels and scenarios. The L02 midlevel wall section notably presented the warmest mean surface temperatures for the summer and winter *Nv* and *AC* datasets (save for summertime green façade and living wall application *Nv* and *AC* scenario $T_{surf_1}$ datasets). This suggested the significance of disproportionate internal gains, with relatively greater received by the midlevel from surrounding occupied building zones; the effect of which was pronounced for the heating period than in the summer.

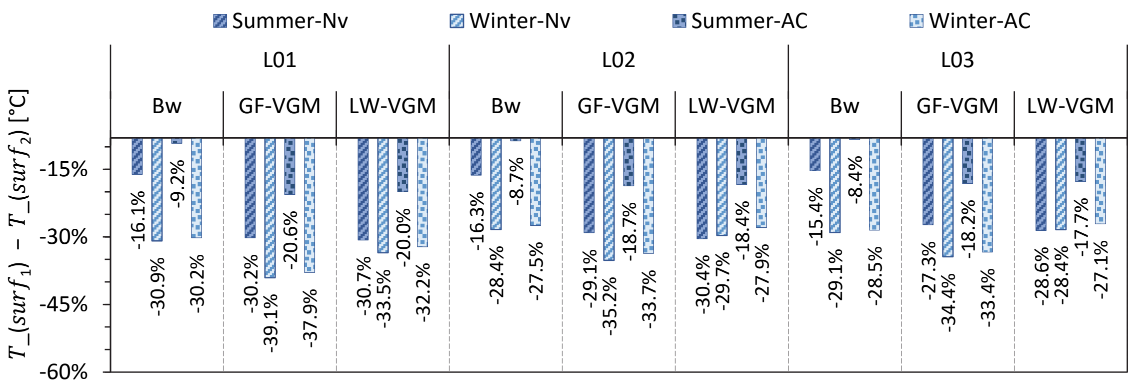


*Fig. 73. DAB, summer and winter mean $T_{surf_1} - T_{surf_2}$ difference for floor levels and scenarios.*

The surface temperature of the atrium wall hosting the installation (i.e., $T_{surf_1}$) was always cooler than the other side facing into the adjoining room (i.e., $T_{surf_2}$), for all floor levels and scenarios including the bare wall (*Bw*) scenarios (Fig. 73). This is expected given that the atrium has relatively lower internal gains than the surrounding occupied zones. The addition of installations substantially increased most differences relative to *Bw* simulations, with slightly greater $T_{surf_1} - T_{surf_2}$ differences presented with green façade than living wall application to suggest the moderating significance of the latter's substrate.

### *Surface flux*

The annual surface flux results showed that the mean net flux out of the walls (and into the atrium) had substantially decreased following vertical greening application, relative to the bare wall (*Bw*) simulation and under both space-conditioning scenarios (Fig. 74, p. 171). With green façade addition the net annual flux was in fact directed into the installation for day and night-time durations, while with living wall application this was valid for the daytime only. The inward flux was mostly affected by the summer mean flux, which was directed inwards for all vertical greening application scenarios. Winter mean flux in contrast was always in the outward direction for all scenarios.

The summer mean convective surface flux partitioning for the green façade scenarios (*Nv* and *AC*) highlighted the contribution made by the canopy latent flux ($Q_{E_{veg}}$) to range between the wall floor levels from 45.0-49.1% for the daytime when transpiration is active (i.e., $Q_{R_{sw}}$ >0), and 39.3-41.1% for the night-time when respiration is dominant (Fig. 75, p. 172 and Fig. 76, p. 173). In the wintertime, this partitioning representation reduced to 41.5-43.2% for the daytime given that solar penetration into the atrium was relatively lower, while at night-time increased to between 42.4-43.8% to suggest the contribution significance of internal gains stored in the building materials. With living wall scenarios (*Nv* and *AC*) the trend was similar, only with reduced partitioning percentage ranges given the added contribution from the substrate flux ($Q_{E_{sub}}$). The summertime $Q_{E_{veg}}$ representation range was therefore relatively lower and between 36.3-38.7% for the daytime and 32.1-33.1% for the night-time. In the winter, this representation reduced to 34.9-35.8% for the daytime and increased to 34.2-34.7% for the night-time. The mean $Q_{E_{sub}}$ flux representation also followed this trend and ranged between the wall floor levels from 14.0-14.8% for the summer daytime, which reduced to 13.5-14.5% for the winter, while during the night-time contributed between 12.4-12.9% for the summer, which increased to 13.1-14.1% in winter.

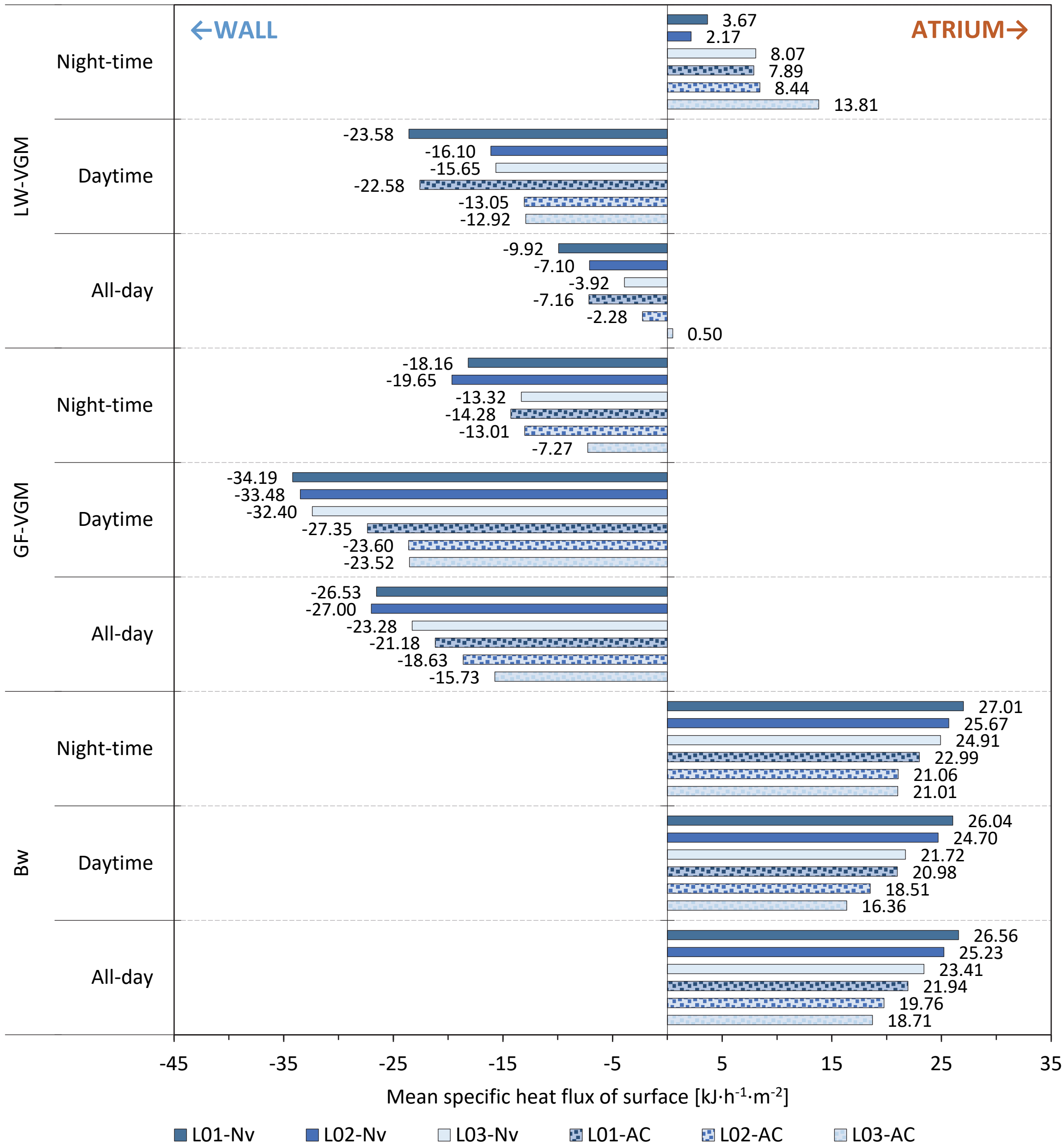


*Fig. 74. DAB atrium, annual mean specific surface flux for walls, by floor level and scenarios.*

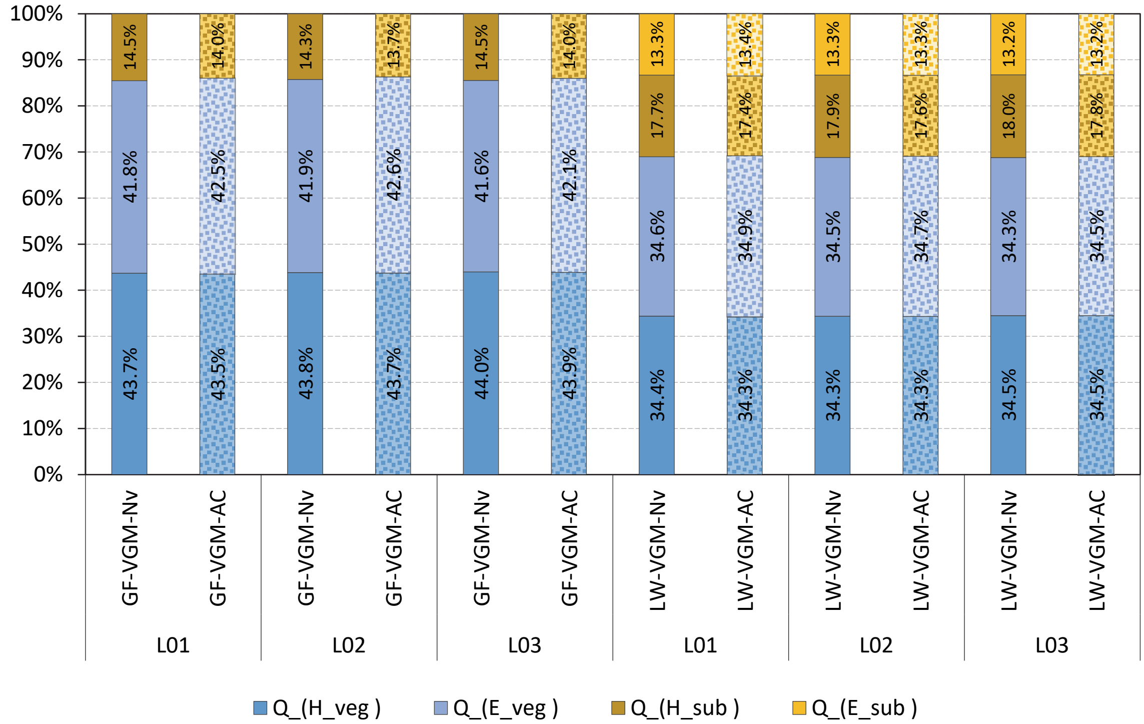


Note: For green façade: $Q_{H_{Hw}}$; and living wall: $Q_{H_{sub}}$.

*Fig. 75. DAB, annual mean surface convective flux partitioning by floor levels and scenarios.*

The summertime $Q_{E_{veg}}$ mean flux was substantially greater, given the greater availability of energy within the system (Fig. 76, p. 173). The mean flux data also highlighted the L02 wall section to present slightly higher contribution than L01 and L03, with both green façade and living wall application (and *Nv* and *AC* scenarios). As with surface temperature means earlier, this suggested the significance of disproportionate internal gains received by the midlevel (L02). Overall, the living wall canopy presented higher $Q_{E_{veg}}$ means relative to the green façade for both *Nv* and *AC* scenarios to suggest higher cooling influence.

The influence of air-conditioning (i.e., *AC* scenarios) was highlighted by decreases in $Q_{E_{veg}}$ means (relative to *Nv*), with reductions ranging between the wall floor levels from 21.7-26.0% for green façades, and 21.4-25.6% for living walls in the summer, while in winter the ranges were lower at 9.8-15.4% for green façades, and 8.7-13.6% for living walls. Air-conditioning (*AC*) reduction influence on living wall $Q_{E_{sub}}$ means was in the range between 22.1-26.4% for the summer, and again lower at 12.0-17.6% for the winter. These reductions suggested the significance of air-conditioning heat rejection, which reduces the energy availability for evaporation in the atrium system, with higher operation in the summer resulting in greater reducing influence on the latent flux than winter.

a)

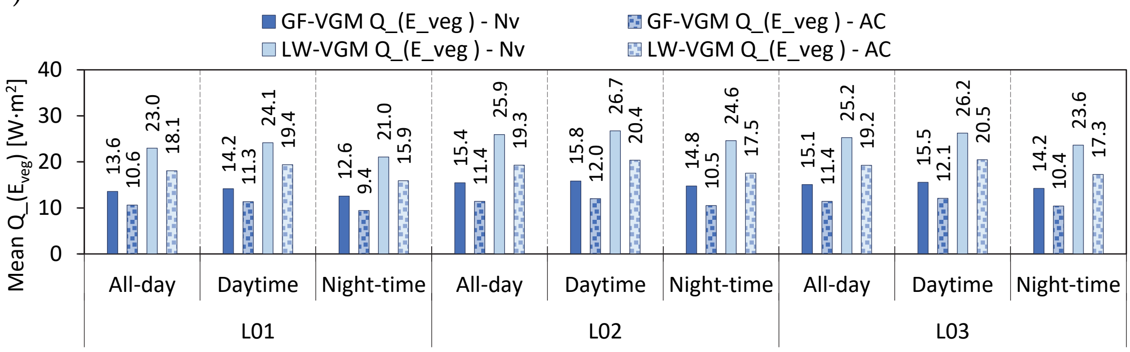


b)

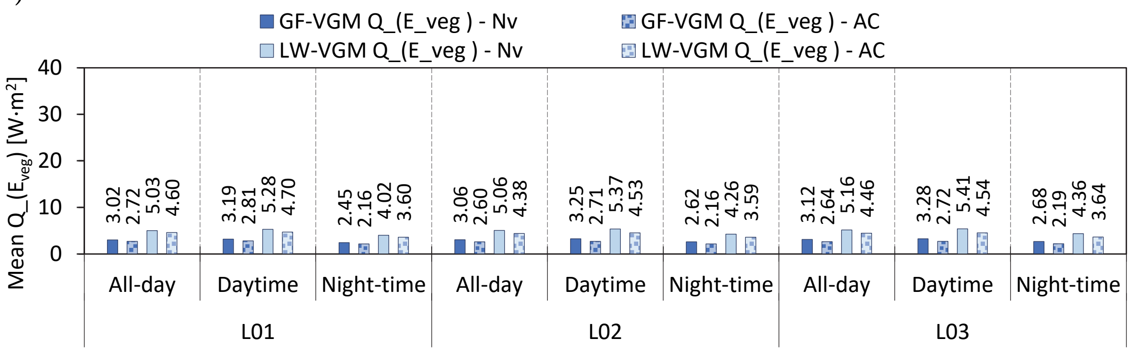


*Fig. 76. DAB, summer (a) and winter (b) mean vegetation latent flux contributions by floor levels for GF- and LW-VGM scenarios.*

### Energy use

The surface flux modifications of vertical greening application impacted on space-conditioning energy consumption of the scenarios. Both green façade and living wall application marginally increased annual heating energy consumption in the adjoining rooms under the *Nv* scenario by 1.48 and 0.87% respectively, and by 1.20 and 0.80% under the *AC* scenario (Fig. 78, p. 174). Living wall application therefore presented a relatively lower annual increase than with green façade application, which suggested influence from the wintertime insulating function of the additional substrate layer. The annual increase however was mostly contributed to by the summertime increase, with living wall application presenting greater contribution than green façade application to suggest the significance of increased heat loss from greater evapotranspiration at the living wall surface. With the *AC* scenario adjoining room cooling energy, both green façade and living wall application decreased annual consumption by 4.53 and 2.57% respectively, owing largely to summertime reductions (i.e., increased heat loss to the atrium volume). Green façade application in this regard was more beneficial with cooling consumption reductions offered in both summer and winter, which in turn suggested that the insulation uplift of the living wall substrate to have countered some of its surface cooling benefit.

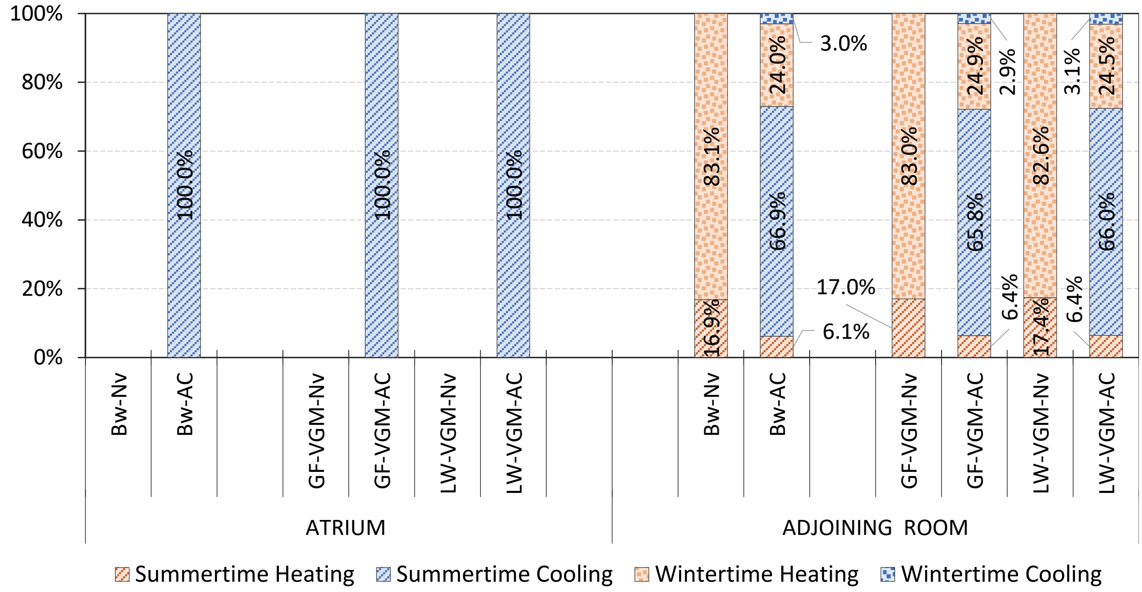


*Fig. 77. DAB, annual mean energy usage representation for scenarios.*

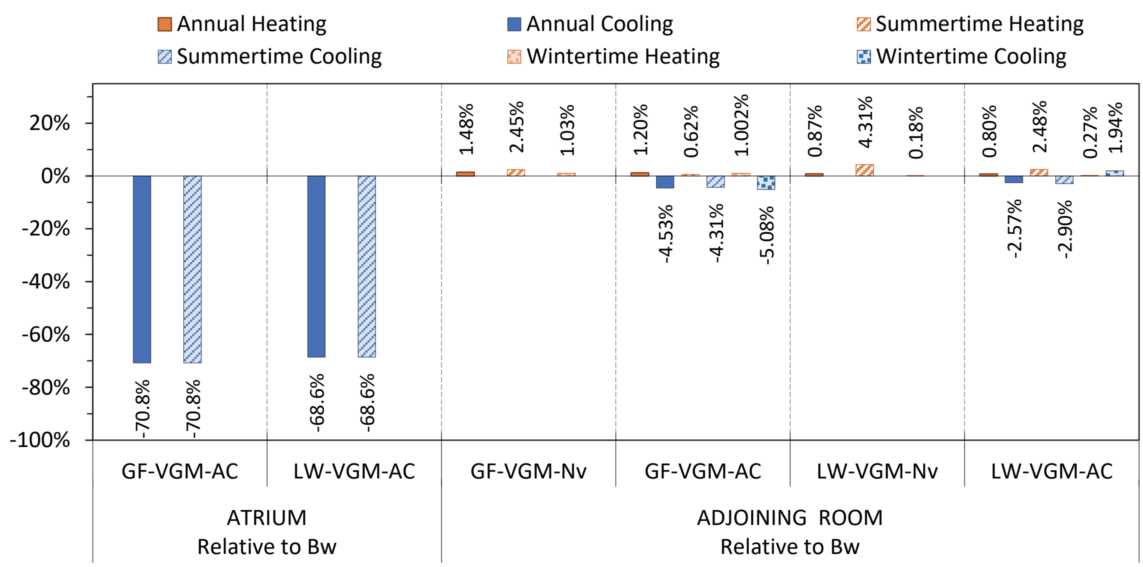


*Fig. 78. DAB, space-conditioning energy consumption modifications for rooms and scenarios.*

Heating loads were not included for the atrium given the reasons mentioned earlier, with space-conditioning consideration limited to the *AC* scenario representing 100% of simulated consumption (Fig. 77). The addition of vertical greening had significant impact relative to the hypothetical *Bw-AC* scenario (i.e., air-conditioned atrium with bare host wall); with >68% reduction in summertime consumption simulated following both green façade and living wall application to highlight the highest cooling consumption benefit by far for the atrium volume including the installation relative to the adjacent rooms (Fig. 78). The latter living wall application (i.e., *LW-VGM-AC*) also presented the greatest reduction to highlight better performance relative to the green façade application (i.e., *GF-VGM-AC*).

### *Humidity*

**a)**

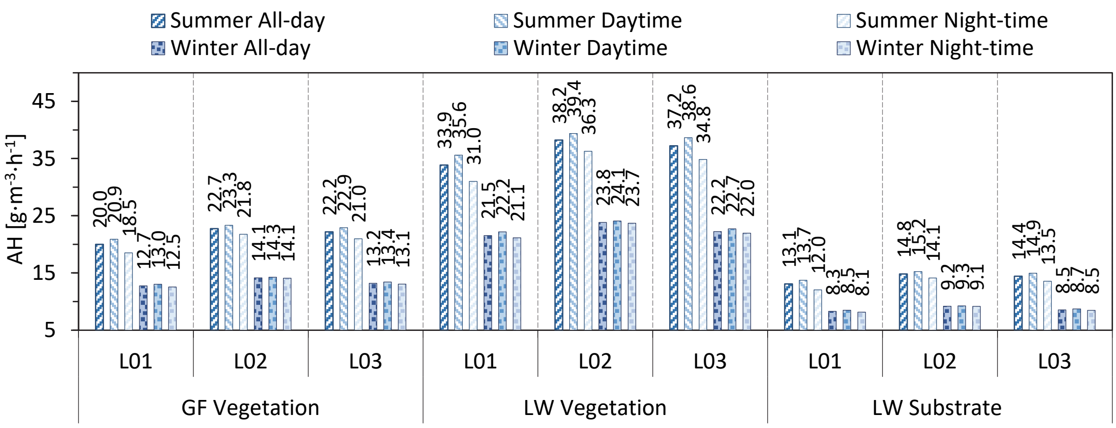


**b)**

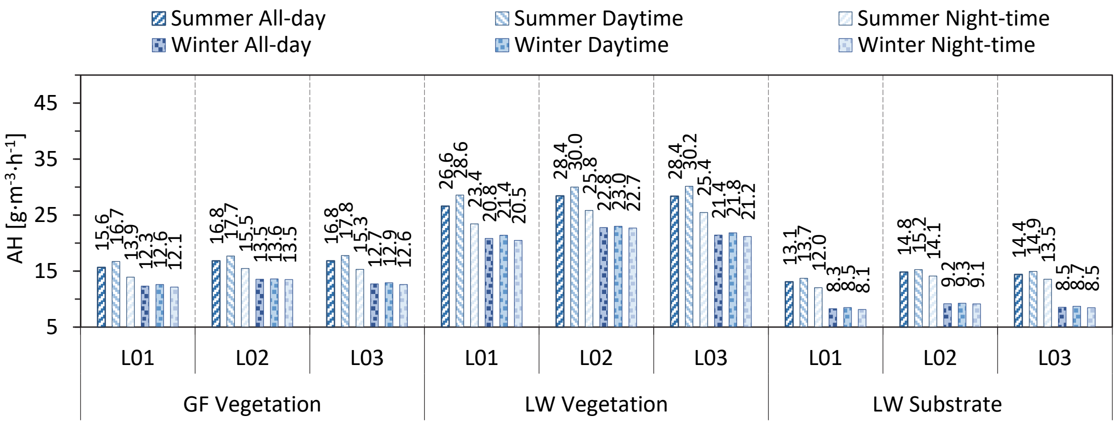


*Fig. 79. DAB, summer and wintertime mean absolute humidity ($AH$) contributions to the atrium from GF- and LW-VGM Nv (a) and AC (b) scenarios.*

Humidity modifications were assessed with reference to mean absolute humidity ($AH$) contributions from the vertical greening surface, and relative humidity proximate to the leaf surface ($RH_{leaf}$). Absolute humidity additions for the *Nv* scenarios highlighted increased contribution during the summer (Fig. 79a), resulting from the increased latent flux for the same period identified earlier. With green façade application, the summer daytime | night-time contribution divide range for the levels was between 52-53 | 47-48% for the vegetation canopies, while for the winter period this was 50-51 | 49-50%. With living wall application, the contribution divide range was broadly similar. Higher contribution during the daytime and in the summer with both vertical greening applications is again attributable to the earlier identified increased latent flux evident during such periods. Notably, the living wall vegetation | substrate contribution divide highlighted significantly higher vegetation influence, with the divide range at ~72 | 28% and consistent for the three levels, and during both summer and winter to suggest relatively consistent latent flux throughout the year.

For the *AC* scenarios (Fig. 79b), $AH$ additions again highlighted increased summer contributions, although less pronounced than with *Nv* given the *AC* reduction influence on the latent flux identified earlier. With green façade application, the summer daytime | night-time contribution divide range for the levels was between 53-55 | 45-47% for the vegetation canopies, while for the winter period this was 50-51 | 49-50%. With living wall application, the daytime | night-time summer contribution divide range was 54-55 | 45-46% for the vegetation and 52-53 | 47-48% for the substrate, while for the winter was between 50-51 | 49-50% for both. The wintertime contribution divide for both vertical greening applications was around the same as with *Nv* scenarios. With the living wall vegetation | substrate contribution, the divide range was modified to present lower summertime vegetation influence (66-67 | 33-34%), given the *AC* reduction influence on the latent flux identified earlier; while for the winter this was comparable to the *Nv* scenario range of between ~71-72 | 28-29%, given the negligible use of air-conditioning and resulting influence on the latent flux.

With leaf proximate relative humidity ($RH_{leaf}$), the variation for the levels was significant with values for the summer ranging between 51.5-59.7% and for the winter between 53.5-58.5% under the *Nv* scenarios, while under the *AC* scenarios summer values ranged between 57.6-66.0% and between 54.5-59.2% for the winter. The increase in values with the living wall relative to the green façade (given the increase in latent flux and $AH$ noted above), ranged between the levels from 2.2-2.8% for the summer and 1.9-2.1% for the winter under the *Nv* scenarios, while under the *AC* scenarios was lower and between 2.0-2.6% for the summer and the same (1.9-2.1%) for the winter; given that higher summer and lower *AC* influence is complimentary to the latent flux and $AH$ observations identified earlier.

### SET, London case study

The simulated microclimate modification results for the defined SET vertical greening application scenarios (in Table 26, p. 161) are detailed in the following sections.

#### *Surface temperatures*

Surface temperature modifications were assessed again with reference to mean $T_{leaf}$ and $T_{Hw} \mid T_{sub}$, as well as $T_{surf_1}$ that represented the TRNSYS output surface temperature for the wall surface facing into the open court. As expected, the isolated summertime data presented much warmer surface temperature means than winter, for all wall orientations and scenarios (Fig. 80). While most surface temperature dataset means were within ±1 K variation between the orientations and scenarios, a marked difference was presented between green façade $T_{Hw}$ and living wall $T_{sub}$, with the latter presenting cooler means by up to 1.9 K for the summer and 0.9 K for winter. This highlighted the influence of the living wall substrate's evaporative flux, with greater impact in the summer than winter. Mean $T_{leaf}$ in contrast was barely modified between green façade and living wall application, with only a minor increase for the south-facing orientation evident with the latter.

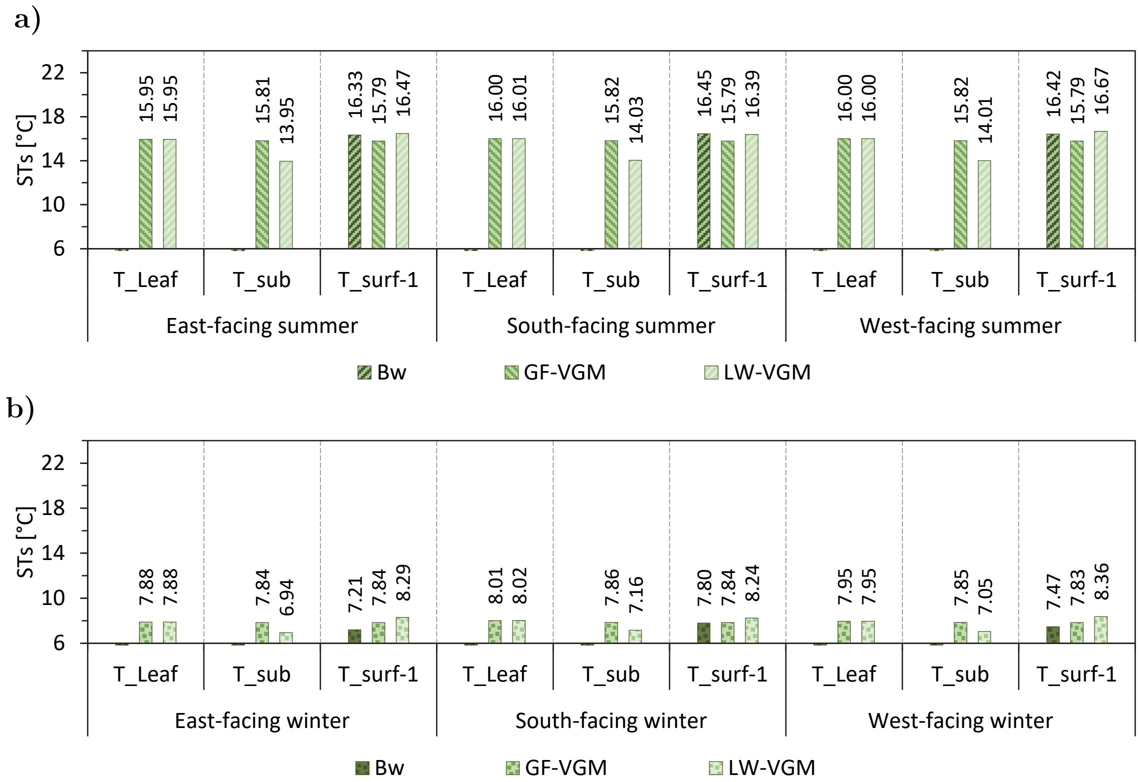


Note: $T_{sub} = T_{Hw}$ for *GF-VGM.*

*Fig. 80. SET, summer (a) and winter (b) mean STs for wall orientations of scenarios.*

The addition of green façades reduced $T_{surf_1}$ means relative to the bare wall (*Bw*) scenario for the summer period (most for the south-facing wall, 0.7 K), while in winter increased means (least for the south-facing wall). This summer cooling and winter warming surface temperature trend is expected with green façades, with several previous monitoring studies confirming this observation (see Chapter 3, e.g., [138]). The addition of living walls in contrast mostly increased $T_{surf_1}$ means relative to the *Bw* scenario in the summer (excluding the south-facing wall), and even more so in winter. This suggested solar irradiance associated influence of the living wall substrate, given that $T_{leaf}$ means had negligible difference between green façade and living wall application.

a)

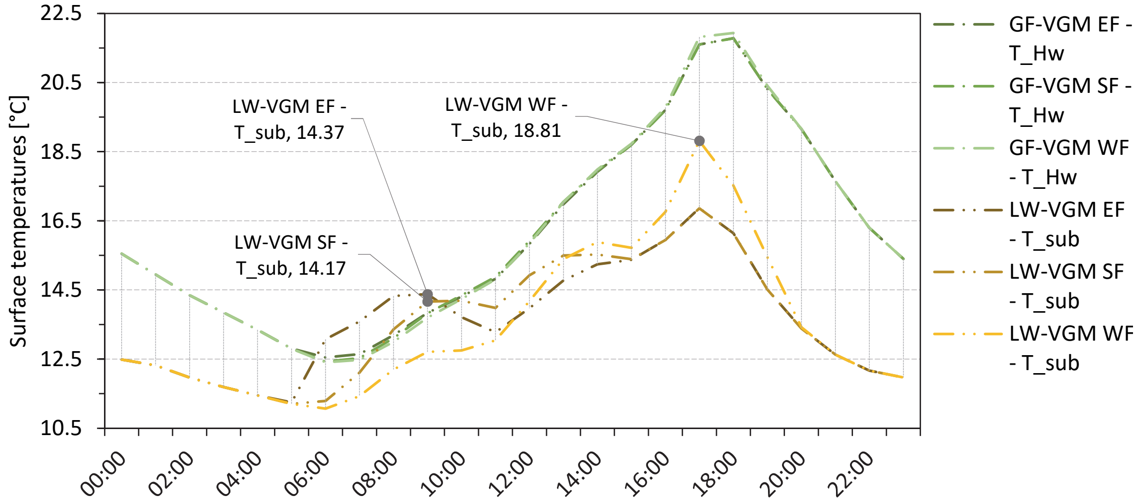


b)

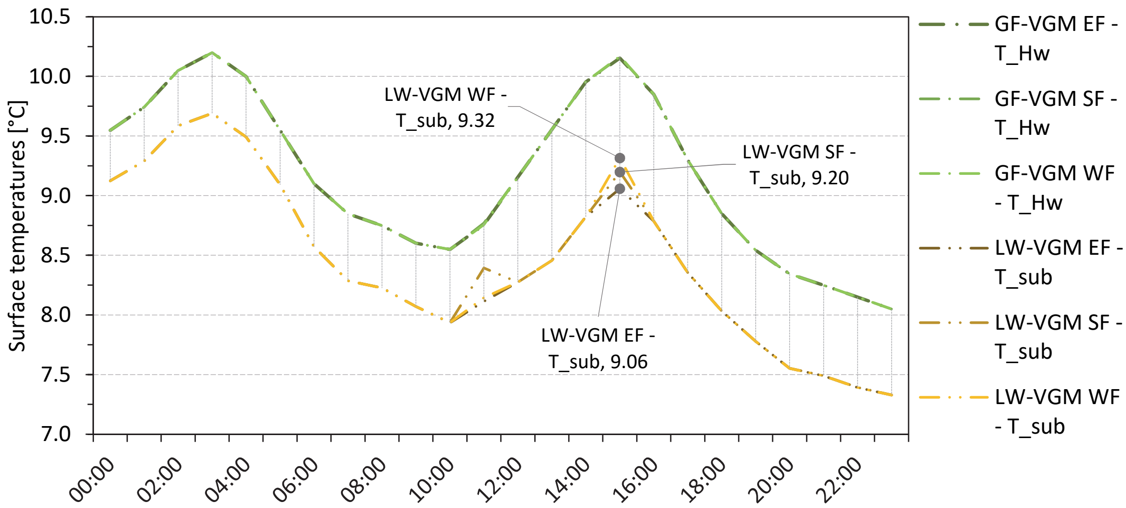


*Fig. 81. SET, summer (a) and winter (b) solstice $T_{Hw}$ | $T_{sub}$ profiles for GF and LW scenarios.*

The solstice day $T_{Hw}$ profiles highlighted little divergence for green façade wall orientations (Fig. 81). For living wall orientations however, $T_{sub}$ profile deviation was evident and pronounced for the summer solstice. The influence of orientation and solar irradiance interaction with substrate thermal properties was confirmed with higher east-facing, followed by south-facing early morning $T_{sub}$; while in the evening the highest peak was for the west-facing wall. Modest temperature lags also highlighted the influence of substrate thermal properties to distinguish living wall from green façade application.

Given that the boundary wall construction considered for all orientations was the same, the temperatures of the surface facing away from the court (i.e., non-vegetated side, $T_{surf_2}$) provided an indication of heat loss modifications from the court to the surroundings. In all scenarios the east-facing wall presented the warmest means to highlight the significance of low solar altitude irradiance during the morning hours (Fig. 82). Vertical greening addition served to marginally decrease the summer means (reduced heat transfer to the non-vegetated side), but marginally increased winter means (increased transfer). Living wall application influence in this regard was marginally greater than green façade, again to suggest the significance of the thermal property modifications offered by its substrate layer.

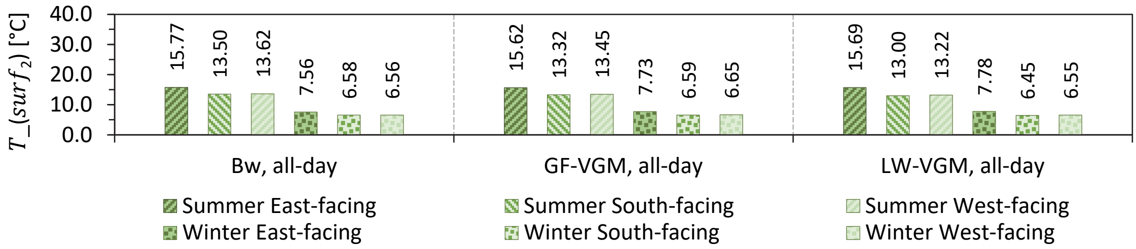


*Fig. 82. SET, non-vegetated $T_{surf_2}$ summer and winter means for wall orientations and scenarios.*

### Surface flux

The surface flux results showed that the mean annual net flux out of the walls (and into the court microclimate) had significantly decreased relative to the *Bw* simulation following vertical greening application (Fig. 83). This was mostly affected during the winter, with living wall daytime east- and west-facing orientations notably presenting flux into the walls. Living wall application reduced the extent of the outward annual mean flux the most with all wall orientations (84-90%), relative to green façade application (37-44%), while the east-facing wall offered the least reduction for both vertical greening applications.

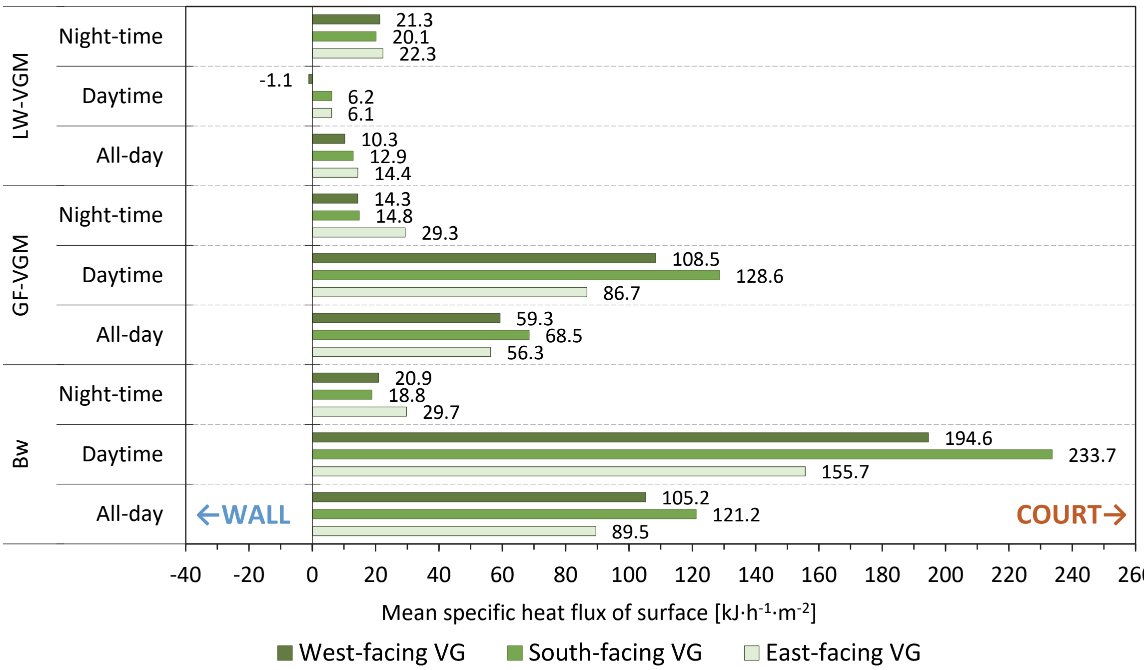


*Fig. 83. SET, annual mean specific surface flux for wall orientations and scenarios.*

The summertime convective flux partitioning for the green façades highlighted the contribution made by the canopy latent flux ($Q_{E_{veg}}$) to range between the wall orientations from 22.7-27.0% during daylight hours when transpiration is active, while during the night-time hours was lower and between 16.2-16.8% (Fig. 84 and Fig. 85, p. 181). During the wintertime, this partitioning reduced further to between 11.8-25.6% for daylight hours and 14.7-16.9% for the night-time. With living wall application, the summertime $Q_{E_{veg}}$ contribution ranges were again lower than with green façade application, given the additional contribution from the substrate latent flux. The ranges were thus between 13.1-13.6% during daylight hours, and significantly lower at <1.2% during the night-time. During the wintertime, these contributions reduced further to be between 9.9-12.3% for daylight hours and <1.0% for the night-time. Absolute living wall latent flux contribution was always greater than with green façades to suggest greater cooling from its canopy (Fig. 85), although this did not translate to significant mean $T_{leaf}$ differences as noted earlier. The living wall substrate latent flux ($Q_{E_{sub}}$) representation on the other hand was relatively high, with the daytime ranging between the wall orientations from 46.2-47.0% for the summer and relatively lower and between 43.3-47.3% for the winter. During the night-time the contribution range was slightly higher and showed minimal seasonal variance, with the summer range between 51.5-51.6% and winter between 51.7-51.9% (Fig. 84).

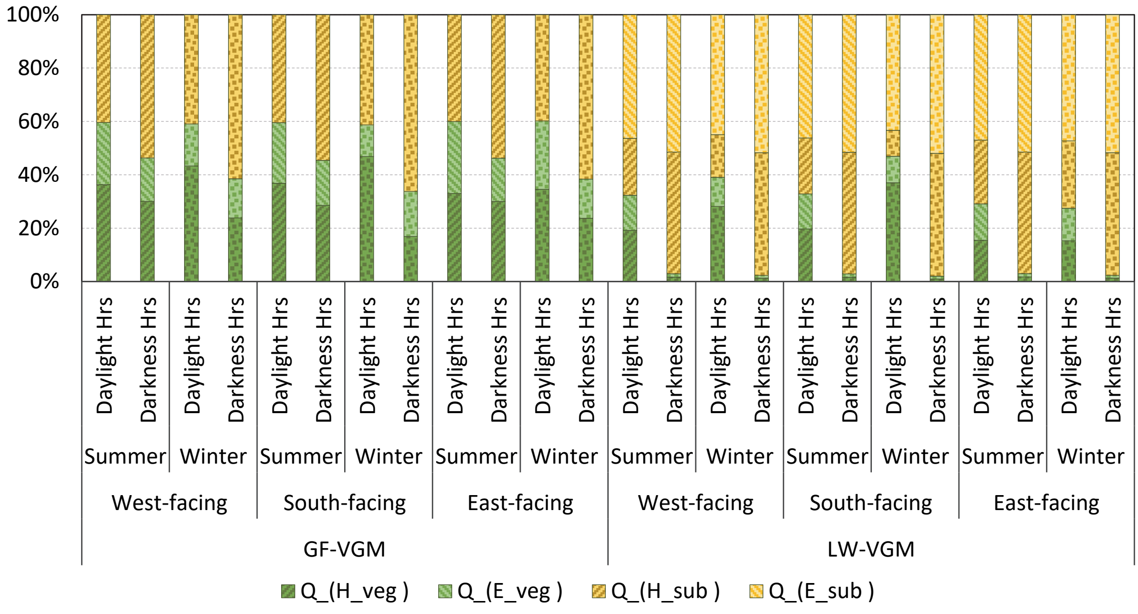


Notes: For green façade: $Q_{H_{Hw}}$; and living wall: $Q_{H_{sub}}$.

*Fig. 84. SET, mean summer and winter surface convective flux partitioning for wall orientations of GF- and LW-VGM scenarios.*

With both vertical greening applications, the canopy latent flux ($Q_{E_{veg}}$) contribution partition was greatest for either east-facing or south-facing orientations to suggest the greater significance of morning and afternoon solar irradiance than later in the evening (Fig. 85). However, when absolute contributions were considered, the west-facing orientation presented the greatest mean in the summer to suggest the significance of accumulated heat, while the south-facing orientation presented the greatest in winter to suggest the significance of solar exposure.

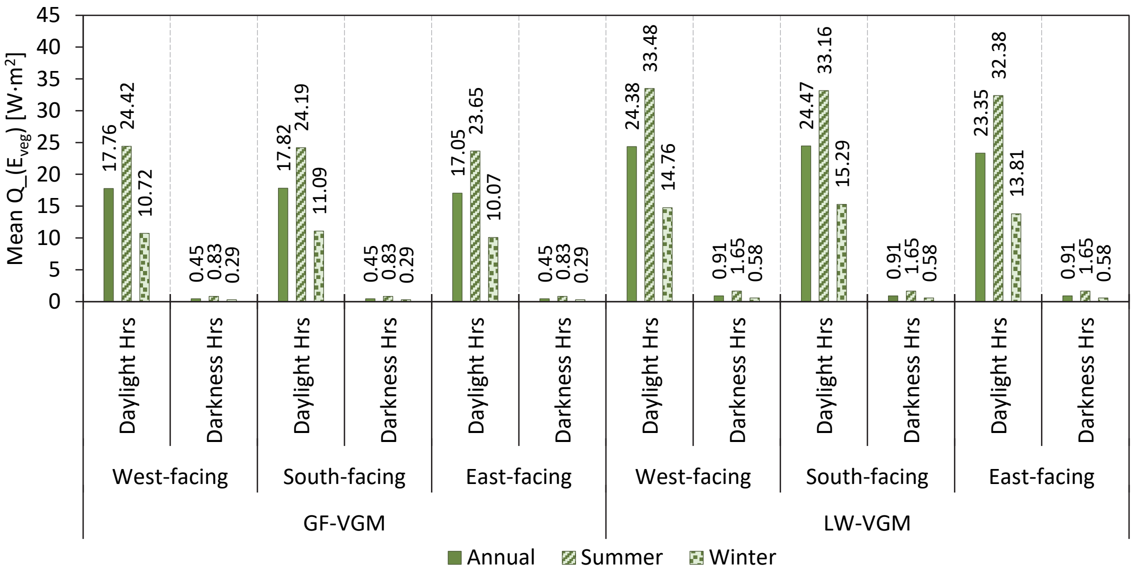


*Fig. 85. SET, annual, summer, and winter mean canopy latent flux ($Q_{E_{veg}}$) contributions for wall orientations of GF- and LW-VGM scenarios.*

### *Humidity*

Humidity modifications were assessed here again with reference to mean $AH$ contributions from the vertical greening surface and $RH_{leaf}$. Absolute humidity additions for all scenarios and orientations highlighted clear increased contribution for the summer period than winter to complement the latent flux trend (Fig. 86, p. 182). With green façade application, the summer daytime | night-time contribution divide was ~95 | ~05% for the vegetation canopies of the considered orientations, while for the winter period this range was between 94-95 | 05-06%. With living wall application, the summer daytime | night-time contribution divide range was between 93-94 | 06-07% for the vegetation and 64-66 | 34-36% for the substrate, while for the winter the divide was ~93-94 | 06-07% for the vegetation (similar to summer) and 65-70 | 30-35% for the substrate. This highlighted substrate contribution to be substantial even during the night-time hours. Substrate contribution was also larger than the vegetation generally, with the summer living wall vegetation | substrate contribution divide range between 18-19 | 81-82%, and the winter even higher at ~14 | ~86% for the orientations. The highest vegetation contribution was during the summer daytime at ~22%, which reduced to between 3-4% during the night-time. In winter, the contribution was lower and between 19-20% during the daytime and dropped to ~3% during the night-time to complement the $Q_{E_{veg}}$ trend. The latter winter contributions highlighted the significance of orientation, with the lower solar altitude irradiance in the morning hours contributing to the east-facing orientation presenting the highest $AH$ contribution.

With $RH_{leaf}$, values for all orientations had minimal variance. Summer mean $RH_{leaf}$ was therefore between 75-76% for all orientations, while for the winter the range was higher at 84-85%. Notably, living wall values were only marginally lower than for green façades (by <0.02%), to highlight little difference between the two canopies.

**a)**

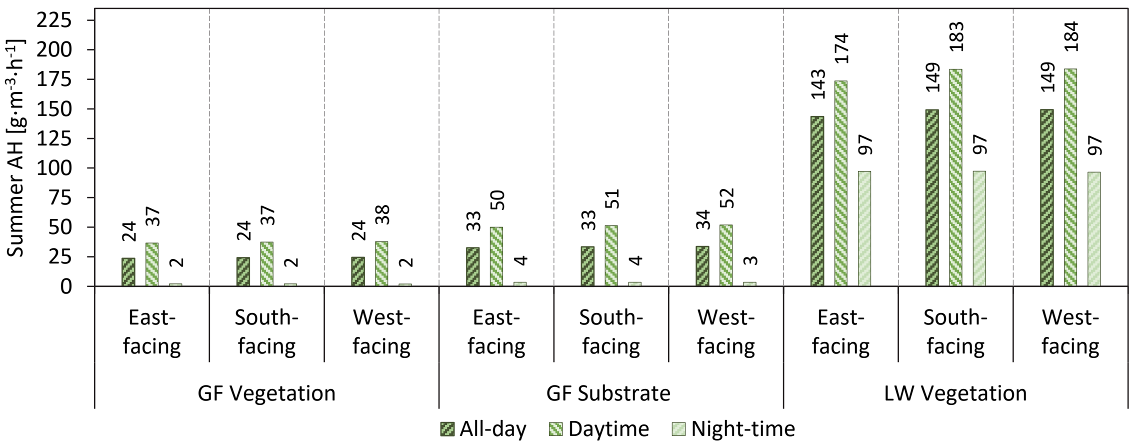


**b)**

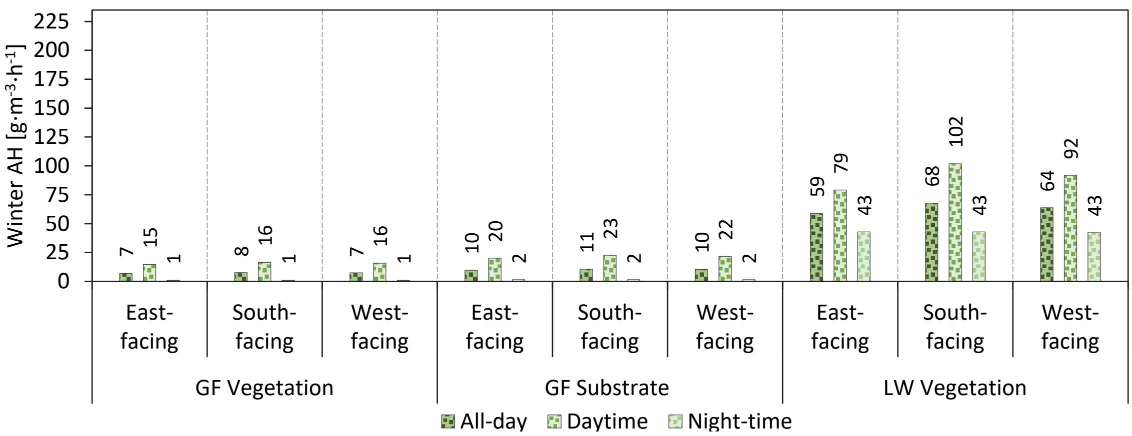


Note: Green façade host-wall has no latent flux (assumed to be dry).

*Fig. 86. SET, summer (a) and winter (b) mean $AH$ additions from GF- and LW-VGM scenarios.*

## 6.4 Discussion

### 6.4.1 Model and validation

The parameter sensitivity analysis demonstrated most plant parameters to have moderate-to-strong influence on final outcomes of the model. With the identified parameters with moderate influence, there is reasonable flexibility to input assumed or mean values representing several species when measurement data is not available. The moderate influence of such parameters also justifies the use of constants for the durations defined, which helps to disregard their dynamic variation typically experienced in in-situ environments. The sensitivities of such parameters however were still potent enough to encourage the input of accurate values where possible, to acquire best approximations.

Most background climate variables in contrast had critical influence, and thus there is a requirement to provide accurate inputs to ascertain reliable simulation results. The issue with TRNSYS is that it considers the air within each zone to be mixed to present mean $T_{air}$ and $RH$ values for the airnode. Study 1 however demonstrated the installation proximate microclimate in indoor environments to be considerably complex. The input of nodal mean $T_{air}$ and $RH$ is therefore unrepresentative, which in turn contributes to poorer approximation as demonstrated by the first DAB living wall validation exercise. When this shortcoming was addressed with the input of measured installation proximate values, the subsequent VGM approximation vastly improved. This clarified any approximation shortfall in such indoor simulations to be dependent primarily on the building energy model's shortfall in approximating the complexity of such microclimates, as opposed to the VGM's. An ideal indoor environment application of this coupling pathway therefore requires the input of installation proximate $T_{air}$ and $RH$ values.

Table 33. DAB, impact between TRNSYS nodal and measured $T_{air}$ and $RH$ input for space-conditioning energy consumption estimation.

| **DAB scenario** | **Heating consumption** | | **Cooling consumption** | |
|---|---|---|---|---|
| | Atrium volume with wall (%) | Adjoining rooms behind wall (%) | Atrium volume with wall (%) | Adjoining rooms behind wall (%) |
| *GF-VGM-Nv* | N/A | -1.11% | N/A | N/A |
| *GF-VGM-AC* | N/A | -1.07% | +1.96% | +0.60% |
| *LW-VGM-Nv* | N/A | -0.92% | N/A | N/A |
| *LW-VGM-AC* | N/A | -0.88% | +1.74% | +0.47% |

Note: Prefix '+' and '-' denotes over- and underestimation by the TRNSYS coupling simulation.

Installation proximate data however is not available to most studies, while improving TRNSYS outputs would also be beyond their scope. Utilising the default TRNSYS airnode coupling approach therefore requires accounting for this shortcoming when interpreting outcomes. With the DAB atrium space-conditioning consumption for example, this meant an approximation error of up to +2% (Table 33, p. 183). While such errors cancel-out with comparative studies, it must be accounted for when interpreting absolute values.

With both indoor and semi-outdoor studies, the validation results highlighted reduced agreement for the summer, particularly during the daytime. This was most pronounced at the indoor study, particularly with living wall application. Monitoring results from Study 1 highlighted surface airflow movement to be evident during these periods, with pronounced influence observed at the indoor DAB study. Such airflow movement off the surface translates to modifications in both vertical and lateral heat flux, as well as vertical and lateral mass flow. The VGM's limitation of only considering one-dimensional horizontal heat flux means that such vertical and lateral modifications are not included in the energy balance. This in turn explains the divergence in agreement results for the periods identified, when buoyancy driven thermal activity and disruption is expected (see Study 1). The consideration of the DAB study for the validation of the VGM for indoor application simulations was therefore a challenge, given that it represents somewhat of an exceptional vertical arrangement with experimental evidence demonstrating vertical flow disruption. This study acknowledges this as requiring further review and evidence in the future to justify simulation accuracy and wider applicability[XX].

For a given exercise if the analysis intent from onset is to obtain a higher resolution of approximation, this would require the calculation of three-dimensional mass, momentum, and energy flux for the defined volume. To achieve this to the highest degree of precision requires a CFD approach with appropriate mesh resolution for the accuracy sought. This would be the most appropriate progression for analysing environments like at the DAB, where complex flow regimes have been demonstrated to occur. The drawback to such an approach however is the increased complexity in simulation setup, computational demand, and simulation clock-time; all of which the VGM and its TRNSYS coupling seeks to avoid. Understanding this trade-off at the onset of an assessment is critical for the appropriate application of this pathway (Pathway-A), and the interpretation of its simulation results.

---

[XX] Prevailing circumstances (Covid-19 pandemic) prevented the consideration of an alternative indoor site.

Given that the VGM is in its testing phase with a direct MATLAB coupling, further development is necessary to ensure the computational efficiency aims of the project. This development would seek to compile the VGM as a specific 'Type' as recommended in the TRNSYS documentation [367]. This is expected to reduce the current simulation clock-time by more than an order of magnitude (as all calculations will be performed within TRNSYS itself). Furthermore, a Type enables multiple coupling with a Multi-Zone Building (Type 56) and to concurrently simulate a vertical greening installation in vertical layers (one per zone, or greater if multiple nodes are specified), as means to improve accuracy and better the representation of hygrothermal stratification influence.

### 6.4.2 Case study influence

The DAB atrium is an indoor volume that can be modelled within the TRNSYS environment to calculate surface and spatial energy balances. In addition to surface metrics, air-node metrics including space-conditioning loads were as a result available for discussing vertical greening thermal performance. The representation of the atrium in the TRNSYS environment however presented limitations that must be acknowledged and considered when interpreting results. For such atrium arrangements where multiple airnodes are coupled, TRNSYS documentation recommends longwave radiation exchange to be calculated with the 'detailed view-factor method'. However, as the VGM is applied as an overriding surface gain, only the standard 'Starnode model' can be applied at present. This means that longwave exchanges from other atrium zones and multiple reflections within the zone are not included. Furthermore, no airmass balance is calculated between the coupled atrium zones, which means that vertical flux exchanges resulting from buoyancy flow that exists at the study are not included. These limitations mean that the TRNSYS approximation of this atrium environment is relatively coarse, which then feedbacks to the VGM estimation.

Despite the SET court being considered in this study as a sheltered environment, it is still an open system with considerable interaction with the wider climate. The thermal model of the court was therefore created by adding background bounding geometry to form the court arrangement as an open void. Given that there is no airnode specified for this void, and as a result no energy balance calculated by TRNSYS, it was not possible to characterise vertical greening application influence on the void's microclimate with reference to airnode metrics. Instead, the bounding geometry output metrics of mean surface flux and exterior surface temperature were utilised to characterise influence.

### Thermal performance

With the DAB indoor study, the central location of the atrium within the building's general arrangement, and the disparity in occupational demands of adjoining spaces means that an energy deficit within the atrium volume is expected. This means that the dominant flux direction from the adjoining rooms will be into the atrium volume; from the said rooms, through the shared partywalls, and in the case of the vertical greening host, through to its outer surface represented by the installation. The occurrence of this is validated by the simulated vertical greening surface temperature at all floor levels (i.e., $T_{surf_1}$), being always cooler than the other side of the wall facing into the adjoining rooms (i.e., $T_{surf_2}$).

The addition of the hypothetical vertical greening installation served to decrease the mean flux into the DAB atrium volume, and thereby reduce mean $T_{surf_1}$, and increase the $T_{surf_1} - T_{surf_2}$ difference relative to the bare host wall scenario (i.e., *Bw*). The flux reduction was negative (i.e., into the wall) during the summertime to highlight a heat sinking or cooling influence for the atrium volume. This influence was best demonstrated with reference to the air-conditioned scenario (*AC*), where it contributed to substantial reductions in cooling energy consumption. With the adjoining rooms, atrium vertical greening addition also served to increase the drawing or sinking of energy from the said rooms. Relatively higher outward flux/heat loss in this manner resulted in the increased heating demand and consumption simulated for these rooms; while when the *AC* scenario was considered a beneficial reduction in cooling energy consumption was simulated. The flux modifications presented were therefore beneficial in the summer, although an adverse influence in winter (given that the installations are evergreen and provide continuous annual ecosystem service provision). With both the atrium and adjoining rooms, the marginally better performance simulated with the green façade application (i.e., *GF-VGM*) relative to the living wall (i.e., *LW-VGM*) is attributed to the influence of the heat storage properties of the latter's substrate layer. This was exemplified with reference to mean $T_{surf_1}$, where living wall temperatures were marginally warmer than with green façade application.

The above highlighted the partitioning of the installation surface flux as latent flux to contribute towards a cooling energy consumption reduction for the DAB atrium. Examining net annual expenditure however revealed that this saving only materialised with the *AC* scenarios (possible future state), with green façade application providing a greater saving (71%), than with living wall application (69%). The adjacent rooms in contrast reported only marginal net energy use savings, with green façade application again providing a greater 2.0% saving, than the 1.1% with living wall application. The natural ventilation (*Nv*) scenarios highlighted that net energy use for the adjacent rooms increased by a larger 1.5% with green façade application, than 0.9% with living wall application (given that the atrium included no space-conditioning energy demands). These net consumption results[XXI] highlighted the relative significance of installation siting within a given building's arrangement, while the influence of the living wall substrate zone and its thermal properties had significant bearing on whether the installation presented a net benefit.

With the SET semi-outdoor study, surface flux results showed that the net annual mean was mostly out of the walls and into the court volume for all scenarios (Fig. 83, p. 179). The walls on average were therefore contributing thermal energy to the court's microclimate. The daytime flux being much greater than the night-time with the bare wall scenario (i.e., *Bw*) is expected, given that the highest energy input from solar radiation is received and reradiated back to the court microclimate during this period of the day. The significance of orientation was highlighted here with the south-facing wall presenting the greatest flux, characterised by the surface presenting the warmest $T_{surf_1}$ means (Fig. 80, p. 177).

The SET green façade application (i.e., *GF-VGM*) net annual flux profile broadly followed the *Bw* scenario, only with reduced mean flux that translated to reduced mean $T_{surf_1}$. The annual $T_{surf_1}$ reductions were supported by summertime contributions when the walls were between 3.3-4.0% cooler than the *Bw* scenario. During the winter, $T_{surf_1}$ means in contrast were increased to be between 0.5-8.7% warmer than the *Bw* scenario (Fig. 87, p. 188). These findings clarified the green façade canopy's function as a thermal moderator that intercepts and dissipates radiation at the surface to reduce penetration, while also acting as an insulator that abates rapid energy loss. This simulated moderating influence of green façades supports previous findings discussed in section 3.4.2 (e.g., [138,189,252,253]).

The SET living wall application (i.e., *LW-VGM*) application mean flux profile differed from the above, with the highest outward flux evident during the night-time period (Fig. 83). The walls were therefore a heat source for the court microclimate, more so during the night than daytime. The daytime mean flux was considerably lower than for the *Bw*

[XXI] Error cancelled-out given the comparisons (refer to section 6.4.1).

scenario, with the west-facing wall notably presenting flux into the wall to highlight a modest heat sinking effect for the court microclimate. These flux reductions were mostly attributed to significant energy dissipation enhancement introduced by the substrate latent flux, which represented around half of the convective surface flux for all the walls. This increased latent heat loss however was not directly translated to reductions in mean $T_{surf_1}$. Living wall application means were therefore warmer than the *Bw* and green façade application for all orientations (less warm during the summer). This is attributed to the added thermal storage contribution from the substrate, which is further enhanced when saturated. The substrate addition also affected the overall wall's thermal resistance to limit energy transfer through to the other side of the boundary wall, and out of the court's microclimate system. The living wall application scenario therefore offered cooler mean $T_{surf_2}$ relative to both the *Bw* and green façade application scenarios (Fig. 82, p. 179).

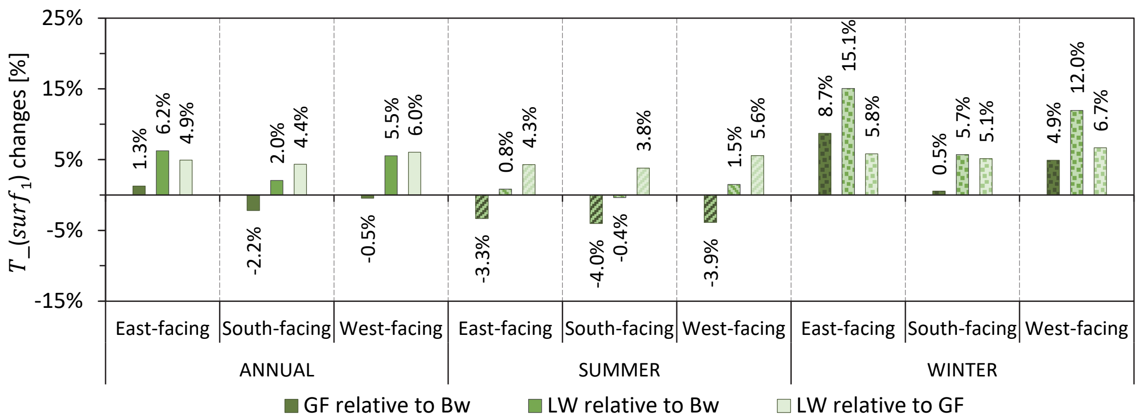


*Fig. 87. SET, annual, summer, and wintertime mean $T_{surf_1}$ modifications for wall orientations of GF- and LW-VGM scenarios.*

In general, vertical greening application served to reduce outward mean net flux relative to the *Bw* scenario to dampen energy contributions to the court's microclimate. Relative to the green façade scenario, living wall application reduced the extent of this the most for all wall orientations, which in turn would benefit the thermal microclimate of the court the most. Any modification to the court microclimate's $T_{air}$ however would be dependent on the flux exchange with the wider climate (not accounted for in this TRNSYS simulation pathway). This would be significantly aided by background wind flow, of which the dominant south-westerly flow would typically benefit the case study siting, if not for the constraint presented by the court's sheltered geometry and surrounding morphology. The most accurate approximation of such complex interactions however is beyond the scope of this study and the analysis pathway presented.

Both case studies established the addition of vertical greening installations to dampen the flux output to the immediate microclimate. Whether this damping effect leads to a cooling or energy sinking effect is dependent on the potency of the convective flux and its partitioning, which in turn is dependent on the energy input to the system (i.e., seasonality). Overall, living walls performed better in this regard, mainly attributed to the latent flux contribution from its substrate, followed by higher latent flux contribution from the vegetation. The beneficial substrate contribution however in certain circumstances can be countered by its heat storage properties, which is enhanced to an extent when saturated.

### Humidity influence

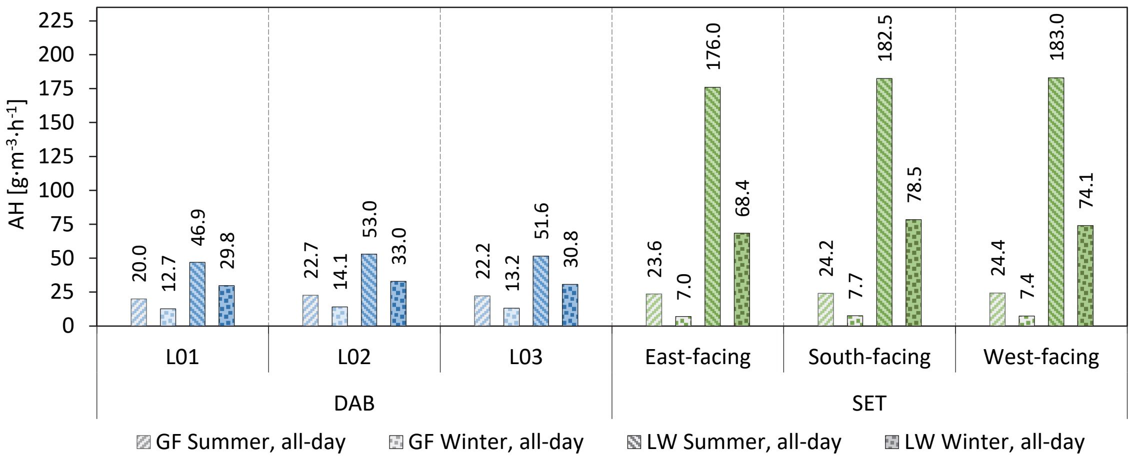


*Fig. 88. DAB and SET, summer and winter mean $AH$ contributions from GF and LW scenarios.*

Any increase in surface latent flux translates to increases in proximate $AH$ and $RH$, with subsequent diffusion into the surrounding microclimate. Both the DAB atrium and SET court simulation data highlighted an uplift in surface vapour flux following vertical greening application, with daytime evapotranspiration output as the largest contributor (plant transpiration at night is minimal as stomata are closed, [53,54]). The SET south-facing wall also presented the relative highest output, while summer output for all SET wall orientations and DAB installation levels was significantly greater than in winter (Fig. 88). This is explained by $\Delta/P_{air}$ rapidly increasing with background $T_{air}$, which in turn means that the latent flux is dominated by radiant energy input, received most by south-facing façades and during the summer [53]. The greater vegetation contribution from living walls relative to green façades is attributed to the former's plant profile, which has a greater $LAI$ and canopy depth ($z_{veg}$); while the overall greater installation latent flux contribution from living walls is attributed to the additional flux from its saturated substrate.

As identified in the Chapter 3 review and by Study 1 measurements, humidity additions could remain trapped in sheltered environments if background wind velocities and resultant humidity advection is minimal. This in turn could present a challenge to both the health and comfort of occupants of such sheltered environments by increasing fungal colony-forming units (CFU) [374], while also increasing the risk of thermal discomfort to occupants by inhibiting evaporative cooling from perspiration [10]. These risks are far greater in indoor environments such as at the DAB, where the atrium could be considered as a near closed system with only controlled ventilation. The dissipation of contributions is somewhat aided by the presence of a prevailing stack-flow, as identified by the monitoring results in Study 1. This however is unique to the spatial arrangement of the atrium system and not relatable to all indoor application environments. In generic sheltered environments the necessity for providing enhanced ventilation flow paths is therefore a key consideration of vertical greening installation design and siting. This will not only mitigate risks from humidity accumulation but will also serve to enhance the evaporative flux of the plants (and living wall substrate) by keeping the foliage coupled to relatively desaturated airflow.

## 6.5 Summary

This chapter presented a one-dimensional VGM that can be coupled by any building performance analyst familiar with the TRNSYS building energy modelling framework to obtain a reasonable estimate of energy and microclimate modification implications of vertical greening application. The agreement results demonstrated that this is achievable and applicable in semi-outdoor environments, although the promising results from indoor environment application, particularly with living wall assessment requires further validation.

At the DAB indoor study, vertical greening application **reduced cooling energy consumption mostly in the atrium** that contained the installation, and to a lesser extent in the adjoining rooms. This consumption reduction resulting from the partitioning of the installation sensible flux as latent flux translated to a **net annual energy use saving** for the atrium volume. This however would only be realised **if air-conditioning is eventually implemented**, while with the **current naturally ventilated atrium** with heating in adjoining rooms only, a **modest net energy use increase is expected** from the wintertime cooling influence of the evergreen installation.

At the SET semi-outdoor study, vertical greening addition **reduced the outward annual mean surface flux** to present the prevalence of a thermally moderated microclimate for the sheltered court, with **living walls reducing the flux the most relative to green façade application.** The extent of this moderation was dependent on the dynamic latent-to-sensible partitioning efficiencies of the installation surface flux. This in turn was dependent on wall orientation as well as the time of day, which highlighted the **significance of solar radiation loading received** and its dynamic moderation by contextual morphological and material features.

# Chapter 7

## STUDY 4: NEIGHBOURHOOD SIMULATION PATHWAY-B

## 7.1 Introduction

Progressing from Studies 1-3, this chapter presents Study 4, which addresses the fourth-of-five secondary research questions introduced in Chapter 1.

> *Q IV. To what extent would neighbourhood-scale application contribute to enhancing urban climate resilience?*

This question is examined here through a comparison study between office building construction build-ups including vertical greening applications, sited within the morphological contexts of central urban and suburban areas. The study approaches this by simulating the respective street canyons, utilising a multiscale urban climate framework including the coupling of the VGM developed in Study 3 (referred to as simulation Pathway-B). The chapter includes material and data extracts from the paper by Gunawardena *et al.* [45].

### 7.1.1 Simulating the urban climate

Sourcing measurement data from direct methods (i.e., using eddy flux stations with anemometers, thermocouples, gas analysers etc.) to compile localised weather profiles offer the most accurate means of accounting for urban site-specific climate loading. For such measurements to be representative, longitudinal data collection is necessary to account for the spatial and temporal diversity of heat island influence [2]. This requirement favours methodologies utilising relatively high-resolution networks of fixed stations as opposed to mobile traverse observations that offer only cross-sectional data. There is however no general framework or accepted standard practice to direct such fixed-station measurement campaigns currently in place in cities [375]. This means that proposed studies would have to establish their own networks at the representative grid resolution required. Although such measurement projects exist (e.g., [33,376,377]), the infrastructural cost to achieve similar campaigns of data collection is unlikely to be available for typical urban climate studies [378]. As an alternative, data collected from private networks and enthusiasts may be considered (i.e., community-based data sharing). This data however is likely to be inconsistent, with limited and divergent parameters collected, or include data gaps that would in turn require laborious interpolation methods to complete.

### 7.1.2 Adapting a climate framework

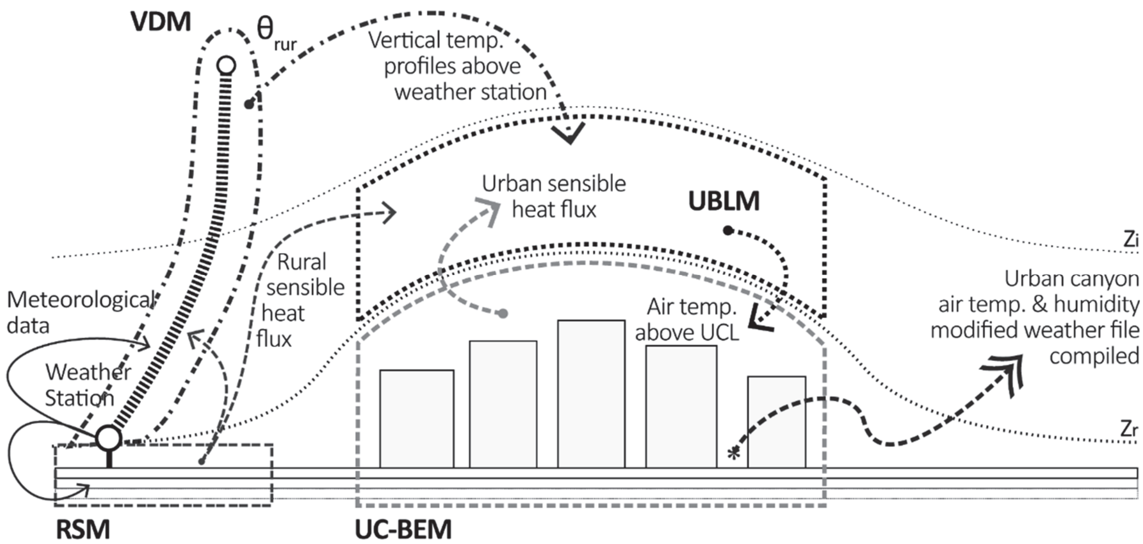


*Fig. 89. Physical domain of the UWG modules and data exchanges for an idealised city; based on* [1], *published in* [379].

In order to approximate urban climate processes and influences, this study instead utilised a revised version of the model framework published as the 'Urban Weather Generator' or UWG *V4.1.0* [1,380]. This framework is based on multiscale energy balances and Monin-Obukhov similarity theory [381], and is composed of the following four coupled sub-models: Rural Station Model (RSM); Vertical Diffusion Model (VDM); Urban Boundary-layer Model (UBLM); and the Urban Canopy and Building Energy Model (UC-BEM). The latter UC-BEM sub-model integrates the established Town Energy Balance scheme [382], with a simplified building energy model developed by Bueno *et al.* [383]. A summary of the principal data interactions of the framework is schematically represented in Fig. 89, while detailed mathematical descriptions are offered in Bueno *et al.* [1,384]. Field data verifications from the cities of Basel (Cfb), Toulouse (Cfb), and Singapore (Af) are presented in Bueno *et al.* [1,384], and Nakano *et al.* [385], while modified framework application studies by the author are presented in [27,379,386,387].

The UWG framework is primed with the input of a rural weather file, which is used by the sub-models to calculate the principal outcomes of canyon-specific air temperature ($T_{can}$) and relative humidity ($RH_{can}$); finally compiled as a modified canyon weather file in the EnergyPlus (*.epw*) format. This output weather file may then be used by any dynamic building thermal modelling software to simulate and output in detail building zone-specific indoor environmental conditions, space-conditioning loads, and building energy use.

The modified version of the UWG (*V5.2.0 beta* [388]) included general restructuring and consolidating of the preceding MATLAB code (*V4.1.0*) to enhance input and computational efficiency, as well as the following principal modifications:

- Input modified to accept xml, MATLAB script, or Excel proforma as an input file using new processing functions. Modification of outputs to include UC-BEM data, including BEM space-conditioning loads and building energy use data.
- New diagnostic functions added to assess input weather file and soil-layer profile. Where <3 soil-layer temperatures are present, the Kusuda & Achenbach [389] model is applied to generate missing layer temperatures.
- Building-stock material definition database constraint removed (United States context specific modification introduced by the previous version's authors[XXII]), and manual input definition improved to provide flexibility to assess any material configurations for wall, roof, mass, and rural and urban surface elements.
- Where specified, a default surface greening influence assessment added to account for sensible/latent partitioning of roof or wall flux. This coarse calculation is based on a surface flux partitioning fraction that must be input by the user (assessed in this study).
- Batch-processing capabilities added to facilitate parametric simulations.

The validation of these changes were examined through a case study based simulation study published in Gunawardena *et al.* [45].

[XXII] While this 'improvement' made sense from an American application perspective, it presented significant inflexibility for research purposes, as well as being a hindrance for any non-USA-based application exercises.

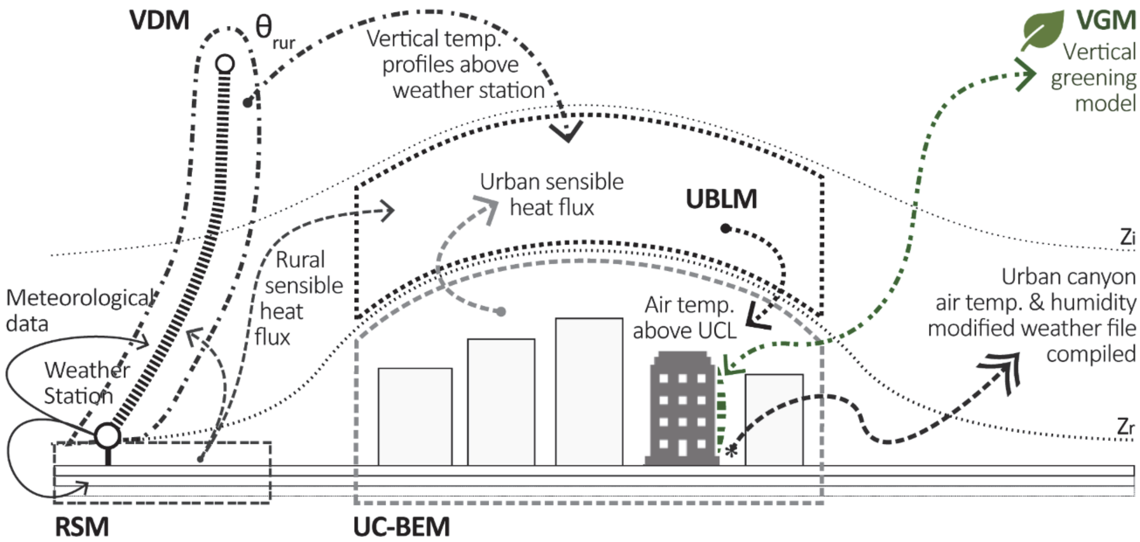


*Fig. 90. Modified urban framework pathway including the VGM coupling.*

To approximate vertical greening application on street canyon building walls, the new VGM developed in Study 3 was integrated into the MATLAB code of the UWG *V5.2.0 beta* version (Fig. 90). The VGM code was first modified to be compatible with the data exchanges of the framework (i.e., TRNSYS integration specific code blocks removed), and then integrated by inserting the code blocks as a method function into the defined 'Element Class', which calculates building envelope surface flux and passes this to the UC-BEM.

## 7.2 Methodology

The case study morphologies used for this study are of Moorgate and Wimbledon areas of London (Fig. 91, p. 196). Moorgate represents the central urban condition and is located within the City of London, the city's thermal core as identified by Watkins *et al.* [390]. It is regarded as the financial centre, and typically includes many banks housed in Portland stone-faced traditional buildings. Wimbledon in contrast represents the suburban condition located in southwest London; typically represented by residential and retail buildings with dominant brick-faced façades. Although there are expansive greenspaces in Wimbledon (i.e., the Common), the area selected for the study represents a built-up area of moderate density (currently characterised as a residential neighbourhood).

The case study urban morphologies of both Moorgate and Wimbledon were idealised by averaging parameters to generate roughness profiles with a 500 m characteristic radius (Fig. 92; Fig. 93, p. 196; & Table 35, p. 198). At both sites, the canyon buildings were given the same use, occupancy schedule, and space-conditioning (heating and cooling) and gains profiles of a medium-sized office building, and only differed between scenarios described in Table 34, p. 197, in terms of their façade constructions detailed in Table 35 and Table 36, p. 199. These roughness and material profiles (including evergreen vegetation data where applicable), together with a rural weather file were then input to the UWG (*V5.2.0 beta*) to generate new canyon climate and energy use data for the scenarios.

*Fig. 91. Typical 'central urban' street canyon view of Moorgate (left); and 'suburban' street canyon view of Wimbledon, London (right); images from ©Google Earth, Street-view 2019.*

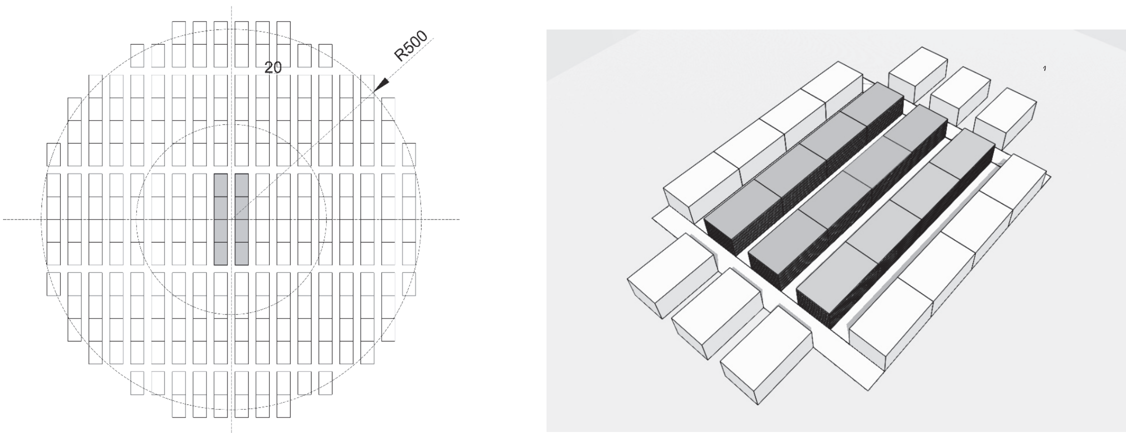


*Fig. 92. Idealised radial area of the central urban condition used for UWG simulations (based on Moorgate); and the canyon's simplified three-dimensional representation (right).*

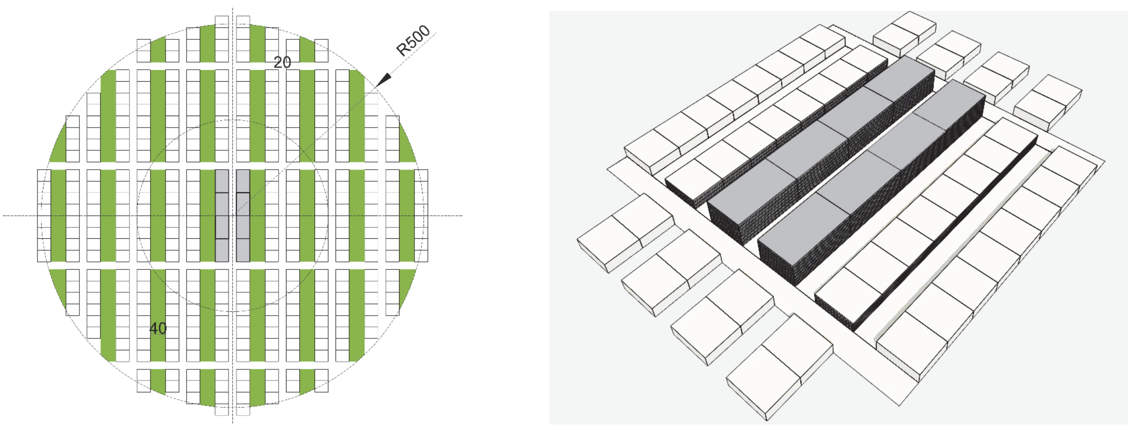


*Fig. 93. Idealised radial area of the suburban condition used for UWG simulations (based on Wimbledon); and the canyon's simplified three-dimensional representation (right).*

The rural weather data used for this study is the Design Summer Year (DSY) for the Reading area (~60 and ~52 km due west of the Moorgate and Wimbledon sites respectively) created using the UKCP09 Weather Generator, the full methodology of which is described in Eames *et al.* [391]. This input weather data represents the rural boundary condition where the influence of the city of London is assumed to be negligible. The Reading file was selected for this purpose as it represents conditions well-beyond urbanised London, while preceding research has confirmed the heat island of the city of Reading itself to make negligible contribution to the gridded data output of the UKCP09 Weather Generator [392]. The weather file also presented clear conditions for both the summer and winter solstice (low cloud cover), which represents ideal conditions for heat island formation and serve as benchmark days to compare and assess the different canyon climates generated.

Table 34. Simulation scenarios considered.

| **Scenario** | **Weather data used** | **Constructions** (detailed in Table 35) |
|---|---|---|
| **Urban \| *'Urb'* (Moorgate)** | | |
| *Def-Urb-Stone* | Unmodified Reading DSY. | *Default scenario:* using stone façades with glazing ratio (GR) of 0.30. |
| *Urb-Stone* (*base*) | Reading DSY modified using the UWG to include UHI influence. | *Base scenario:* using stone façades with GR of 0.30. |
| *Urb-Def-VG* | Reading DSY modified using the UWG to include UHI influence and default canyon vertical greening cover. | *Default vertical greening scenario:* using stone façades with vertical greening (i.e., direct green façade) and GR of 0.30. |
| *Urb-GF* | Reading DSY modified using the UWG to include UHI influence and canyon GF cover. | *Green façade scenario:* using stone façades with direct green façade and GR of 0.30. |
| *Urb-LW* | Reading DSY modified using the UWG to include UHI influence and canyon LW cover. | *Living wall scenario:* using stone façades with living wall and GR of 0.30. |
| **Suburban \| *'SUrb'* (Wimbledon)** | | |
| *Def-SUrb-Brick* | Unmodified Reading DSY. | *Default scenario:* using brick façades with glazing ratio (GR) of 0.30. |
| *SUrb-Brick* (base) | Reading DSY modified using the UWG to include UHI influence. | *Base scenario:* using brick façades with GR of 0.30. |
| *SUrb-Def-VG* | Reading DSY modified using the UWG to include UHI influence and default canyon vertical greening cover. | *Default vertical greening scenario:* using brick façades with vertical greening (i.e., direct green façade) and GR of 0.30. |
| *SUrb-GF* | Reading DSY modified using the UWG to include UHI influence and canyon GF cover. | *Green façade scenario:* using brick façades with direct green façade and GR of 0.30. |
| *SUrb-LW* | Reading DSY modified using the UWG to include UHI influence and canyon LW cover. | *Living wall scenario:* using brick façades with living wall and GR of 0.30. |

Output from the UWG was first used to characterise the respective canyon climates generated (described in Table 34, p. 197). The output was then used to characterise exterior building wall temperatures ($T_{canWall}$) and resulting surface flux modifications, followed by indoor space-conditioning energy consumption impact for the buildings facing the respective canyons (normalised and reported as consumption per square meter of building area).

The generated Moorgate and Wimbledon base scenario UWG canyon climate files were also applied to their respective thermal models (created using the dynamic simulation platform IES-VE, [393]), to simulate the space-conditioning energy use influence of including the heat island effect; i.e., the comparison between *Def-Urb-Stone* | *Def-SUrb-Brick* and *Urb-Stone* | *SUrb-Brick* base scenarios (see Table 34).

Table 35. Parameter inputs used for simulations.

| **Parameter** | | **Moorgate (central urban)** | **Wimbledon (suburban)** |
|---|---|---|---|
| **Urban building block** | Canyon block dimensions: | L 60 × D 35 × H 24.5 m | L 60 × D 35 × H 24.5 m |
| | Context block dimensions: | L 60 × D 35 × H 24.5 m | L 60 × D 35 × H 10.5 m |
| | Mean floor height: | 3.5 m | |
| | Assumed building use: | Medium office | |
| | Total office area in radius: | 3,410,400 m$^2$ | 2,360,400 m$^2$ |
| **Simplified base building constructions** (existing) | **Wall**<br>Material and thickness: | Type: *Stone*<br>Portland stone \| plaster<br>Thickness: 0.3 \| 0.025 m<br>U-value: 2.33 W·m$^{-2}$·K$^{-1}$<br>Albedo, $\rho_{surf}$: 0.62<br>Emissivity, $\varepsilon_{surf}$: 0.90 | Type: *Brick*<br>Brick \| gypsum plaster<br>Thickness: 0.215 \| 0.035 m<br>U-value: 1.96 W·m$^{-2}$·K$^{-1}$<br>Albedo, $\rho_{surf}$: 0.30<br>Emissivity, $\varepsilon_{surf}$: 0.93 |
| | Glazing: | Ratio (GR): 0.3 (30%)<br>Unit U-value: 1.93 W·m$^{-2}$·K$^{-1}$ | |
| | **Roof**<br>Material and thickness: | Type: Flat roof<br>Gravel \| expanded polystyrene \| concrete \| ceiling tiles<br>Thickness:<br>0.075 \| 0.1 \| 0.3 \| 0.05 m<br>U-value: 0.24 W·m$^{-2}$·K$^{-1}$ | Type: Inclined roof (45°)<br>Clay tiled \| timber insulation \| gypsum plasterboard<br>Thickness:<br>0.015 \| 0.1 \| 0.25 \| 0.015 m<br>U-value: 0.23 W·m$^{-2}$·K$^{-1}$ |
| **Priming** | Initial construction temperature: | 20°C | |
| **Building gains** | Lighting and equipment: | 12 and 25 W·m$^{-2}$ | |
| | Occupancy: | 6 m$^2$·person$^{-1}$ | |
| | Gains profile used: | Weekdays 07:00-19:00 @0.9 load.<br>Saturday 07:00-17:00 @0.4 load.<br>Sunday Full-day @0.1 load. | |
| | Infiltration: | 0.5 ach | |
| | Ventilation: | 0.002 m$^3$·s$^{-1}$·m$^{-2}$ | |

| Parameter | | | Moorgate (central urban) | Wimbledon (suburban) |
|---|---|---|---|---|
| **Building space-conditioning** | Cooling system: | | Air | |
| | Heating efficiency: | | 0.80 | |
| | Heating setpoint schedule: | Weekdays and Saturday | 00:00-05:00 @05°C \| 05:00-06:00 @15°C \| 06:00-22:00 @20°C \| 22:00-23:00 @15°C \| and 23:00-00:00 @05°C. | |
| | | Sundays | Full-day @5°C. | |
| | Cooling setpoint schedule: | Weekdays | 00:00-05:00 @35°C \| 05:00-06:00 @27°C \| 06:00-22:00 @23°C \| 22:00-23:00 @27°C \| and 23:00-00:00 @35°C. | |
| | | Saturday | 00:00-06:00 @35°C \| 06:00-18:00 @23°C \| 18:00-19:00 @27°C \| and 19:00-00:00 @35°C. | |
| | | Sunday | 00:00-06:00 @35°C \| 06:00-18:00 @50°C \| and 18:00-00:00 @35°C. | |
| | Heat rejected to canyon: | | 50% | 25% |
| **Roads** | Material and thickness: | | Asphalt \| 0.5 m | |
| **Urban & Rural** | Vegetation coverage ratio: | | Urban: 0.005<br>Rural: 0.8 | 0.2<br>0.8 |
| **Urban area** | *Mean building height*:* | | *24.5 m* | *10.8 m* |
| | *Horizontal building density ratio*:* | | *0.598* | *0.480* |
| | *Vertical-to-horizontal area ratio*:* | | *0.99* | *0.35* |
| | Tree coverage ratio: | | 0.001 | 0.080 |
| | Non-building sensible heat rejection: | | 22.68 W·m$^{-2}$ | 1.77 W·m$^{-2}$ |
| | Non-building latent heat rejection: | | 2.268 W·m$^{-2}$ | 0.18 W·m$^{-2}$ |
| | Daytime boundary-layer height: | | 1000 m | 850 m |
| | Night-time boundary-layer height: | | 80 m | 50 m |
| | Characteristic neighbourhood length: | | 500 m | |
| | Tree and grass latent fractions: | | 0.7 and 0.5 | |
| | Vegetation albedo ($\rho_{veg}$): | | 0.25 | |
| | Vegetation contribution start-to-end: | | April-to-September (deciduous) | |
| **Reference weather site** | Latitude, longitude (for Reading): | | 51.446, - 0.957 | |
| | Distance from study sites: | | ~60 km due west | ~52 km due west |

* Key neighbourhood morphological parameters.

Table 36. Construction parameters of vertical greening additions.

| Parameter | | Green façade (GF) | Living wall (LW) |
|---|---|---|---|
| **Vertical greening construction** (hypothetical) | Material and thickness: | Evergreen climbing plants (*H. helix*) \| host-wall<br><br>Thickness:<br>$z_{veg}$: 0.2 m \| from Table 35 | Herbaceous evergreens \| saturated soil (substrate) \| host-wall<br><br>Thickness:<br>$z_{veg}$: 0.25 \| 0.1 m \| from Table 35 |
| | U-value (excluding host-wall): | 1.49 W·m$^{-2}$·K$^{-1}$ | 0.46 W·m$^{-2}$·K$^{-1}$ |
| | Wall vegetation coverage ratio: | 0.5 (50%) | |

| **Parameter** | | **Green façade (GF)** | **Living wall (LW)** |
|---|---|---|---|
| **Vegetation** (evergreen) | Canopy absorptivity ($\alpha_{veg}$): | $(1 - \rho_{veg} - \tau_{veg})$ | |
| | Canopy albedo ($\rho_{veg}$): | 0.20 | |
| | Canopy emissivity ($\varepsilon_{veg}$): | 0.95 | |
| | Leaf-width ($W_{leaf}$): | 0.075 m | 0.060 m |
| | Open stomatal conductance ($g_s$): | 0.30 mol·m$^{-2}$·s$^{-1}$ | 0.20 mol·m$^{-2}$·s$^{-1}$ |
| | Closed stomatal conductance ($g_s$): | 0.01 mol·m$^{-2}$·s$^{-1}$ | |
| | Radiation attenuation coefficient ($k$): | 0.5 (assumed) | |
| | Stomatal arrangement: | Hypostomatous | Amphistomatous (assumed) |
| | Leaf-angle ($\theta_{leaf}$): | 45° (assumed) | |
| **Substrate** (LW only) | Density ($\dot{\rho}_{sub}$): | N/A | 1,230 kg·m$^{-3}$ |
| | Specific heat capacity ($c_{p_{sub}}$): | N/A | 1,140 J·kg$^{-1}$·K$^{-1}$ |
| | Volumetric heat capacity: | N/A | 2,310,000 J·m$^{-3}$·K$^{-1}$ |
| | Albedo ($\rho_{sub}$): | N/A | 0.4 |
| | Emissivity ($\varepsilon_{sub}$): | N/A | 0.9 |
| | Soil moisture, permanent wilting threshold ($\eta_{wilt}$): | N/A | 0.39 (peat soil) |
| | Soil moisture, root zone min. ($\eta_{root}$): | N/A | 0.70 (assumed) |

## 7.3 Findings

The following presents firstly, a parameter sensitivity assessment for the '*Def-VG*' application approach; followed by key features of the canyon climates generated by the UWG for the scenarios; their resulting influence on external building surface temperatures and flux; and finally, indoor space-conditioning energy consumption impact for the buildings off the Moorgate and Wimbledon street canyons.

### 7.3.1 Parameter sensitivity of default vertical greening application

The Moorgate and Wimbledon configurations were simulated first to ascertain the sensitivity of key user-specified input parameters on the principal summertime canyon outputs of the default vertical greening application approach (i.e., *Def-VG,* see Table 34, p. 197). This default approach relies on two essential user-specified inputs: the 'latent fraction' that determines the partitioning of the canyon wall flux ($Q_{canWall}$), and the specified 'vegetation coverage ratio' for the canyon walls that determines the extent of this partitioned flux. With these two parameters considered as independent variables, a one-at-a-time (OAT) parametric approach was implemented to determine their sensitivity to outcomes.

The results showed that the correlation coefficients for the two variables were very strong for most model outputs in both configurations, save for the relatively lower $Q_{canWall}$ latent fraction variation for the urban configuration (Table 37). Negative correlations were presented for $T_{can}$, $V_{can}$, $\Delta T_{UHI}$, and canyon building wall temperature ($T_{canWall}$) latent fraction variation, as well as $RH_{can}$, $T_{canWall}$, and $Q_{canWall}$ for the vegetation coverage ratio variation (Fig. 94). Notably, the urban configuration correlations were marginally stronger for $T_{can}$, $V_{can}$, $\Delta T_{UHI}$, and $T_{canWall}$ latent fraction variation, while this was also true for $T_{can}$ and $\Delta T_{UHI}$ vegetation coverage ratio variation.

Table 37. Sensitivity correlation coefficients from OAT parameter assessment.

| UWG summer outputs | Latent fraction | | | | Vegetation coverage ratio | | | |
|---|---|---|---|---|---|---|---|---|
| | Urban | | Suburban | | Urban | | Suburban | |
| | $r$ | $r^2$ | $r$ | $r^2$ | $r$ | $r^2$ | $r$ | $r^2$ |
| $T_{can}$ | **-0.95** | 90% | **-0.96** | 92% | **0.97** | 94% | **0.88** | 77% |
| $RH_{can}$ | **0.94** | 88% | **0.95** | 90% | **-0.99** | 98% | **-0.97** | 94% |
| $V_{can}$ | -0.87 | 76% | -0.94 | 88% | 0.99 | 98% | 1.00 | 100% |
| $\Delta T_{UHI}$ | -0.95 | 90% | -0.96 | 92% | 0.97 | 94% | 0.88 | 77% |
| $T_{canWall}$ | -0.92 | 85% | -0.92 | 85% | -0.99 | 98% | -0.84 | 71% |
| $Q_{canWall}$ | 0.79 | 62% | 0.90 | 81% | -1.00 | 100% | -0.99 | 98% |

Notes: Summertime results from 20 simulations per configuration (i.e., total = 40). All datasets normally distributed; and all Pearson's $r$, *p-values* <0.01.

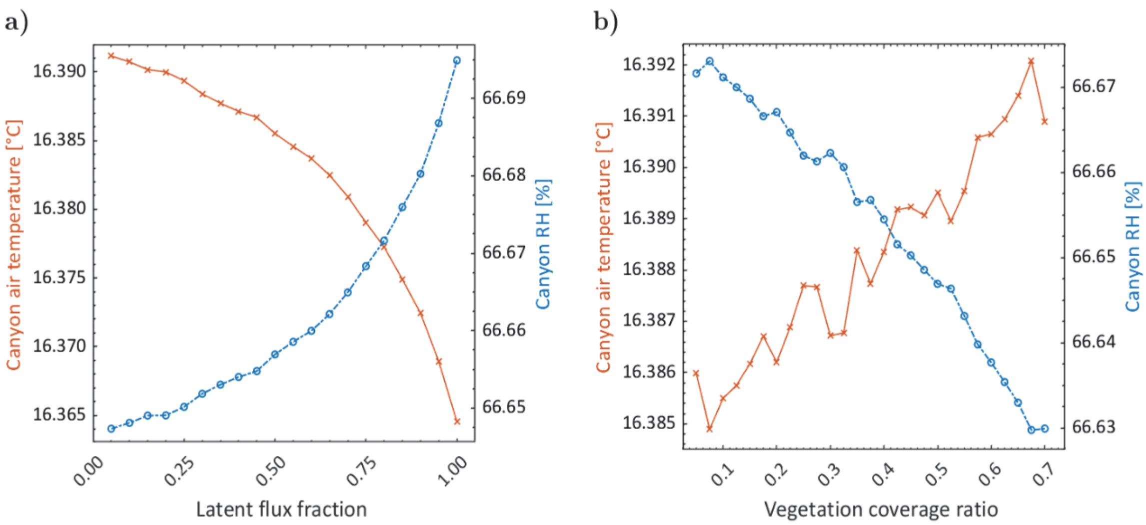


*Fig. 94. Summertime mean $T_{can}$ and $RH_{can}$ variation by latent fraction (0-to-1), (a); and vegetation coverage ratio (0-to-0.7* [XXIII]*) variation (b).*

[XXIII] Given that the default glazing ratio used for the study was 0.3.

## 7.3.2 Canyon microclimate profiles

The summertime heat island mean daily maxima for urban and suburban scenarios ranged between 3.34, ±2.09 and 4.41, ±2.32 K (N = 153 days), while mean daily minima ranged between -0.32, ±0.52 and 0.20, ±0.52 K (Fig. 95a, p. 202). Notably the latter mean daily minima for the urban scenarios presented positive values, while the suburban scenarios presented negative values to suggest greater ‘cool island’ occurrences[XXIV]. When hourly resolution $\Delta T_{UHI}$ was examined (Fig. 95b), such cool island occurrences were identified in all scenarios with intensities ranging between <0 and -2.5 K representing a range between ~2.9 and 4.0% for the urban scenarios, while the suburban scenarios showed a significantly higher proportional range between 8.2 and 9.2% of the hours simulated (N = 3,672). The hourly $\Delta T_{UHI}$ resolution also identified peak values ranging between >6.5 and ≤12.5 K to range between 2.7 and 3.0% for the urban scenarios, while for the suburban scenarios this was notably a lower and narrower range of around 1% of the total hours simulated.

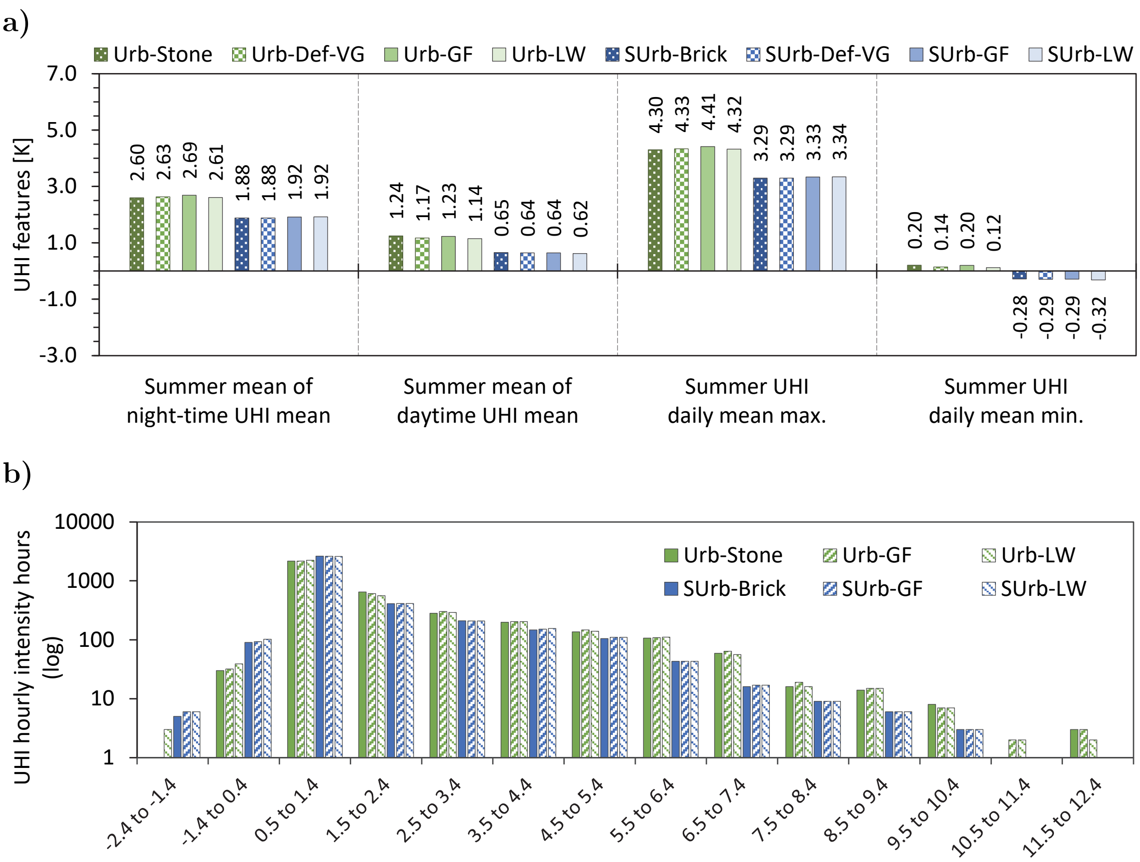


*Fig. 95. Summertime mean heat island features (a); and urban and suburban $\Delta T_{UHI}$ log₁₀ frequencies (b) for the scenarios simulated.*

[XXIV] Cool island occurrences are indicative of the area having warmed less rapidly than the surrounding context during the period highlighted, and does not necessarily mean that an actual sink or cooling effect had occurred.

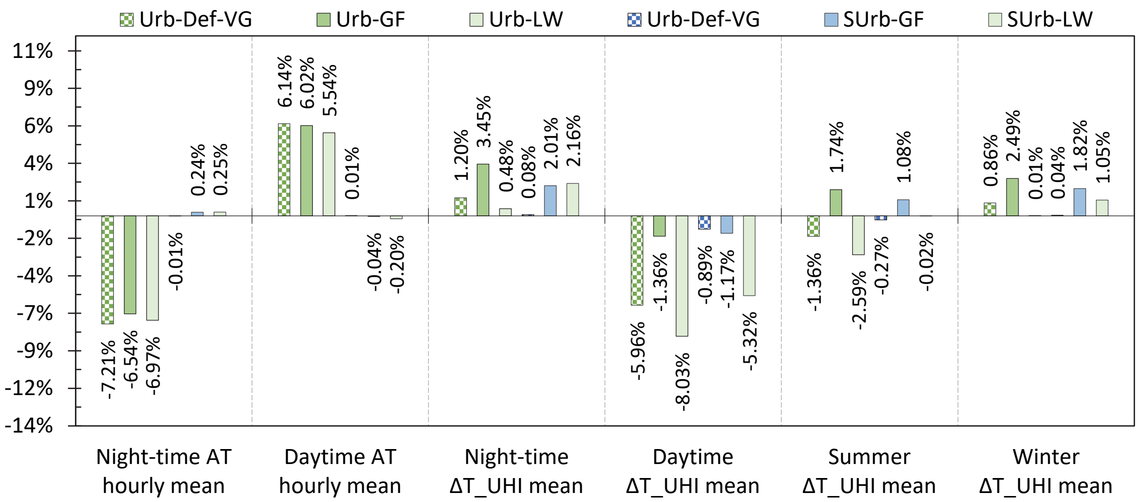


*Fig. 96. Summertime mean air temperature (AT) and $\Delta T_{UHI}$ modifications for scenarios following vertical greening application.*

When all hours of the day were included (i.e., 24-hours), urban $\Delta T_{UHI}$ means were considerably higher than suburban scenarios (increase ranging between 0.60-0.67 K). However, when the hours of the day were divided between daytime (12 hours from 06:00-to-18:00) and night-time (residual hours) urban and suburban $\Delta T_{UHI}$ means, the daytime values ranged between 0.62, ±0.47 and 1.24, ±0.59 K, while the night-time ranged between 1.88, ±1.11 and 2.69, ±1.38 K (Fig. 95a, p. 202). Across all scenarios night-time $\Delta T_{UHI}$ means were always higher than the daytime (in agreement with literature), while vertical greening application served to increase night-time means, and reduce daytime means (Fig. 96).

When the daytime | night-time divide of $\Delta T_{UHI}$ maxima and minima were considered, the urban context generated greater night-time maxima occurrences (where $\Delta T_{UHI}$ was >6.5 K; *Urb-Stone:* 1.95%, relative to *SUrb-Brick:* 0.58%). The application of vertical greening modified these occurrences for the urban setting from 1.95→2.19% and 1.89% with green façade and living wall application respectively, while for the suburban setting the influence was minimal (constant for green façade application at 0.58%, and marginally increased for living walls at 0.60%). Living wall application notably reduced night-time $\Delta T_{UHI}$ maxima occurrences in the urban setting, annually by 2.8%, and by 1.6% in the summer. With daytime cool island conditions, the suburban context presented greater occurrences (*SUrb-Brick:* 10.8%, relative to *Urb-Stone:* 3.84%). Vertical greening application increased these cool island occurrences for the urban setting from 3.84→4.09% and 4.89% for green façade and living wall application respectively, while for the suburban setting these occurrences were also increased from 10.77→11.06% and 11.17% respectively.

The *Def-VG* approach means broadly complemented above trends, with the values typically falling between those for the base scenario and green façade application (Fig. 95a, p. 202 and Fig. 96, p. 203). The magnitude of changes output for this approach however is determined by the above considered user-input latent fraction, and thus is only significant for situations where this value has been accurately prescribed based on the available literature or determined by empirical means (i.e., only developed as a simulation option). The data output from this approach is therefore not assessed beyond this point in the study.

**a)**

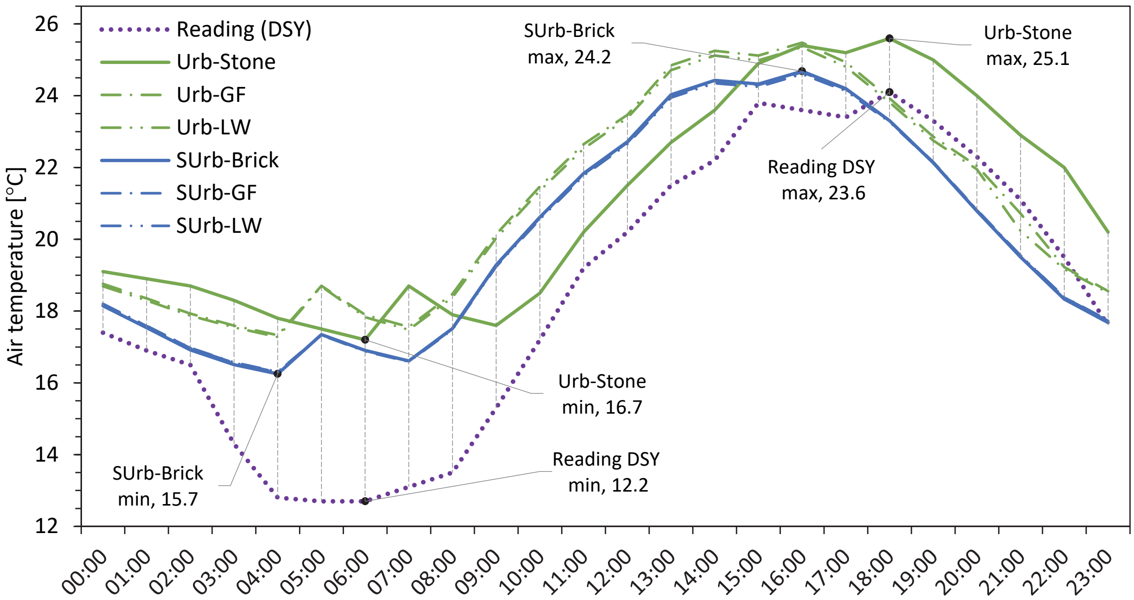


**b)**

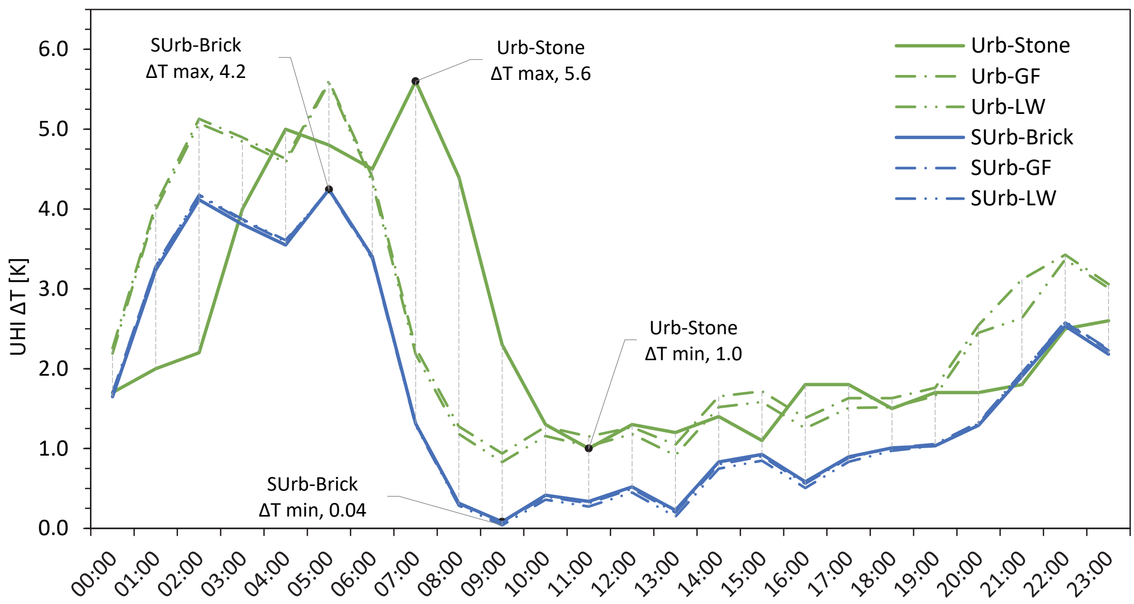


*Fig. 97. Summer solstice $T_{can}$ profiles relative to the Reading DSY profile (a); and summer solstice $\Delta T_{UHI}$ (intensity) profiles (b) for the scenarios simulated.*

While the above observations can be made for means, examining daily profiles highlighted eccentric features. For example, profiles for the summer solstice (21-June) highlighted the situation when the hourly $\Delta T_{UHI}$ maximum for the day was reached after sunrise (~04:50), at ~05:30 for the *SUrb-Brick,* and much later and with greater intensity at ~07:30 for the *Urb-Stone* scenario (Fig. 97a & b, p. 204). Notably, the addition of vertical greening (GF or LW) to the *Urb-Stone* base scenario meant that this peak was reached much earlier (i.e., eliminated the lag), to be around the same time as all *SUrb-Brick* scenarios. The summer solstice profiles also showed greater variation between urban green façade and living wall profiles relative to the *Urb-Stone* base scenario, while the suburban profiles were broadly similar for all. In general, the daily profiles highlighted urban setting $\Delta T_{UHI}$ profiles to be much higher in amplitude (i.e., warmer), than corresponding suburban profiles (Fig. 97b).

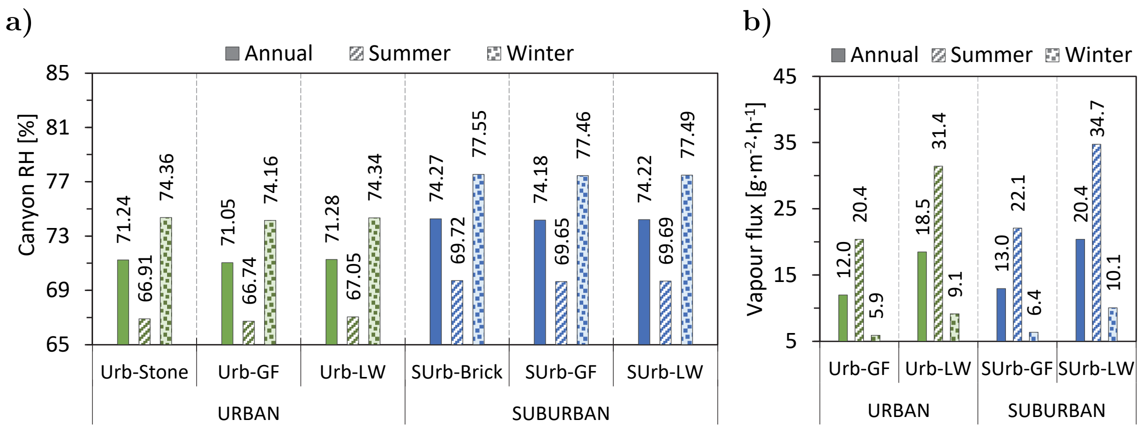


*Fig. 98. Mean annual, summer, and winter $RH_{can}$ (a); and vapour flux densities (b) for scenarios.*

The mean $RH_{can}$ values highlighted higher values for the suburban scenarios than for the urban (Fig. 98a), while winter means were much greater than the summer for all scenarios. The addition of vertical greening to both urban and suburban scenarios marginally reduced means with green façade application, while the converse was true with living wall application. Vapour flux densities highlighted summer contributions from vertical greening to be significantly higher than in winter, with living wall application patently contributing much higher values than green façades (Fig. 98b).

### 7.3.3 Canyon building surface temperatures and flux

When annual canyon building wall temperature ($T_{canWall}$) hourly means were considered, base *Urb-Stone* and *SUrb-Brick* surfaces were marginally cooler than the respective vertical greening scenarios (by 0.01-0.86 K), while green façade surfaces were always the warmest

(Fig. 99). Notably, living wall $T_{canWall}$ means were relatively cooler than green façade means, with greater influence during the summer (*Urb-Stone*: 1.10; and *SUrb-Brick*: 0.51 K cooler), than in winter (*Urb-Stone*: 0.65; and *SUrb-Brick*: 0.36 K cooler).

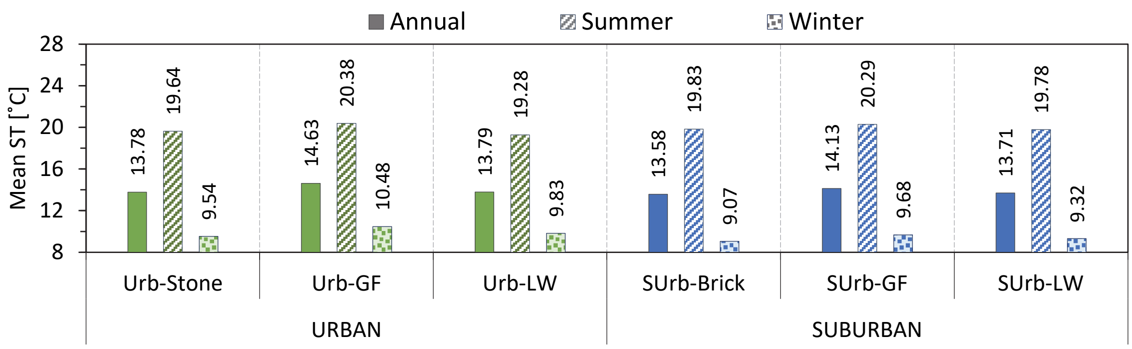


*Fig. 99. Mean annual, summer, and winter $T_{canWall}$ for scenarios.*

a)

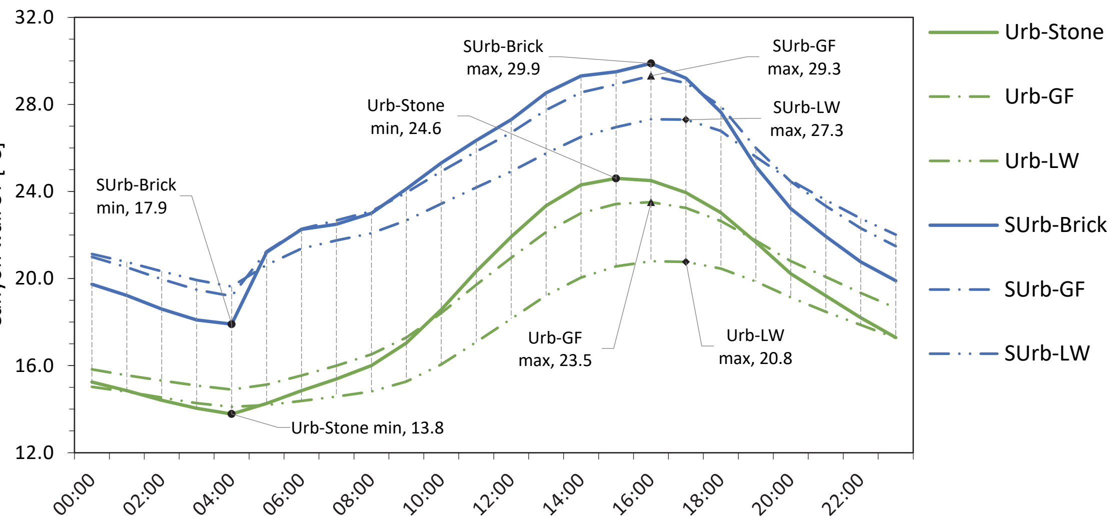


b)

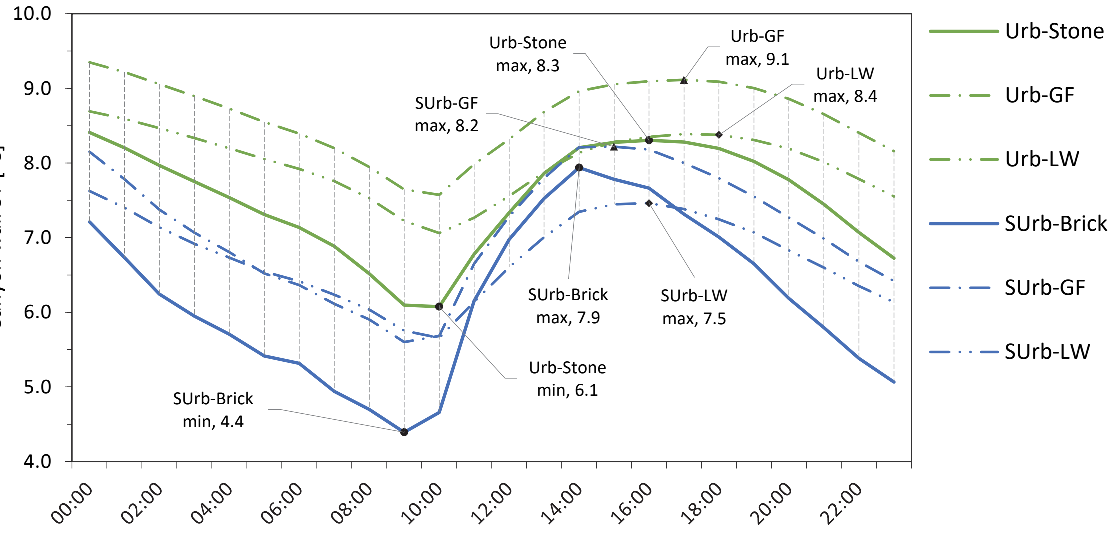


*Fig. 100. Summer (a); and winter solstice (b) building $T_{canWall}$ profiles for scenarios.*

The profiles for the summer solstice demonstrated higher $T_{canWall}$ for *SUrb-Brick* surfaces relative to *Urb-Stone* (Fig. 100a, p. 206), while the converse was true with the winter solstice profiles (Fig. 100b). Vertical greening addition reduced the peak-to-peak amplitudes to ‘flatten’ the $T_{canWall}$ profiles, which translated to cooler peak temperatures for the summer solstice and mostly (except for *SUrb-LW*) warmer peak temperatures for the winter solstice. The summer solstice cooling influence was greater with living wall than green façade profiles, while the winter solstice warming influence was greater with green façade than living wall profiles, with pronounced influence evident with the urban scenario. The solstice profiles for *Urb-Stone* and *SUrb-Brick* also indicated a temporal shift for when peak temperatures occur, with a lag of two hours for the summer and one for the winter solstice profiles. Adding vertical greening marginally delayed the peak occurrence, with living wall scenarios presenting a greater delay relative to green façade scenarios.

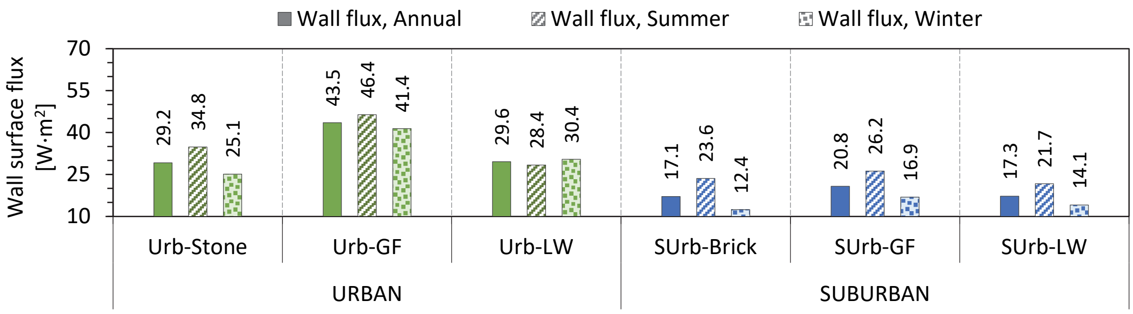


*Fig. 101. Mean canyon $Q_{canWall}$ for scenarios.*

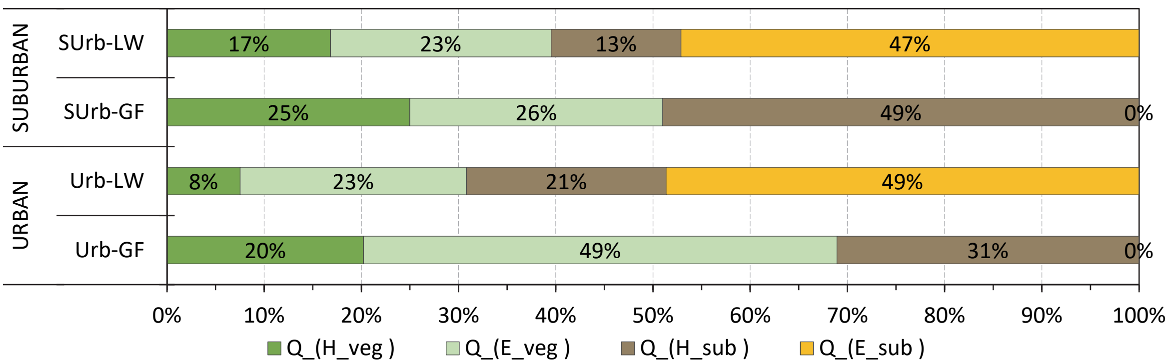


Note: For green façade: $Q_{H_{Hw}}$; and living wall: $Q_{H_{sub}}$.

*Fig. 102. Mean canyon wall surface convective flux partitioning for vertical greening scenarios.*

Canyon wall surface flux ($Q_{canWall}$) data revealed urban mean values to be significantly higher than suburban, with summertime flux making dominant contributions in all except the urban living wall application scenario (i.e., *Urb-LW*, Fig. 101). Green façade application made higher contribution relative to living wall application, which was pronounced greatest for the urban context. The surface convective flux partitioning revealed living wall substrate latent flux ($Q_{E_{sub}}$) to be dominant for both urban and suburban contexts, while green façade host-wall sensible flux ($Q_{H_{Hw}}$) was dominant for the suburban, and vegetation sensible flux ($Q_{H_{veg}}$) was dominant for the urban context (Fig. 102, p. 207).

### 7.3.4 Canyon building space-conditioning

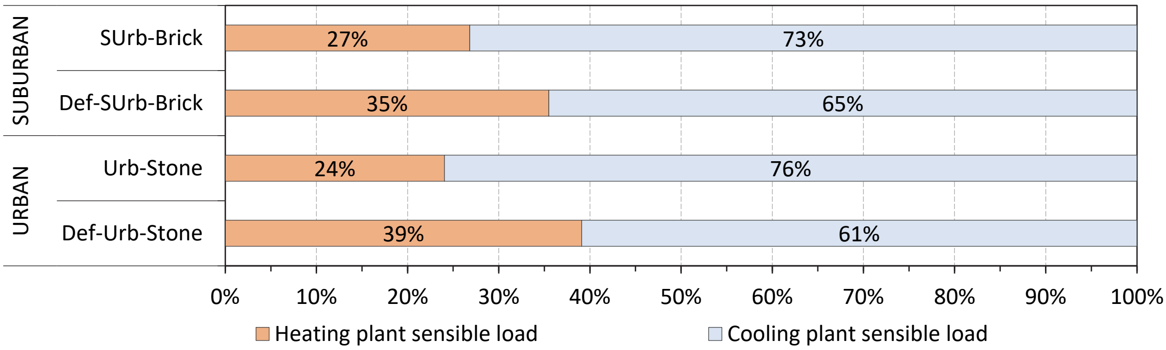


*Fig. 103. Annual space-conditioning load partitioning for default and base scenarios.*

Including heat island influence on summer cooling and winter heating loads demonstrated significant differences between urban and suburban scenarios [45]. The IES-VE simulation of the urban *Def-Urb-Stone* scenario (i.e., without UWG modification) relative to the *Urb-Stone* base scenario (i.e., with UWG modification), highlighted the inclusion of heat island influence to have resulted in a 30% increase in summertime cooling demand, while winter heating demand was reduced by 36%. Overall, this meant that heat island influence had increased net annual space-conditioning demand by 4.2%. For the suburban context, the IES-VE simulation of *Def-SUrb-Brick* relative to the *SUrb-Brick* base scenario highlighted heat island influence to have increased the summer cooling demand by 16%, while winter heating demand was reduced by 23%. Overall, this meant that heat island influence had increased net annual space-conditioning demand by 2.5%. With both urban and suburban contexts, the inclusion of heat island influences patently increased the proportional significance of summer cooling to the respective annual space-conditioning profiles (Fig. 103).

Annual mean consumption was significantly higher for the suburban scenarios, with winter heating dominating. Vertical greening application had most impact on reducing mean summer heating consumption; followed by winter heating, winter cooling, and summer cooling. All means therefore were reduced to some extent, with reductions pronounced for the urban context than suburban, and with living wall application than green façade (Fig. 104).

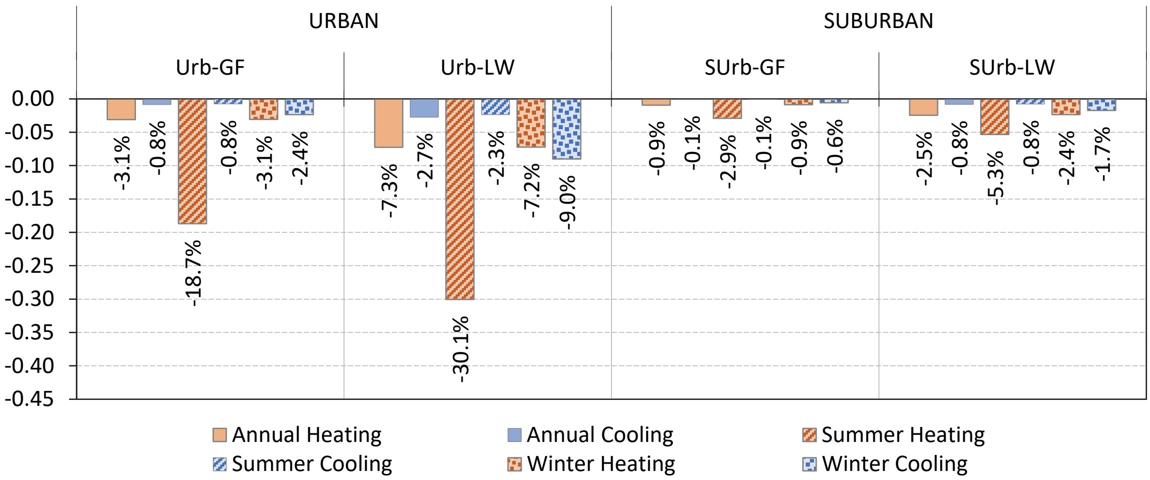


Note: Negative values signify relative savings.

*Fig. 104. Space-conditioning energy consumption impact of vertical greening application.*

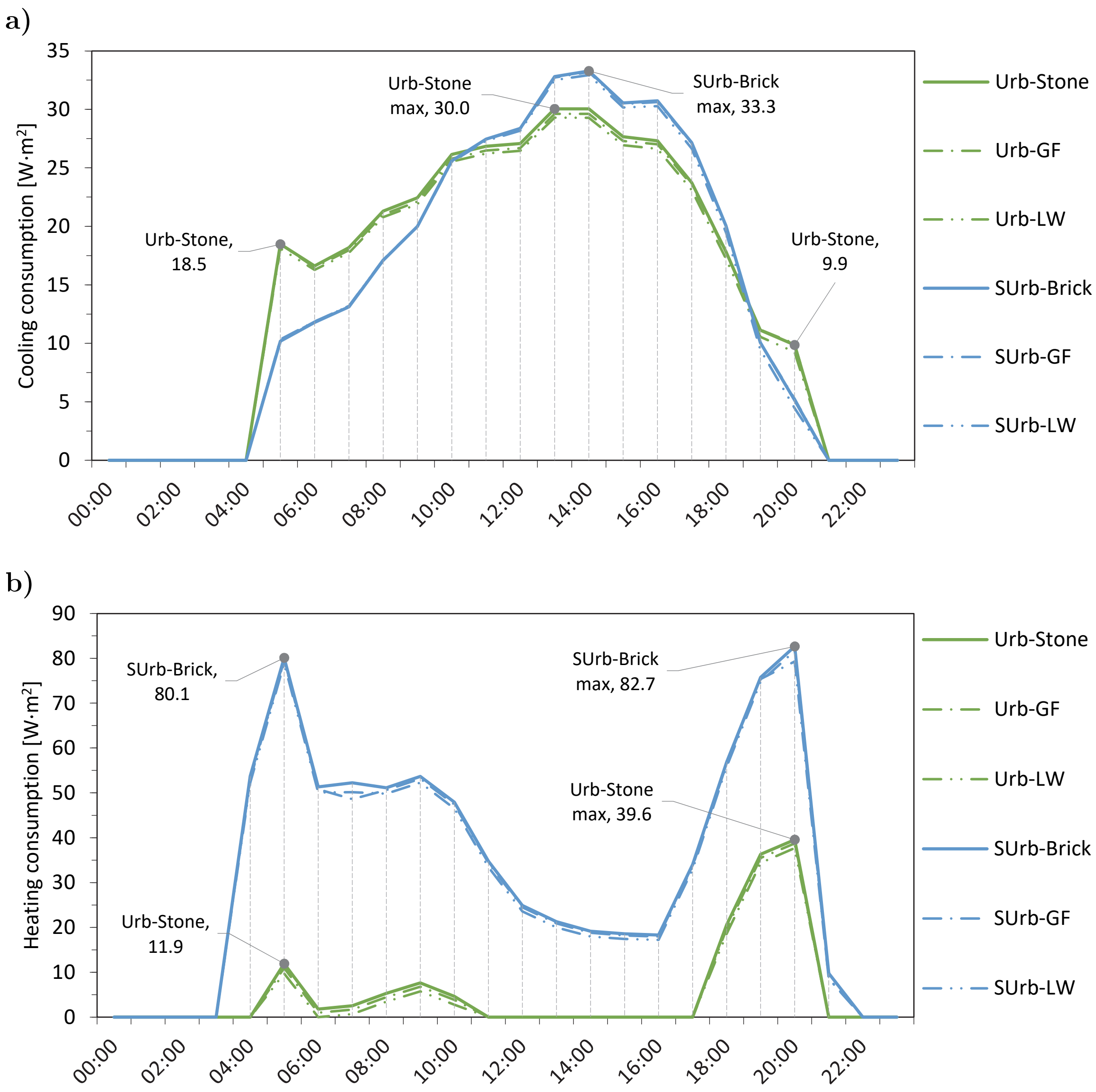


*Fig. 105. Summer solstice cooling (a); and winter solstice heating energy consumption (b) profiles for scenarios (per m² of building floor area).*

Examining the summer solstice cooling consumption profiles highlighted urban scenarios to have a higher consumption period early in the morning (i.e., priming), and a relatively smaller, and shorter higher consumption period later in the evening relative to suburban scenarios (Fig. 105a, p. 209). The suburban cooling peaks however were higher than the urban peaks. The winter solstice heating profiles in comparison showed significantly increased consumption for the suburban scenarios relative to the urban, while both demonstrated twin peaks with one in the morning and the other later in the evening (Fig. 105b). The solstice profiles in general demonstrated vertical greening application to reduce consumption, mostly evident nearer to the peaks (Fig. 105).

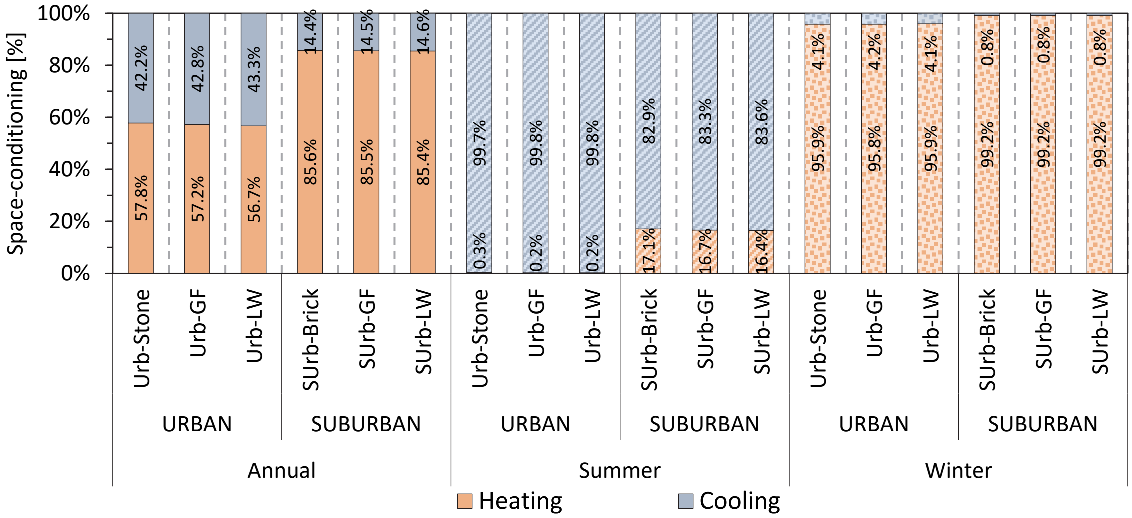


*Fig. 106. Annual, summer, and winter, space-conditioning load partitioning for scenarios.*

The space-conditioning energy consumption partitioning demonstrated cooling to be of greater significance to urban annual profiles than suburban (Fig. 106). In the summer, cooling consumption was near 100% for urban scenarios, while some transitional heating consumption was still evident for suburban scenarios (<17.1%). This contrasted against the winter, where urban scenarios still presented some transitional cooling consumption (<4.2%), while in the suburban context this was near negligible (<0.8%).

## 7.4 Discussion

The following introduces preceding work on London's heat island to aid the comparative discussion of UWG outcomes including simulated heat island influence. Thereafter it considers the significance of façade materials and vertical greening application scenarios, followed by impact on indoor space-conditioning energy use.

### 7.4.1 London's heat island and the scenarios simulated

The earliest recorded heat island observations are of the city of London, when Luke Howard [47] published urban air temperature ($T_{urb}$) timeseries data spanning a decade of measurements to identify the city to be 0.6 K warmer in the summer and 1.2 K warmer in the winter than surroundings. Howard [47] also observed the city to be warmest at night by 2.05 K, while during the day it was 0.18 K cooler to demonstrate a modest 'cool island' effect (in [390]). The study of the relative warming of London has since been furthered by several longitudinal surveys to confirm these findings and identify trends. As examples, Moffitt [394] identified ~0.8 K mean $T_{urb}$ increase at Kew Gardens relative to a rural site at Rothamsted (between 1878-to-1968); while Chandler [112] identified the annual central London mean to be 1.4 K warmer (1931-to-1960), with a monthly mean value of 1.6 K for the summer and 1.2 K for winter (in [390]). More recent timeseries analysis by Lee [395] had identified the central London warming trend to have increased in relation to minimum $T_{urb}$ (1962-to-1989), while maxima had decreased, and the mean had remained constant. Furthermore, the study found the summer daytime mean $\Delta T_{UHI}$ to have decreased from ~0.5 to 0.25 K, and the night-time $\Delta T_{UHI}$ to have increased by ~0.5 K [395]. Wilby [396] broadly found similar results considering the period between 1958 and 1998, while the Jones & Lister [397] study considering data from several central sites also found the relative increasing warming trend noted for periods earlier in the twentieth century to have stabilised in recent times. Considering these observations, central London sites are projected as likely to maintain their $\Delta T_{UHI}$, while sites in suburban London are hypothesised to demonstrate intensification [397]. The significant variable affecting the experience of this trend is therefore the radial distance from the core of the city [396,398]. Watkins *et al.* [390] found that 77% of the variance of the mean night-time $T_{urb}$ measured across London to be strongly correlated to the radial distance of each location (daytime presented weaker association given the higher daytime thermal inversion elevation presenting greater dispersion), while the radial centre or thermal core was identified as the City of London, characterised by its high-density development with reduced green-cover and high anthropogenic emissions [390]. These observations suggested the transition in morphologies and materiality typically observed when traversing from the urban core to the peripheries to be significant factors affecting the potency of the heat island load experienced at specific localities, with changes following densification trends likely to influence future heat island intensification.

London's heat island maxima and minima are discussed in higher resolution studies typically considering central sites that have been monitored for limited durations. As summertime examples, Watkins *et al.* [390] presented data from 1999 to highlight peaks of ~7 K; and Kolokotroni & Giridharan [399] also presented data from 1999 to highlight a maximum daytime peak of 8.9 K, and a nocturnal maximum of 8.6 K observed during clear-sky periods with low wind velocities; while Doick *et al.* [79] highlighted even higher nocturnal peaks of >10 K from west London data. Wintertime studies have also highlighted high peaks, with data gathered by Giridharan & Kolokotroni [400] for example having identified maximum peaks of ~9 K for both day and night-time under low wind velocity conditions (<5 m·s$^{-1}$). In summary, these examples present ample evidence for $\Delta T_{UHI}$ maxima reaching significantly high values at central sites during the day and night-time, and throughout the year. However, a comparison between urban core values and those at the peripheries is difficult to consider, given that studies seldom attempt to assess the intermediary condition represented by suburban localities.

Considering the above historic observations and trends for London, the heat island simulated by the UWG could be said to fall within a plausible range, with the summertime daily means for the street canyons ranging between 1.81, ±0.83 to 1.89, ±0.85 K (N = 153) for urban scenarios, and relatively lower at 1.21, ±0.69 to 1.23, ±0.69 K for the suburban scenarios simulated. The wintertime daily means were lower as expected, with urban context values ranging from 1.56, ±0.50 to 1.60, ±0.51 K (N = 212 days), and suburban means ranging from 0.94, ±0.33 to 0.96, ±0.34 K. The suburban scenarios generated relatively milder canyon temperatures and as a result $\Delta T_{UHI}$, which is clearly illustrated by the summer solstice profiles (Fig. 97, p. 204). This urban-to-suburban disparity is therefore consistent with previous observations noted above in relation to the decreasing heat island intensity trend when traversing away from the city centre and into the peripheries [390]; which is generally an indication of morphological spread (low density development, dispersal/sprawl), and associated changes in construction types and materiality. This disparity however could become narrower as suburban areas are intensified with development. The suggestion by Jones & Lister [397] that London's suburban areas are likely to show increasing $\Delta T_{UHI}$ in the future is based on the assumption of growth-related policies intensifying development density, associated material use, and reducing green-cover in such areas to transform their character to a more urbanised state with increased heat storage.

When summer daytime and night-time heat island means were considered, the lower values simulated across the scenarios for the day relative to the night-time is consistent with previous studies that highlight its peak influence as a nocturnal occurrence [2,47,396]. Howard's [47] finding of a cooler daytime mean temperature (i.e., cool island) however was not relatable to any of the simulations. This is explained by the fact that cool island conditions simulated tended to be modest and restricted to shorter durations. Notably, occurrences with the urban scenarios were less than expected and limited to hourly incidences as highlighted in the results earlier. This may be attributed to the 20 m street width being broad enough to minimise the canyon self-shading effect (a key contributing factor, [401]), as well as the notably higher anthropogenic heat output used for the Moorgate area (based on Iamarino *et al.* simulations [402]) contributing to relatively higher daytime canyon temperatures. The suburban scenarios in contrast presented relatively cooler daytime canyon temperatures, and a higher number of hours presenting cool island conditions to be experienced in the canyon. This may be attributed to the relatively lower anthropogenic heat output from the suburban context, as well as increased vegetation coverage contributing to a higher proportion of the ground surface flux partitioned as latent flux.

Building fabrics with dominant heavyweight constructions are also identified to generate a warmer heat island effect to be experienced in street canyons at night, while the converse may be true during the daytime [45]. The denser stone material of the *Urb-Stone* base scenario generated greater night-time heat island maxima occurrences in agreement, while in contrast the *SUrb-Brick* base scenario presented greater daytime cool island occurrences. Vertical greening application modified heat island maxima occurrences, with living wall application in the urban context notably reducing night-time instances. This would typically be a benefit given that nocturnal temperatures are more critical for human health [2], although the canyon profile of including office use means that this is unlikely to serve many pedestrians. Daytime cool island occurrences in contrast were increased with vertical greening application. This is significant for daytime pedestrians, with the urban canyon benefiting substantially with living wall application to present a 38.8% increase in occurrences during the critical summer period (i.e., when heat relief is most sought), compared to 3.4% increase for the suburban context. This suggests living wall application to offer greater summertime advantage in improving the urban canyon climate than suburban, while green façade application benefit in both contexts was lower (12 and 3% respectively).

### 7.4.2 Facade material influence

The materiality of the built environment modifies the urban surface energy balance by affecting net radiation and heat storage. The radiative properties of materials are emissivity ($\varepsilon_{surf}$) and albedo ($\rho_{surf}$), while heat storage is affected by mass ($m$), heat capacity ($c$), and thermal conductivity ($\kappa$). Albedo is defined as the ratio of solar energy reflected by a surface (mainly 250-2500 nm wavelengths), and is a determinant of its temperature [2,31,57]. Since 43% of solar energy is in the visible wavelengths (400-700 nm), material colour is strongly correlated with albedo, with lighter coloured surfaces having higher values (>0.7) than darker (<0.2) [100,403]. Higher albedo values lower radiation absorption by building façade materials, which in turn helps to reduce their surface temperature and canyon wall temperature ($T_{canWall}$). The direct effect of this is to reduce canyon air temperature ($T_{can}$), as relatively cooler surfaces have lower sensible flux output to the canyon climate. The indirect effect works in conjunction with material emissivity and thermal storage properties to modify indoor building energy use and eventual feedback to the outdoor canyon climate (i.e., by reducing anthropogenic emissions). This façade albedo influence would have benefited the urban context considered in this study, where the stone was assumed to be homogenous Portland (typical for the Moorgate neighbourhood), which is of a lighter colour and has a high mean albedo ($\rho_{surf}$ = 0.6, [404]), relative to the outer-leaf brick considered for the suburban context ($\rho_{surf}$ = 0.3). However, there was no apparent effect on mean canyon wall temperature to report, given that the mean for the *SUrb-Brick* base scenario was cooler than the *Urb-Stone* base scenario (Fig. 99, p. 206). This suggested that the heat storage properties of the urban canyon walls had greater influence in characterising their wall temperature.

From the energy that is absorbed after reflection ($1 - \rho_{surf}$), a material's ability to store heat (specific heat capacity $c_p$, which at times is referred to as 'thermal mass'), and thermal diffusivity (ease by which heat penetrates the material, $\dot{D} = \kappa / \dot{\rho}\ c_p$), determines its thermal inertia ($I$); a measure of the responsiveness of the material to temperature variations. Heavyweight materials such as stone, and to a lesser extent brick, have relatively higher diffusivity, heat capacity, and thermal inertia, which means that their temperature fluctuations are moderated [405]. When radiation energy is received by such surfaces, the non-reflected energy is absorbed and mostly stored in the material bulk, which serves to increase its temperature. Given the relative higher heat storage property values of stone compared to brick (Table 38), partly explains the higher canyon wall temperature means simulated for the former than latter (Fig. 99, p. 206).

Table 38. Thermal properties of stone and brick materials.

| **Properties** | **Stone*** | **Outer-leaf brick** | **Units** |
|---|---|---|---|
| Density ($\dot{\rho}$) | 2,200 | 1,700 | [kg·m$^{-3}$] |
| Albedo ($\rho$) | 0.62 | 0.30 | |
| Emissivity ($\varepsilon$) | 0.90 | 0.93 | |
| Thermal conductivity ($\kappa$) | 1.70 | 0.84 | [W·m$^{-1}$·K$^{-1}$] |
| Specific heat capacity ($c_p$) | 1,000 | 800 | [J·kg$^{-1}$·K$^{-1}$] |
| Volumetric heat capacity ($\dot{\rho}\ c_p$) | 2,200,000 | 1,360,000 | [J·m$^{-3}$·K$^{-1}$] |
| Thermal diffusivity ($\dot{D} = \kappa/\dot{\rho}\ c_p$) | 0.77 | 0.62 | [mm$^2$·s$^{-1}$] |

Note: * Values for Portland limestone [404].

As the surrounding climate cools during the evening, the stored energy in façade materials becomes a heat source that is reradiated back to the local environment as longwave infrared radiation. The diffused nature of this reradiation encourages reabsorption by other surfaces to trap energy within the street canyon. The delay or lag in the release of stored energy and its inefficient dissipation results in the surrounding canyon climate remaining warmer for longer than expected. The presence of this lag effect is evident when examining canyon wall temperature solstice profiles for the simulated scenarios (Fig. 100, p. 206), where a delay in the peak (i.e., phase shift) was observed between *SUrb-Brick* and *Urb-Stone* profiles, while vertical greening application to both also resulted in relative phase shifts. Living wall application notably presented a greater delay relative to green façade application, which is explained by the additional heat storage benefit contributed from the 100 mm zone of substrate included in its system build-up.

The influence of vertical greening application is best demonstrated by the canyon wall temperature solstice profiles, where the peak-to-peak amplitudes were reduced to flatten or moderate the profiles. The cooler peak temperatures that resulted presented a beneficial summertime influence, while the warmer peaks were a wintertime benefit. This translated best with living wall application for longer durations, where summer means were cooler (by 0.36 K with *Urb-Stone*; and 0.05 K with *SUrb-Brick*), and in winter means were warmer than for base scenarios (by 0.29 K with *Urb-Stone*; and 0.25 K with *SUrb-Brick*). This moderating benefit of living wall application is explained by the joint action of added heat storage and the evaporative flux from the substrate and vegetation. The latter evaporative flux represented >70% of the canyon wall convective surface flux, with marginally greater contribution in the urban context (*Urb-Stone*: 72%). Green façade application in contrast presented warmer means for both summer (by 0.74 K with *Urb-Stone;* and 0.46 K with *SUrb-Brick*), and winter periods (0.94 with *Urb-Stone*; and 0.61 K *with SUrb-Brick*). The insulating effect of the green façade vegetation layer seemed to counter the cooling benefit offered from its evaporative flux, with the latter having represented a relatively moderate significance of 49% of the convective surface flux for the urban context, while in the sub-urban context represented only 26% (Fig. 102, p. 207).

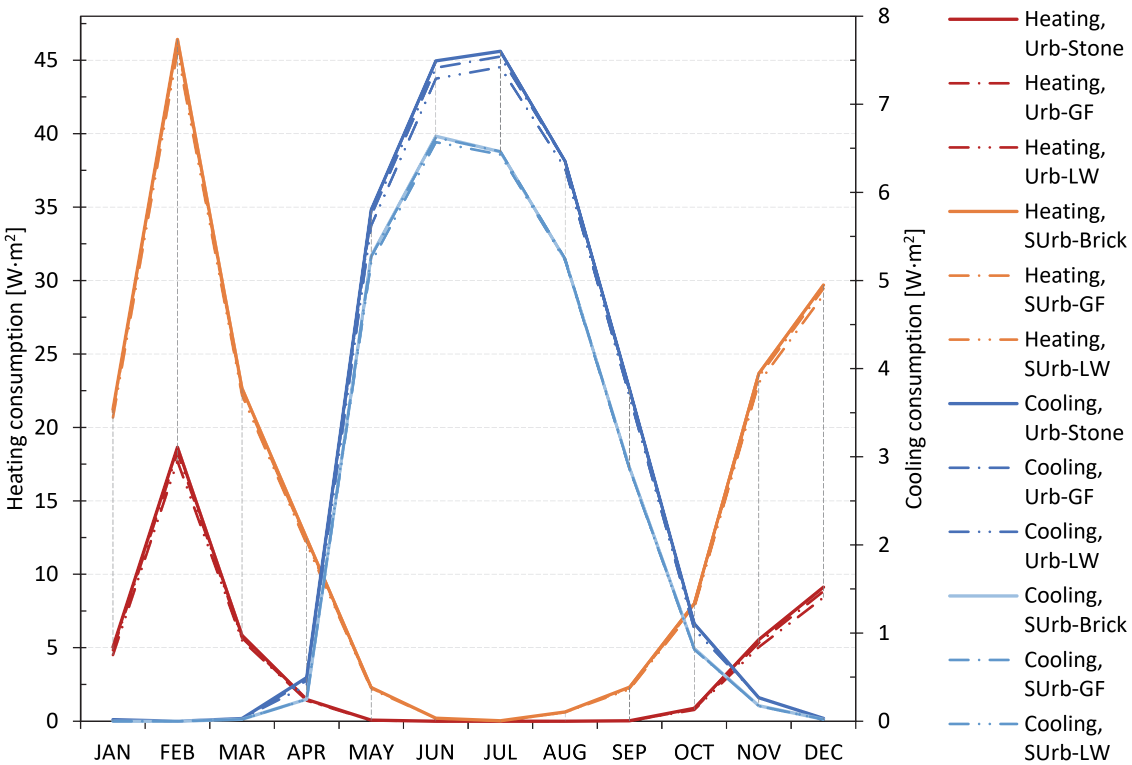


*Fig. 107. Monthly mean space-conditioning consumption for scenarios.*

The damping of summer and winter canyon wall temperature peaks following vertical greening application translated to reductions in indoor space-conditioning energy consumption. All consumption demands were reduced to some extent, with reductions pronounced for the urban context than suburban, and with the above canyon wall temperature observations translating to better performance from living wall application than green façade. Notably, the damping influence worked mostly to reduce heating consumption in contrast to cooling consumption anticipated. Summertime cooling consumption in fact benefited the least from vertical greening application. This is due to absolute heating demand peaks being greater than cooling demand peaks, with any relative reductions also amounting to larger savings in absolute terms (Fig. 107). The overall net influence of vertical greening application was thus a significant saving, with urban scenarios presenting greater savings than suburban, and living wall application presenting greater savings than green façade (savings from *Urb-Stone-GF*: 2.1%; *Urb-Stone-LW*: 5.2%; *SUrb-Brick-GF*: 0.8%; and *SUrb-Brick-LW*: 2.2%). These net annual savings in turn demonstrated the potential for wider applicability of evergreen vertical greening application in temperate climate street canyons (particularly living walls). When utilised in conjunction with material heat storage in the right locations and adequate night-time purge ventilation, vertical greening applied heavyweight constructions could therefore facilitate the creation of thermally comfortable indoor environments with reduced space-conditioning loads in both summer and winter. Optimal conditions however are dependent on not only the duration and magnitude of climate loading experienced, but also on the relevant occupancy groups and their activity schedules.

## 7.5 Summary

This chapter considered the extent to which scaled-up application of vertical greening contributes towards enhancing urban climate resilience. It examined this through a simulation comparison study of office building construction build-ups situated within the morphological contexts of central urban and suburban neighbourhoods. The study achieved this by simulating the respective street canyons, utilising a multiscale urban climate framework incorporating the coupling of the VGM developed in Study 3. The findings however must be cautioned here as the model utilised still requires validation with reference to data from an in-situ canyon, which was beyond the scope of this project.

Table 39. Summary of vertical greening application influence on space-conditioning consumption.

| | **Annual (%)** | | | | **Summer (%)** | | | | **Winter (%)** | | | |
|---|---|---|---|---|---|---|---|---|---|---|---|---|
| | *Urb-Stone* | | *SUrb-Brick* | | *Urb-Stone* | | *SUrb-Brick* | | *Urb-Stone* | | *SUrb-Brick* | |
| | GF | LW | GF | LW | GF | LW | GF | LW | GF | LW | GF | LW |
| **Relative to base** | -2.1 | -5.2 | -0.8 | -2.2 | -0.8 | -2.4 | -0.5 | -1.5 | -3.0 | -7.1 | -0.9 | -2.3 |
| **Heating** | -3.1 | -7.0 | -0.9 | -2.4 | -18.3 | -24.6 | -2.8 | -5.2 | -3.0 | -7.0 | -0.9 | -2.3 |
| **Cooling** | -0.8 | -2.7 | -0.1 | -0.8 | -0.7 | -2.3 | -0.1 | -0.8 | -2.2 | -8.8 | -0.6 | -1.7 |
| **Relative to GF** | | -3.2 | | -1.4 | | -1.6 | | -1.0 | | -4.2 | | -1.5 |
| **Heating** | | -4.1 | | -1.5 | | -7.6 | | -2.4 | | -4.1 | | -1.5 |
| **Cooling** | | -1.9 | | -0.7 | | -1.6 | | -0.7 | | -6.8 | | -1.2 |

Note: Negative values signify relative savings.

The simulation study found the application of vertical greening to present immediate **benefit to canyon pedestrians by reducing the intensity of the daytime heat island and increasing the occurrences of cool island conditions to be experienced**. These effects were pronounced for the urban setting than suburban, while living wall application offered greater advantage towards improving the urban canyon climate.

The results also demonstrated the heat island effect to adversely influence space-conditioning loads to stress the necessity for accounting for this climate load when estimating energy use in urban and suburban buildings. The improvements to the respective canyon climates resulting from vertical greening application translated to **significant net annual space-conditioning savings to the buildings fronting the canyons** (Table 39, p. 217), with urban scenarios presenting greater savings than suburban, and **living wall application presenting greater savings than green façades**. These net annual savings in turn demonstrated the potential for **wider applicability of evergreen vertical greening in temperate climates**, with emphasised value from living wall application.

# Chapter 8

## STUDY 5: SITE INSPECTIONS

### 8.1 Introduction

Notwithstanding the growth trend identified in Chapter 3, and ecosystem benefits clarified by the preceding four studies, criticism of vertical greening application persists. This is principally associated with service-life maintenance and sustainability concerns. Study 5 investigated such practical concerns to address the final and fifth-of-five secondary research questions introduced in Chapter 1.

> *Q V. What are the key challenges in sustaining the positive contributions of vertical greening installations in temperate climates?*

This has been addressed through the inspection of ten European case studies and associated interviews with their management authorities. The chapter also represents an expanded version of the published study in Gunawardena & Steemers [46].

### 8.2 Methodology

This study involved structured case study site inspections and associated unstructured interviews (following methodological guidance in Bryman [406]). The site visits were carried out over the period between 2017 and 2019 at ten installations located in the European cities detailed in Table 40, p. 220; Fig. 108, p. 221; and Fig. 109, p. 221. These were selected for representing significant evergreen plant coverage areas (>30 m$^2$) in outdoor (#8) and indoor (#2) environments; as well as for offering accessibility to carryout direct observational studies and conduct interviews with maintenance authorities[XXV]. Save for one installation from the Mediterranean (Csa) climate zone, the rest are all located in maritime temperate (Cfb) climates, where Chapter 3 had highlighted observational in-situ data to be lacking [10]. The failed installation considered (henceforth referred to as 'Project-A'), has been anonymised here to comply with the management authority's requirements.

Table 40. The ten living wall case studies inspected (to be read with Fig. 108, p. 221).

| **Case study** | **Use** | **Location (Köppen climate)** | **Installed (removed)** | **Instllation environment** | **Description of system & canopy** |
|---|---|---|---|---|---|
| Project-A, *corner façade* | Services facility | Southeast England<br>Temperate (Cfb) | 2014<br>(2015) | Outdoor | Mineral wool modular plates<br>Evergreens |
| David Attenborough Building (DAB), *atrium wall* | Multi-occupancy office | Cambridge, England<br>Temperate (Cfb) | 2015 | Indoor | Soil-based interlocking modular crates<br>Evergreens |
| St. Edmund's Terrace (SET), *court walls* | Private residence | London, England<br>Temperate (Cfb) | 2017 | Outdoor | Soil-based modular-felt pocket panels<br>Evergreens |
| Rubens at the Palace, *gable-end façade* | Hotel | London, England<br>Temperate (Cfb) | 2013 | Outdoor | Soil-based modular<br>Evergreens mostly, with some seasonals |
| The Athenaeum, *corner façade* | Hotel | London, England<br>Temperate (Cfb) | 2009 | Outdoor | *Mur Vegetal* (MV); continuous felt-based hydroponic<br>Evergreens (with some seasonals at the Athenaeum) |
| CaixaForum (CF), *gable-end façade fronting urban court* | Museum | Madrid, Spain<br>Mediterranean (Csa) | 2008 | Outdoor | |
| Oasis of Aboukir, *gable-end façade fronting urban court* | Mixed-use | Paris, France<br>Temperate (Cfb) | 2013 | Outdoor | |
| Quai Branly (QB), *façade fronting street* | Museum | Paris, France<br>Temperate (Cfb) | 2004 | Outdoor | |
| Toulouse Natural History Museum (TNHM), *atrium wall* | Museum | Toulouse, France<br>Temperate (Cfb) | 2008 | Indoor | |
| Henri Gaussen Botanical Garden (HGBG), *greenhouse wall* | Museum greenhouse | Toulouse, France<br>Temperate (Cfb) | 2008* | Indoor | |

* Original Patrick Blanc designed installation from 1996 dismantled during major renovation.

[XXV] Installations visited as part of the project included additional European sites in England, France, Italy, and Spain, as well as further afield in California (United States) and Colombo (Sri Lanka), although were discounted owing to lack of accessibility and response from management authorities.


*Fig. 108. The ten living wall case studies inspected.*

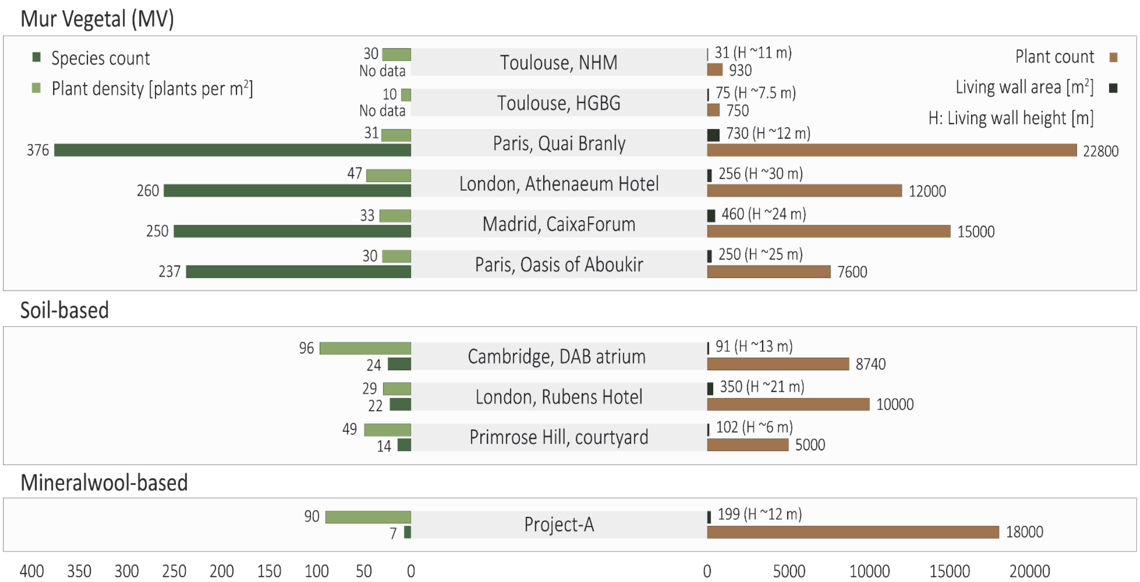


*Fig. 109. Plant coverage properties of the ten case studies inspected.*

The site visits included two principal objectives. The first involved structured installation inspections (SI) carried out by an inspector (the author). They included the identification of plant and system failures (flourishing state), biodiversity presence (healthy ecosystem), and evidence of resource oversupply (resource management). The non-structured observations also gathered during these visits included examples of watering, replacement planting, and horticultural practices (Table 44, p. 228). The second objective involved systematic non-participant direct observation of human engagement behaviours, recorded by a ‘rater’ (the author) at each sampling visit typically lasting for an hour. The engagement observation schedule recorded incidents or instances distinguished per visit between *building occupant* and *visitor or public* instances, as well as the type of engagement between those *taking visual notice; making connections by means of conversation or taking photographs; active movement towards the feature*; and *physical contact and interaction with plants*. The frequency of instances gathered in relation to this observational schedule (Table 43, p. 227) was ordinally categorised based on frequencies representing ‘none’ (0), ‘very low’ (<2), ‘low’ (≥2 and <5), ‘moderate’ (≥5 and <7), ‘high’ (≥7 and <9), and ‘very high’ (≥9).

The above site visit data was complemented by unstructured interviews with expert practitioners, and installation managers or key decisionmakers associated with the installations inspected. The expert practitioners consulted included agricultural engineers, horticulturalists, ecologists, and individuals that identified themselves as ‘living wall consultants’ with suitable qualification in the management of plant integrated systems. They were recruited through the recommendations received from the relevant installation managers, who themselves were defined as individuals responsible for the day-to-day management of the inspected installations and answerable to the end-occupiers of the buildings concerned. For the failed Project-A however, the key decisionmaker responsible for project procurement was interviewed given the absence of an installation manager. The topics discussed at the interviews included installation and service-life incidents; failures of plants and systems; maintenance programmes and their operation; resource consumption (mainly water and nutrients); maintenance costs; as well as the influence of human engagement aspects (as a distinct topic). As these unstructured interviews involved contact with human participants (i.e., interview subjects), requisite Departmental ethical guidance and Supervisor approval was obtained. Material from these interviews have also been anonymised to comply with interviewee wishes, while certain sources in relation to projects discussed are intentionally not referenced to comply with the confidential nature of such material (e.g., meeting minutes, reports, correspondence etc.). The response notes taken at the interviews were later processed using the MATLAB R2019b, Text Analytics Toolbox to ‘clean’ the data and reduce complexity. This involved the implementation of six steps including (1) the removal of confidential references; (2) tokenising the text into smaller units; (3) removal of a list of stop-words (‘and’, ‘the’, etc.); (4) lemmatisation or the grouping together of inflected forms of a word [407]; (5) removal of punctuations; and (6) the removal of words with <2 characters [392]. The resulting text analytics histogram was used to develop a preliminary coding scheme of fourteen themes, which was then consolidated to eight distinct maintenance-related themes and used to manually code the text data (given the modest dataset). The responses concerning engagement behaviour were gathered discretely from the other interview topics and thus required no additional coding.

## 8.3 Findings

### 8.3.1 Maintenance observations

A summary of key incidents reported in interviews and during the inspection campaign are detailed in Table 44, p. 228, while the key themes of concern coded in the interviews are discussed in section 8.4 under eight maintenance-related subtopics.

From the structured observations recorded at inspections, installations were nominally categorised as either ‘flourishing’ or ‘failed’ predicated on the estimated percentage of plant failures. Any installation with over 30% (upper limit for expected failures, [134]) was deemed a failed state, with only Project-A designated as such given the removal of the entire installation (Fig. 110a, p. 224). The failure rates for the remaining installations were relatively stable over the campaign, all within 5-10% of expected failures (Table 41, p. 224). The flourishing state was further qualified by the biodiversity presence recorded (i.e., to indicate a healthy ecosystem). This nominal categorisation required invertebrate and/or vertebrate presence, with most inspections (90%) having recorded invertebrates (e.g., insects), while a few outdoor installations also included vertebrates (8%, e.g., bird-nesting). There was however a marked difference between indoor and outdoor installations, with the latter presenting greater presence of visually apparent diversity (mostly invertebrates). The final structured observation considered resource management (watering supply). All *Mur Vegetal* systems in this regard showed watering oversupply dripping into their waste drains (e.g., Fig. 110d), while a few demonstrated significant overspray to surroundings (e.g., at the CaixaForum and Quai Branly installations; Fig. 114, p. 235).

The non-structured observations also gathered during these visits, including watering, replacement planting, and horticultural practices are discussed in section 8.4.

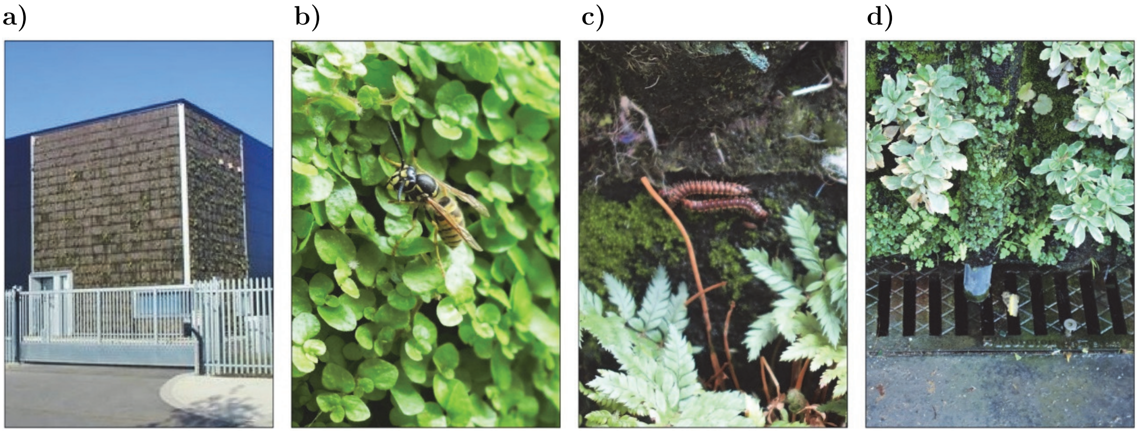


*Fig. 110. Substantial plant failures at Project-A, taken circa early-2015 (a); biodiversity presence, e.g., wasp (b) and millipedes (c); excess water flowing into base drain (d).*

Table 41. Aspects recorded during site inspections [46].

| **Case study** | **Design** | | **Structured installation inspections** | | | | | |
|---|---|---|---|---|---|---|---|---|
| | **Designed public interface** | **Direct wall access** | **Number of inspections** | **Flourishing state** | **Biodiversity presence** | *invertebrate* | *vertebrate* | **Resource* management** |
| Project-A | *No* | *No* | 01 | *No (0%)* | N/A | (N/A) | (N/A) | N/A‡ |
| DAB | *No* | *No* | 08 | *Yes (~90%)* | *Yes* | *(6/8)* | *(0/8)* | *No (0/8)* |
| SET | *No* | *No* | 04 | *Yes (~85%)* | *Yes* | *(4/4)* | *(0/4)* | *No (0/4)* |
| Rubens Hotel | *Yes* | *No* | 03 | *Yes (~95%)* | *Yes* | *(2/3)* | *(0/3)* | *No (0/3)* |
| The Athenaeum | *Yes* | *Yes* | 02 | *Yes (~90%)* | *Yes* | *(2/2)* | *(0/2)* | *Yes (1/2)* |
| CaixaForum | *Yes* | *Yes* | 20 | *Yes (~95%)* | *Yes* | *(20/20)* | *(0/20)* | *Yes (11/20)* |
| Oasis of Aboukir | *Yes* | *No* | 02 | *Yes (~95%)* | *Yes* | *(2/2)* | *(1/2)* | *Yes (1/2)* |
| Quai Branly | *Yes* | *Yes* | 08 | *Yes † (~90%)* | *Yes* | *(8/8)* | *(3/8)* | *Yes (6/8)* |
| Toulouse Natural History Museum | *Yes* | *Yes* | 01 | *Yes (~95%)* | *Yes* | *(1/1)* | *(1/1)* | *Yes (1/1)* |
| Henri Gaussen Botanical Garden | *Yes* | *Yes* | 01 | *Yes (~95%)* | *No* | *(0/1)* | *(0/1)* | *Yes (1/1)* |

Notes: † Disregarding areas being replanted at the time; ‡ historically recorded; * resource management assessed in terms of watering oversupply.

Save for Project-A, all other installations demonstrated only localised failures. These included species-specific ill-health or death; stress symptoms at installation edges; crown domination associated issues; and localised heat stress. With the Project-A failure, the trigger event had been identified as wintertime dry-out, which then led to other complications arising from remedial irrigation measures taken. The project however was climatically challenged from the onset when it was sited in a remote location with minimal surrounding shelter, followed by the application of the installation with considerable height to a building corner. The resultant wind-loading burden was therefore stressed in the post-failure assessment as a significant climate risk for the project. The lack of human engagement resulting from the building's use also meant that there had been little acknowledgment of the installation's ecosystem contributions, while stress symptoms and failures reported to the procurement team had been rapidly perceived and deemed as a defect of the installation, and to an extent the greening solution itself. This latter negative reaction is partly explained by the cost associated with its removal and replacement with an alternative, which was reported as a loss to the client of around £1,500 per m$^2$.

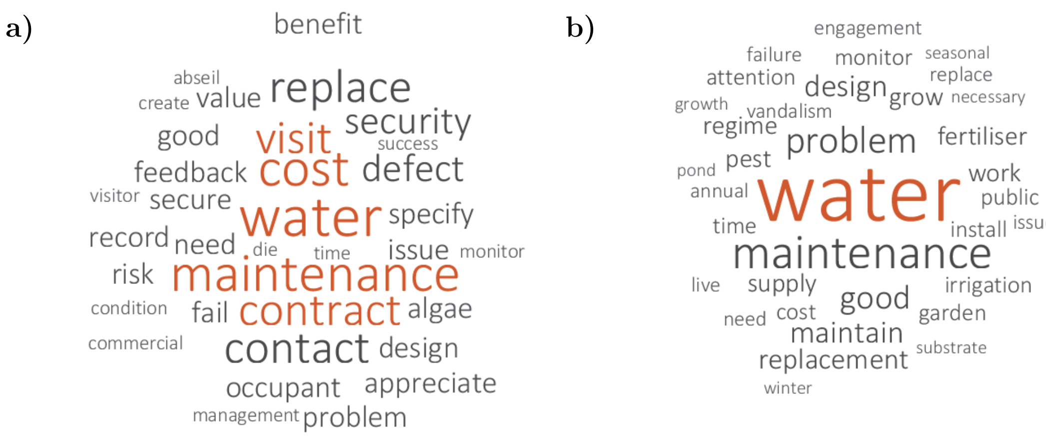


*Fig. 111. Word-clouds from manager/key decisionmaker (a) and expert (b) interview notes.*

As demonstrated by interview response word-clouds (Fig. 111), concern for cost was stressed greater by managers/key decisionmakers relative to experts. Installation cost represented the primary concern given its proportional relevance to maintenance pricing, which varies with the system used. From the examples presented in Table 42, p. 226, felt-based systems (e.g., *Mur Vegetal*) presented the highest estimation between £600-650 per m$^2$, while specialist substrates could cost >£1,000 [408,409]. The secondary concern was annual maintenance cost, which was typically quoted as a percentage of installation cost ranging between 6% (£29 per m$^2$) and 12.5% (£62 per m$^2$) for mineral wool and soil-based systems, while for *Mur Vegetal* installations it could be high as 15-20% (according to a Madrid-based supplier). These rates vary depending on whether the installations are outdoor or indoor (higher for latter), and on the services included. A UK-based supplier for example quoted per plant replacement costs of £3.00 for outdoor and £4.50 for indoor installations, although this was said to be included for expected failures in most maintenance contracts. Complete substrate replacement and/or replanting for any installation system is a substantial cost burden. With the mineral wool-based £550 per m$^2$ system in Table 42 as an example, substrate replacement would cost 22.5% of installation, while complete replanting was said to cost a further 45%.

Table 42. Reported vertical greening installation and maintenance costs.

| VG | Vertical greening system description | Installation cost (£\|€*/m²) | Annual maintenance (£\|€*/m²) | Supplier/ source |
|---|---|---|---|---|
| Green façades (GF) | Direct GF | €30-45 (~£25-40) | €2-5 (~£2-4) | Europe-based [408] |
| | Direct GF (wire) | €35 (~£30) | - | Turkey-based [409] |
| | Indirect GF, with wire mesh | €40-75 (~£35-65) | €2-5 (~£2-4) | Europe-based [408] |
| | Indirect GF, planter box (zinc-coated steel) | €600-800 (~£520-695) | | [408] |
| | Indirect GF, planter box (coated steel) | €400-500 (~£350-435) | | [408] |
| | Indirect GF, planter box (HDPE) | €100-150 (~£90-130) | | [408] |
| Living walls (LW) | LW soil-based planter box (HDPE) | €400-600 (~£350-520) | €40-100 (~£35-90) | Europe-based [408] |
| | LW foam-based | €750-1,200 (~£650-1,040) | | (as above) |
| | LW felt-based | €350-750 (~£305-650) | | (as above) |
| | LW felt-based | €416 (~£370) | - | Turkey-based [409] |
| | LW mineral wool-based modular plates | £550 | £55 | UK, Cambridgeshire-based† |
| | LW mineral wool-based | £375-425 | | Spain, Madrid-based† |
| | LW soil-based modular-felt pocket panels | £500 | £29 outdoor<br>£62 indoor | UK, London-based† |
| | LW soil-based interlocking modular crates | £500-600 | £50-60 | Global, UK representative† |
| | LW felt-based *Mur Vegetal* continuous | £425-600 | £42.50-60 | Spain, Madrid-based† |

Notes: † Quoted rates between 2017-2020; *Euro-to-GBP conversion based on 2019 mean rate (rounded).

### 8.3.2 Flourishing state and human engagement behaviour

Five of the flourishing projects offered direct access to their living walls, while seven presented a designed public interface (Table 41, p. 224). Notably, three sites included circulation arrangements with enhanced building-user and public accessibility, namely the outdoor installations at the Quai Branly, CaixaForum, and Athenaeum Hotel. At all three, pedestrian level access to the installations facilitated physical contact with plants (no threat of plant injury or vandalism was recorded during inspections; nor were any reported), with the *Mur Vegetal* installations recording the highest frequencies and complete range of behavioural interactions rated (Fig. 112, p. 227).

The gathered frequency data on the six human engagement behavioural aspects (Fig. 112), was ordinally ranked by the earlier defined frequency thresholds as represented in Table 43, p. 227. This categorisation highlighted *visitor or public engagement,* as well as *taking notice*, *making a connection*, and *movement towards the feature* to present the highest frequency in the 'very high' category, while *building occupant engagement* and *physical* *contact* demonstrated the highest frequency in the 'low' category. The overall lower engagement of building occupants could be partly explained by the sample studies underrepresenting indoor projects, where in isolation this was in the 'high' category.

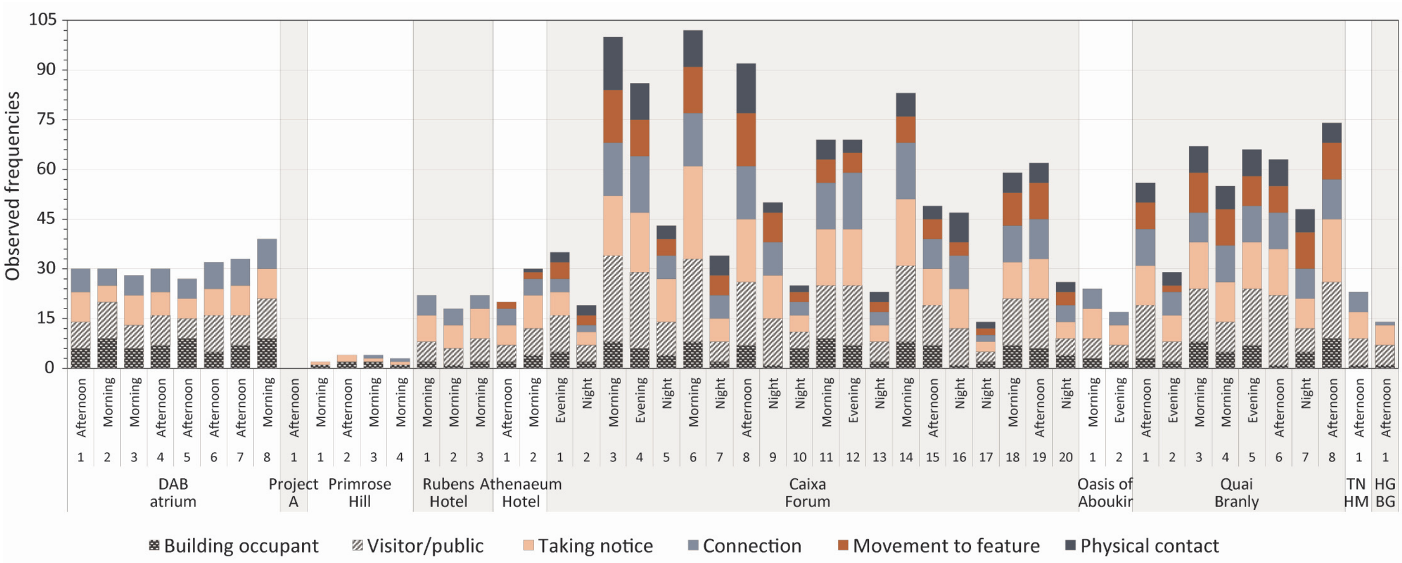


*Fig. 112. Frequencies of human engagement aspects rated during site visits; in* [46].

Table 43. Human engagement and interaction categories.

| Percentage within flourishing state | Valid visits | None | Very low | Low | Medium | High | Very high |
|---|---|---|---|---|---|---|---|
| *Building occupant engagement* | 49 | 0.0% | 16.3% | **32.7%** | 18.4% | 22.4% | 10.2% |
| *Visitor or public engagement* | 50 | 8.2% | 6.1% | 6.1% | 16.3% | 16.3% | **55.1%** |
| *Taking notice* | 49 | 0.0% | 6.1% | 6.1% | 16.3% | 16.3% | **55.1%** |
| *Making a connection* | 49 | 4.1% | 6.1% | 14.3% | 20.4% | 12.2% | **42.9%** |
| *Movement towards the feature* | 39 | 23.1% | 0.0% | 23.1% | 10.3% | 10.3% | **33.3%** |
| *Physical contact with plants* | 36 | 19.4% | 2.8% | **27.8%** | 16.7% | 16.7% | 16.7% |

The unstructured interview responses were coded as eight maintenance-related categories, while human engagement behaviour was defined as a unique category. The latter showed value assignment to human engagement behaviour, aligned closely with the agendas of the associated building function. For example, at museum installations they valued public perception mostly, while at the DAB with its multi-organisation building occupancy, both occupant and visitor perception was equally valued. At Project-A however the agenda contrasted, with the planning authority's acceptance of the 'concept of a flourishing installation' highlighted as the principal driver for the 'willingness to pay'. The minimal occupancy and technical function of the building use had also presented little experience of engagement behaviours to influence the installation owner's value assignment.

Table 44. Summary of incidents and issues reported in interviews and recorded at site inspections (SI); published in [46].

| Case study | Plant health | General maintenance |
|---|---|---|
| **Project-A** (***bulding façade***) | Plants had suffered high wind exposure as it is in a remote location with no contextual buildings.<br>Cold stress in winter, and frost damage mitigation had led to dry-out.<br>**SI:** Entire installation removed in 2015. | Water and nutrient blow-out (high wastage) had presented a slip-hazard in summer and black-ice risk in winter (i.e., health and safety risk).<br>Water wastage had encouraged algae growth on paving and façade.<br>Envelope water ingress became a major defect. |
| **David Attenborough Building (DAB)** (***indoor atrium***) | The atrium has four ground-level entrance heaters (now decommissioned), which during the first winter had caused localised heat stress.<br>*Maranta leuconeura* affected by entrance heaters, crown shading from neighbouring *M. deliciosa*, and a spider mite infestation.<br>**SI:** Above *M. leuconeura* replaced and *M. deliciosa* trimmed in June 2018. | Irrigation leakages reported and repaired. Six watering zones remotely monitored, and valves controlled utilising an *app*.<br>**SI:** Routine horticultural visit with two abseilers descending, with system details assessed and issues rectified in-situ. |
| **St. Edmund's Terrace (SET)** (***court walls***) | *Helleborus* sp. had suffered aphid attack, although successfully treated.<br>**SI:** Plants in shaded wall corners in poor health. | Typical issues with weed presence and trimming.<br>**SI:** Moderate amounts of detritus accumulation. |
| **Rubens Hotel** (***bulding façade***) | Seasonal flowering plants rotated to satisfy client aesthetic requirements.<br>Increased soil depth (~0.20 m) allows for rapid growth, which demands regular trimming.<br>**SI:** Intermittent plant failures, although few (<5%) and far apart (i.e., expected failures). | Rainwater harvester and rainfall monitoring are added maintenance tasks. Remote monitoring and control of watering valves utilised.<br>**SI:** Inspections and works require a gantry to be installed (three personnel involved). |
| **The Athenaeum Hotel** (***bulding façade***) | Initial plant-plan modified over first few years to adapt to local constraints, e.g., some had failed under pollution stress. Seasonal plants are also used and rotated as per client demands.<br>**SI:** Crown domination from certain plants, with adverse impact on those overshadowed; and dead plants at corner apex, possibly from wind stress. | Challenge to balance watering requirements given the installation height (>30 m).<br>**SI:** Several window openings were overshadowed by excessive growth and required trimming. |
| **CaixaForum Museum** (***bulding façade***) | Initial plant-plan modified to adapt to south-facing exposure. Some evergreen shade-loving plants had struggled to flourish.<br>**SI:** *Hosta patriot* exhibited leaf edge browning; some new additions to the wall-edge returns had failed to take root; and at the apex, some plants exhibited wind stress symptoms. | Major plant failures (~90%) during construction in the summer caused by accidental water cut-off.<br>Major refurbishment including full replanting ~four years ago, owing to felt deterioration and invasive root growth into pipework.<br>Higher water volume delivered to the first few drippers in contrast to peripheries; initial nine sectors extended to eleven to address. The problem was acute enough that for a period, sedum plants had to be introduced.<br>Weeds are a major problem and grow rapidly; takes 2-4 days to de-weed. No pest problems, possibly due to their aversion to higher irradiation from the south-facing aspect. |
| **Oasis of Aboukir** (***bulding façade***) | **SI:** Mild wind stress noted at the apex; and crown domination from certain plants, although no adverse consequences noted. | **SI:** The gable-end wall had several window openings overshadowed by excessive growth and required urgent trimming to prevent obstruction. |

| Case study | Plant health | General maintenance |
|---|---|---|
| **Quai Branly Museum** (***bulding façade***) | Higher frequency of detailed inspections (six per year) to address horticultural needs and plant replacement.<br>**SI:** Installation was undergoing replanting (to celebrate 10th anniversary), with half the wall completed and young plants taking root. | Significant trimming in 2007 to mitigate plant fall-off risk (i.e., health and safety risk).<br>Major refurbishment, including full replanting undertaken between 2017-18.<br>Laboratory analysis of felt routinely carried out.<br>**SI:** Irrigation sessions showed significant oversupply draining into the waste collection channel at the installation base. |
| **Toulouse Natural History Museum** (***indoor atrium***) | Some plants (e.g., *M. deliciosa*) exhibited aggressive growth in the well-lit atrium.<br>**SI:** Few plants exhibited leaf-edge browning. | Plants regularly trimmed to limit growth.<br>Drainage tray at the bottom requires regular clearing out, as detritus is visible.<br>**SI:** Installation artificially lit even during the day. |
| **Henri Gaussen Botanical Garden** (***indoor greenhouse***) | Orchidaceae and Bromeliaceae had failed due to insufficient light.<br>Plant pushback and fall-out (e.g., *Philodendron* sp.) from excessive weight.<br>Some plants (e.g., *Drynaria* sp., *Kohleria* sp., and *Ficus* sp.) frequently trimmed.<br>**SI:** High levels of algae growth. | Original 1996 installation dismantled during major renovation works.<br>Intermittent failures with automated water and humidity control apparatus (*RH* within the greenhouse is maintained at 80%).<br>**SI:** Significant water supply drains into the installation base-pond (although is not an aquaponic arrangement). Environment thermally uncomfortable for human occupants. |

## 8.4 Discussion

The installation managers highlighted plant stress management as the principal challenge in sustaining an urban installation's flourishing state (given the availability of adequate financial and other resources). While short-term demands within species tolerance limits are addressed by their self-management mechanisms, atypical demand extremes present the risk of irrecoverable injury and rapid escalation to installation-level failure. Human management processes must therefore recognise stress symptoms as early as possible and intervene with appropriate measures, with the following stress management aspects highlighted by the respective experts as requiring significant attention.

### 8.4.1 Managing local climate extremes

Managing local climate loading is critical for the sustainable maintenance of urban living walls, with outdoor installations strongly influenced by local light, temperature, moisture, and wind climates. While plants are capable of acclimatising to reasonable extremes by dynamically adjusting their optimal, management experts must select plants with complementing climate hardiness ratings to limit exposure risk (e.g., [410]). Atypical extremes however are a significant risk. For example, the principal contributing factors at Project-A's failure was identified as atypical lower winter temperatures and drought.

Installation monitoring frequency during atypical extremes caused by heatwaves or cold snaps must therefore be increased to ensure rapid response to stress. In indoor conditions the climate is controlled to meet occupant comfort, which correspondingly satisfies optimal conditions for most plants. This limits thermal and water stress risk, although draughts from both hot (e.g., as experienced with heaters at the DAB, [134]) and cold sources have been reported to cause localised stress. Space-conditioning objectives could also present complications as humidity is maintained at lower levels to ensure occupant comfort (relative humidity ~40-70%), which contradicts requirements for tropical shade-loving plants typically selected for such installations (85-95%). The monitoring burden at indoor installations is as a result reported to be higher during the early establishing period, while afterward the climate variables are typically balanced by the managers to provide optimal growth conditions throughout the year [134].

The challenge of managing the light climate in cities is presented by contextual building overshadowing. Although this is addressed at the design stage and with the specification of shade-loving plants for surfaces in frequent shadow; the dynamic nature of urban renewal could result in unforeseen overshadowing risk. A few experts referred to past projects where this had been a major issue, although none of the installations inspected have thus far encountered such problems. Low-light availability in indoor installations on the other hand is a constant risk [42,134]. Although this is also addressed by specifying shade-loving plants, failures from low light availability are not uncommon even when tolerant species have been used (e.g., Orchidaceae failures at the Henri Gaussen Botanical Garden installation, [411]). The converse condition of high light exposure is an unlikely risk in indoor environments, although significant in outdoor conditions particularly with shade-loving plants. At the CaixaForum for example, leaves of *Hosta* spp. exhibited irradiance stress symptoms, while tropical evergreens in general were reported to be frequently stressed from higher irradiation at the south-facing installation [156]. None of the installations inspected however seemed to employ real-time monitoring, with managers reporting light-level monitoring only as an essential task during regular site visits.

With low velocities wind flow is acknowledged to alleviate heat stress by enhancing heat and humidity advection, although at higher velocities increased humidity advection could encourage water stress, while directly causing wind-induced mechanical stress. Symptoms of wind stress are identified as thigmomorphogenesis features, which includes limited growth extents, canopy compaction, greater stem radial growth, and reduced number of leaves than typical. At several outdoor installations (e.g., the Athenaeum), high-level plants demonstrated compact canopy arrangements to suggest prolonged exposure to wind stress. As these installations extend canopies to higher levels of exposure than otherwise typical (e.g., the Athenaeum height is >30 m), edges and apexes are likely to be vulnerable to negative pressures resulting from eddy diffusion [55]. This is likely to increase heat and mass transfer to increase the risk of drying, while in colder climates may also cause localised cold stress (e.g., experienced at Project-A). If such conditions cannot be avoided by design, plant selection with high hardiness ratings mitigates the risk to an extent.

Most local climate risks discussed above could be managed by using active thermal, humidity, or lighting controls to facilitate constant plant growth conditions. The feasibility to do so is greater with indoor conditions relative to outdoors, given the near closed nature of such systems. In any scenario however, the increased energy demand necessary to implement such active measures are likely to counter the beneficial ecosystem services and passive climate modifications expected. This in turn would call into question the sustainability of operating and maintaining such installations.

### 8.4.2 Irrigation

Irrigation manages plant water demand, and an integrated supply is necessary for living walls given their limited substrate volume and vertical arrangement enhancing percolation flow [412]. The frequency required is dependent on the background climate, exposure, season, species, installation height, and system (substrate). With felt-based hydroponic systems, a relatively higher watering frequency is necessary to maintain a saturated substrate [158]. The *Mur Vegetal* designer for example has recommended frequencies between 3-5 times a day [136]. Organic or soil substrate systems in contrast have greater water retention capacity that translates to reduced frequencies [158]; as exemplified by the 1-2 frequency reported at the Rubens Hotel in London [132]. Programmes are also adjusted for seasonality with the growth season in spring and summer requiring higher frequency and volume (e.g., 3:1 summer-to-winter frequency ratio at the CaixaForum in Madrid; and 3:2 at the Henri Gaussen Botanical Garden in Toulouse). Wintertime frequency is therefore lower, and in colder conditions restricted to mitigate frost damage [134].

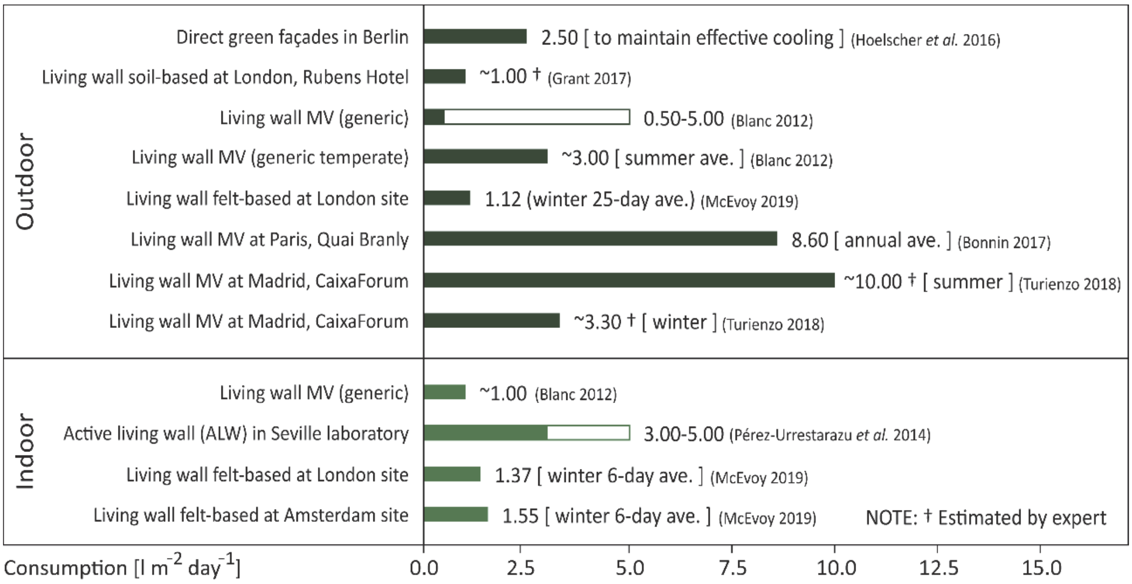


*Fig. 113. Water consumption estimated or reported for indoor and outdoor installations by various sources; published in* [46].

The frequency of watering required dictates water-use volume, with consumption data not widely reported (few examples in Fig. 113). With sheltered indoor applications, consumption is reported to be relatively lower given the controlled climate. Some specialist indoor walls however require higher use as the plants used (i.e., bryophytes) require a saturated environment to thrive (e.g., ALW in Fig. 113, [158,311]). In outdoor conditions, consumption is greater given the exposure to the drying power of the atmosphere. Blanc [136] had claimed *Mur Vegetal* supply burdens to be lower than typical for gardens and urban parks, although reported values at the Quai Branly for example are higher than those for other systems. The *Mur Vegetal* rates in drier climates like the CaixaForum are also more pronounced, particularly in the summer months [156]. Water demands of such hydroponic, felt-based, capillarity systems must be implemented through closed-loop recycling to avoid unsustainable consumption. At the Henri Gaussen Botanical Garden for example, the high volumes supplied (15-30 $l \cdot m^{-3} \cdot day^{-1}$ in the winter and 30-60 $l \cdot m^{-3} \cdot day^{-1}$ in the summer) are recirculated through a pond arrangement to maintain flow consistency [411]. Laboratory assessments have demonstrated these high flow rates to be necessary to achieve distribution uniformity and prevent asymmetric dry-out, despite the increased risk of wastage [311]. It is significant to note that closed-loop systems in practice waste ~30-40% of supply, resulting from spillage, blow-out onto adjoining areas, or other leakages [156]. Spillage and blow-out for example was observed at outdoor *Mur Vegetal* installations at the Quai Branly and CaixaForum (Fig. 114, p. 235); identified as a ‘defect’ at Project-A; and reported as a significant problem with several installations with considerable height [156]. It is significant to account for wastage and precipitation retention to prevent oversupply. While accounting for wastage is challenging, precipitation is accounted for at most outdoor installations by rain sensors (e.g., Rubens Hotel in London [132]). Although there is potential for employing precision irrigation strategies, none of the installations inspected were managing consumption to that degree of accuracy.

While oversupply must be prevented to ensure water-use efficiency, it is also necessary for plant health. Hypoxic stress from waterlogging is reported as a challenge to identify given the external symptoms including reduced growth, chlorosis, leaf margin browning, root-rot, and wilting [54], could easily be misinterpreted as early signs of water stress and lead to an erroneous increase in supply. Examining system features could clarify oversupply, with high algal growth on the substrate and vicinity (e.g., at Project-A), and a high proportion of the irrigation supply accumulating as waste, indicative of oversaturation.

### 8.4.3 Nutrient supply

External supply is necessary for living walls as the vertical growth substrate receives only a small fraction of the biomass litter. Nitrogen (N), phosphorous (P), and potassium (K), along with essential trace-elements must therefore be supplied with concentrations varying across systems, their height, seasonality, and plant profile. Seasonal changes demand the most significant alteration, with summertime typically demanding greater. The Urrestarazu *et al.* [413] study for example found the summertime average to be 2.9 $l \cdot m^{-2} \cdot day^{-1}$, with maximum use reaching 5.1 $l \cdot m^{-2} \cdot day^{-1}$, while wintertime use was between 1.7-1.9 $l \cdot m^{-2} \cdot day^{-1}$. The installation height is also a factor. The same study found greater consumption at the top section of the installation canopy, which incidentally also demanded between 60-90% more irrigation [413]. In practice however, most installations inspected maintained a constant supply (e.g., monthly usage at the Henri Gaussen Botanical Garden *Mur Vegetal* was reported at ~1 kg of N:P:K delivered at a 19:10:18 ratio, [411]), while only a few reported bespoke adjustment. The CaixaForum regime for example is noteworthy, where a varied N:P:K balance was reported including a high-N balance of 18:11:11 delivered at the start of the growth season in spring when growth is rapid (mostly with deciduous plants), while in the autumn a low-N and high-P and -K balance of 9:18:18 is used to prepare plant roots for cold stress [156]. For a given installation, the exact balance is advised to be adjusted with levels monitored regularly to maintain both appropriate concentrations and pH. Excess concentrations are cautioned as it alters salinity and substrate pH to disrupt necessary nutrient availability, or at worst lead to mineral toxicity associated failures.

### 8.4.4 Pollution stress

Although the phytoremediation of pollutants is promoted as a vital ecosystem service [10], high concentrations were acknowledged as a significant stress source in outdoor conditions. The main offenders are particulate matter, minerals, and inorganic gaseous pollutants such as Sulphur dioxide, Nitrogen oxides, and Ozone. Service-life contamination is unavoidable given that anthropogenic activity and deposition of pollutants are typically higher in urban environments, particularly adjacent to streets and construction sites [265]. The outdoor installations inspected however have yet to report on critical stress incidents, with the Athenaeum adjacent to a busy London street as the only project reporting minor issues. Save for plant replacement, experts highlighted few solutions to address pollution stress. Excessive deposition was suggested to be washed off, although this was cautioned given that closed-loop systems are likely to accumulate such pollutants that would in turn require intensive filtering or lead to water wastage.

### 8.4.5 Microbiome management

Management experts demonstrated general awareness of the significance of the plant microbiome in pollutant phytoremediation and nutrient recycling, with the greater significance of the rhizosphere microbiome acknowledged (see [108]). Most however attached relevance of this aspect when considering indoor installations and specifically ALWs, while the only exception was reported by the Quai Branly, where the expert acknowledged laboratory analysis to ensure substrate microbial balance as a regular maintenance task [414].

### 8.4.6 Growth management

Given the verticality, the risk of uprooting and fall-out from wind-induced canopy changes was stressed as a critical concern raised by installation owners. Maintenance pruning is therefore a necessary task, with the outdoor installations inspected yet to report a major fall-out incident. The high planting densities also mean that certain canopies must be trimmed to prevent overshadowing from crown domination. The DAB installation for example had reported crown domination as a contributing factor for the poor health of adjacent lower-level plants [134]. Root competition could similarly lead to certain adjacent plants failing, which stresses the necessity to test planting combinations prior to deployment at installations [415]. Other growth management tasks mentioned included training (e.g., climbing plants), realignment, and in certain instances replanting when dislodged from excessive root growth (pushback). Pushback was reported as a typical concern with indoor installations where optimal growth conditions are maintained throughout the year. The DAB and Henri Gaussen Botanical Garden installations as examples, reported root growth out of the root zone, and in the latter case, fall-out [134,411]. In general, the experts suggested indoor installations to require a higher frequency of growth management tasks, which is reflected in their higher annual maintenance cost (e.g., 6.0% of installation cost for an outdoor project relative to 12.5% for an indoor one, managed by the same supplier).

### 8.4.7 Biotic stress management

Synthetic ecosystems attract biotic stress from colonising species of flora, fauna, and pathogens as an abundance of resources are made available for enhancing biodiversity with little to no control mechanisms. This vulnerability was reported to be greater with indoor installations, where controlled microclimates present near constant favourable conditions [134,156]. A degree of resilience is provided by installation planting density and diversity, as pests and diseases are often species-specific. Managers however are likely to deploy immediate remedial measures following threat detection. These may include the use of pesticides, herbicides, or antipathogens, although these are cautioned given the potential for unintended results. As an ecologically sound alternative, the introduction and maintenance of natural control mechanisms was strongly advocated by most experts [134,156].

a) b) c) d)

*Fig. 114. Watering wastage (a); weeds taken root at the CaixaForum (b); the Quai Branly replanting using an articulated lift (c); canopy trimming by an abseiler at the DAB (d).*

Although verticality has been claimed to limit weed propagation (e.g., [136]), installation inspections demonstrated it to present a recurring maintenance problem (e.g., at the CaixaForum, Fig. 114b). Most experts advocated preference for addressing weeds as well as pests and diseases with biological control, where the mechanisms of predation, parasitism, or herbivory of other organisms is utilised [134,162]. As an alternative, mild threats may be managed with biopesticides, while the use of stronger synthetic pesticides was cautioned in indoor spaces given the potential to adversely affect building occupant health. Synthetic pesticide use is also a problem with closed-loop irrigation systems, as they accumulate in wastewater leading to toxicity stress risk that is challenging to filter-out [134].

Human physical contact is also a source of plant biotic stress. Excessive handling of foliage and vandalism are significant concerns typically highlighted by designers, particularly with publicly accessible arrangements (e.g., at the CaixaForum, Quai Branly, and the Athenaeum). With the inspected installations however, the managers reported the threat from accidental damage or vandalism to be less than presumed. Most human physical interactions with plants have been reported as non-injurious [156]; an observation reinforced by the behavioural engagement findings from the case studies.

### 8.4.8 Infrastructure maintenance

Irrigation and fertigation are typically implemented as an integrated delivery system, and involves a range of tasks including the maintenance of flow networks and active apparatus; accumulated waste disposal; filtering; and frost protection [156,414]. In contrast to modular systems, embedded networks in continuous arrangements are reported to be onerous to maintain given the difficulty in detecting and remedying leaks, blockages, or invasive root growth into pipework [132]. Hydroponic arrangements (e.g., *Mur Vegetal*), consider the substrate as an integrated element of the delivery system, with monitoring of felt degradation as an additional task [414]. At a certain point however, significant felt replacement and replanting is reported as necessary (e.g., at the CaixaForum and Quai Branly). The time frame varies dependent on the degradation rate, although is likely to be necessary in advance of the twenty-five-year service life-span typical for an installation (e.g., the CaixaForum was replaced in approximately seven years, and the Quai Branly replaced in approximately ten years). This replacement is therefore a significant disadvantage and maintenance cost of such felt-based living wall systems [156].

All maintenance tasks require infrastructure and apparatus to be used, with some requiring permanent support features, while others are introduced per site visit [132,156]. Access particularly at larger installations is a key consideration that installation designers must address, with some requiring the use of cranes or gantries with substantial access and loading burdens, or inbuilt infrastructure necessary for climbers or abseilers (Fig. 114, p. 235). When such considerations have not been adequately addressed during the design stage, onerous alternatives may need to be considered during the installation service-life, which inevitably increases maintenance costs.

Notably, a significant proportion of tasks at most installations are still reported to be managed manually, requiring the physical presence of the installation manager. Remote management apparatus at present is only reported to be used for irrigation flow control, with several experts utilising mobile applications to monitor conditions through embedded sensors and valves operated to complement. Real-time stress detection and automated response mechanisms were not in operation at any of the installations inspected, despite the significant prominence and resource availability at some installations.

## 8.5 Summary

Installation managers highlight **atypical extremes of abiotic stressors** including water, temperature, and light as the most challenging to address with outdoor urban installations; particularly during the construction phase and initial establishing period; as well as when local climate variability has been underestimated. The challenge is highlighted by the rapid escalation of adverse effects, as experienced at the failed project reported in this study. With indoor installations, vulnerability to such extremes is significantly limited by the near closed nature of the local climate. Instead, optimal growth conditions maintained throughout the year often translate to higher growth management requirements.

The sustained success of an installation depends on resource consumption and the diligent and consistent management of the maintenance programme. At any installation, the failure of a proportion of plants would be explained by the challenges presented by plant stressors and the ability of the plants to self-manage the resulting consequences, as well as by the management and maintenance team's ability to respond with necessary interventions when such efforts are failing. In contrast, the complete failure of installations is more likely to stem from fundamental design flaws or substantial management and maintenance team failures to maintain plant stress management infrastructure. It is significant to note that the management tasks inspected seemed to be dependent on the monitoring diligence and competence of the managers, with **none employing smart sensor data-driven technologies to automate** processes. The adoption of such technologies in the future is likely to offer the opportunity to reduce existing maintenance burdens and resource consumption.

The methodologies employed by the respective managers highlighted varying complexity, with a few bespoke to the installation profile. In terms of resource consumption, soil-based systems were expressed to offer significant water-use and material replacement advantage, along with higher planting densities and flexibility. The popular hydroponic felt-based systems in contrast were expressed to present higher water-use and material replacement burdens in agreement with previous studies (e.g., [182,416]). The latter however offered the highest planting diversity (order of magnitude greater) to present visually flourishing installations, which suggested association with the increased frequency of human engagement behaviour observed. Sustaining flourishing installations could be said to be influenced by the ability to sustain human engagement interest, with the **interaction from public and building occupants highlighted as a key motivator** by installation managers. This hypothesis however needs to be investigated further in future research, as the modest sample size and number of site visits in this study limits significant correlations from being identified. Further observational study is therefore encouraged including failed projects, while the limited number of failed projects in the European context at present could be considered as an indicator of the general commitment of installation managers towards sustaining thriving ecosystems.

PART III

# Chapter 9

## SYNTHESIS AND RECOMMENDATIONS

The findings of the two-part review and following five studies are summarised and synthesised in this chapter to present the project's final outcomes. It first presents concise answers to the five secondary research questions raised at the onset, followed by key recommendations for built environment practice. Finally, the chapter concludes with an introduction to future development opportunities and subsidiary interests, and project reflections.

### 9.1 Research questions answered

From the review of literature in Part I, mitigation and adaptation were stressed as being equally significant when considering climate resilience. In relation to urban heat risks this translates to measures that address the mitigation of prolonged heat storage in cities (long-term), as well as the moderation of heat extremes that enable adaptation (short-term). Urban green infrastructure contributes to both these demands. The significance of the contributions made depend principally on the scale of the intervention, along with associated secondary parameters discussed in Chapter 2. Climatological evidence has confirmed the need for substantial coverage areas to make city-scale modifications, while microscale thermal relief is achievable with modestly scaled, well-arranged interventions. The latter is a significant benefit to communities in densely built cities, with added value from the identified greater microscale cooling influence observed during harsher conditions typical of heatwaves and high heat island intensity.

As alleviating city-wide heat-related impacts with green infrastructure interventions become progressively more challenging in densely constructed cities, the focus has shifted towards localised thermal mitigation/relief measures. Reducing thermal loads in such settings is expected to reduce demands on health, comfort, and wellbeing, as well as energy used to modify these immediate climates. The study of green infrastructure enables city-planners, policymakers, engineers, and architects to determine appropriate types and their efficient urban arrangements, with the exponential increase in attention received in recent years indicative of the subject's acknowledged value to urban planning. Surface greening and its subcategory of vertical greening exists within this milieu of expanding interest. This thesis sought to address shortfalls in the evidence base to promote their wider application based on technical reasoning, as opposed to aesthetic fascination.

The second stage of the Part I review stressed the lack of relatability of observations derived from outdoor application studies in relation to sheltered and indoor settings, particularly with reference to in-situ observations. This represented the point of departure for the five secondary research questions raised and addressed in Part II of this project. The first and second questions sought to establish the empirical evidence for microclimate influence in underreported in-situ environments. Considering their findings, the third and fourth questions sought the development of influence approximation pathways, for building (Pathway-A) and urban neighbourhood-scale (Pathway-B) applications. Finally, the fifth question sought to address the challenges of widespread application and its sustainability.

### 9.1.1 Q I

*To what extent does the presence of a vertical greening installation modify the microclimate of a sheltered environment?*

#### Q I Answer

To address this question, monitoring was carried out at an indoor atrium and a semi-outdoor court including living walls. The results highlighted only a modest surface proximate cooling and humidifying influence at the **indoor study (maximum $T_{air}$: M = 0.3 K and $RH$: M = 5.5%)**, in contrast to **relatively greater influence at the semi-outdoor study (maximum $T_{air}$: M = 0.9 K and $RH$: M = 13.7%)**. Both studies therefore presented less influence than typically reported for outdoor installations in the literature (see Chapter 3). From the results it is also evident that the potency of hygrothermal modifications (characterised by horizontal distribution) to be most apparent within the 1-2 m proximity zone from installation surfaces. Beyond this range other phenomena such as the stack-flow at the indoor atrium study, caused interference and mixing to disrupt distribution. Notably, air movement data from the same indoor study presented a dominant daytime downward flow, which together with the stack-flow could be contributing to the function of a microscale centripetal thermal system in the atrium. The potency of this flow when combined with other flow disruptions was however modest (PPD between 10-15%), with **significance only for presenting thermal sensation and diversity to proximate occupants.**

### 9.1.2 Q II

*How does the plant canopy morphology of a vertical greening installation influence its surface temperature?*

#### Q II Answer

The purpose of this question was to examine how installation canopies influence their surface temperatures ($ST_{leaf}$), which in turn affects their surface flux. To address this, the study investigated the influence that the non-destructively measurable living wall canopy morphological features of protuberance ($z_{veg}$) and leaf size ($W_{leaf}$) has on its $ST_{leaf}$, using qualitative and quantitative thermography. The preliminary qualitative, and subsequent quantitative assessment confirmed that large and broadleaf canopies with substantial protuberance to present much warmer $ST_{leaf}$ relative to small-leaf canopies that are more surface spreading. This finding highlighted that both these canopy morphological parameters are significant and must be input for the reasonable approximation of $T_{leaf}$, and as a result the surface flux from a given installation.

The above findings informed the coding of the developed model, with the sensitivity of the two parameters assessed against the model's final outcomes as part of the subsequent exercises in Study 3.

### 9.1.3 Q III

*How can vertical greening influence be approximated for building-scale assessments in a computationally efficient manner?*

#### Q III Answer

To address this problem, the study developed and presented a one-dimensional vertical greening model (VGM) that can be coupled with the TRNSYS building energy modeller to obtain reasonable estimates of microclimate modification and energy use implications of vertical greening application. The agreement results demonstrated that this is achievable and applicable in semi-outdoor environments, while the promising results from indoor environment application, particularly with living wall assessment requires further validation.

Application of the VGM coupling to the DAB indoor atrium case study highlighted vertical greening addition to present a net annual space-conditioning energy consumption saving when air-conditioning was considered (69 or 71% for the atrium and 1.1 or 2.0% for the rooms behind, with either living wall or green façade application respectively). The current natural ventilation and heating only profile however presented a modest net increase resulting from the wintertime cooling influence provided by the evergreen installation (0.9 or 1.5% for the rooms behind with living wall or green façade application respectively). Green façade application therefore had greater influence on net annual space-conditioning energy consumption at the indoor study than with living wall addition.

The application of the VGM coupling to the SET semi-outdoor court case study simulated surface flux reductions to present a thermally moderated microclimate, with living walls reducing the flux the most (84-90%) relative to green façade application (37-44%). The extent of this was dependent on the dynamic latent-to-sensible partitioning efficiencies, which in turn is dependent on the solar radiation loading received and moderated by contextual morphological and material features.

Although the two sheltered application environments examined in this study cannot be compared like-for-like, it is noteworthy that the greater influence of living wall application simulated at the SET semi-outdoor study contrasted against the greater influence of green façade application simulated at the DAB indoor study. This highlighted the complex significance of the substrate feature of living wall installations, which in certain circumstances could present counterproductive influence.

### 9.1.4 Q IV

*To what extent would neighbourhood-scale application contribute to enhancing urban climate resilience?*

#### Q IV Answer

To address this question, a simulation comparison study was carried out of office buildings with construction build-ups including vertical greening applications sited within the contexts of central urban and suburban neighbourhoods. The results showed that vertical greening application contributed to urban climate resilience by improving the thermal climate of the outdoor environment, which in turn impacted on the energy consumption of the street canyon buildings including the installations.

The application of vertical greening simulated benefit to canyon pedestrians by reducing daytime heat island intensity and increasing the occurrences of cool island conditions experienced. This in turn would contribute to relieving heat stress and facilitate the creation of thermally comfortable street canyon environments for pedestrians. These benefits were pronounced for the central urban context than suburban, and with living wall application than green façade. The better performance from living wall application is therefore complementary to the findings from the semi-outdoor simulations in Study 3.

The study also found the heat island load to adversely influence space-conditioning demands of buildings fronting the canyon, and stressed the necessity for accounting for this load when estimating building energy consumption. The improvements in the respective canyon climates from vertical greening application translated to significant net annual space-conditioning savings to these buildings (between 0.8 and 5.2%), with urban scenarios presenting greater savings than suburban, and living wall application presenting greater savings than green façades. These net annual savings in turn demonstrated the potential for wider applicability of vertical greening in temperate climates, with greater value from living wall application.

### 9.1.5 Q V

*What are the key challenges in sustaining the positive contributions of vertical greening installations in temperate climates?*

#### Q V Answer

To address this question, inspections were carried out at ten European case studies, with associated interviews with their management authorities. The results highlighted atypical extremes of abiotic stressors including water, temperature, and light as the most challenging to address with outdoor urban installations; particularly during the construction phase and initial establishing period; as well as when local climate variability has been underestimated. With indoor installations, the vulnerability to such extremes is limited by the near closed nature of the local climate. Instead, optimal growth conditions maintained throughout the year had often translated to higher growth management requirements.

The inspected management tasks were entirely dependent on the monitoring diligence and competence of the installation managers, with none employing smart sensor, data-driven technologies to automate processes (e.g., real-time thermography). Sustaining flourishing installations was stressed as a key motivator in delivering this diligence, with the flourishing state determined by aesthetics. This aesthetic perception had similar significance on human engagement interest, demonstrated by both the public and building occupants alike.

## 9.2 Synthesis

By collating the answers to the five secondary research questions, an answer could now be forwarded for the principal research question this project and thesis set out to answer at its commencement:

*To what extent does architectural vertical greening enhance heat-related climate resilience in urban built environments, and is there value in advocating for wider application in temperate climates?*

At the monitored sheltered living wall installations, Study 1 and 2 identified modest surface proximate cooling and humidifying influence, as well as surface temperature asymmetry and airflow modifications. The distinction between the two studies was highlighted by the magnitude of hygrothermal influence, with greater presented at the semi-outdoor study than at the indoor one. This greater influence from the former however was still less potent than values typically reported for outdoor installations in the available literature. From this evidence it could be argued that the degree of microclimate modification presented by vertical greening application to depend on the degree of shelter relevant for the given environment; with the spectrum of influence highlighting outdoor installations to present the most, followed by semi-outdoors, and least by indoor installations. The modest influences observed were also most apparent and potent within the 1-2 m proximity zone from installation surfaces, while background climate mixing often disrupted detection and distribution beyond this range. The key benefit for occupants inhabiting these environments is thus limited to **experiencing thermal sensation and diversity**, which broadly contributes to their wellbeing enhancements. The degree to which this is significant however is dependent on occupant proximity, thereby highlighting the arrangement and siting of the installation as a key design consideration.

The simulation results from Study 3 identified the above influences to generate thermally moderated microclimates in the modestly scaled sheltered environments examined. This in turn could translate to energy use savings if the said environments require and implement space-conditioning, particularly mechanical cooling. The simulations however highlighted the cooling extent provided by such passive vertical greening installations to be insufficient to entirely negate the need for mechanical cooling provision. The advantage presented is therefore to do with **significantly reducing energy consumption** needed to satisfy such demands (i.e., reducing peak demands). In such instances a net annual space-conditioning energy consumption saving could be expected, although in indoor environments this is dependent on the internal gains from contextual building zones. Any such saving gained may be a significant advantage in commercial or institutional buildings such as healthcare facilities, sheltered accommodation, and community centres, where worsening heat-related risks will eventually necessitate some form of mechanical cooling to be introduced. The living wall category in this regard presented greater influence than green façade application at the semi-outdoor study, owing to the added contribution from its saturated substrate. At the indoor study however, green façade application in contrast offered better relative performance as the heat storage contribution of the living wall substrate countered some of the benefit offered from its evaporative flux. The latter substrate performance complexities coupled with internal gains disparities mean that the nature of vertical greening influence is more finely balanced in indoor environments, and thus requires situation-specific assessments to conclude vertical greening contributions.

The simulation results from Study 4 found widespread vertical greening application to also improve the thermal climate of the outdoor street canyon environment to benefit pedestrians, as well as present energy use savings to buildings including the façade installations. These benefits were pronounced for the more densely arranged central urban context than suburban, which justifies their appropriateness as a strategy for enhancing urban greening where space is at a premium, and where retrofitting would be the only option available. The higher net energy savings simulated for the canyon therefore stressed the **significance of wider applicability in temperate climate compacted cities**, with emphasised value gained from living wall application. Study 5 on the other hand identified atypical extremes of abiotic stressors including water, temperature, and light as the most challenging to address when considering such temperate climate applications.

From a methodological perspective, the project was commenced with the principle aim of utilising and contributing to an existing urban modelling framework (or ecology) to situate and analyse the defined set of problems presented by vertical greening application. This approach ensures greater reproducibility and continuity of research, with future researchers able to extract the relevant module/component to either upgrade or adapt to complement their research agenda. As such, the project successfully **delivered two novel model coupling Pathways as its principal contribution** (Fig. 115).

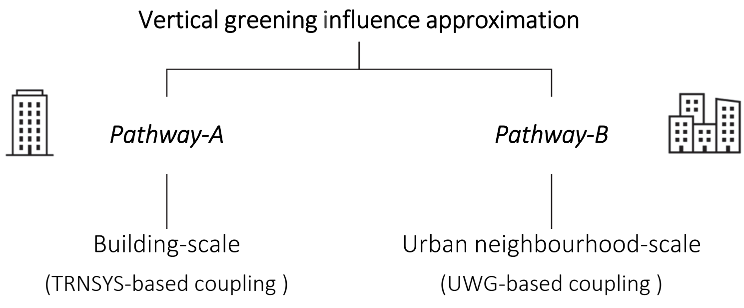


*Fig. 115. VGM coupling pathways delivered.*

### 9.2.1 Recommendations

The following presents a concise list of recommendations:

#### Multiples

- The addition of multiple smaller green infrastructure interventions that take advantage of dominant wind flow patterns (in the summer), offer greater cooling transport across a larger canopy layer area than with a solitary larger feature. Useful greenspace can therefore be introduced as infilling features in urban regeneration and compaction projects, while any shortfall should be addressed by well-planned and diverse surface greening additions. Vertical greening in this regard provides the means to utilise the abundant, yet underutilised vertical surfaces of urban buildings to deliver meaningful enhancement in green coverage. Advancements in systems available mean that this is now achievable in both newbuild and retrofit projects.

#### Diversity

- While initial surface greening applications were mostly of the extensive variety, system advancements now enable more diverse, intensive plant communities to be implemented at relatively low cost. The evidence base stresses that the diversity added from the introduction of shrubs and small trees to the plant community to present greater ecosystem service provision. This can be amplified for any given project by concurrently implementing a range of green infrastructure solutions (e.g., combinations of extensive and intensive vertical and horizontal greening coupled with contextual landscaping and waterbodies). This hybrid implementation means the establishment of a more intersected and self-regulating ecosystem that better copes with threats, which in turn offers sustained ecosystem service provision.

#### Moderator

- Both building-scale simulation findings in Study 3 and neighbourhood-scale simulation findings in Study 4 stressed that although vertical greening is commonly promoted as a summertime cooling contributor, in practice it performs overall as a thermal moderator that regulates fluctuations to present benefit in both cooling and heating seasons. The neighbourhood-scale simulations highlighted that wintertime and transitional season heating energy reductions could contribute to substantial net annual expenditure savings. Wider-scale evergreen vertical greening application (living wall application in particular) therefore has significant value in temperate climates, with future urban planning policy and strategies needing to acknowledge and promote this energy saving benefit. This benefit however can be realised only with the successful growth of evergreen flora, which means that greater attention needs to be given to identifying flora with sufficient hardiness ratings to sustain ecosystem service provision throughout the challenging winter months.

### Proximity

- ❖ The monitoring evidence from Study 1 highlighted the discomfort risk from down-draught flow and radiation asymmetry to be negligible in sheltered environments (where such effects are likely to present the greatest risk). The hygrothermal and surface flow effects however are potent enough to present thermal sensation and diversity to occupants, thereby enhancing their comfort, wellbeing, and health. At present however, the design of most observed installation arrangements precludes such thermal relief from being experienced by the respective building occupants. This in turn highlights the necessity for installation designers to take account of the proximity influence identified in this thesis and seek to increase building occupant access at future installation implementations. This will involve advising and directing clients to accept the best siting of installations to be in well-lit circulation routes such as corridors and stairwells, as opposed to large open volumes.

### Expectations

- ❖ The clients of a project must be informed from the onset of the challenges of introducing and sustaining an ecosystem (i.e., introducing a community of interacting organisms). They should also be advised of the extent and variability of ecosystem service provision that can be reasonably expected. For example, the monitoring and simulation findings of this project highlighted cooling benefit from passive installations to be modest in sheltered environments. In such circumstances they should not be engaged for the exclusive purpose of introducing microclimate cooling relief. If substantial cooling indeed is a prerequisite, active installations should be considered (e.g., ALWs).

### Aesthetics

- Study 5 highlighted aesthetic considerations to be high on the agenda of installation managers, given their perception that it is the principal client focus when determining the success of an installation. The reality is that much of the application growth witnessed in recent times has also been driven by this aesthetic demand, which in some settings has even encouraged the implementation of pseudo-installations. The danger therefore is that once the aesthetic fascination has passed, the drive to implement installations will also diminish. It is therefore in the interest of designers to expediently utilise the aesthetic driver to realise projects and broaden the evidence base, and while doing so to educate clients of the valuable ecosystem benefits gained. This will in turn ensure installation longevity and proliferation within urban fabrics is sustained.

### Engagement

- The evidence suggested the attraction and physical interaction with installations to be driven by the public/building occupant perception of their flourishing state; assessed aesthetically. While previous design direction has cautioned proximity and encouraged separation from human interaction fearing vandalism risk, the survey and inspections conducted suggested this fear to be unfounded. Human interactions with vertical greening plant communities in large part are non-injurious, and given the evidence highlighting the value of such interactions to a person's wellbeing, it should be encouraged.

### Systems

- Hydroponic felt-based continuous systems offer the highest planting diversity to present visually flourishing installations, which also suggested association with the increased frequency of human engagement behaviour observed. The maintenance and management experience data gathered however showed higher water-use and material replacement to present significant burden. Modular systems in response offer greater flexibility, adaptability, and scalability. From a sustainability and architectural assembly perspective, such modular systems are therefore the future of widespread application.

### 9.2.2 Limitations

Section 6.1.2 presented the key assumptions and limitations of the developed VGM. While most modelling aims were addressed in its development, several areas are acknowledged here as requiring further advancement. The following details a ‘wish-list’ of such improvements that the author plans to address and integrate into the next version of the model:

*Short term:*

→ Enhance data validation diagnostics and warnings.

→ Add parameter inputs using an Excel proforma (i.e., enhance user-input interface and options), as currently this is done through a MATLAB script.

→ Complete translating the VGM’s MATLAB coding as a TRNSYS component Type, which would vastly improve its computational efficiency[XXVI] and application flexibility, as well as promoting engagement within the building energy modelling community.

→ Following the publishing of the model, to upload the MATLAB code onto an online repository to aid dissemination amongst fellow researchers.

*Medium term:*

→ UWG and VGM coupling (i.e., Pathway-B) validation with reference to data from an in-situ canyon, which was beyond the scope of this project.

→ Include an interstitial ‘air-gap layer’ to simulate more advanced indirect green façade and living wall system arrangements.

→ The integration of a water balance to estimate hydration demands, as well as to accurately simulate humidity interactions (currently no water stress is assumed).

→ Increase dimensional representation to enhance simulation accuracy (e.g., in indoor environments), and aid the assessment of more complex situations.

---

[XXVI] Currently the Type 155 annual (8,760 hrs) green façade simulation clock-time varies between 10-30 minutes, while living wall simulations vary between 60-120 minutes.

## 9.3 Future research opportunities

Reflecting on the findings of this project, the following presents future research opportunities. They include the application and development of methodologies, as well as opportunity to assess the potential of another ecosystem benefit of enhancing urban greening.

### 9.3.1 Methodological opportunities

The use of thermography in this project was a direct response to the challenges of attempting to reasonably characterise canopy surface temperature ($ST_{leaf}$) through single-point measurements. By engaging with the methodology and researching its agricultural applications, the opportunity to transfer and advance approaches for the sustainable management of vertical greening systems became apparent.

#### Thermography and automation

Plant science studies have applied quantitative thermography to understand and aide stress management, particularly focusing on agricultural crops. This application is predicated on canopy surface temperature increases observed with plant senescence, typically induced by disruptions in water and nutrient uptake and transportation triggered by biotic or abiotic stressors. Biotic stress induced by pest or pathogen attack for example can result in distinct canopy surface temperatures, with thermography utilised to diagnose conditions prior to patent chromatic or morphological symptoms [417]. The method can also be used to assess abiotic stressors such as nutrient uptake, with deficiencies distinguishable between nutrient and water stress [336,418]. The latter aspect of water stress detection is by far the most significant abiotic stress management focus at present [331,419]. As thermography could be used to quantify $T_{leaf} - T_{air} = \Delta T_{veg}$, a canopy energy balance could thus be used to quantify the vapour pressure deficit, and from that calculate stomatal conductance ($g_s$), transpiration rate, and water status [337,346,420].

Although the thermography-based monitoring systems being developed at present focus on applying these benefits to monitor horizontally distributed agricultural or natural ecosystem canopies (e.g., [337]), there is potential for such systems to be adapted for vertical greening canopies and aid the application of automated precision irrigation and fertigation systems, including real-time biotic stress detection. Preliminary exercises of coupling the developed VGM with the canopy segmentation approach described in Study 2 revealed promising results (e.g., Fig. 116). The further development and deployment of this thermography coupled pathway would mean that vertical greening installation maintenance and resource costs could be lowered, which in turn could promote their widespread application and contribute to the efficient enhancement of urban climate resilience.

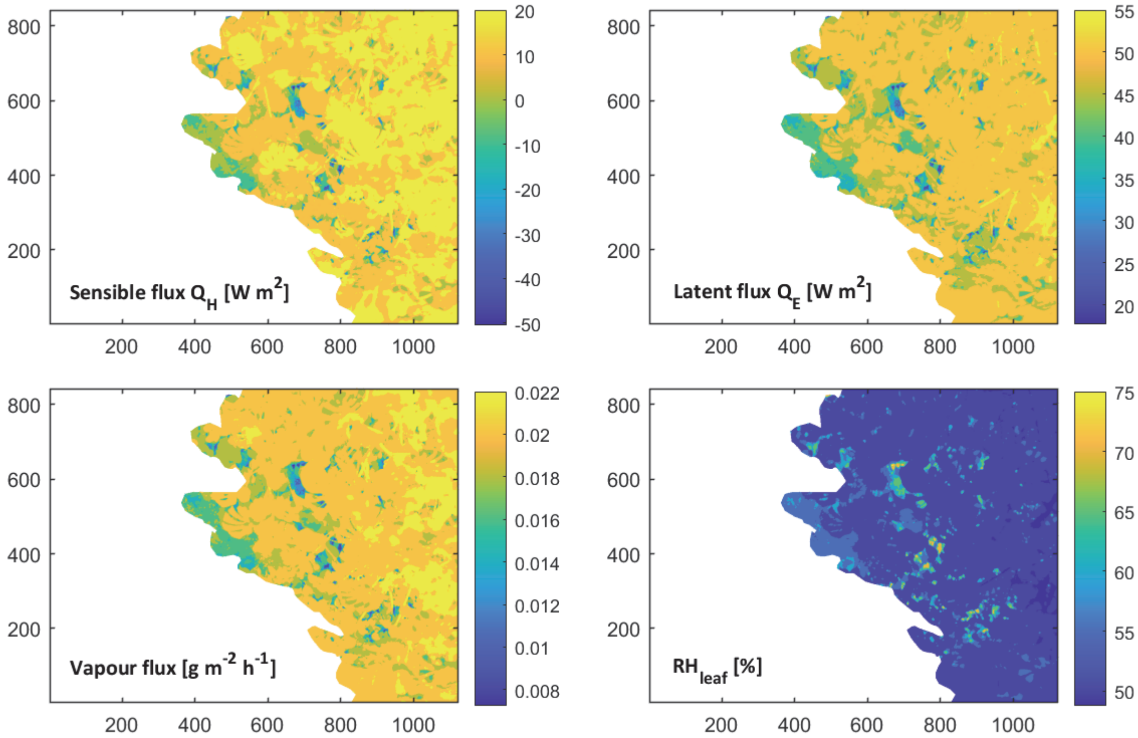


*Fig. 116. Coupling the VGM with thermography application to assess M. deliciosa canopy water status at the DAB indoor living wall installation.*

### 9.3.2 Simulation pathway expansion

In keeping with the aims established at the onset, the project presented the VGM and the resulting two model coupling pathways with built-in flexibility for future adaptation and modification, as well as opportunity to couple with any other compatible design simulation pathway. Amongst the many aspects that could be integrated to this model ecology, the opportunity to expand on the approximation of other plant-based ecosystem service provisions is a patent consideration. In this regard, the consideration of the productivity potential of urban vertical greening applications is an emerging interest for the author.

#### Enhancing urban food-security

Urban produce sourcing has historically received interest in times of crises when rural-to-urban supply routes have been disrupted. Notable experience is recorded during the War years, and more recently with the ongoing pandemic where movement restrictions have posed significant food-security challenges to many urban populations across the world [421]. The latter has thus reignited support for urban cultivation as a valuable community-based reinforcement strategy. Food-security experts however have long argued the necessity for urban cultivation to be based on the reality that rural harvests alone are unlikely to fully address the nutritional demands of ever-growing urban populations. They have therefore repeatedly called for greater food system infrastructure investments to be made by urban planning authorities [422–426].

Advancements in soilless cultivation has provided the technological opportunity. Such methods have not only demonstrated the ability to gain substantial yields from compact footprints, but also challenge the necessity for vacant horizontal cultivation areas. Vegetated architectural strategies such as living walls therefore present the potential to address the food-security challenge. By extending the VGM to couple a productivity model and a water balance, the pathways presented in this project could thus be explored to investigate the hypothesis that such 'suitably planted vegetated architectural features could make substantial contribution towards improving urban food-security'.

## 9.4 Project reflections

The overarching aim of the project was to address the climate emergency call and contribute towards the necessary development of passive climate resilience strategies. The two-stage review in Part I focused this broad aim to consider the contribution to be made by the enhanced application of the green infrastructural strategy of vertical greening and its novel variants. By investigating this focus through a sequence of five independent but connected studies, the project was able to make valuable and novel contribution towards improving the understanding of vertical greening performance, and the developing of principles for their efficient application in future urban developments.

Given the nature of the problem, a multidisciplinary approach was embraced to bring together several bodies of knowledge to address the research questions raised. This included engagement with public health, climate change, urban climatology, city-planning, plant science, building physics, and architectural resources. The interdisciplinary value gained from this engagement is of significant merit not only to the development of the subject, but also the author's own comprehension of the research endeavour.

### 9.4.1 Project outcomes

The project's aim of delivering analysis pathways that enable built environment practitioners to determine the expedient application of vertical greening was met with the development of the VGM and resulting analysis coupling pathways (elaborated through exemplar application studies). These Pathways (A & B) now provide the means for vertical greening application considerations to be front-loaded to building and urban design approaches, which in turn will offer technically sound reasoning for utilising such strategies and prevent costly and unsightly failures of future installations.

The development of a novel simulation model and its validation is a protracted and iterative process. The first model coded accordingly underwent several rounds of development involving the addition of layers of complexity (on occasion rollback), followed by testing to arrive at the working version presented here. The publications achieved and this thesis therefore only presents to the reader the narrative of the most fruitful avenue pursued. Notwithstanding this effort, the outcome achieved is still cautioned with areas identified for further development. The advantage of planning the project from onset to follow a model ecology is that many of such tasks can now be implemented and tested in subsequent releases with ease, and significantly with the rigor introduced by addressing the critique of building energy modelling peers. It also facilitates for future collaborative development.

### 9.4.2 Academic outcomes

The principal academic aim of this project was to engage with real-world conditions to inform the study of urban green infrastructure, specifically explored through the typology of vertical greening. To achieve this, the monitoring of in-situ case studies was utilised, which then informed the simulation-based analysis Pathways proposed. Overcoming the challenges of carrying out in-situ measurements was a key learning outcome, met to varying degrees of success throughout the course of the project. The acquisition of measurement apparatus was particularly challenging, with interdepartmental loans utilised where possible to part address the Departmental shortfall. Addressing full requirements however meant the need to acquire new assets, with the decision made to procure pre-calibrated off-the-shelf apparatus to facilitate accurate and immediate deployment. The budget however was limited and only permitted the procurement of essential requirements. The consequence of this was a reduction in scope, with case study selection reduced to only two of the three sites initially named. The reduced number of probs also meant that the deployment programme required continuous rearranging to acquire meaningful data covering the desired time periods. The entire programme was therefore an exercise in how to resourcefully achieve the established measurement objectives of the project.

Although these monitoring tasks were delayed by university-wide industrial action during the first year of the project, the most substantial disruption by far was presented by the global Covid-19 pandemic (active at the time of writing). While most of the monitoring exercises were completed prior to its escalation, the subsequent movement restrictions imposed disrupted data collection and thwarted all plans for supplementary experiments. The project consequently had to depend entirely on the data gathered from the previous year, with acknowledged need for further model validation exercises to be carried out following the removal of the said restrictions. Given these difficulties, the successful completion of most tasks set out at the project's commencement must be considered as a privilege.

A secondary academic objective of the project sought the validation of findings and developed analysis pathways by engaging and seeking publication in peer-reviewed journals, as well as presenting at pertinent international conferences. The thesis presented here is as a result a 'hybrid', which combines these published and presented materials to date with the overarching research narrative set-out at commencement. The publishing and conference engagement also presented the advantage of addressing criticism from external expert reviewers, which in turn has reinforced the material and outcomes presented.

***The most rewarding accomplishment of this thesis project was the successful delivery of the vertical greening model (VGM), followed by the two associated analysis Pathways to determine the expedient application of installations in cities. These Pathways (A & B), now pave the way for application considerations to be front-loaded to building and urban design processes. This in turn addressed the author's aspiration to present built environment analysts with efficient pathways for early assessments, as well as in facilitating the agenda for evidence-based decision-making in the delivery of climate resilient urban environments.***

*****

# BIBLIOGRAPHY

[1] B. Bueno, L. Norford, J. Hidalgo, G. Pigeon, The urban weather generator, *Journal of Building Performance Simulation*. 6 (2013) 269–281.

[2] T.R. Oke, Boundary Layer Climates, 2nd ed., Methuen, London, 1987.

[3] A. Stevenson, ed., Oxford Dictionary of English, 3rd ed., Oxford University Press, Oxford, 2010.

[4] C. Park, M. Allaby, A Dictionary of Environment and Conservation, 3rd ed., Oxford University Press, Oxford, 2017.

[5] K. Williams, Government Office for Science, Foresight, Urban form and infrastructure, a morphological review, London, 2014.

[6] C. Gorse, D. Johnston, M. Pritchard, A Dictionary of Construction, Surveying and Civil Engineering, 2nd ed., Oxford University Press, Oxford, 2020.

[7] J. Law, E. Martin, Concise Medical Dictionary, 10th ed., Oxford University Press, Oxford, 2020.

[8] T. Parkinson, R. De Dear, Thermal pleasure in built environments: Physiology of alliesthesia, *Building Research and Information*. 43 (2015) 288–301.

[9] ASHRAE, ASHRAE Handbook 2013 Fundamentals, American Society of Heating, Refrigerating and Air Conditioning Engineers, Atlanta, 2013.

[10] K. Gunawardena, K. Steemers, Living walls in indoor environments, *Building and Environment*. 148 (2019) 478–487.

[11] A. Rogers, N. Castree, R. Kitchin, A Dictionary of Human Geography, Oxford University Press, Oxford, 2013.

[12] UK Committee on Climate Change Adaptation Sub-Committee, UK Climate Change Risk Assessment 2017, Synthesis report: Priorities for the next five years, Climate Change Committee, London, 2017.

[13] UK Committee on Climate Change Adaptation Sub-Committee, Independent Assessment of UK Climate Risk: Advice to Government For the UK's third Climate Change Risk Assessment (CCRA3), London, 2021.

[14] UN IPCC, Climate Change 2021: The Physical Science Basis. Contribution of Working Group I to the Sixth Assessment Report of the Intergovernmental Panel on Climate Change, Cambridge University Press, Cambridge, 2021.

[15] UK Met Office, UK Climate Projections: Headline Findings, Exeter, 2019.

[16] UN, World Urbanization Prospects: Highlights, United Nations, New York, 2014.

[17] K.R. Gunawardena, Heat vulnerability: risk to health and wellbeing in the built environment [M.Phil paper], University of Cambridge, 2015.

[18] S.N. Gosling, J.A. Lowe, G.R. McGregor, M. Pelling, B.D. Malamud, Associations between elevated atmospheric temperature and human mortality: a critical review of the literature, *Climatic Change*. 92 (2009) 299–341.

[19] K.G. Arbuthnott, S. Hajat, The health effects of hotter summers and heat waves in the population of the United Kingdom: A review of the evidence, *Environmental Health: A Global Access Science Source*. 16 (2017) 1–13.

[20] H. Johnson, R.S. Kovats, G. McGregor, J. Stedman, M. Gibbs, H. Walton, E. Black, The impact of the 2003 heatwave on mortality and hospital admissions in England, *Health Statistics Quarterly*. 25 (2005) 6–11.

[21] S. Hajat, S. Vardoulakis, C. Heaviside, B. Eggen, Climate change effects on human health: projections on temperature-related mortality for the UK during the 2020s, 2050s and 2080s, *Journel Epidemiol Community Health*. 0 (2013) 1–8.

[22] R.S. Kovats, S. Hajat, Heat stress and public health: A critical review, *Annual Review of Public Health*. 29 (2008) 41–55.

[23] C.E. Reid, M.S. O'Neill, C.J. Gronlund, S.J. Brines, D.G. Brown, A. V. Diez-Roux, J. Schwartz, Mapping community determinants of heat vulnerability, *Environmental Health Perspectives*. 117 (2009) 1730–1736.

[24] S. Hajat, R.S. Kovats, K. Lachowycz, Heat-related and cold-related deaths in England and Wales: who is at risk?, *Occupational and Environmental Medicine*. 64 (2007) 93–100.

[25] L.S. Kalkstein, R.E. Davis, Weather and Human Mortality - an Evaluation of Demographic and Interregional Responses in the United-States, *Annals of the Association of American Geographers*. 79 (1989) 44–64.

[26] T.R. Oke, The Energetic Basis of the Urban Heat-Island, *Quarterly Journal of the Royal Meteorological Society*. 108 (1982) 1–24.

[27] K. Gunawardena, K. Steemers, Adaptive comfort assessments in urban neighbourhoods: Simulations of a residential case study from London, *Energy and Buildings*. 202 (2019) 109322.

[28] O. Buchin, M.T. Hoelscher, F. Meier, T. Nehls, F. Ziegler, Evaluation of the health-risk reduction potential of countermeasures to urban heat islands, *Energy and Buildings*. 114 (2016) 27–37.

[29] K. Steemers, Energy and the city: density, buildings and transport, *Energy and Buildings*. 35 (2003) 3–14.

[30] M. Santamouris, On the energy impact of urban heat island and global warming on buildings, *Energy and Buildings*. 82 (2014) 100–113.

[31] H. Taha, Urban climates and heat islands: albedo, evapotranspiration, and anthropogenic heat, *Energy and Buildings*. 25 (1997) 99–103.

[32] B. Boardman, S. Darby, G. Killip, M. Hinnells, C.N. Jardine, J. Palmer, G. Sinden, 40 Percent House, Environmental Change Institute University of Oxford, Oxford, 2005.

[33] M. Kolokotroni, Y.P. Zhang, R. Watkins, The London Heat Island and building cooling design, *Solar Energy*. 81 (2007) 102–110.

[34] UK Committee on Climate Change Adaptation Sub-Committee, Reducing emissions and preparing for climate change: 2015 Progress Report to Parliament, Committee on Climate Change, London, 2015.

[35] S. Diamond, C. Das Bhaumic, A. Mylona, G. Virk, Zero Carbon Hub evidence review: assessing overheating risk, London, 2015.

[36] GB DCLG, Investigation into overheating in homes: literature review, Department for Communities and Local Government, London, 2012.

[37] UK Committee on Climate Change Adaptation Sub-Committee, Managing climate risks to well-being and the economy, Committee on Climate Change, London, 2014.

[38] D.J. Sailor, A review of methods for estimating anthropogenic heat and moisture emissions in the urban environment, *International Journal of Climatology*. 31 (2011) 189–199.

[39] K.R. Gunawardena, T. Kershaw, Green and blue-space significance to urban heat island mitigation, in: S. Emmit, K. Adeyeye (Eds.), Integrated Design International Conference (ID@50), University of Bath, Bath, 2016: pp. 1–15.

[40] A. Dimoudi, M. Nikolopoulou, Vegetation in the urban environment: microclimatic analysis and benefits, *Energy and Buildings*. 35 (2003) 69–76.

[41] K.R. Gunawardena, M.J. Wells, T. Kershaw, Utilising green and bluespace to mitigate urban heat island intensity, *Science of the Total Environment*. 584–585 (2017) 1040–1055.

[42] K. Gunawardena, K. Steemers, Living wall influence on microclimates: an indoor case study, in: CISBAT 2019, Special Issue of Journal of Physics: Conference Series, IOP Science, 2019.

[43] K. Gunawardena, K. Steemers, Characterising living wall microclimate modifications in sheltered urban conditions: findings from two monitored case studies, in: J. Rodríguez-Álvarez, J.C. Gonçalves (Eds.), Planning Post Carbon Cities. Proceedings of the 35th PLEA Conference on Passive and Low Energy Architecture. Volume 1, University of A Coruña, A Coruña, 2020: pp. 606–611.

[44] K. Gunawardena, K. Steemers, Living wall influence on the microclimates of sheltered urban conditions: results from monitoring studies, *Architectural Science Review.* 64 (2020) 235–246.

[45] K. Gunawardena, T. Kershaw, K. Steemers, Simulation pathway for estimating heat island influence on urban/suburban building space-conditioning loads and response to facade material changes, *Building and Environment.* 150 (2019) 195–205.

[46] K. Gunawardena, K. Steemers, Urban living walls: reporting on maintenance challenges from a review of European installations, *Architectural Science Review.* 63 (2020) 526–535.

[47] L. Howard, The climate of London: deduced from meteorological observations made in the metropolis and at various places around it, Harvey and Darton, J. and A. Arch, Longman, Hatchard, S. Highley [and] R. Hunter, London, 1833.

[48] A. Sundborg, Climatological studies in Uppsala with special regard to the temperature conditions in the urban area, Appelbergs Boktryckeri Aktiebolag, Uppsala, 1951.

[49] T.R. Oke, The Urban Energy-Balance, *Progress in Physical Geography.* 12 (1988) 471–508.

[50] T.R. Oke, The distinction between canopy and boundary-layer urban heat islands, *Atmosphere.* 14 (1976) 268–277.

[51] C.S.B. Grimmond, M. Roth, T.R. Oke, Y.C. Au, M. Best, R. Betts, G. Carmichael, H. Cleugh, W. Dabberdt, R. Emmanuel, Climate and more sustainable cities: climate information for improved planning and management of cities (producers/capabilities perspective), *Procedia Environmental Sciences.* 1 (2010) 247–274.

[52] H.G. Jones, Plants and microclimate: A quantitative approach to environmental plant physiology, 3rd ed., Cambridge University Press, Cambridge, 2013.

[53] G.S. Campbell, J.M. Norman, An Introduction to Environmental Biophysics, 2nd ed., Springer Science & Business Media, New York, 1998.

[54] Hans Lambers, F.S. Chapin III, T.L. Pons, Plant Physiological Ecology, 2nd ed., Springer New York, New York, 2008.

[55] J. Monteith, M. Unsworth, Principles of environmental physics, 4th ed., Academic Press, an imprint of Elsevier, Oxford, 2013.

[56] R. Crang, S. Lyons-Sobaski, R. Wise, Plant anatomy, 1st ed., Springer Nature, New York, 2018.

[57] M.Z. Jacobson, Fundamentals of atmospheric modeling, Cambridge University Press, Cambridge, 2005.

[58] W. Zhou, X. Shen, F. Cao, Y. Sun, Effects of Area and Shape of Greenspace on Urban Cooling in Nanjing, China, *Journal of Urban Planning and Development.* 145 (2019).

[59] X.D. Xiao, L. Dong, H. Yan, N. Yang, Y. Xiong, The influence of the spatial characteristics of urban green space on the urban heat island effect in Suzhou Industrial Park, *Sustainable Cities and Society.* 40 (2018) 428–439.

[60] K. Ward, S. Lauf, B. Kleinschmit, W. Endlicher, Heat waves and urban heat islands in Europe: A review of relevant drivers, *Science of the Total Environment.* 569–570 (2016) 527–539.

[61] E. Ng, L. Chen, Y. Wang, C. Yuan, A study on the cooling effects of greening in a high-density city: An experience from Hong Kong, *Building and Environment.* 47 (2012) 256–271.

[62] T. Honjo, T. Takakura, Simulation of thermal effects of urban green areas on their surrounding areas, *Energy and Buildings.* 15 (1990) 443–446.

[63] L. Zhao, X. Lee, R.B. Smith, K. Oleson, Strong contributions of local background climate to urban heat islands, *Nature.* 511 (2014) 216–219.

[64] R. Emmanuel, A. Loconsole, Green infrastructure as an adaptation approach to tackling urban overheating in the Glasgow Clyde Valley Region, UK, *Landscape and Urban Planning*. 138 (2015) 71–86.

[65] C. Skelhorn, S. Lindley, G. Levermore, The impact of vegetation types on air and surface temperatures in a temperate city: A fine scale assessment in Manchester, UK, *Landscape and Urban Planning*. 121 (2014) 129–140.

[66] A. Bernatzky, The Contribution of Trees and Green Spaces to a Town Climate, *Energy and Buildings*. 5 (1982) 1–10.

[67] A. Bernatzky, Tree ecology and preservation, 3rd ed., Elsevier, Amsterdam, 1978.

[68] J. Heusinger, S. Weber, Surface energy balance of an extensive green roof as quantified by full year eddy-covariance measurements, *Science of the Total Environment*. 577 (2017) 220–230.

[69] M.V. Monteiro, T. Blanuša, A. Verhoef, P. Hadley, R.W.F. Cameron, Relative importance of transpiration rate and leaf morphological traits for the regulation of leaf temperature, *Australian Journal of Botany*. 64 (2016) 32–44.

[70] C. de Munck, A. Lemonsu, V. Masson, J. Le Bras, M. Bonhomme, Evaluating the impacts of greening scenarios on thermal comfort and energy and water consumptions for adapting Paris city to climate change, *Urban Climate*. 23 (2018) 260–286.

[71] K. Qiu, B. Jia, The roles of landscape both inside the park and the surroundings in park cooling effect, *Sustainable Cities and Society*. 52 (2020).

[72] H. Yan, F. Wu, L. Dong, Influence of a large urban park on the local urban thermal environment, *Science of the Total Environment*. 622–623 (2018) 882–891.

[73] B. Vidrih, S. Medved, Multiparametric model of urban park cooling island, *Urban Forestry & Urban Greening*. 12 (2013) 220–229.

[74] H. Sugawara, S. Shimizu, H. Takahashi, S. Hagiwara, K. Narita, T. Mikami, T. Hirano, Thermal Influence of a Large Green Space on a Hot Urban Environment, *Journal of Environmental Quality*. 45 (2016) 125–133.

[75] J. Park, J.H. Kim, D.K. Lee, C.Y. Park, S.G. Jeong, The influence of small green space type and structure at the street level on urban heat island mitigation, *Urban Forestry and Urban Greening*. 21 (2017) 203–212.

[76] C. Yu, W.N. Hien, Thermal benefits of city parks, *Energy and Buildings*. 38 (2006) 105–120.

[77] F. Aram, E. Solgi, E.H. García, A. Mosavi, A.R. Várkonyi-Kóczy, The cooling effect of large-scale urban parks on surrounding area thermal comfort, *Energies*. 12 (2019).

[78] C. Jansson, P.E. Jansson, D. Gustafsson, Near surface climate in an urban vegetated park and its surroundings, *Theoretical and Applied Climatology*. 89 (2006) 185–193.

[79] K.J. Doick, A. Peace, T.R. Hutchings, The role of one large greenspace in mitigating London's nocturnal urban heat island, *Science of the Total Environment*. 493 (2014) 662–671.

[80] I. Hamilton, J. Stocker, S. Evans, M. Davies, D. Carruthers, The impact of the London Olympic Parkland on the urban heat island, *Journal of Building Performance Simulation*. 7 (2014) 119–132.

[81] C. Li, C.W. Yu, Mitigation of urban heat development by cool island effect of green space and water body, in: Proceedings of the 8th International Symposium on Heating, Ventilation and Air Conditioning, Springer, 2014: pp. 551–561.

[82] J. Xu, Q. Wei, X. Huang, X. Zhu, G. Li, Evaluation of human thermal comfort near urban waterbody during summer, *Building and Environment*. 45 (2010) 1072–1080.

[83] S. Leuzinger, R. Vogt, C. Körner, Tree surface temperature in an urban environment, *Agricultural and Forest Meteorology*. 150 (2010) 56–62.

[84] K. Doick, T. Hutchings, The Forestry Commission, Air Temperature regulation by urban trees and green infrastructure, The Forestry Commission, Farnham, 2013.

[85] W. Wang, B. Zhang, L. Xiao, W. Zhou, H. Wang, X. He, Decoupling forest characteristics and background conditions to explain urban-rural variations of multiple microclimate regulation from urban trees, *PeerJ*. 2018 (2018).

[86] L. Shashua-Bar, M.E. Hoffman, Vegetation as a climatic component in the design of an urban street - An empirical model for predicting the cooling effect of urban green areas with trees, *Energy and Buildings*. 31 (2000) 221–235.

[87] L.L.H. Peng, Z. Jiang, X. Yang, Y. He, T. Xu, S.S. Chen, Cooling effects of block-scale facade greening and their relationship with urban form, *Building and Environment*. 169 (2020) 106552.

[88] K. Perini, M. Ottele, A.L.A. Fraaij, E.M. Haas, R. Raiteri, Vertical greening systems and the effect on air flow and temperature on the building envelope, *Building and Environment*. 46 (2011) 2287–2294.

[89] N.H. Wong, A.Y.K. Tan, Y. Chen, K. Sekar, P.Y. Tan, D. Chan, K. Chiang, N.C. Wong, Thermal evaluation of vertical greenery systems for building walls, *Building and Environment*. 45 (2010) 663–672.

[90] J.A. Acero, E.J.Y. Koh, X.X. Li, L.A. Ruefenacht, G. Pignatta, L.K. Norford, Thermal impact of the orientation and height of vertical greenery on pedestrians in a tropical area, *Building Simulation*. 12 (2019) 973–984.

[91] H. Saaroni, J.H. Amorim, J.A. Hiemstra, D. Pearlmutter, Urban Green Infrastructure as a tool for urban heat mitigation: Survey of research methodologies and findings across different climatic regions, *Urban Climate*. 24 (2018) 94–110.

[92] Y. Su, L. Liu, J. Liao, J. Wu, P. Ciais, J. Liao, X. He, X. Liu, X. Chen, W. Yuan, G. Zhou, R. Lafortezza, Phenology acts as a primary control of urban vegetation cooling and warming: A synthetic analysis of global site observations, *Agricultural and Forest Meteorology*. 280 (2020).

[93] M. Santamouris, L. Ding, F. Fiorito, P. Oldfield, P. Osmond, R. Paolini, D. Prasad, A. Synnefa, Passive and active cooling for the outdoor built environment – Analysis and assessment of the cooling potential of mitigation technologies using performance data from 220 large scale projects, *Solar Energy*. 154 (2017) 14–33.

[94] C. Bartesaghi Koc, P. Osmond, A. Peters, Evaluating the cooling effects of green infrastructure: A systematic review of methods, indicators and data sources, *Solar Energy*. 166 (2018) 486–508.

[95] M. Santamouris, Cooling the cities - A review of reflective and green roof mitigation technologies to fight heat island and improve comfort in urban environments, *Solar Energy*. 103 (2014) 682–703.

[96] D.E. Bowler, L. Buyung-Ali, T.M. Knight, A.S. Pullin, Urban greening to cool towns and cities: A systematic review of the empirical evidence, *Landscape and Urban Planning*. 97 (2010) 147–155.

[97] R.A. Bustami, M. Belusko, J. Ward, S. Beecham, Vertical greenery systems: A systematic review of research trends, *Building and Environment*. 146 (2018) 226–237.

[98] S.E. Gill, J.F. Handley, A.R. Ennos, S. Pauleit, Adapting cities for climate change: the role of the green infrastructure, *Built Environment*. 33 (2007) 115–133.

[99] T. Matthews, A.Y. Lo, J.A. Byrne, Reconceptualizing green infrastructure for climate change adaptation: Barriers to adoption and drivers for uptake by spatial planners, *Landscape and Urban Planning*. 138 (2015) 155–163.

[100] H. Taha, H. Akbari, A. Rosenfeld, J. Huang, Residential Cooling Loads and the Urban Heat-Island - the Effects of Albedo, *Building and Environment*. 23 (1988) 271–283.

[101] G.Y. Qiu, H.Y. Li, Q.T. Zhang, W. Chen, X.J. Liang, X.Z. Li, Effects of Evapotranspiration on Mitigation of Urban Temperature by Vegetation and Urban Agriculture, *Journal of Integrative Agriculture*. 12 (2013) 1307–1315.

[102] L. Shashua-Bar, M.E. Hoffman, The Green CTTC model for predicting the air temperature in small urban wooded sites, *Building and Environment*. 37 (2002) 1279–1288.

[103] D. Armson, P. Stringer, A.R. Ennos, The effect of tree shade and grass on surface and globe temperatures in an urban area, *Urban Forestry & Urban Greening*. 11 (2012) 245–255.

[104] S.E. Gill, M.A. Rahman, J.F. Handley, A.R. Ennos, Modelling water stress to urban amenity grass in Manchester UK under climate change and its potential impacts in reducing urban cooling, *Urban Forestry & Urban Greening*. 12 (2013) 350–358.

[105] T.R. Oke, The Micrometeorology of the Urban Forest, *Philosophical Transactions of the Royal Society of London Series B-Biological Sciences*. 324 (1989) 335–349.

[106] E.G. Mcpherson, D.J. Nowak, R. a Rowntree, US Department of Agriculture, Chicago's Urban Forest Ecosystem: Results of the Chicago Urban Forest Climate Project, *Urban Ecosystems*. (1994) 201.

[107] K. Perini, A. Magliocco, The Integration of Vegetation in Architecture, Vertical and Horizontal Greened Surfaces, *International Journal of Biology*. 4 (2012) 79–91.

[108] N. Weyens, S. Thijs, R. Popek, N. Witters, A. Przybysz, J. Espenshade, H. Gawronska, J. Vangronsveld, S.W. Gawronski, The role of plant-microbe interactions and their exploitation for phytoremediation of air pollutants, *International Journal of Molecular Sciences*. 16 (2015) 25576–25604.

[109] A.G. McDonald, W.J. Bealey, D. Fowler, U. Dragosits, U. Skiba, R.I. Smith, R.G. Donovan, H.E. Brett, C.N. Hewitt, E. Nemitz, Quantifying the effect of urban tree planting on concentrations and depositions of PM 10 in two UK conurbations, *Atmospheric Environment*. 41 (2007) 8455–8467.

[110] Q. Xiao, E.G. McPherson, Surface water storage capacity of twenty tree species in Davis, California, *Journal of Environmental Quality*. 45 (2016) 188–198.

[111] P.K. Cheung, C.Y. Jim, Differential cooling effects of landscape parameters in humid-subtropical urban parks, *Landscape and Urban Planning*. 192 (2019).

[112] T.J. Chandler, The Climate of London, Hutchinson & Co Ltd, London, 1965.

[113] J.X. Shi, J.S. Deng, X.M. Wang, C.F. Luo, X.C. Qiu, Thermal effect and adjusting mechanism of rural landscape patterns, *Scientia Silvae Sinicae*. 47 (2011) 7–15.

[114] R. Sun, L. Chen, How can urban water bodies be designed for climate adaptation?, *Landscape and Urban Planning*. 105 (2012) 27–33.

[115] ARUP, Reducing urban heat risk: a study on urban heat risk mapping and visualization, London, 2014.

[116] S.I. Bohnenstengel, S. Evans, P.A. Clark, S.E. Belcher, Simulations of the London urban heat island, *Quarterly Journal of the Royal Meteorological Society*. 137 (2011) 1625–1640.

[117] A. Mavrogianni, M. Davies, M. Batty, S.E. Belcher, S.I. Bohnenstengel, D. Carruthers, Z. Chalabi, B. Croxford, C. Demanuele, S. Evans, R. Giridharan, J.N. Hacker, I. Hamilton, C. Hogg, J. Hunt, M. Kolokotroni, C. Martin, J. Milner, I. Rajapaksha, I. Ridley, J.P. Steadman, J. Stocker, P. Wilkinson, Z. Ye, The comfort, energy and health implications of London's urban heat island, *Building Services Engineering Research & Technology*. 32 (2011) 35–52.

[118] N.E. Theeuwes, A. Solcerova, G.J. Steeneveld, Modeling the influence of open water surfaces on the summertime temperature and thermal comfort in the city, *Journal of Geophysical Research-Atmospheres*. 118 (2013) 8881–8896.

[119] Greater London Authority, Green infrastructure and open environments: the all London Green Grid, Greater London Authority, London, 2012.

[120] Met Office, Southern England: Climate, (2012).

[121] Parliament UK, Hansard: Written answers for 7 February 2002, *Bound Volume Hansard - Written Answers*. 2016 (2002).

[122] GiGL, Greenspace Information for Greater London (GiGL), (2016).

[123] LVRPA, Lee Valley Regional Park Authority, (2016).

[124] Google Maps, Image data, (2016) 22 February 2016.

[125] S. Peng, S. Piao, P. Ciais, P. Friedlingstein, C. Ottle, F.M. Bréon, H. Nan, L. Zhou, R.B. Myneni, Surface urban heat island across 419 global big cities, *Environmental Science and Technology*. 46 (2012) 696–703.

[126] M.M.H. Echenique, A.J.A. Hargreaves, G. Mitchell, A. Namdeo, Growing Cities Sustainably. Does Urban Form Really Matter?, *Journal of the American Planning Association*. 78 (2012) 121–137.

[127] B. Stone, J.J. Hess, H. Frumkin, Urban form and extreme heat events: Are sprawling cities more vulnerable to climate change than compact cities?, *Environmental Health Perspectives*. 118 (2010) 1425–1428.

[128] V. Masson, C. Marchadier, L. Adolphe, R. Aguejdad, P. Avner, M. Bonhomme, G. Bretagne, X. Briottet, B. Bueno, C. de Munck, O. Doukari, S. Hallegatte, J. Hidalgo, T. Houet, J. Le Bras, A. Lemonsu, N. Long, M.P. Moine, T. Morel, L. Nolorgues, G. Pigeon, J.L. Salagnac, V. Viguié, K. Zibouche, Adapting cities to climate change: A systemic modelling approach, *Urban Climate*. 10 (2014) 407–429.

[129] Y.J. Huang, H. Akbari, H. Taha, A.H. Rosenfeld, The potential of vegetation in reducing summer cooling loads in residential buildings, *Journal of Climate and Applied Meteorology*. 26 (1987) 1103–1116.

[130] R. William, A. Goodwell, M. Richardson, P.V. V Le, P. Kumar, A.S. Stillwell, An environmental cost-benefit analysis of alternative green roofing strategies, *Ecological Engineering*. 95 (2016) 1–9.

[131] D.J. Sailor, T.B. Elley, M. Gibson, Exploring the building energy impacts of green roof design decisions – a modeling study of buildings in four distinct climates, *Journal of Building Physics*. 35 (2012) 372–391.

[132] G. Grant, Ecologist and living wall consultant. Interviewed by Gunawardena, K. 15 November, (2017).

[133] T. Beatley, Handbook of biophilic city planning and design, Island Press, Washington, DC, 2017.

[134] T. Ward, Living wall consultant. Interviewed by Gunawardena, K. 22 January, (2018).

[135] M. Keeley, The Green Area Ratio: an urban site sustainability metric, *Journal of Environmental Planning and Management*. 54 (2011) 937–958.

[136] P. Blanc, The Vertical Garden: From Nature to the City, Revised Ed, W.W. Norton, New York, 2012.

[137] D.C. Gunawardena, Genera et species plantarum Zeylaniae: an etymological and historical account of the flowering plants of Ceylon, Lake House Investments, Colombo, 1968.

[138] T. Sternberg, H. Viles, A. Cathersides, Evaluating the role of ivy (Hedera helix) in moderating wall surface microclimates and contributing to the bioprotection of historic buildings, *Building and Environment*. 46 (2011) 293–297.

[139] H. Viles, T. Sternberg, A. Cathersides, Is ivy good or bad for historic walls?, *Journal of Architectural Conservation*. 17 (2011) 25–41.

[140] A.K. Mishra, K.K. Jain, K.L. Garg, Role of higher plants in the deterioration of historic buildings, *Science of The Total Environment*. 167 (1995) 375–392.

[141] C. Darwin, The Power of Movement in Plants, John Murray, London, 1880.

[142] L.J. Clark, W.R. Whalley, P.B. Barraclough, How do roots penetrate strong soil?, in: J. Abe (Ed.), Plant and Soil, Springer Netherlands, Dordrecht, 2003: pp. 93–104.

[143] P. Taylor, The Oxford Companion to the Garden, Oxford University Press, 2006.

[144] N. Dunnett, N. Kingsbury, Planting green roofs and living walls, Timber Press, Portland, OR, 2008.

[145] M. Köhler, Green facades-a view back and some visions, *Urban Ecosystems*. 11 (2008) 423–436.

[146] G. Boccaccio, The Decameron, 2007 ed., Project Gutenberg Literary Archive Foundation, Salt Lake City, USA, 1358.

[147] F. Colonna, Hypnerotomachia Poliphili, Aldus Manutius (ca. 1450–1515), Venice, 1499.

[148] M. Thornbush, A Photo-Based Environmental History of the Use of Climbing Plants in Central Oxford, UK, *International Journal of Geosciences*. 2013 (2013) 1083–1094.

[149] M.F. Bernstein, Football: the Ivy League origins of an American obsession, University of Pennsylvania Press, Pennsylvania USA, 2001.

[150] C.Y. Jim, Greenwall classification and critical design-management assessments, *Ecological Engineering*. 77 (2015) 348–362.

[151] M. Manso, J. Castro-Gomes, Green wall systems: A review of their characteristics, *Renewable and Sustainable Energy Reviews*. 41 (2015) 863–871.

[152] A. Medl, R. Stangl, F. Florineth, Vertical greening systems – A review on recent technologies and research advancement, *Building and Environment*. 125 (2017) 227–239.

[153] C. Darwin, On the Movements and Habits of Climbing Plants, *The Journal of the Linnean Society*. 9 (1865) 107.

[154] S. Isnard, W.K. Silk, Moving with climbing plants from Charles Darwin's time into the 21st century, *American Journal of Botany*. 96 (2009) 1205–1221.

[155] S.C. Lenaghan, M. Zhang, Real-time observation of the secretion of a nanocomposite adhesive from English ivy (Hedera helix), *Plant Science*. 183 (2012) 206–211.

[156] J.L. Turienzo, Agricultural Engineer and living wall consultant. Interviewed by Gunawardena, K. 09 August, (2018).

[157] R.W.F. Cameron, J.E. Taylor, M.R. Emmett, What's "cool" in the world of green façades? How plant choice influences the cooling properties of green walls, *Building and Environment*. 73 (2014) 198–207.

[158] R. Fernández-Cañero, L.P. Urrestarazu, A. Franco Salas, Assessment of the cooling potential of an indoor living wall using different substrates in a warm climate, *Indoor and Built Environment*. 21 (2012) 642–650.

[159] L. Pérez-Urrestarazu, R. Fernández-Cañero, A. Franco, G. Egea, Influence of an active living wall on indoor temperature and humidity conditions, *Ecological Engineering*. 90 (2016) 120–124.

[160] W.T. Hong, K. Ibrahim, S.C. Loo, Urging green retrofits of building facades in the tropics: A review and research agenda, *International Journal of Technology*. 10 (2019) 1140–1149.

[161] D. Holm, Thermal improvement by means of leaf cover on external walls - A simulation model, *Energy and Buildings*. 14 (1989) 19–30.

[162] N. McEvoy, Living wall consultant. Personal communication. 11 March, (2019).

[163] I. Susorova, M. Angulo, P. Bahrami, Brent Stephens, A model of vegetated exterior facades for evaluation of wall thermal performance, *Building and Environment*. 67 (2013) 1–13.

[164] A.M. Hunter, N.S.G. Williams, J.P. Rayner, L. Aye, D. Hes, S.J. Livesley, Quantifying the thermal performance of green façades: A critical review, *Ecological Engineering*. 63 (2014) 102–113.

[165] R.A. Francis, J. Lorimer, Urban reconciliation ecology: The potential of living roofs and walls, *Journal of Environmental Management*. 92 (2011) 1429–1437.

[166] S. Charoenkit, S. Yiemwattana, Living walls and their contribution to improved thermal comfort and carbon emission reduction: A review, *Building and Environment*. 105 (2016) 82–94.

[167] B. Jänicke, F. Meier, M.-T. Hoelscher, D. Scherer, Evaluating the Effects of Façade Greening on Human Bioclimate in a Complex Urban Environment, *Advances in Meteorology*. 2015 (2015) 1–15.

[168] European Environment Agency, Green infrastructure and territorial cohesion. The concept of green infrastructure and its integration into policies using monitoring systems, Luxembourg, 2011.

[169] European Commission, Building a Green Infrastructure for Europe, Luxembourg, 2013.

[170] UK Department for Environment Food and Rural Affairs, The Natural Choice: securing the value of nature, Norwich, 2011.

[171] S. Albon, K. Turner, R. Watson, A. Anger, J. Baker, I. Bateman, S. Bentley, N. Blyth, N. Bowles-Newark, C. Brown, I. Brown, J. Byrne, A. Church, P. Coates, C. Cowap, I. Dickie, M. Elliott, M. Everard, L. Gosling, N. Grayson, R. Haines-Young, P. Harrison, M. Kelly, J. Kenter, K. Martin, S. Maxwell, D. Mccarthy, L. Mee, K. Monk, D. Mortimer, D. Osborn, R. Owen, S. Ranger, M. Reed, D. Russel, A. Scott, D. Thompson, M. Tierney, R. Waters, J. Wharfe, T. Whitbread, D. Williams, B. Wilson, L. Wilson, U. NEA, UK National Ecosystem Assessment Synthesis of the Key Findings, *UK National Ecosystem Assessment*. (2014) 100.

[172] LP&B, BGMR, The Biotope Area Factor as an Ecological Parameter, Berlin, 1990.

[173] A. Kruuse, The Green Space Factor and the Green Points System, Malmö, 2011.

[174] R. Giordano, E. Montacchini, S. Tedesco, A. Perone, Living Wall Systems: A Technical Standard Proposal, *Energy Procedia*. 111 (2017) 298–307.

[175] R. Collins, M. Schaafsma, M.D. Hudson, The value of green walls to urban biodiversity, *Land Use Policy*. 64 (2017) 114–123.

[176] Transport for London, Delivering Vertical Greening, 2012.

[177] G. Grant, D. Gedge, Living Roofs and Walls from policy to practice, London, 2019.

[178] M. Ottelé, K. Perini, A.L.A. Fraaij, E.M. Haas, R. Raiteri, Comparative life cycle analysis for green façades and living wall systems, *Energy and Buildings*. 43 (2011) 3419–3429.

[179] P. Rosasco, K. Perini, Evaluating the economic sustainability of a vertical greening system: A Cost-Benefit Analysis of a pilot project in mediterranean area, *Building and Environment*. 142 (2018) 524–533.

[180] Natural England, Green Infrastructure – Valuation Tools Assessment, Exeter, 2013.

[181] L. Pérez-Urrestarazu, A. Blasco-Romero, R. Fernández-Cañero, Media and social impact valuation of a living wall: The case study of the Sagrado Corazon hospital in Seville (Spain), *Urban Forestry and Urban Greening*. 24 (2017) 141–148.

[182] K. Perini, P. Rosasco, Cost-benefit analysis for green façades and living wall systems, *Building and Environment*. 70 (2013) 110–121.

[183] K. Veisten, Y. Smyrnova, R. Klæboe, M. Hornikx, M. Mosslemi, J. Kang, Valuation of green walls and green roofs as soundscape measures: Including monetised amenity values together with noise-attenuation values in a cost-benefit analysis of a green wall affecting courtyards, *International Journal of Environmental Research and Public Health*. 9 (2012) 3770–3778.

[184] Z. Huang, Y. Lu, N.H. Wong, C.H. Poh, The true cost of “greening” a building: Life cycle cost analysis of vertical greenery systems (VGS) in tropical climate, *Journal of Cleaner Production*. 228 (2019) 437–454.

[185] F.R. Torpy, P.J. Irga, M.D. Burchett, Profiling indoor plants for the amelioration of high CO2 concentrations, *Urban Forestry and Urban Greening*. 13 (2014) 227–233.

[186] E. Cuce, Thermal regulation impact of green walls: An experimental and numerical investigation, *Applied Energy*. 194 (2017) 247–254.

[187] A. Hoyano, Climatological uses of plants for solar control and the effects on the thermal environment of a building, *Energy and Buildings*. 11 (1988) 181–199.

[188] M.T. Hoelscher, T. Nehls, B. Jänicke, G. Wessolek, Quantifying cooling effects of facade greening: Shading, transpiration and insulation, *Energy and Buildings*. 114 (2016) 283–290.

[189] J. Coma, M. Chàfer, G. Pérez, L.F. Cabeza, How internal heat loads of buildings affect the effectiveness of vertical greenery systems? An experimental study, *Renewable Energy*. 151 (2020) 919–930.

[190] L.S.H. Lee, C.Y. Jim, Subtropical summer thermal effects of wirerope climber green walls with different air-gap depths, *Building and Environment*. 126 (2017) 1–12.

[191] L. Zhang, Z. Deng, L. Liang, Y. Zhang, Q. Meng, J. Wang, M. Santamouris, Thermal behavior of a vertical green facade and its impact on the indoor and outdoor thermal environment, *Energy and Buildings*. 204 (2019).

[192] L.S.H. Lee, C.Y. Jim, Transforming thermal-radiative study of a climber green wall to innovative engineering design to enhance building-energy efficiency, *Journal of Cleaner Production*. 224 (2019) 892–904.

[193] F. Convertino, G. Vox, E. Schettini, Convective heat transfer in green façade system, *Biosystems Engineering*. 188 (2019) 67–81.

[194] G. Vox, I. Blanco, E. Schettini, Green façades to control wall surface temperature in buildings, *Building and Environment*. 129 (2018) 154–166.

[195] C. Li, J. Wei, C. Li, Influence of foliage thickness on thermal performance of green façades in hot and humid climate, *Energy and Buildings*. 199 (2019) 72–87.

[196] H.F. Di, D. Wang, Cooling effect of ivy on a wall, *Experimental Heat Transfer*. 12 (1999) 235–245.

[197] E.A. Eumorfopoulou, K.J. Kontoleon, Experimental approach to the contribution of plant-covered walls to the thermal behaviour of building envelopes, *Building and Environment*. 44 (2009) 1024–1038.

[198] I. Susorova, P. Azimi, B. Stephens, The effects of climbing vegetation on the local microclimate, thermal performance, and air infiltration of four building facade orientations, *Building and Environment*. 76 (2014) 113–124.

[199] R.W.F. Cameron, J. Taylor, M. Emmett, A Hedera green façade - Energy performance and saving under different maritime-temperate, winter weather conditions, *Building and Environment*. 92 (2015) 111–121.

[200] C. Bolton, M.A. Rahman, D. Armson, A.R. Ennos, Effectiveness of an ivy covering at insulating a building against the cold in Manchester, U.K: A preliminary investigation, *Building and Environment*. 80 (2014) 32–35.

[201] H. Yin, F. Kong, A. Middel, I. Dronova, H. Xu, P. James, Cooling effect of direct green façades during hot summer days: An observational study in Nanjing, China using TIR and 3DPC data, *Building and Environment*. 116 (2017) 195–206.

[202] G. Pérez, L. Rincón, A. Vila, J.M. González, L.F. Cabeza, Green vertical systems for buildings as passive systems for energy savings, *Applied Energy*. 88 (2011) 4854–4859.

[203] G. Pérez, J. Coma, S. Sol, L.F. Cabeza, Green facade for energy savings in buildings: The influence of leaf area index and facade orientation on the shadow effect, *Applied Energy*. 187 (2017) 424–437.

[204] J. Coma, G. Pérez, A. de Gracia, S. Burés, M. Urrestarazu, L.F. Cabeza, Vertical greenery systems for energy savings in buildings: A comparative study between green walls and green facades, *Building and Environment*. 111 (2017) 228–237.

[205] T. Koyama, M. Yoshinaga, H. Hayashi, K. ichiro Maeda, A. Yamauchi, Identification of key plant traits contributing to the cooling effects ofgreen façades using freestanding walls, *Building and Environment*. 66 (2013) 96–103.

[206] M.A. Kenaï, L. Libessart, S. Lassue, D. Defer, Impact of plants occultation on energy balance: Experimental study, *Energy and Buildings*. 162 (2018) 208–218.

[207] F. Yang, F. Yuan, F. Qian, Z. Zhuang, J. Yao, Summertime thermal and energy performance of a double-skin green facade : A case study in Shanghai, *Sustainable Cities and Society*. 39 (2018) 43–51.

[208] D. Tudiwer, A. Korjenic, The effect of living wall systems on the thermal resistance of the façade, *Energy and Buildings*. 135 (2017) 10–19.

[209] X. Nan, H. Yan, R. Wu, Y. Shi, Z. Bao, Assessing the thermal performance of living wall systems in wet and cold climates during the winter, *Energy and Buildings*. 208 (2020).

[210] M. Ottelé, K. Perini, Comparative experimental approach to investigate the thermal behaviour of vertical greened façades of buildings, *Ecological Engineering*. 108 (2017) 152–161.

[211] M. Solera Jimenez, Green walls: a sustainable approach to climate change, a case study of London, *Architectural Science Review*. 61 (2018) 48–57.

[212] C.Y. Cheng, K.K.S. Cheung, L.M. Chu, Thermal performance of a vegetated cladding system on facade walls, *Building and Environment*. 45 (2010) 1779–1787.

[213] F. Olivieri, L. Olivieri, J. Neila, Experimental study of the thermal-energy performance of an insulated vegetal façade under summer conditions in a continental mediterranean climate, *Building and Environment*. 77 (2014) 61–76.

[214] T. Safikhani, M. Baharvand, Evaluating the effective distance between living walls and wall surfaces, *Energy and Buildings*. 150 (2017) 498–506.

[215] S. Charoenkit, S. Yiemwattana, Role of specific plant characteristics on thermal and carbon sequestration properties of living walls in tropical climate, *Building and Environment*. 115 (2017) 67–79.

[216] U. Mazzali, F. Peron, P. Romagnoni, R.M. Pulselli, S. Bastianoni, Experimental investigation on the energy performance of Living Walls in a temperate climate, *Building and Environment*. 64 (2013) 57–66.

[217] Q. Chen, B. Li, X. Liu, An experimental evaluation of the living wall system in hot and humid climate, *Energy and Buildings*. 61 (2013) 298–307.

[218] F. Victorero, S. Vera, W. Bustamante, F. Tori, C. Bonilla, J. Gironás, V. Rojas, Experimental study of the thermal performance of living walls under semiarid climatic conditions, *Energy Procedia*. 78 (2015) 3416–3421.

[219] G. Pérez, L. Rincón, A. Vila, J.M. González, L.F. Cabeza, Behaviour of green facades in Mediterranean Continental climate, *Energy Conversion and Management*. 52 (2011) 1861–1867.

[220] T. Safikhani, A.M. Abdullah, D.R. Ossen, M. Baharvand, Thermal impacts of vertical greenery systems, *Environmental and Climate Technologies*. 14 (2014) 5–11.

[221] W.J. Stec, A.H.C. Van Paassen, A. Maziarz, Modelling the double skin facade with plants, *Energy and Buildings*. 37 (2005) 419–427.

[222] M.S. Penaranda-Moren, A. Korjenic, Hotter and colder – How Do Photovoltaics and Greening Impact Exterior Facade Temperatures: The synergies of a Multifunctional System, *Energy and Buildings*. 147 (2017) 123–141.

[223] M. Scarpa, U. Mazzali, F. Peron, Modeling the energy performance of living walls: Validation against field measurements in temperate climate, *Energy and Buildings*. 79 (2014) 155–163.

[224] M.P. de Jesus, J.M. Lourenço, R.M. Arce, M. Macias, Green façades and in situ measurements of outdoor building thermal behaviour, *Building and Environment*. 119 (2017) 11–19.

[225] R. Djedjig, E. Bozonnet, R. Belarbi, Experimental study of the urban microclimate mitigation potential of green roofs and green walls in street Canyons, *International Journal of Low-Carbon Technologies*. 10 (2015) 34–44.

[226] N. Katsoulas, D. Antoniadis, I.L. Tsirogiannis, E. Labraki, T. Bartzanas, C. Kittas, Microclimatic effects of planted hydroponic structures in urban environment: measurements and simulations, *International Journal of Biometeorology*. 61 (2017) 943–956.

[227] C.L. Tan, N.H. Wong, S.K. Jusuf, Effects of vertical greenery on mean radiant temperature in the tropical urban environment, *Landscape and Urban Planning*. 127 (2014) 52–64.

[228] A.B. Daemei, M. Azmoodeh, Z. Zamani, E.M. Khotbehsara, Experimental and simulation studies on the thermal behavior of vertical greenery system for temperature mitigation in urban spaces, *Journal of Building Engineering*. 20 (2018) 277–284.

[229] A.J. Ghazalli, C. Brack, X. Bai, I. Said, Alterations in use of space, air quality, temperature and humidity by the presence of vertical greenery system in a building corridor, *Urban Forestry and Urban Greening.* 32 (2018) 177–184.

[230] T. Koyama, M. Yoshinaga, K. ichiro Maeda, A. Yamauchi, Room temperature reductions in relation to growth traits of kudzu vine (Pueraria lobata): Experimental quantification, *Ecological Engineering.* 70 (2014) 217–226.

[231] P. Sunakorn, C. Yimprayoon, Thermal performance of biofacade with natural ventilation in the tropical climate, *Procedia Engineering.* 21 (2011) 34–41.

[232] J. Kronvall, H. Rosenlund, Hygro-thermal and energy related performance of vertical greening on exterior walls, in: Proceedings of the 10th Symposium on Building Physics in the Nordic Countries, Lund University, Lund, 2014: pp. 247–254.

[233] K.J. Kontoleon, E.A. Eumorfopoulou, The effect of the orientation and proportion of a plant-covered wall layer on the thermal performance of a building zone, *Building and Environment.* 45 (2010) 1287–1303.

[234] G. Kokogiannakis, J. Darkwa, S. Badeka, Y. Li, Experimental comparison of green facades with outdoor test cells during a hot humid season, *Energy and Buildings.* 185 (2019) 196–209.

[235] Q. Xing, X. Hao, Y. Lin, H. Tan, K. Yang, Experimental investigation on the thermal performance of a vertical greening system with green roof in wet and cold climates during winter, *Energy and Buildings.* 183 (2019) 105–117.

[236] R.F. De Masi, F. de Rossi, S. Ruggiero, G.P. Vanoli, Numerical optimization for the design of living walls in the Mediterranean climate, *Energy Conversion and Management.* 195 (2019) 573–586.

[237] O.H. Akinwolemiwa, C. Bleil de Souza, L.M. De Luca, J. Gwilliam, Building community-driven vertical greening systems for people living on less than £1 a day: A case study in Nigeria, *Building and Environment.* 131 (2018) 277–287.

[238] P. Abdo, B.P. Huynh, P.J. Irga, F.R. Torpy, Evaluation of air flow through an active green wall biofilter, *Urban Forestry and Urban Greening.* 41 (2019) 75–84.

[239] M.M. Davis, A.L. Vallejo Espinosa, F.R. Ramirez, Beyond green façades: active air-cooling vertical gardens, *Smart and Sustainable Built Environment.* 8 (2019) 243–252.

[240] D. Tudiwer, A. Korjenic, The effect of an indoor living wall system on humidity, mould spores and CO2-concentration, *Energy and Buildings.* 146 (2017) 73–86.

[241] P. Heiselberg, Draught risk from cold vertical surfaces, *Building and Environment.* 29 (1994) 297–301.

[242] H. Manz, T. Frank, Analysis of thermal comfort near cold vertical surfaces by means of computational fluid dynamics, *Indoor and Built Environment.* 13 (2004) 233–242.

[243] G. Perez, J. Coma, I. Martorell, L.F. Cabeza, Vertical Greenery Systems (VGS) for energy saving in buildings: A review, *Renewable and Sustainable Energy Reviews.* 39 (2014) 139–165.

[244] S. Poddar, D. Park, S. Chang, Energy performance analysis of a dormitory building based on different orientations and seasonal variations of leaf area index, *Energy Efficiency.* 10 (2017) 887–903.

[245] N.H. Wong, A.Y.K. Tan, P.Y. Tan, N.C. Wong, Energy simulation of vertical greenery systems, *Energy and Buildings.* 41 (2009) 1401–1408.

[246] R. Djedjig, E. Bozonnet, R. Belarbi, Modeling green wall interactions with street canyons for building energy simulation in urban context, *Urban Climate.* 16 (2016) 75–85.

[247] R. Djedjig, R. Belarbi, E. Bozonnet, Experimental study of green walls impacts on buildings in summer and winter under an oceanic climate, *Energy and Buildings.* 150 (2017) 403–411.

[248] K. Perini, F. Bazzocchi, L. Croci, A. Magliocco, E. Cattaneo, The use of vertical greening systems to reduce the energy demand for air conditioning. Field monitoring in Mediterranean climate, *Energy and Buildings.* 143 (2017) 35–42.

[249] Y. Stav, G. Lawson, Vertical vegetation design decisions and their impact on energy consumption in subtropical cities, *WIT Transactions on Ecology and the Environment*. 155 (2011) 489–500.

[250] S. Yuan, D. Rim, Cooling energy saving associated with exterior greenery systems for three US Department of Energy (DOE) standard reference buildings, *Building Simulation*. 11 (2018) 625–631.

[251] K.C. Dahanayake, C.L. Chow, Comparing reduction of building cooling load through green roofs and green walls by EnergyPlus simulations, *Building Simulation*. 11 (2018) 421–434.

[252] L. Libessart, M.A. Kenai, Measuring thermal conductivity of green-walls components in controlled conditions, *Journal of Building Engineering*. 19 (2018) 258–265.

[253] J.S. Carlos, Simulation assessment of living wall thermal performance in winter in the climate of Portugal, *Building Simulation*. 8 (2015) 3–11.

[254] M. Marchi, R.M. Pulselli, N. Marchettini, F.M. Pulselli, S. Bastianoni, Carbon dioxide sequestration model of a vertical greenery system, *Ecological Modelling*. 306 (2015) 46–56.

[255] B.C.C. Wolverton, W.L. Douglas, K. Bounds, A study of Interior Landscape Plants for Indoor Air Pollution Abatement, Mississippi, 1989.

[256] T.A. Moya, A. van den Dobbelsteen, M. Ottelé, P.M. Bluyssen, A review of green systems within the indoor environment, *Indoor and Built Environment*. 0 (2018) 1–12.

[257] World Health Organization, WHO Air quality guidelines for particulate matter, ozone, nitrogen dioxide and sulfur dioxide: summary of risk assessment, Geneva, 2006.

[258] K. Dzierzanowski, R. Popek, H. Gawrońska, A. Saebø, S.W. Gawroński, Deposition of particulate matter of different size fractions on leaf surfaces and in waxes of urban forest species, *International Journal of Phytoremediation*. 13 (2011) 1037–1046.

[259] U. Weerakkody, J.W. Dover, P. Mitchell, K. Reiling, Evaluating the impact of individual leaf traits on atmospheric particulate matter accumulation using natural and synthetic leaves, *Urban Forestry and Urban Greening*. 30 (2018) 98–107.

[260] M. Rajkumar, S. Sandhya, M.N.V. Prasad, H. Freitas, Perspectives of plant-associated microbes in heavy metal phytoremediation, *Biotechnology Advances*. 30 (2012) 1562–1574.

[261] H. Qin, B. Hong, R. Jiang, Are green walls better options than green roofs for mitigating PM10 pollution? CFD simulations in urban street canyons, *Sustainability (Switzerland)*. 10 (2018).

[262] U. Weerakkody, J.W. Dover, P. Mitchell, K. Reiling, Topographical structures in planting design of living walls affect their ability to immobilise traffic-based particulate matter, *Science of the Total Environment*. 660 (2019) 644–649.

[263] M. Ottelé, H.D. van Bohemen, A.L.A. Fraaij, Quantifying the deposition of particulate matter on climber vegetation on living walls, *Ecological Engineering*. 36 (2010) 154–162.

[264] P.N. Pegas, C.A. Alves, T. Nunes, E.F. Bate-Epey, M. Evtyugina, C.A. Pio, Could houseplants improve indoor air quality in schools?, *Journal of Toxicology and Environmental Health - Part A: Current Issues*. 75 (2012) 1371–1380.

[265] F. Weber, I. Kowarik, I. Säumel, Herbaceous plants as filters: Immobilization of particulates along urban street corridors, *Environmental Pollution*. 186 (2014) 234–240.

[266] A. Przybysz, R. Popek, H. Gawronska, K. Grab, K. Loskot, M. Wrochna, S.W. Gawronski, Efficiency of Photosynthetic Apparatus of Plants Grown in Sites Differing in Level of Particulate Matter, 13 (2014) 17–30.

[267] J. Laothawornkitkul, J.E. Taylor, N.D. Paul, C.N. Hewitt, Biogenic volatile organic compounds in the Earth system: Tansley review, *New Phytologist*. 183 (2009) 27–51.

[268] T. Salthammer, E. Uhde, Organic Indoor Air Pollutants. Occurrence, Measurement, Evaluation, 2nd ed., John Wiley & Sons, New York, 2009.

[269] A.P. Jones, Indoor air quality and health, *Atmospheric Environment*. 33 (1999) 4535–4564.

[270] F. Torpy, N. Clements, M. Pollinger, A. Dengel, I. Mulvihill, C. He, P. Irga, Testing the single-pass VOC removal efficiency of an active green wall using methyl ethyl ketone (MEK), *Air Quality, Atmosphere and Health*. 11 (2018) 163–170.

[271] M. Dela Cruz, J.H. Christensen, J.D. Thomsen, R. Müller, Can ornamental potted plants remove volatile organic compounds from indoor air? - a review, *Environmental Science and Pollution Research*. 21 (2014) 13909–13928.

[272] R.G.S. Bidwell, G.P. Bebee, Carbon monoxide fixation by plants, *Canadian Journal of Botany*. 52 (1974) 1841–1847.

[273] I. Florentina, B. Io, The Effects of Air Pollutants on Vegetation and the Role of Vegetation in Reducing Atmospheric Pollution, in: M. Khallaf (Ed.), The Impact of Air Pollution on Health, Economy, Environment and Agricultural Sources, InTech, Rijeka, 2011: pp. 241–280.

[274] P.J. Irga, F.R. Torpy, M.D. Burchett, Can hydroculture be used to enhance the performance of indoor plants for the removal of air pollutants?, *Atmospheric Environment*. 77 (2013) 267–271.

[275] A. Rondeau, A. Mandon, L. Malhautier, F. Poly, A. Richaume, Biopurification of air containing a low concentration of TEX: Comparison of removal efficiency using planted and non-planted biofilters, *Journal of Chemical Technology and Biotechnology*. 87 (2012) 746–750.

[276] G. Pérez, J. Coma, C. Barreneche, A. De Gracia, M. Urrestarazu, S. Burés, L.F. Cabeza, Acoustic insulation capacity of Vertical Greenery Systems for buildings, *Applied Acoustics*. 110 (2016) 218–226.

[277] N.H. Wong, A.Y.K. Tan, P.Y. Tan, K. Chiang, N.C. Wong, Acoustics evaluation of vertical greenery systems for building walls, *Building and Environment*. 45 (2010) 411–420.

[278] M.J.M. Davis, M.J. Tenpierik, F.R. Ramírez, M.E. Pérez, More than just a Green Facade: The sound absorption properties of a vertical garden with and without plants, *Building and Environment*. 116 (2017) 64–72.

[279] Z. Azkorra, G. Pérez, J. Coma, L.F. Cabeza, S. Bures, J.E. Álvaro, A. Erkoreka, M. Urrestarazu, Evaluation of green walls as a passive acoustic insulation system for buildings, *Applied Acoustics*. 89 (2015) 46–56.

[280] A.M. Lacasta, A. Penaranda, I.R. Cantalapiedra, C. Auguet, S. Bures, M. Urrestarazu, Acoustic evaluation of modular greenery noise barriers, *Urban Forestry and Urban Greening*. 20 (2016) 172–179.

[281] S. Loh, Living Walls - a way to Green the Built Environment, *BEDP Environment Design Guide*. 1 (2008) 1–7.

[282] F. Madre, A. Vergnes, N. Machon, P. Clergeau, Green roofs as habitats for wild plant species in urban landscapes: First insights from a large-scale sampling, *Landscape and Urban Planning*. 122 (2014) 100–107.

[283] R.N. Belcher, K.R. Sadanandan, E.R. Goh, J.Y. Chan, S. Menz, T. Schroepfer, Vegetation on and around large-scale buildings positively influences native tropical bird abundance and bird species richness, *Urban Ecosystems*. 22 (2019) 213–225.

[284] M.A. Benedict, E.T. McMahon, Green Infrastructure: Smart conservation for the 21st Century, *Renewable Resources Journal*. 20 (2002) 32.

[285] S. Matt, Green facades provide habitat for arthropods on buildings in the Washington, D.C. Metro area [Thesis], University of Maryland, 2012.

[286] F. Madre, P. Clergeau, N. Machon, A. Vergnes, Building biodiversity: Vegetated façades as habitats for spider and beetle assemblages, *Global Ecology and Conservation*. 3 (2015) 222–233.

[287] R.S. Ulrich, Aesthetic and Affective Response to Natural Environment, in: Behavior and the Natural Environment, Springer US, Boston, MA, 1983: pp. 85–125.

[288] S.H. Park, R.H. Mattson, Effects of flowering and foliage plants in hospital rooms on patients recovering from abdominal surgery, *HortTechnology*. 18 (2008) 563–568.

[289] M.P. White, I. Alcock, J. Grellier, B.W. Wheeler, T. Hartig, S.L. Warber, A. Bone, M.H. Depledge, L.E. Fleming, Spending at least 120 minutes a week in nature is associated with good health and wellbeing, *Scientific Reports*. 9 (2019) 1–11.

[290] B.C. Wolverton, R.C. Mcdonald, E.A. Watkins, Foliage plants for removing indoor air pollutants from energy-efficient homes, *Economic Botany*. 38 (1984) 224–228.

[291] G. Berg, A. Mahnert, C. Moissl-Eichinger, Beneficial effects of plant-associated microbes on indoor microbiomes and human health?, *Frontiers in Microbiology*. 5 (2014) 1–5.

[292] R. Ulrich, View through a window may influence recovery from surgery, *Science*. 224 (1984) 420–421.

[293] R. Kaplan, S. Kaplan, The experience of nature: A psychological perspective, Cambridge University Press, Cambridge, 1989.

[294] S.H. Park, R.H. Mattson, E. Kim, Pain tolerance effects of ornamental plants in a simulated hospital patient room, *Acta Horticulturae*. 639 (2004) 241–247.

[295] K. Dijkstra, M.E. Pieterse, A. Pruyn, Stress-reducing effects of indoor plants in the built healthcare environment: The mediating role of perceived attractiveness, *Preventive Medicine*. 47 (2008) 279–283.

[296] R.K. Raanaas, K.H. Evensen, D. Rich, G. Sjøstrøm, G. Patil, Benefits of indoor plants on attention capacity in an office setting, *Journal of Environmental Psychology*. 31 (2011) 99–105.

[297] A.E. van den Berg, J.E. Wesselius, J. Maas, K. Tanja-Dijkstra, Green Walls for a Restorative Classroom Environment: A Controlled Evaluation Study, *Environment and Behavior*. 49 (2017) 791–813.

[298] H. Ikei, M. Komatsu, C. Song, E. Himoro, Y. Miyazaki, The physiological and psychological relaxing effects of viewing rose flowers in office workers, *Journal of Physiological Anthropology*. 33 (2014) 1–5.

[299] S.A. Park, C. Song, J.Y. Choi, K.C. Son, Y. Miyazaki, Foliage plants cause physiological and psychological relaxation as evidenced by measurements of prefrontal cortex activity and profile of mood states, *HortScience*. 51 (2016) 1308–1312.

[300] J. Yin, S. Zhu, P. MacNaughton, J.G. Allen, J.D. Spengler, Physiological and cognitive performance of exposure to biophilic indoor environment, *Building and Environment*. (2018).

[301] M. Elsadek, B. Liu, Z. Lian, Green façades: Their contribution to stress recovery and well-being in high-density cities, *Urban Forestry and Urban Greening*. 46 (2019).

[302] C. Gubb, T. Blanusa, A. Griffiths, C. Pfrang, Can houseplants improve indoor air quality by removing CO2 and increasing relative humidity?, *Air Quality, Atmosphere and Health*. 11 (2018) 1191–1201.

[303] D.P. Karunananda, W.K. Abeysinghe, Suitability of foliage plants for indoor decoration based on $CO_2$ emission and absorption rate and stomata density, *Sri Lanka Journal of Food and Agriculture*. 5 (2019) 49.

[304] A. V. Arundel, E.M. Sterling, J.H. Biggin, T.D. Sterling, Indirect health effects of relative humidity in indoor environments, *Environmental Health Perspectives*. VOL. 65 (1986) 351–361.

[305] B.C. Wolverton, How to grow fresh air: 50 houseplants that purify your home or office, Weidenfeld & Nicolson, London, 1997.

[306] B.C. Wolverton, J.D. Wolverton, Interior Plants: Their Influence on Airborne Microbes inside Energy-efficient Buildings, *Journal of the Mississippi Academy of Sciences*. 41 (1996) 99–105.

[307] G. D'Amato, L. Cecchi, S. Bonini, C. Nunes, I. Annesi-Maesano, H. Behrendt, G. Liccardi, T. Popov, P. Van Cauwenberge, Allergenic pollen and pollen allergy in Europe, *Allergy: European Journal of Allergy and Clinical Immunology*. 62 (2007) 976–990.

[308] A. Kinghorn, Toxic Plants, Columbia University Press, New York, 1979.

[309] S.C. Smolinske, Toxicity of Houseplants, CRC Press, Boca Raton, Florida, 1990.

[310] K. Perini, M. Ottelé, S. Giulini, A. Magliocco, E. Roccotiello, Quantification of fine dust deposition on different plant species in a vertical greening system, *Ecological Engineering*. 100 (2017) 268–276.

[311] L. Pérez-Urrestarazu, G. Egea, A. Franco-Salas, R. Fernández-Cañero, Irrigation systems evaluation for living walls, *Journal of Irrigation and Drainage Engineering.* 140 (2014) 1–11.

[312] W.Y. Hung, W.K. Chow, A review on architectural aspects of atrium buildings, *Architectural Science Review.* 44 (2001) 285–295.

[313] S. Sharples, R. Bensalem, Airflow in courtyard and atrium buildings in the urban environment: A win tunnel study, *Solar Energy.* 70 (2001) 237–244.

[314] F. Mills, N. Baker, P. Linden, Construction Industry Conference Centre, Atrium buildings: architecture and engineering, CICC Publications, Welwyn, 1991.

[315] J. Foxall, CCI Campus Manager interviewed by Gunawardena, K. (08 November), (2017).

[316] B. Lee-Rodgers, Hampstead NW3, London Weather Station Dataset, (2020).

[317] A. Kylili, P.A. Fokaides, P. Christou, S.A. Kalogirou, Infrared thermography (IRT) applications for building diagnostics: A review, *Applied Energy.* 134 (2014) 531–549.

[318] S.G. West, J.F. Finch, P.J. Curran, Structural equation models with nonnormal variables, in: R.H. Hoyle (Ed.), Structural Equation Modeling: Concepts, Issues, and Applications, Sage Publications, Inc., 1995: pp. 56–75.

[319] Digital Technology Group, Cambridge University Weather Station Data, (2019).

[320] BSI, BS EN ISO 7730: Ergonomics of the thermal environment - Analytical determination and interpretation of thermal comfort using calculation of the PMV and PPD indices and local thermal comfort criteria, (2005) 605–615.

[321] K. V. Mardia, Statistics of Directional Data, *Journal of the Royal Statistical Society. Series B (Methodological).* 37 (1975) 349–393.

[322] A.S. Muhaisen, Shading simulation of the courtyard form in different climatic regions, *Building and Environment.* 41 (2006) 1731–1741.

[323] M. Taleghani, L. Kleerekoper, M. Tenpierik, A. Van Den Dobbelsteen, Outdoor thermal comfort within five different urban forms in the Netherlands, *Building and Environment.* 83 (2015) 65–78.

[324] G. Öquist, N.P.A. Huner, Photosynthesis of Overwintering Evergreen Plants, *Annual Review of Plant Biology.* 54 (2003) 329–355.

[325] CIBSE, Guide A: Environmental design, 8th ed., Chartered Institution of Building Services Engineers, Norwich, 2018.

[326] P.O. Fanger, B.M. Ipsen, G. Langkilde, B.W. Olessen, N.K. Christensen, S. Tanabe, Comfort limits for asymmetric thermal radiation, *Energy and Buildings.* 8 (1985) 225–236.

[327] P.O. Fanger, N.K. Christensen, Perception of draught in ventilated spaces, *Ergonomics.* 29 (1986) 215–235.

[328] A.K. Hegazy, M.I. El Amry, Leaf temperature of desert sand dune plants: Perspectives on the adaptability of leaf morphology, *African Journal of Ecology.* 36 (1998) 34–43.

[329] A. Leigh, S. Sevanto, J.D. Close, A.B. Nicotra, The influence of leaf size and shape on leaf thermal dynamics: does theory hold up under natural conditions?, *Plant Cell and Environment.* 40 (2017) 237–248.

[330] Y. Cohen, V. Alchanatis, M. Meron, Y. Saranga, J. Tsipris, Estimation of leaf water potential by thermal imagery and spatial analysis, *Journal of Experimental Botany.* 56 (2005) 1843–1852.

[331] Y. Kim, C.J. Still, D.A. Roberts, M.L. Goulden, Thermal infrared imaging of conifer leaf temperatures: Comparison to thermocouple measurements and assessment of environmental influences, *Agricultural and Forest Meteorology.* 248 (2018) 361–371.

[332] D.M. Aubrecht, B.R. Helliker, M.L. Goulden, D.A. Roberts, C.J. Still, A.D. Richardson, Continuous, long-term, high-frequency thermal imaging of vegetation: Uncertainties and recommended best practices, *Agricultural and Forest Meteorology.* 228–229 (2016) 315–326.

[333] S. Leuzinger, C. Körner, Tree species diversity affects canopy leaf temperatures in a mature temperate forest, *Agricultural and Forest Meteorology*. 146 (2007) 29–37.

[334] J. Padhi, R.K. Misra, J.O. Payero, Estimation of soil water deficit in an irrigated cotton field with infrared thermography, *Field Crops Research*. 126 (2012) 45–55.

[335] B. Kluge, A. Peters, J. Krüger, G. Wessolek, Detection of soil microbial activity by infrared thermography (IRT), *Soil Biology and Biochemistry*. 57 (2013) 383–389.

[336] J.M. Costa, O.M. Grant, M.M. Chaves, Thermography to explore plant-environment interactions, *Journal of Experimental Botany*. 64 (2013) 3937–3949.

[337] J.M. Blonquist, J.M. Norman, B. Bugbee, Automated measurement of canopy stomatal conductance based on infrared temperature, *Agricultural and Forest Meteorology*. 149 (2009) 1931–1945.

[338] H.G. Jones, R.A. Vaughan, Remote sensing of vegetation: principles, techniques, and applications, Oxford University Press, Oxford, 2010.

[339] A. Kirimtat, O. Krejcar, A review of infrared thermography for the investigation of building envelopes: Advances and prospects, *Energy and Buildings*. 176 (2018) 390–406.

[340] FLIR Systems, The Ultimate Infrared Handbook for R&D Professionals, Wilsonville, Oregon, 2012.

[341] British Standards Institution, BS EN 13187:1999 Thermal performance of buildings. Qualitative detection of thermal irregularities in building envelopes. Infrared method, (1999) 16.

[342] M. Fox, S. Goodhew, P. De Wilde, Building defect detection: External versus internal thermography, *Building and Environment*. 105 (2016) 317–331.

[343] B. Tejedor, M. Casals, M. Gangolells, X. Roca, Quantitative internal infrared thermography for determining in-situ thermal behaviour of façades, *Energy and Buildings*. 151 (2017) 187–197.

[344] M. Vollmer, K.-P. Möllmann, Infrared thermal imaging: fundamentals, research and applications, 2nd ed., John Wiley & Sons, Weinheim, 2018.

[345] J. Kelly, N. Kljun, P.-O. Olsson, L. Mihai, B. Liljeblad, P. Weslien, L. Klemedtsson, L. Eklundh, Challenges and Best Practices for Deriving Temperature Data from an Uncalibrated UAV Thermal Infrared Camera, *Remote Sensing*. 11 (2019) 567.

[346] H.G. Jones, Use of thermography for quantitative studies of spatial and temporal variation of stomatal conductance over leaf surfaces, *Plant, Cell and Environment*. 22 (1999) 1043–1055.

[347] P. Berdahl, M. Martin, Emissivity of clear skies, *Solar Energy*. 32 (1984) 663–664.

[348] K. Zhang, T.P. Mcdowell, M. Kummert, Sky temperature estimation and measurement for longwave radiation calculation, in: Proceedings of the 15th IBPSA Conference, IBPSA, San Francisco, 2017: pp. 769–778.

[349] O. Lapidot, T. Ignat, R. Rud, I. Rog, V. Alchanatis, T. Klein, Use of thermal imaging to detect evaporative cooling in coniferous and broadleaved tree species of the Mediterranean maquis, *Agricultural and Forest Meteorology*. 271 (2019) 285–294.

[350] I.J. Wright, N. Dong, V. Maire, I.C. Prentice, M. Westoby, S. Díaz, R. V. Gallagher, B.F. Jacobs, R. Kooyman, E.A. Law, M.R. Leishman, Ü. Niinemets, P.B. Reich, L. Sack, R. Villar, H. Wang, P. Wilf, Ü. Niinemets, M.R. Leishman, I.J. Wright, I.C. Prentice, R. Kooyman, M. Westoby, P.B. Reich, B.F. Jacobs, R. V. Gallagher, V. Maire, N. Dong, E.A. Law, H. Wang, R. Villar, V. Maire, I.C. Prentice, M. Westoby, S. Díaz, R. V. Gallagher, B.F. Jacobs, R. Kooyman, E.A. Law, M.R. Leishman, Ü. Niinemets, P.B. Reich, Global climatic drivers of leaf size, *Science*. 357 (2017) 917–921.

[351] W.K. Smith, G.N. Geller, Leaf and environmental parameters influencing transpiration: Theory and field measurements, *Oecologia*. 46 (1980) 308–313.

[352] D.M. Gates, Transpiration and Leaf Temperature, *Annual Review of Plant Physiology*. 19 (1968) 211–238.

[353] W.K. Smith, G.A. Carter, Shoot Structural Effects on Needle Temperatures and Photosynthesis in Conifers, *American Journal of Botany*. 75 (1988) 496.

[354] H.G. Jones, Application of Thermal Imaging and Infrared Sensing in Plant Physiology and Ecophysiology, *Advances in Botanical Research*. 41 (2004) 107–163.

[355] B. Lehmann, K. Ghazi Wakili, T. Frank, B. Vera Collado, C. Tanner, Effects of individual climatic parameters on the infrared thermography of buildings, *Applied Energy*. 110 (2013) 29–43.

[356] F. Meier, D. Scherer, J. Richters, A. Christen, Atmospheric correction of thermal-infrared imagery of the 3-D urban environment acquired in oblique viewing geometry, *Atmospheric Measurement Techniques*. 4 (2011) 909–922.

[357] W. Minkina, S. Dudzik, Infrared thermography: errors and uncertainties, J. Wiley, West Sussex, 2009.

[358] R.D. Jackson, Remote Sensing of Biotic and Abiotic Plant Stress, *Annual Review of Phytopathology*. 24 (2003) 265–287.

[359] R.G. Allen, L.S. Pereira, D. Raes, M. Smith, Crop evapotranspiration-Guidelines for computing crop water requirements-FAO Irrigation and drainage paper 56, *FAO, Rome*. 300 (1998) D05109.

[360] M.M. Davis, S. Hirmer, The potential for vertical gardens as evaporative coolers: An adaptation of the "Penman Monteith Equation," *Building and Environment*. 92 (2015) 135–141.

[361] P.M.F. van de Wouw, E.J.M. Ros, H.J.H. Brouwers, Precipitation collection and evapo(transpi)ration of living wall systems: A comparative study between a panel system and a planter box system, *Building and Environment*. 126 (2017) 221–237.

[362] E. Alexandri, P. Jones, Developing a one-dimensional heat and mass transfer algorithm for describing the effect of green roofs on the built environment: Comparison with experimental results, *Building and Environment*. 42 (2007) 2835–2849.

[363] D.J. Sailor, A green roof model for building energy simulation programs, *Energy and Buildings*. 40 (2008) 1466–1478.

[364] D.B. Crawley, L.K. Lawrie, F.C. Winkelmann, W.F. Buhl, Y.J. Huang, C.O. Pedersen, R.K. Strand, R.J. Liesen, D.E. Fisher, M.J. Witte, J. Glazer, EnergyPlus: creating a new-generation building energy simulation program, *Energy and Buildings*. 33 (2001) 319–331.

[365] F. Olivieri, R.C. Grifoni, D. Redondas, J.A. Sánchez-Reséndiz, S. Tascini, An experimental method to quantitatively analyse the effect of thermal insulation thickness on the summer performance of a vertical green wall, *Energy and Buildings*. 150 (2017) 132–148.

[366] R. Djedjig, S.E. Ouldboukhitine, R. Belarbi, E. Bozonnet, Development and validation of a coupled heat and mass transfer model for green roofs, *International Communications in Heat and Mass Transfer*. 39 (2012) 752–761.

[367] University of Wisconsin Solar Energy Laboratory, TRNSYS: A Transient System Simulation Program, (1994).

[368] K. Grabowiecki, A. Jaworski, T. Niewczas, A. Belleri, Green Solutions-Climbing Vegetation Impact on Building -Energy Balance Element, *Energy Procedia*. 111 (2017) 377–386.

[369] J. Levitt, Responses of Plants to Environmental Stresses, 2nd ed., Academic Press, Inc., London, 1980.

[370] W. Larcher, Physiological plant ecology: ecophysiology and stress physiology of functional groups, 3rd ed., Springer, Heidelberg, 2003.

[371] P.C. Tabares-Velasco, J. Srebric, A heat transfer model for assessment of plant based roofing systems in summer conditions, *Building and Environment*. 49 (2012) 310–323.

[372] L.F. Shampine, I. Gladwell, S. Thompson, Solving ODEs with MATLAB, Cambridge University Press, Cambridge, 2003.

[373] R.D. Peacock, P.A. Reneke, W. D. Davis, W.W. Jones, Quantifying fire model evaluation using functional analysis, *Fire Safety Journal*. 33 (1999) 167–184.

[374] T. Takahashi, Airborne fungal colony-forming units in outdoor and indoor environments in Yokohama, Japan, *Mycopathologia*. 139 (1997) 23–33.

[375] C.S.B. Grimmond, M. Blackett, M.J. Best, J. Barlow, J.J. Baik, S.E. Belcher, S.I. Bohnenstengel, I. Calmet, F. Chen, A. Dandou, K. Fortuniak, M.L. Gouvea, R. Hamdi, M. Hendry, T. Kawai, Y. Kawamoto, H. Kondo, E.S. Krayenhoff, S.H. Lee, T. Loridan, A. Martilli, V. Masson, S. Miao, K. Oleson, G. Pigeon, A. Porson, Y.H. Ryu, F. Salamanca, L. Shashua-Bar, G.J. Steeneveld, M. Tombrou, J. Voogt, D. Young, N. Zhang, The International Urban Energy Balance Models Comparison Project: First Results from Phase 1, *Journal of Applied Meteorology and Climatology*. 49 (2010) 1268–1292.

[376] G. Pigeon, A. Lemonsu, N. Long, J. Barrié, V. Masson, P. Durand, Urban thermodynamic island in a coastal city analysed from an optimized surface network, *Boundary-Layer Meteorology*. 120 (2006) 315–351.

[377] J. Hidalgo, G. Pigeon, V. Masson, Urban-breeze circulation during the CAPITOUL experiment: observational data analysis approach, *Meteorology and Atmospheric Physics*. 102 (2008) 223–241.

[378] S. Oxizidis, A. V Dudek, A.M. Papadopoulos, A computational method to assess the impact of urban climate on buildings using modeled climatic data, *Energy and Buildings*. 40 (2008) 215–223.

[379] K.R. Gunawardena, T. Kershaw, Urban climate influence on building energy use, in: M.P. Burlando, Massimiliano; Canepa, Maria; Magliocco, Adriano; Perini, Katia, Repetto (Ed.), International Conference on Urban Comfort and Environmental Quality URBAN-CEQ, Genoa University Press, Genoa, 2017: pp. 175–184.

[380] B. Bueno, J. Sullivan, M. Street, L. Zhang, B.T. Lopez-Pineda, Urban Weather Generator (V4.1.0), (2015).

[381] T. Monin-obukhov, Momentum and Heat Exchanges with Homogeneous Surfaces, in: S.P. Arya (Ed.), Introduction to Micrometeorology, Academic Press Inc., Cambridge, Massachusetts, 1988: pp. 157–181.

[382] V. Masson, A physically-based scheme for the urban energy budget in atmospheric models, *Boundary-Layer Meteorology*. 94 (2000) 357–397.

[383] B. Bueno, L. Norford, G. Pigeon, R. Britter, A resistance-capacitance network model for the analysis of the interactions between the energy performance of buildings and the urban climate, *Building and Environment*. 54 (2012) 116–125.

[384] B. Bueno, M. Roth, L. Norford, R. Li, Computationally efficient prediction of canopy level urban air temperature at the neighbourhood scale, *Urban Climate*. 9 (2014) 35–53.

[385] A. Nakano, B. Bueno, L. Norford, C.F. Reinhart, Urban Weather Generator - A novel workflow for integrating urban heat island effect within urban design process, *Building Simulation 2015*. (2015).

[386] K.R. Gunawardena, N. Mccullen, T. Kershaw, Heat island influence on space-conditioning loads of urban and suburban office buildings, in: Cities and Climate Conference 2017, Potsdam Institute for Climate Impact Research, Potsdam, 2017: pp. 1–13.

[387] K. Gunawardena, T. Kershaw, N. McCullen, The influence of urban climate on building energy use, in: 8th International Conference on Structural Engineering and Construction Management, ICSECM, Kandy, 2017.

[388] B. Bueno, J. Sullivan, M. Street, L. Zhang, B.T. Lopez-Pineda, J. Yang, K. Gunawardena, Urban Weather Generator (V5.1.0 beta), (2019).

[389] T. Kusuda, P.R. Achenbach, Earth temperature and thermal diffusivity at selected stations in the United States, DTIC Document, 1965.

[390] R. Watkins, J. Palmer, M. Kolokotroni, P. Littlefair, The London heat island: Results from summertime monitoring, *Building Services Engineering Research and Technology*. 23 (2002) 97–106.

[391] M. Eames, T. Kershaw, D. Coley, On the creation of future probabilistic design weather years from UKCP09, *Building Services Engineering Research & Technology*. 32 (2011) 127–142.

[392] T. Kershaw, M. Sanderson, D. Coley, M. Eames, Estimation of the urban heat island for UK climate change projections, *Building Services Engineering Research and Technology*. 31 (2010) 251–263.

[393] IES-VE, IES-Virtual Environment (V2017.2.0.0), (2017).

[394] B.J. Moffitt, The effects of urbanization on mean temperatures at Kew observarotory, *Weather*. 27 (1972) 121–129.

[395] D.O. Lee, Urban warming? - An analysis of recent trends in London's urban heat island, *Weather*. 47 (1992) 50–56.

[396] R.L. Wilby, Past and projected trends in London ' s urban heat island, *Weather*. 58 (2003) 251–260.

[397] P.D. Jones, D.H. Lister, The urban heat island in central London and urban-related warming trends in central London since 1900, *Weather*. 64 (2009) 323–327.

[398] M. Kolokotroni, Y. Zhang, R. Giridharan, Heating and cooling degree day prediction within the London urban heat island area, *Building Services Engineering Research and Technology*. 30 (2009) 183–202.

[399] M. Kolokotroni, R. Giridharan, Urban heat island intensity in London: An investigation of the impact of physical characteristics on changes in outdoor air temperature during summer, *Solar Energy*. 82 (2008) 986–998.

[400] R. Giridharan, M. Kolokotroni, Urban heat island characteristics in London during winter, *Solar Energy*. 83 (2009) 1668–1682.

[401] T.R. Oke, Street Design and Urban Canopy Layer Climate, *Energy and Buildings*. 11 (1988) 103–113.

[402] M. Iamarino, S. Beevers, C.S.B. Grimmond, High-resolution (space, time) anthropogenic heat emissions: London 1970-2025, *International Journal of Climatology*. 32 (2012) 1754–1767.

[403] M. Santamouris, D. Kolokotsa, eds., Urban climate mitigation techniques, Routledge, 2016.

[404] T. Yates, BRE, Jordans basebed technical data sheet, Building Research Establishment (BRE) on behalf of Albion Stone, Surrey, 2017.

[405] L. Gartland, Heat islands: understanding and mitigating heat in urban areas, Routledge, Oxford, 2008.

[406] A. Bryman, Social research methods, 5th ed., Oxford University Press, Oxford, 2016.

[407] C.D. Manning, P. Raghavan, H. Schutze, Introduction to Information Retrieval, Cambridge University Press, Cambridge, 2008.

[408] K. Perini, M. Ottelé, E.M. Haas, R. Raiteri, Greening the building envelope, facade greening and living wall systems, *Open Journal of Ecology*. 01 (2011) 1–8.

[409] A. Meral, N. Başaran, E. Yalçinalp, E. Doğan, M.K. Ak, E. Eroğlu, A comparative approach to artificial and natural green walls according to ecological sustainability, *Sustainability (Switzerland)*. 10 (2018).

[410] J. David, Royal Horticultural Society, A New System of Plant Hardiness Ratings for the British Isles, *The Plantsman*. 138 (2013) 68–69.

[411] N. Séjalon-Delmas, Senior Lecturer at Université Toulouse III - Paul Sabatier. Personal communication. 21 February, (2019).

[412] A. Medl, F. Florineth, S.B. Kikuta, S. Mayr, Irrigation of 'Green walls' is necessary to avoid drought stress of grass vegetation (Phleum pratense L.), *Ecological Engineering*. 113 (2018) 21–26.

[413] M. Urrestarazu, G. Carrasco, J.E. Álvaro, Design of a modular vegetative unit and fertigation management for noise-abatement walls in a semiarid climate, *Journal of Irrigation and Drainage Engineering*. 143 (2017).

[414] J. Bonnin, Deputy Director of Technical Resources. Personal communication. 29 November, (2017).

[415] L. Jørgensen, K. Thorup-Kristensen, D.B. Dresbll, Against the wall—Root growth and competition in four perennial winter hardy plant species grown in living walls, *Urban Forestry and Urban Greening*. 29 (2018) 293–302.

[416] K. Perini, M. Ottelé, E.M. Haas, R. Raiteri, Vertical greening systems, a process tree for green façades and living walls, *Urban Ecosystems*. 16 (2013) 265–277.

[417] H.E. Nilsson, Remote sensing and image analysis in plant pathology, *Annual Review of Phytopathology*. 33 (1995) 489–527.

[418] L. Chaerle, D. Hagenbeek, X. Vanrobaeys, D. Van Der Straeten, Early detection of nutrient and biotic stress in Phaseolus vulgaris, *International Journal of Remote Sensing*. 28 (2007) 3479–3492.

[419] H.G. Jones, R. Serraj, B.R. Loveys, L. Xiong, A. Wheaton, A.H. Price, Thermal infrared imaging of crop canopies for the remote diagnosis and quantification of plant responses to water stress in the field, *Functional Plant Biology*. 36 (2009) 978–989.

[420] H.G. Jones, Plants and microclimate: a quantitative approach to environmental plant physiology, 3rd ed., Cambridge, 2014.

[421] UN High Level Panel of Experts, Impact of COVID-19 on Food Security and Nutrition (FSN), Rome, 2020.

[422] M. Ableman, Farm the City: A Toolkit for Setting Up a Successful Urban Farm, New Society Publishers, 2020.

[423] A. Viljoen, J. Howe, Continuous Productive Urban Landscapes, Routledge, London, 2012.

[424] A. Viljoen, J.S.C. Wiskerke, Sustainable food planning: evolving theory and practice: Evolving Theory and Practice, Wageningen Academic Publishers, Wageningen, 2012.

[425] C. Steel, Hungry City: How Food Shapes Our Lives, Random House, London, 2013.

[426] C. Steel, Sitopia: How Food Can Save the World, Random House, London, 2020.

[427] M. Grašič, T. Sovdat, A. Gaberščik, Frond optical properties of the fern phyllitis scolopendrium depend on light conditions in the habitat, *Plants*. 9 (2020) 1–17.

[428] M.S. Jayalakshmy, J. Philip, Thermophysical properties of plant leaves and their influence on the environment temperature, *International Journal of Thermophysics*. 31 (2010) 2295–2304.

University of Cambridge